



# **COMPARATIVE STUDY OF GAS-BUBBLE LESIONS USING EXPERIMENTAL MODELS**

**ALICIA SOFÍA VELÁZQUEZ WALLRAF**

Doctorado en Sanidad Animal y Seguridad Alimentaria

Las Palmas de Gran Canaria. Julio 2023.









## **TESIS DOCTORAL**

# **COMPARATIVE STUDY OF GAS- BUBBLE LESIONS USING EXPERIMENTAL MODELS**

**ESTUDIO COMPARATIVO DE LAS LESIONES  
CAUSADAS POR BURBUJAS DE GAS  
MEDIANTE MODELOS EXPERIMENTALES**

**ALICIA SOFÍA VELÁZQUEZ WALLRAF**

**DOCTORADO EN SANIDAD ANIMAL Y SEGURIDAD  
ALIMENTARIA**

**ESCUELA DE DOCTORADO - UNIVERSIDAD DE LAS PALMAS  
DE GRAN CANARIA**

**LAS PALMAS DE GRAN CANARIA**

**JULIO DE 2023**



**D. ANTONIO FERNÁNDEZ RODRIGUEZ, COORDINADOR  
DEL PROGRAMA DE DOCTORADO DE SANIDAD ANIMAL Y  
SEGURIDAD ALIMENTARIA DE LA UNIVERSIDAD DE LAS  
PALMAS DE GRAN CANARIA**

**INFORMA,**

De que la Comisión Académica del Programa de Doctorado, en su sesión de fecha .../.../....., tomó el acuerdo de dar el consentimiento para su tramitación, a la tesis doctoral titulada **“Comparative study of gas-bubble lesions using experimental models (Estudio comparativo de las lesiones causadas por burbujas de gas mediante modelos experimentales)”** presentada por la doctoranda D<sup>a</sup> **Alicia Sofía Velázquez Wallraf** y dirigida por el Dr. D **Antonio J. Fernández Rodríguez**, la Dra. D<sup>a</sup> **Maria José Caballero Cansino** y la Dra. D<sup>a</sup> **Yara Bernaldo de Quirós Miranda**.

Y para que así conste, y a efectos de lo previsto en el Artº 11 del Reglamento de Estudios de Doctorado (BOULPGC 04/03/2019) de la Universidad de Las Palmas de Gran Canaria, firmo la presente en Las Palmas de Gran Canaria, a ... de ..... de dos mil veintitrés.



**UNIVERSIDAD DE LAS PALMAS DE GRAN CANARIA**

**ESCUELA DE DOCTORADO**

Programa de doctorado

DOCTORADO EN SANIDAD ANIMAL Y SEGURIDAD  
ALIMENTARIA

Título de la Tesis

**COMPARATIVE STUDY OF GAS-BUBBLE LESIONS  
USING EXPERIMENTAL MODELS**

(ESTUDIO COMPARATIVO DE LAS LESIONES  
CAUSADAS POR BURBUJAS DE GAS MEDIANTE  
MODELOS EXPERIMENTALES)

Tesis Doctoral presentada por D<sup>a</sup>  
ALICIA SOFÍA VELÁZQUEZ WALLRAF

Dirigida por el Dr. D ANTONIO J. FERNÁNDEZ RODRÍGUEZ

Codirigida por la Dra. D<sup>a</sup> MARIA JOSÉ CABALLERO CANSINO y la  
Dra. D<sup>a</sup> YARA BERNALDO DE QUIRÓS MIRANDA

Las Palmas de Gran Canaria, a ..... de ..... de 2023

El Director

Las Codirectoras

La Doctoranda







*A mis padres y mi hermano,*

*A mis abuelos y mi familia,*

*A Rosa.*



“La vie n’est facile pour aucun de nous. Mais il faut avoir de la persévérance, et surtout de la confiance en soi. Il faut croire que l’on est doué pour quelque chose, et que, cette chose, il faut l’atteindre coûte que coûte.”

“La vida no es fácil para ninguno de nosotros. Pero hay que tener perseverancia y, sobre todo, confianza en sí mismo. Hay que creer que estamos capacitados para algo y, ese algo, conseguirlo cueste lo que cueste”.

*Marie Skłodowska-Curie.*



# **TABLE OF CONTENTS**

<b>1. INTRODUCTION AND OBJECTIVES</b>	<b>1</b>
<b>2. STATE OF THE ART</b>	<b>7</b>
<b>2.1. DECOMPRESSION ILLNESS</b>	<b>9</b>
<b>2.2. HISTORY OF DECOMPRESSION SICKNESS</b>	<b>10</b>
<b>2.3. DECOMPRESSION THEORY</b>	<b>19</b>
<b>2.4. DECOMPRESSION SICKNESS IN HUMANS</b>	<b>24</b>
2.4.1. Clinical manifestations	24
2.4.2. Risk factors	24
2.4.3. Diagnostic	26
2.4.4. Treatment	27
<b>2.5. DECOMPRESSION SICKNESS IN MARINE</b>	
<b>ANIMALS</b>	<b>28</b>
2.5.1. Decompression sickness in sea turtles	28
2.5.2. Decompression-like sickness in cetaceans	31
<b>2.6. PATHOLOGY OF DECOMPRESSION SICKNESS</b>	<b>38</b>
2.6.1. Decompression pathology in humans	38
2.6.2. Decompression pathology in marine animals	40
2.6.3. Endothelial damage and associated biomarkers	45
<b>2.7. EXPERIMENTAL MODELS OF DECOMPRESSION</b>	
<b>SICKNESS</b>	<b>51</b>
2.7.1. Treatment	52
2.7.2. Diagnostic and risk factors	53
2.7.3. Pathology	54

<b>2.8. GAS BUBBLE DISEASE AS A MODEL OF</b>	
<b>DECOMPRESSION SICKNESS</b>	56
2.8.1. Definition	56
2.8.2. History	59
2.8.3. Pathogenesis	63
2.8.4. Clinical features, risk factors and treatment	64
2.8.5. Pathology	68
2.8.6. Comparative pathophysiology between Gas bubble disease and decompression sickness	70
<b>3. METHODOLOGY</b>	73
<b>3.1. RABBIT EXPERIMENTAL MODEL</b>	75
<b>3.2. FISH EXPERIMENTAL MODEL</b>	80
3.2.1. Water supersaturation	80
3.2.2. Pilot tests	87
3.2.3. Fish model of gas-bubble lesions	90
<b>4. SCIENTIFIC PUBLICATIONS</b>	103
<b>5. CONCLUSIONS</b>	155
<b>6. RESUMEN EXTENDIDO</b>	159
<b>6.1. ANTECEDENTES Y OBJETIVOS</b>	161
<b>6.2. RESUMEN DE LAS PUBLICACIONES</b>	
<b>CIENTÍFICAS</b>	163
6.2.1. PUBLICACIÓN I: Patología descompresiva en cetáceos basada en un modelo patológico experimental	163

6.2.2. PUBLICACIÓN II: Establecimiento de un modelo en peces para estudiar las lesiones por burbujas de gas	167
6.2.3. PUBLICACIÓN III: Biomarcadores relacionados con embolismo gaseoso: gas score, patología y expresión génica en un modelo de enfermedad de las burbujas de gas	172
<b>6.3. CONCLUSIONES</b>	179
<b>7. REFERENCE LIST</b>	181
<b>8. ABBREVIATIONS</b>	223
<b>9. ACKNOWLEDGMENTS / AGRADECIMIENTOS / REMERCIEMENTS</b>	231



# 1. INTRODUCTION AND OBJECTIVES





Decompression sickness (DCS) is a syndrome caused when the partial pressure of dissolved gases in the organism exceeds the ambient pressure, triggering the formation of gas bubbles in circulation and tissues (Vann et al., 2011). These gas bubbles can lead to traumatic, embolic, and biochemical/inflammatory alterations (i.e., cellular stress or damage). Its abundance correlated positively with the risk of DCS (Mahon and Regis, 2014). In humans, the main clinical manifestations described in severe DCS are neurological, pulmonary, systemic, and inner ear disorders (Lemaitre et al., 2009). Subjects undergoing the same diving profile have shown a widely different pattern of gas bubble formation (Nishi, 1993). Individual variability remains a factor to be taken into account in this syndrome.

DCS has traditionally been studied in humans. It was first described in the 19th century in caisson workers (Triger, 1845). Nowadays, it is mainly associated with diving (Edmonds et al., 2015). This syndrome has also recently been described in marine species, such as sea turtles (García-Párraga et al., 2014). Cetaceans were assumed to be protected from DCS through a suit of diving adaptations developed in their transition from land to water (Piantadosi and Thalmann, 2004). However, a pathology consistent with DCS (decompression-like sickness (DC-likeS)) was described for the first time in a mass stranding of beaked whales coincidental in time and space with naval exercises and the use of mid-frequency active sonar (Jepson et al., 2003; Fernandez et al., 2005). Since then, DC-likeS in cetaceans has been diagnosed in various beaked whales stranding associated with naval exercises, but also in Risso's dolphins struggling to kill their prey (Arbelo et al., 2008; Bernaldo de Quirós et al., 2011b; Fernández et al., 2012; Bernaldo de Quirós et al., 2019). Regardless the recent literature, the controversy in the scientific community as to whether adaptations to diving prevent the appearance of DC-likeS in cetaceans remains a

scientific debate. Therefore, it is necessary to investigate and provide more evidence of this pathology in this group of marine animals.

In contrast to human and sea turtles, in which the diagnosis and study of DCS is clinical, this syndrome in cetaceans can only be studied by means of postmortem pathological studies in stranded animals. In human medicine, experimental models of DCS have traditionally been used in small mammals such as rabbits, rats, and mice, mainly focused on prevention and potential treatments. Despite the extensive literature on experimental models of DCS, few have delved into the pathological aspects, being necessary an updated complete pathological study to reinforce the pathological diagnosis of decompression pathology consistent with DCS in cetaceans, but also for sea turtles or even humans.

The traditional use of small mammals, mostly rodents, in experimental DCS (e.g., Eggleton et al., 1945; Shim et al., 1967; Tanoue et al., 1987; Arieli et al., 2010) could be replaced by an alternative fish model. This was postulated due to the similarities in intravascular and extravascular gas bubble formation of the gas bubble disease (GBD) in fish and DCS in mammals (D'Aoust and Smith, 1974; Machado et al., 1987). GBD is a pathology widely described in fish living in large dams where masses of water fall from one reservoir to another, causing the trapping and dissolution of atmospheric gases, due to the hydrostatic pressure (Bouck et al., 1976; Weitkamp and Katz, 1980). This water is hence supersaturated with dissolved gases and is responsible for large fish mortalities in dams. The development of a gas embolism and its associated lesions described in GBD are very similar to those observed in experimental and natural decompression (Speare, 2010).

Considering the pathological similarities between GBD and DCS and applying the replacement principle described in the Directive 2010/63/EU of the European Parliament which establishes the need to

use animals with less capacity to feel pain, suffering, or lasting damage, a fish model of gas embolism could be used as a basis to further explore the pathophysiology of DCS. This model could be useful for the study of pathological lesions associated with gas bubbles and for the study of the biochemical/inflammatory alterations caused by the gas bubbles in blood vessels and tissues.

### **OBJECTIVES**

The present thesis project is part of the research line of Histology and Pathology of terrestrial and marine animals from the Animal health and food safety institute (IUSA) and it has been developed to broaden the knowledge on the pathology and cellular alterations associated with gas-bubble lesions. The main objectives were:

1. - To characterize the pathology associated with DCS in a well-established animal model, i.e., the New Zealand White Rabbit, and to compare these results with those described in cetaceans presenting a decompression pathology.
2. - To induce in a reproducible and consistent manner an experimental model of severe gas bubble disease in fish to produce intravascular and extravascular gas bubbles and its associated lesions.
3. - To evaluate and validate the fish model of severe gas bubble disease to study the gas-bubble lesions and its effects at the cellular level in DCS.



## 2. STATE OF THE ART





## **2.1. DECOMPRESSION ILLNESS**

Decompression illness (DCI) is a term used to cover any condition produced by a pressure reduction known as decompression, such as decompression sickness and barotraumas (Lemaitre et al., 2009). This disease can develop either at altitude or at depth; thus, population groups such as divers, aviators, parachutists, or miners can be affected (Ninokawa and Nordham, 2022). The term DCI is used in the clinical field with no distinction between the different conditions but, referring specifically to pathophysiology, is necessary to differentiate between processes (Mitchell, 2019).

### **Barotraumas**

Barotrauma is a physical damage that occurs due to the pressure difference between a gas inside a corporeal space and the ambient gas, causing an expansion of the body gas that may rupture the body cavity where it is retained (Brubakk and Neuman, 2003). In DCI the most frequent condition described is pulmonary barotrauma followed by inner ear barotrauma. In pulmonary barotrauma, arterial gas embolism (AGE) occurs due to the rupture of lung tissue and the entry of alveolar gas into the arterial circulation, forming gas emboli that can reach the brain (Francis and Mitchell, 2003).

### **Decompression sickness**

Other classical condition of DCI is decompression sickness (DCS). DCS is a clinical condition caused by the phase separation of the dissolved gas in the organism when the sum of dissolved gases in blood and organ tissues exceeds the ambient pressure (Vann et al., 2011), resulting in the formation and growth of intravascular and extravascular gas bubbles. This difference in gas tension occurs mostly in tissues and in the venous side, leading to a systemic venous gas embolism (VGE).

VGE will reach the lungs causing interference with gas exchange, cardiac arrhythmias, pulmonary hypertension, and other systemic processes related to systemic gas bubbles (Muth and Shank, 2000). This thesis will focus on the study of DCS.

DCS is generally referred to in the context of divers, as this is the group where it has been most observed. Within the divers, we can differentiate between scuba and breath-hold divers.

## **2.2. HISTORY OF DECOMPRESSION SICKNESS**

DCS has been known since the 17th century, with the most critical advances in this field developed between 1800 and 1900 (Mahon and Regis, 2014). The scientists of this period who, in some cases such as Paul Bert, dedicated their scientific careers to the study of this syndrome, proposed hypotheses and set the basis for the prevention and treatment by studying the symptoms of “caisson disease” or “the bends”, synonyms of DCS. The Irish scientist Robert Boyle (1627-1691) reported the first reference to DCS after observing gas bubbles in a snake's eye placed in an airtight chamber and creating a vacuum (Boyle, 1670).

### **“Caisson disease”: Triger, Pol and Watelle**

In the early 1800s in France, miners faced an unknown and potentially fatal condition. This syndrome began to be observed in 1840 when Charles-Jean Triger (1800-1872), a French civil engineer, implemented a pressurized chamber to work in underground mines in which compressed gas was pumped to ensure that the workers breathed enough oxygen (**Fig. 1**). Coined caisson disease, in reference to the

French term for a box ("Caisson" in French) in which they descended, is the first record of DCS in humans (Triger, 1845).

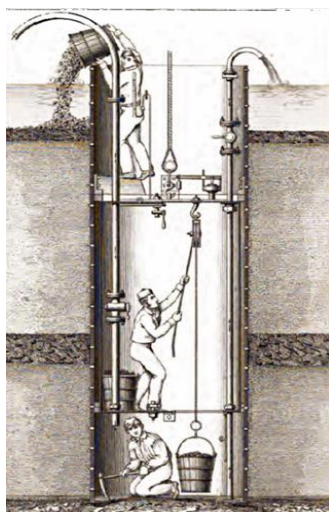


**Figure 1.** Diagram of the first use of the Triger caisson in French mines for coal extraction (Source: *Amédée Burat - Géologie appliquée ou Traité de la recherche et de l'exploitation des Mines*).

These caissons were used all over France during the following years. Triger hired two physicians, Pol and Watelle, to study this mysterious syndrome and the conditions that could lead to it in the different projects where caissons were used. Miners began to report symptoms such as arthralgia, myalgia, pruritus, paralysis, and dyspnea when they returned to the surface and left the caisson. All these symptoms were treated by different symptomatic treatment methods ranging from cold water baths to essential oils. Pol and Watelle correctly attributed the severity of the symptoms to the rate of decompression suffered and postulated recompression for the first time as a possible treatment guideline (Ninokawa and Nordham, 2022).

### **“The bends”: Jaminet and Smith**

The first application of caissons was implemented in mines by Triger but was based on an ingenious solution designed in 1691 for bridge construction (**Fig. 2**) by the French physicist and inventor Denis Papin (1647-1712). Applying the caisson to his original design (**Fig. 3**),

the term “the bends” arises, used as a synonym for the DCS. This designation first emerged in 1868 during the construction of the Eads Bridge in St. Louis, Missouri (**Fig. 4a**), which included underwater work in caissons on the Mississippi River. Workers emerging at the end of their shift adopted a curved position resembling a fashionable Greek female posture called the Grecian Bend (**Fig. 4b**). This position resulted from the joint and abdominal pain they experienced upon returning to the surface (Elliot, 1999).

**Figure 2.** Modern Caisson for bridge construction (Source: *Engineering Discoveries*).

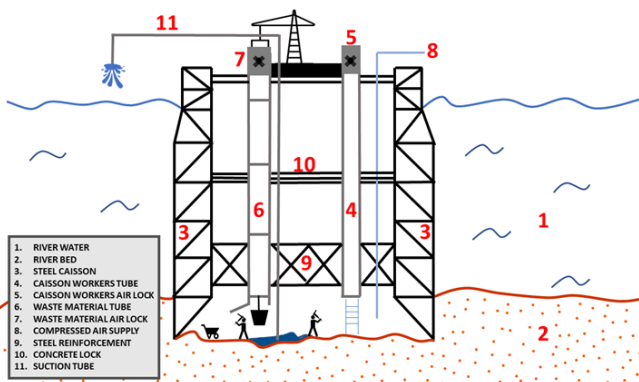
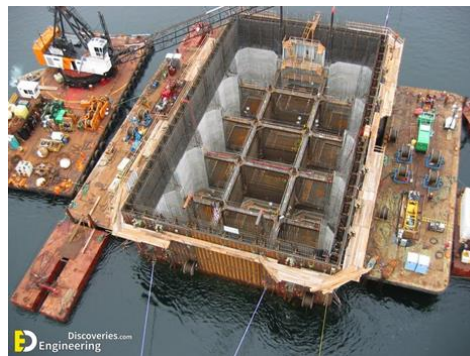


**Figure 3.** Diagram showing the components of a caisson for a bridge construction over a river. The workers of the caisson enter through a locked door (5) that leads to a ladder through a tube (4). At the same time, another conduit (6) is built through which, by means of a pulley, a crane extracts the excavated or waste material via a locked door (7), in addition to a suction tube (11), that returns the extracted water and sand to the river water (1) and bed (2). Compressed air is introduced through a pipe (8) to ensure the workers' breathing. As the caisson deepens, reinforcements (9, 10) are placed between the steel walls of the caisson (3) (Adapted from *Carol Denney*. <https://kshitija.wordpress.com/2006/07/15/caissons/>).

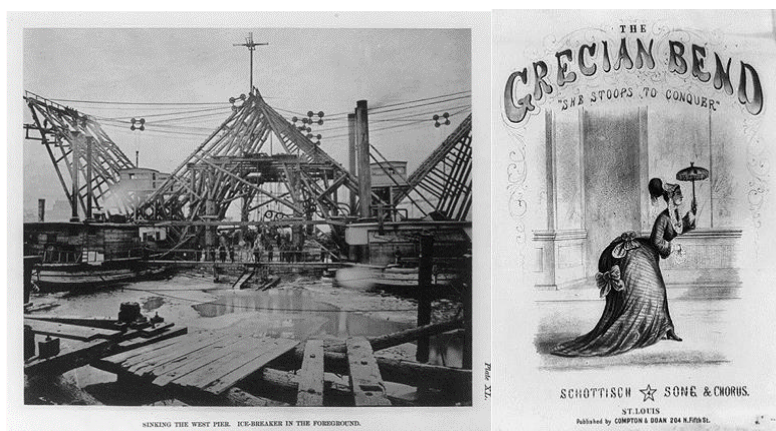


**Figure 4.** From left to right. **a)** Picture of the beginning of the construction of the East Bridge in St. Louis, where DCS began to be described after several worker deaths (Source: *Library of Congress of USA*). **b)** Poster advertisement showing a woman with the Grecian bend posture, similar to the posture observed in bridge caisson workers and from where the synonym the bends for DCS comes from (Source: *Library of Congress of USA*).

Alphonse Jaminet (1825-1890) was the physician in charge of treating the workers when they returned to the surface, creating a field hospital for monitorization, noting that the most affected were those who had worked at greater depths. At the end of the St Louis Bridge project, 25% of the workforce suffered caisson disease, resulting in 13 deaths. Jaminet's findings were purely observational and, even, experimental with himself (Jaminet, 1871). He was the first to postulate standard ratios for compression and decompression, being the first step in today's decompression injuries prevention standards (Ninokawa and Nordham, 2022).

In 1870, the construction project of the Brooklyn Bridge (New York) began, involving working at greater depths, with caissons 3 times larger than those used in the Eads Bridge. Andrew H. Smith (1798-1873) was the physicist in charge of the health of the caisson workers, describing similar symptoms to Jaminet and providing that the time of exposure to compressed air was directly proportional to the severity of the symptoms. Smith was the first to publish the term caisson disease in

a book (Smith, 1873), in addition to describing that worker who died had obesity, a finding that today is supported as a risk factor of DCS.

### Paul Bert

It would not be until 200 years later that the first experimental studies on gas bubbles production after decompression were carried out by the French physiologist Paul Bert (1833-1886) (**Fig. 5a**). Paul Bert described in his book *La Pression Barométrique* (Bert, 1878) all the knowledge he had acquired by performing experiments on dogs, mice and birds subjected to high and low pressures and their scientific significance, explaining the causes of DCS (**Fig. 5b**). Paul Bert is considered the founder of barophysiology.

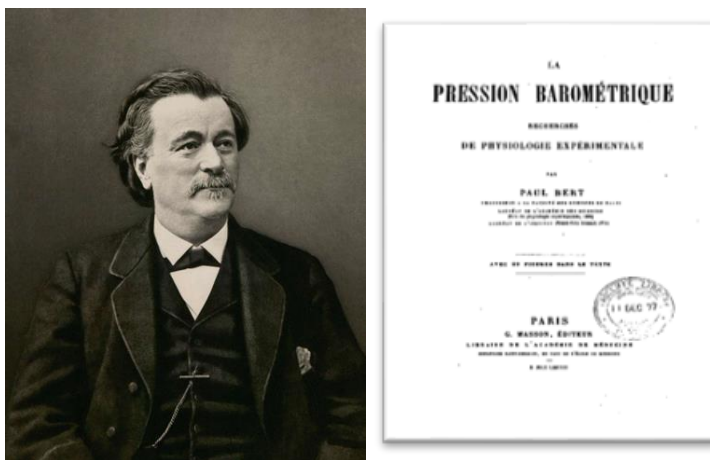


**Figure 5.** From left to right. **a)** Portrait of Paul Bert (Source: *Wikimedia commons*). **b)** Cover of the book "La Pression Barométrique: Recherche de Physiologie Experimentale", a compilation of Bert's considerations in physiology, including his work on scientific experiments with high and low pressures (Source: *Radcliffe Science Library*).

The main points described by Bert in this book were of great importance for physiology. He described, for the first time, the dissociation curves for oxygen and carbon dioxide in blood, and the changes of this curve with temperature. Paul Bert also described how a rapid decompression can lead to mechanical damage, caused by the

expansion of the gas stored in hollow organs such as lungs (swim bladder in fish) or the gastro-intestinal track, or by the formation of gas bubbles from previously dissolved gas in tissues and blood due to changes in pressure. In addition, he established prevention guidelines for decompression accidents through gradual decompression, considering that the more profound the dive, the slower the decompression should be. As for the treatment of DCS, he defined immediate recompression as the only effective treatment for this disease, which could be implemented with the administration of inhaled oxygen (Bert, 1878).

### **John Haldane**

In familiarity with Bert's work and findings on caisson workers, John Scott Haldane (1860-1936), a Scottish physiologist, built a hyperbaric chamber to study caisson disease associated with the Lister Institute of Preventive Medicine and the Royal Navy (**Fig. 6**). In these experiments on animals, Haldane observed that most of the symptoms derived from gas bubbles in the white matter of the nervous system. This finding led him to hypothesize that, this structure was mainly composed of fat, and that there was a relationship between the severity of the disease and the amount of fat in the victims, as Smith had already described. From here arise restrictions for workers who are overweight in the caisson.



**Figure 6:** John Haldane in a hyperbaric chamber (Source: *The Tennessean*).

Haldane created the theory of tissue half-times, that is, the time needed for the slowest tissue to desaturate to half of the partial pressure of its supersaturated state (Haldane, 1908). Based on this theory and the guidelines described by Bert, he established the first decompression tables defining that a worker should decompress to half the pressure at which he has been working and slowly at 10-foot intervals, being the basis of the preventive tables of today (Ninokawa and Nordham, 2022). Haldane was also responsible for implementing the use of canaries inside coal mines to detect harmful gases.

### **Breath-hold divers**

DCS has also been described in breath-hold divers associated with repetitive dives with short surface intervals, as pearl divers or spear fishermen, or single dives at great depths, as diving athletes, both situations causing an accumulation of gases known as supersaturation (Schipke et al., 2006). Humans have been diving with breath-holding since the ancient Greeks who dived in search of sponges, to the current pearl divers, or the Ama, Japanese and Korean women divers who collect shells, pearls, and food (Edmonds et al., 2015).

In the 1960s, the first description of decompression accident in breath-holding divers was noted by Cross (1962), describing an illness called “Taravana”, which means “to fall crazily”, very similar to scuba divers' DCS. This first assumed description of DCS was in pearl divers of Tuamotu Archipelago (French Polynesians islands), who experienced vertigo, nausea, paresis, impaired vision, loss of consciousness, and death, after repeated dives in search of pearls (Cross, 1962). These divers performed an apnea diving pattern characterized by 40 to 60 dives of approximately 2 minutes each and at a depth of 30 meters or more to collect pearls. When they reached the surface they remained in short intervals of approximately 3-4 minutes after which they submerged again, causing a gradual supersaturation (Cross, 1965) (**Fig. 7a**).

With a breath-hold diving pattern very similar to the one described for “Taravana” disease, a group of divers known as the Ama also collect shells and pearls, following a Japanese and Korean tradition of more than 2000 years of existence (Nukada, 1965) (**Fig. 7b**). These divers are usually women who work for more than 20 years, performing two types of dives. The first is called "cachido" and consists of descending to depths of 3 to 10 meters without any assistance. The second is known as "Funado" and involves using weights and ropes to descend and ascend quickly in depths close to 30 meters deep (Lemaitre et al., 2014). This diving pattern is repeated up to 60 times in a single day with very short surface intervals, causing the appearance of neurological symptoms, mainly in the Funado technique (Kohshi et al., 1998). These symptoms are similar to those of “Taravana” disease and are assumed to be decompressive disorders initiated by the formation of gas embolism (Kohshi et al., 2021).



**Figure 7.** From left to right. **a**) Pearl divers reaching the surface with their fishing baskets after an apnea dive (Source: *Bahrain house of Photography*). **b**) An Ama diver during a breath-hold dive in search of pearls (Source: *Yoneo Morita- Argusphoto*).

Freediving competitions started in the 1940s, when Italian spear fishermen began to compete against each other. As it gained followers, this sport began to be divided into different modalities (Edmonds et al., 2015). DCS is unusual for single breath-hold dives as the sum of the accumulated gases is often not enough to generate DCS, although few

cases of this syndrome associated with a single dive have been described, mostly in diving athletes (Fitz-Clarke, 2009). The human world record for depth with breath-holding currently stands at 253 meters in the discipline of no-limit free diving (Guinness World Record, 2012; Checked in July 2023) (**Fig. 8a**). No-limit free diving is the most extreme mode in terms of depth, which consists of sinking by weight to the bottom and, once the desired depth is reached, releasing the weight, and inflating a bag with compressed air to help reach the surface (Edmonds et al., 2015) (**Fig. 8b**).

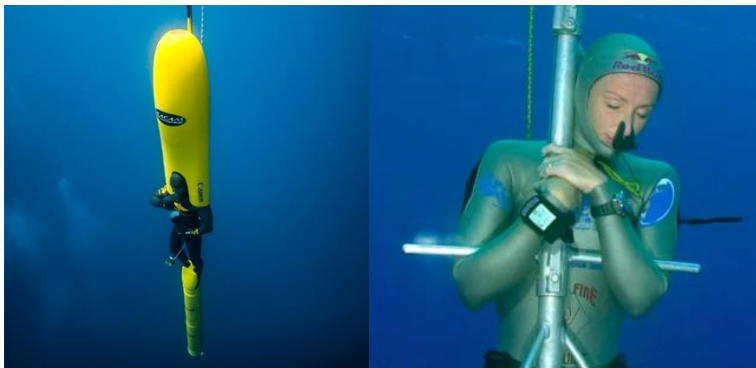


**Figure 8.** From left to right. **a**) The Austrian free diver Herbert Nitsch performing the Guinness depth world record in the no-limits free diving category, helped by a yellow structure that serves in the lower part as a weight for the descent and in the upper part as an air structure for the ascent (Source: <https://www.herbertnitsch.com/freediver>). **b**) Apnea world champion Tanya Streeter performing a weighted dive. She holds the female Guinness record for depth in the no-limits free diving category (160 meters) (Source: <https://www.deeperblue.com/>)

With the introduction of new devices such as fins, wetsuits, weight belts and inflatable bags, it has been possible to reach greater depths with higher risks of DCS episodes (Ferrigno and Lundgren, 2003). Wetsuits help to reach greater depths by maintaining body temperature and reducing the low thermal sensation experienced at depth. Even so, wetsuits near the surface have a positive buoyancy that must be overcome in order to descend, so weight belts are used. In turn, when ascending, these belts will generate more ballast and, to

compensate the effects of these devices, self-inflating bags have been implemented, allowing a faster ascent but leading to increased risk of DCS (Edmonds et al., 2015).

Despite this, research surrounding DCS in this group of divers is limited as it has been poorly described. Unless severe cases, breath-hold divers do not require medical assistance, and cases are rarely reported (Lemaitre et al., 2009).

## **2.3. DECOMPRESSION THEORY**

Scuba divers and breath-hold divers inhale atmospheric gases in which the main component is nitrogen, at a concentration of 78%. The tissue partial pressure of nitrogen will depend on this concentration of nitrogen and the ambient pressure. With the inspired concentration being constant, the partial pressure of inspired nitrogen will be directly proportional to the ambient pressure. On the other hand, the partial pressure of ambient and body gases tends to be in equilibrium (Edmonds et al., 2015). Therefore, as the environmental pressure increases with depth, there is a higher partial pressure of nitrogen in alveoli which favors greater diffusion. This is established first between the alveoli and the blood circulation of the lungs and, secondly, between the systemic blood circulation and the tissues (Tikuissis and Gerth, 2003). Thus, in a healthy lung, the gas assimilated during the gas exchange in the pulmonary alveoli is transferred to the systemic circulation, remaining in solution and, from there, to the organic tissues (Francis, 2002).

### **Nitrogen accumulation and elimination**

The saturation of the tissues with the breathed gases is known as the saturation state, which will depend on two physical properties, their perfusion, and the solubility of the gases in them. Thus, tissues highly

perfused will assimilate gases rapidly being called fast tissues, while slow tissues are poorly perfused tissues, which will assimilate this gas slower (Tikuisis and Gerth, 2003). Since nitrogen is an inert gas that is 6 times more soluble in fat tissues than in blood, the gas balance between blood and tissues will be faster in lipid-rich tissues (e.g., central nervous system and adipose tissue) and slower in lean tissues (Edmonds et al., 2015).

For the study of gas exchange and gas accumulation in tissues, Boycott et al. (1908) proposed to divide the body into parallel compartments corresponding to tissues with the same physical properties (i.e.: blood perfusion and gas solubilities) (**Fig. 9**). At the end of a period of immersion at a given depth, the faster tissues may get saturated and balanced with the bloodstream, while the slower usually don't (Edmonds et al. 2015).

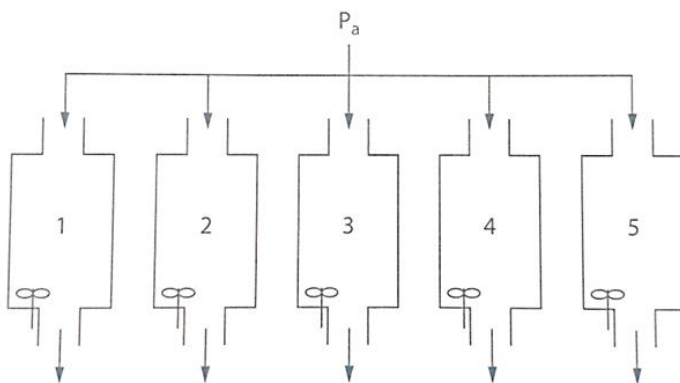


**Figure 9.** Diagram for the concept of parallel compartments simulating tissues with similar properties, mainly perfusion and composition. Compartment 1 is the fastest compartment while compartment 5 the slowest compartment,  $P_a$  is the blood pressure of circulating inert gases (Source: Edmonds et al., 2015).

As divers ascend to the surface, the ambient pressure decreases, causing the alveolar and blood nitrogen pressure to decrease, generating a nitrogen removal gradient. Fast compartments will eliminate nitrogen

rapidly while slower compartments will eliminate nitrogen slowly (**Fig. 10**). If the ascent is rapid, the slow compartments will not be able to equilibrate fast enough, presenting dissolved gas pressures (tension) exceeding the ambient pressure. This condition is known as supersaturation and can cause phase separation of the gases from dissolved to the gaseous state, causing the formation of gas bubbles (Edmonds et al., 2015).

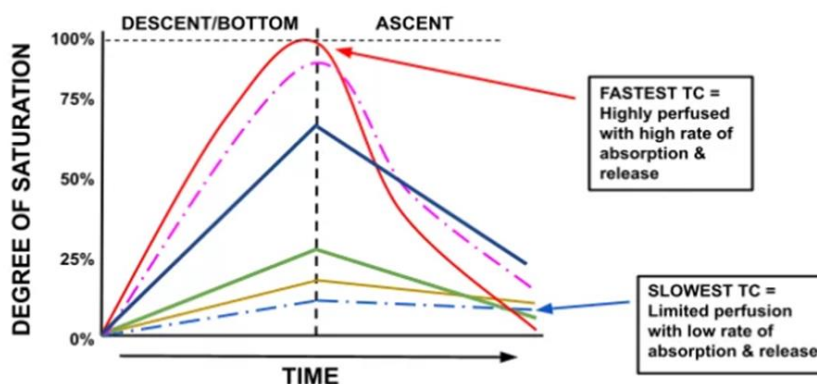


**Figure 10.** Illustration representing the saturation of fast and slow tissues. Fast tissues are the first to saturate on a dive and to desaturate completely after ascent. Meanwhile, slow tissues saturate to a lesser degree but are still off-gassing at the end of the dive. (Source: [www.readydive.com/education](http://www.readydive.com/education)).

In the case of breath-hold divers, DCS is mainly associated with repeated dives with short surface intervals (Schipke et al., 2006), although there are also cases described in single dives, mainly at great depths (Lemaitre et al., 2009). This group of divers has an air supply (nitrogen) limited to the amount of air breathed prior to diving. During immersion, the partial pressure of nitrogen in the organism attempts to reach equilibrium with the ambient pressure, causing the organism to be saturated. As ascent occurs, the partial pressure of nitrogen in tissues and blood begins to be higher than the ambient pressure causing a supersaturation state (Lemaitre et al., 2009). In this situation, dissolved gas may come out of the solution and form intravascular and

extravascular gas bubbles that may be asymptomatic and tolerated by the organism, as they have been described even at shallow depths (Eckenhoff et al., 1990), or caused DCS. Thus, when repetitive dives with short surface intervals occur, the organism is unable to eliminate all the nitrogen from the slower compartments, causing an accumulation phenomenon that ultimately may lead to DCS (Schipke et al., 2006).

### **Origin of gas bubbles**

Although the development of gas bubbles in DCS is not fully understood, several possibilities have been hypothesized, outstanding the growth of gas bubbles from pre-existing micronuclei versus spontaneous or de novo development (Arieli, 2017). In the 1970s, it was proven that spontaneous gas bubble formation in supersaturated pure water only occurred from a pressure reduction of 200 atmospheres absolute (ATA), a process known as cavitation (Gerth and Hemmingsen, 1976; Hemmingsen, 1977). Thus, the theory of pre-existing gas micronuclei is the most accepted and hypothesized over the last 70 years. However, aspects such as nucleation, stabilization, and location of these micronuclei have not yet been proven (Arieli, 2017).

Gas bubble formation can be intra- and/or extra-vascular, the latter being known as autochthonous bubbles. The formation of autochthonous gas bubbles causes structural and microcirculation disruption of the tissue where they are located, varying the damage from less problematic as in adipose tissue to very severe in the spinal cord. The presence of gas bubbles circulating in blood vessels or intravascular bubbles is known as gas embolism (Francis, 2002).

Gas embolism is defined as the circulation of gas within vascular structures. These intravascular gas bubbles lead to obstructive as well as biochemical alterations leading to vascular dysfunction, activation of leukocytes and platelets, among other hematological alterations (Mahon

and Regis, 2014). Besides these gas emboli, the presence of fat embolism has also been described in DCS (Hulman, 1995). The origin of fat embolism in DCS remains unknown, although different hypotheses have been proposed based on the mechanical damage exerted by gas bubbles in bloodstream and tissues (Hulman, 1995; Jones and Neuman, 2003). In this thesis, we will focus on gas embolism.

## **2.4. DECOMPRESSION SICKNESS IN HUMANS**

### **2.4.1. CLINICAL MANIFESTATIONS OF DCS IN HUMANS**

The clinical manifestations of DCS in humans can be classified into two types based on severity. Type I includes musculoskeletal symptoms such as limb pain, skin symptoms, and lymph node swelling. On the other hand, type II is a more severe manifestation of DCS, characterized by neurological, pulmonary, systemic, and inner ear symptoms (Lemaitre et al., 2009). Clinical signs affecting the brain and spinal cord have a rapid and progressive onset, appearing within 30 minutes after reaching the water's surface. Other less specific symptomatology includes headache, anorexia, dizziness, vomiting, confusion, and localized pain, among others (Francis, 2002).

### **2.4.2. RISK FACTORS OF DCS IN HUMANS**

Several factors have been suggested as possible risk factors for DCS, either because they predispose tissues to bubble damage or enhance bubble formation (Lemaitre et al., 2009). They can be classified into predisposing factors, diving-related factors, and post-diving factors, which require more in-depth studies to support them. However, individuality plays a fundamental role. It has been shown that even with the same dive profiles in similar subjects, gas bubble formation differs (Nishi, 1993).

#### **Predisposing factors**

One predisposing factor is body fat, as observed by Smith and later hypothesized by Haldane. Nitrogen is more soluble in lipid tissues than in aqueous tissues, so an organism with more body fat will

accumulate more nitrogen and will be at higher risk of bubble formation (Carturan et al., 1999). This risk factor is the most studied and better supported in the literature, analyzed since the early days of DCS (Mahon and Regis, 2014). As it is associated with obesity, the risk of DCS is susceptible to increase in cases of poor physical condition (Broome et al., 1995).

Another related risk factor would be sex. It is hypothesized that females are more predisposed to DCS because of their relatively higher percentage of body fat (Janssen et al., 2000). However, no variations in DCS prevalence were observed between women and men in a retrospective study of scuba divers (Hagberg and Ornhagen, 2003), and a higher rate of bubble formation has been observed in men with altitude related DCS (Webb et al., 2002). Hence, a conclusive association between sex and DCS has not been demonstrated to date (Mahon and Regis, 2014).

Older divers tend to have more venous gas bubbles than younger divers with similar dive profiles (Eckenhoff et al., 1990). Hence, age has been proposed as a predisposing factor for DCS risk (Carturan et al., 2002).

Patent foramen ovale (PFO) is a defect in the closure of the foramen ovale, a necessary structure in the fetal circulation that causes the passage of blood directly from the right atrium to the left atrium of the heart, preventing pulmonary circulation. At birth, this orifice begins to close, and its persistence causes a right-to-left shunt. It is the most common shunt in humans, being present in almost a quarter of the human population (Hagen et al., 1984). If venous gas embolism occurs in a diver with PFO, blood and gas bubbles can surpass the lungs and enter directly into the arterial circulation through the PFO (i.e., paradoxical gas embolism), causing a pathology similar to an AGE. PFO in association with decompression, is responsible for severe cerebral,

vestibulocochlear, and spinal manifestations (Vann et al., 2011). It has been estimated that the risk of developing severe neurological DCS is 2.5 times more likely in a diver with PFO than without this pathology (Bove, 1998).

DCS has been also associated in cases of dehydration, probably due to the reduction of blood flow and therefore of gas removal; and with previous episodes of DCS (Lemaitre et al., 2009).

### **Diving and post-diving factors**

The dive profile includes time, depth, and ascent speed to the surface. Overall, the more these three parameters increase, the greater the risk of DCS is. In addition, repetitive dives have been associated with increased risk, as well as increased cardiac output (Francis, 2002) and exposure to low temperatures which enhances the solubility of the gases (Gerth et al., 2007).

### **2.4.3. DIAGNOSTIC OF DCS IN HUMANS**

The diagnosis of DCS in humans is based on the presence of symptomatology and confirmation of gas bubbles by imaging techniques. Ultrasound, mainly Doppler ultrasound, is used as a non-invasive method to corroborate the presence and quantity of gas bubbles present in the circulation (Brubakk et al., 1986). The absence of gas bubbles after immersion has been correlated with the absence of clinical symptoms. Similar clinical signs have been associated in divers with various amounts of gas bubbles detected by Doppler (Mahon and Regis, 2014). But there is a correlation between gas bubbles amount and DCS risk (Gardette, 1979; Eckenhoff et al., 1990). Scientific consensus has been reached regarding gas bubbles as the most likely cause of this syndrome. The definitive diagnosis is established by the resolution of gas bubbles and symptoms after hyperbaric treatment (Edmonds et al.,

2015), although some symptoms may persist longer, due to the cytokine cascade (Bigley et al., 2008), or even permanently if irreversible lesions were caused (mainly in the nervous system) (Spira, 1999; Brubakk and Neuman, 2003; Kamtchum Tatuene et al., 2014). Postmortem diagnosis in humans will be explained in the pathology section of this thesis.

#### 2.4.4. TREATMENT OF DCS IN HUMANS

In terms of treatment, recompression and slow decompression in a hyperbaric chamber is the most used treatment (**Fig. 11**). It helps by redissolving the gas in the vascular circulation and tissues and reducing the size of the gas bubbles so they can safely be eliminated through respiration. Bert postulated as early as 1878 the use of oxygen as both prevention and treatment of DCS (Bert, 1878). Since 1960, in addition to recompression in a hyperbaric chamber, oxygen breathing has been added during the procedure, creating a concentration gradient in the lungs and blood vessels that favors the dissolution and elimination of inert gases. In addition, other adjuvant therapies with lidocaine or corticosteroids, among others, have been postulated and are being studied in experimental animal models (Mahon and Regis, 2014).



**Figure 11.** From left to right. Monoplace hyperbaric chamber, where patients with DCS symptomatology are treated, as well as for the treatment of other diseases (Source: *Jirangkul et al., 2021*). Multiplace hyperbaric chamber, where hyperbaric treatment can be performed on several patients at the same time (Source: *Jirangkul et al., 2021*).

## **2.5. DECOMPRESSION SICKNESS IN MARINE ANIMALS**

Both sea turtles and marine mammals have been presumed to be protected from DCS due to their adaptations to the marine environment in which they live. Recent studies demonstrated that sea turtles may suffer from this clinical syndrome on certain occasions (García-Párraga et al., 2014). Cetaceans have also been diagnosed with a decompression-like sickness (DC-like S) following post-mortem studies (Jepson et al., 2003; Fernández et al., 2005).

### **2.5.1. DECOMPRESSION SICKNESS IN SEA TURTLES**

Sea turtles spend almost 90% of their lives in apnea, performing long and deep dives (Lutcavage and Lutz, 1997). The cause described for DCS in these marine animals is bycatch, a conservation problem that causes great deaths of sea turtles and, to a lesser extent, of marine mammals, which are trapped accidentally in large fishing nets and rapidly brought to the surface (Parga et al., 2020).

The adaptations of sea turtles to diving include small and collapsible lungs, the passage of retained air to areas of the lung where gas exchange does not take place and the presence of cartilaginous reinforcements in the airways (Lutcavage et al., 1989). In addition, they also present a muscular sphincter in the pulmonary arteries (White, 1976) and cardiac shunts (Hicks and Wang, 1996), which, in situations of gas embolism, can cause the passage of gas bubbles from the pulmonary area to the systemic circulation (Vann et al., 2011).

### **2.5.1.1. CAUSES OF DCS IN SEA TURTLES**

In some situations, sea turtles may suffer from DCS. This was demonstrated by García-Párraga et al. (2014) in a study conducted on mediterranean sea turtles, being the first report of gas embolism in wild sea turtles. For this study, an active campaign was started with the collaboration of local fishermen to collect live and dead sea turtles accidentally caught in gillnets and trawls. The fishermen provided information on the behavior of the sea turtles during capture and the research team conducted an exhaustive clinical examination of the live animals, including blood tests and imaging techniques. Dead sea turtles were examined by necropsy and histopathology (García-Párraga et al., 2014).

Sea turtles were in good body condition and without apparent traumatic injuries. On reaching the water's surface, those turtles found alive within fishing nets exhibited different behavioral patterns. Some sea turtles presented typical findings of drowning, as abundant fluid on endotracheal intubation and radiological alveolar pattern. Drowning and DCS can be two concurrent causes of death in bycaught sea turtles. Systemic gas embolism on the venous side was observed in several animals. These sea turtles with signs compatible with DCS were examined by computed tomography and different degrees of DCS severity were established (García-Párraga et al., 2014). DCS condition has also been observed in sea turtles outside the Mediterranean Sea (Parga et al., 2020), demonstrating that it is a pathology that can occur worldwide.

Bycatch has been shown to have drastic effects on the physiology and behavior of sea turtles, generating a situation of severe stress. It is hypothesized that DCS in sea turtles may develop by disrupting the response to diving. It has been proposed that particularly the pulmonary artery sphincter in turtles plays an essential role in gas management.

This sphincter constricts during diving causing a pulmonary shunt that limits perfusion and gas exchange in lungs. Therefore, disruption of this diving response mechanism may cause the sphincter opening and promoting the accumulation of nitrogen in the tissues (García-Párraga et al., 2018). When animals are dragged towards the surface, a sudden decompression is generated causing the development of intravascular and extravascular gas bubbles.

It is assumed that the depth, the ascent rate, the immersion time, and the water temperature described as risk factors in humans (Vann et al., 2011) likely influence the severity of DCS in sea turtles (García-Párraga et al., 2014). Fahlman et al. (2017) found a positive correlation between the depth of trawls and severity of DCS. Low water temperature increases nitrogen solubility proportionally. Additionally, sea turtles remain submerged longer and in deeper waters during the coldest periods of the year (Hochscheid et al., 2007). García-Párraga et al. (2014) noted that most bycaught gas embolism cases occurred during the coldest months of the year.

#### **2.5.1.2. CLINICAL MANIFESTATIONS, DIAGNOSTIC AND TREATMENT OF DCS IN SEA TURTLES**

The diagnosis of DCS in sea turtles, as in human medicine, is clinical, based primarily on the symptomatology presented. When sea turtles are found in fishing nets, fishermen report normal, comatose or initially hyperreactive animals. Some of them appear with aspiration of water which is observed on intubation and compatible with drowning as primary cause. Observations of clinical manifestations such as positive buoyancy and erratic swimming when reintroduced have been reported. Neurological signs may be seen progressively until death, which usually occurs within 72 hours post-capture (García-Párraga et al., 2014).

Following observation of symptoms, the diagnosis can be completed through blood tests, with increased hematocrit reported, and imaging studies such as radiology, ultrasound, or computed tomography, where the presence, abundance, and distribution of gas bubbles will be evidenced (García-Párraga et al., 2014, Parga et al., 2020).

Recompression with hyperbaric oxygen has been demonstrated as an effective treatment, similar to human medicine (García-Párraga et al., 2014), resulting in an accurate clinical diagnosis of DCS in sea turtles. Post-mortem examination by means of imaging and necropsy techniques allows the observation of these gas bubbles (García-Párraga et al., 2014; Parga et al., 2020), which will be discussed in the pathology section.

## **2.5.2. DECOMPRESSION-LIKE SICKNESS IN CETACEANS**

Marine mammals returned from land to the marine environment approximately 60 million years ago and had to develop physiological, anatomical, and behavioral adaptations to living in their new habitat (Ponganis et al., 2003). Some of those adaptations promoted specialized diving and were proposed to protect them against the formation of gas bubbles (Piantadosi and Thalmann, 2004).

### **Respiratory system**

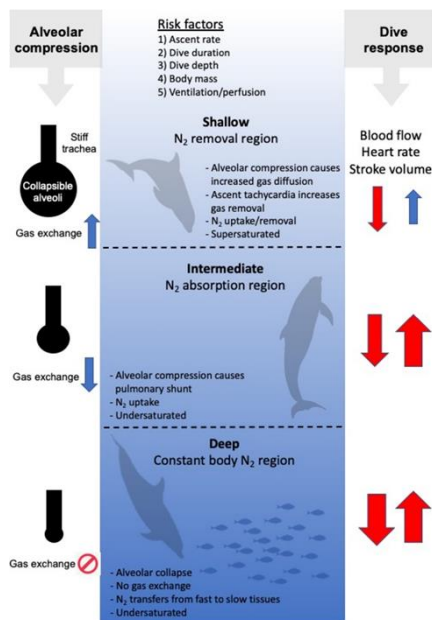
One of the systems most adapted to the marine environment is the respiratory system (Ponganis et al., 2003). Notable features are the flexibility of the chest and the reinforcement of the upper airways, enabling the collapse of the pulmonary alveoli while the upper airways resist the pressure (Fahlman et al., 2015). In this way, the gas is retained in the non-collapsible upper airways during the dive, helping to reduce gas assimilation and the risk of gas embolism (Scholander, 1940;

Fahlman et al., 2021). At the same time, these reinforcements facilitate large tidal volumes with a replacement of 80-90% of lung capacity, resulting in a very efficient gas exchange (Ponganis et al., 2003). Another characteristic unique to cetaceans is the presence of bronchial sphincters. The function of these elastic muscular structures is still under study, probably acting as a valve regulating the flow of air into the alveoli during immersion (Kooyman, 1973).

### Diving response

To conserve the stored oxygen, cetaceans have a very developed dive response (Fig. 12), which consists of apnea, bradycardia, and peripheral vasoconstriction for selective redistribution of blood. Blood perfusion to vital tissues such as the central nervous is maintained, while perfusion to other organs is extremely reduced, reducing the oxygen consumption by those tissues. At the same time, bradycardia allows a decrease both in cardiac output and oxygen consumption (Edmonds et al., 2015).

**Figure 12.** Diagram showing the anatomical and physiological changes that occur in cetaceans in response to diving at different depths (Source: Fahlman et al., 2021).



### 2.5.2.1. HISTORY OF DC-likeS IN CETACEANS

In 1940, Scholander postulated that marine mammals could suffer from DCS due to their repetitive breath-holding dives (Scholander, 1940), although it was not until the early years of the 21st century that the first description of gas bubble lesions in cetaceans was published. This publication in the scientific journal *Nature* (Jepson et al., 2003) and the subsequent publication of the complete pathological study (Fernández et al., 2005), broke an important dogma in the scientific community, raising the possibility that cetaceans do suffer from a form of DCS very similar to that described two centuries ago in caisson workers, named DC-likeS. This first description arises from an atypical mass stranding of beaked whales in temporal and spatial relationship with naval exercises in 2002 in the Canary Islands of Lanzarote and Fuerteventura, involving 14 beaked whales of 3 different species (*Ziphius cavirostris*, *Mesoplodon densirostris* and *Mesoplodon europaeus*).

#### **First description of DC-likeS in cetaceans: beaked whales – military maneuvers**

Simmonds and Lopez-Jurado (1991) noticed in 1991 that mass strandings of beaked whales in the Canary Islands in 1985, 1988 and 1989 were associated in time and space with military naval maneuvers in which medium frequency and high-intensity sonar were used. In 1996 and 2000, this association was corroborated after two other episodes, in Greece (Frantzis, 1998) and Bahamas (Balcomb and Claridge, 2001), respectively.

From the first record in 1874 of beaked whales' mass strandings to 2004, 136 episodes were observed, of which 126 occurred after 1950, coinciding with the implementation of medium-frequency active sonar, known as MFAS, used mainly in international military naval exercises.

Of the mass strandings described after sonar implementation, 37 of them were highly correlated in time and space with training areas or naval bases where sonars were operating (D'Amico et al., 2009).

In 2002, another mass stranding of beaked whales in the Canary Islands was the source of the first description of DC-likeS. Thus, this first cause-effect association in cetaceans was established due to NATO military maneuvers, where several warships and submarines carried out exercises as part of the mission called “Neo-Tapon 2002”. The use of mid-frequency sonar was recorded for 7 hours, stranding 14 beaked whales on the coast of the easternmost islands, the first one 4 hours after the beginning of the maneuvers (Fernández et al., 2005). Even during the attempts to reintroduce the specimens, military ships could be observed several kilometers from the beach (**Fig. 13**). Half of the animals died, and the other half were reintroduced, but within 3 days, the carcasses appeared in nearby locations (Fernández et al., 2005). The lesions presented by the association of sonar and DC-likeS were characterized as acute lesions caused by the formation of gas bubbles in vivo, triggering a systemic gas and fat embolic syndrome (Fernández et al., 2005), as described in cases of “explosive-DCS” in humans (Hulman, 1995).



**Figure 13.** Mass stranding of beaked whales in 2002, in the Canary Islands, showing volunteers trying to reintroduce live specimens into the water (left) and, in the background, ships from the Neo-Tapon2002 naval maneuvers, the causal agents of the strandings (right) (Source: *Cabildo de Fuerteventura*).

With the data supporting this association, in 2004, the European Parliament urged its member states to adopt an anti-sonar moratorium (European Parliament, 2004) until the impact on the marine environment was known. Only the Spanish Government applied this moratorium and limited it to the Canary Islands waters (Daily sessions of the Congress of Deputies, 2004). Since the application of this moratorium to date, no more atypical mass strandings of beaked whales have occurred in the Canary Islands (Fernández et al., 2013). The effectiveness of the application of the European anti-sonar moratorium in Canary Islands waters demonstrated this association since, in other areas, massive strandings of beaked whales continued to occur, such as in Almeria in 2006 (Arbelo et al., 2008) and 2011 (Bernaldo de Quirós et al., 2011b), and Corfu (Greece) in 2011 and 2014 (Bernaldo de Quirós et al., 2019).

#### **Additional findings of DC-likeS in cetaceans: acute dysbaric osteonecrosis (DON) and prey interaction**

In 2004, the association of DC-likeS with DON in sperm whales was described for the first time, hypothesizing that gas embolism is the main cause of the development of this pathology (Moore and Early, 2004). Gas emboli can cause occlusion of the intraosseous microcirculation, leading to this type of avascular necrosis and increasing the risk of bone fractures (Jones and Neuman, 2003). DON in cetaceans was associated with exposure to large environmental pressure changes and was characterized by the presence of multifocal lesions with erosion, ulceration and remodelling of cartilage and bone tissue (Moore and Early, 2004; Rothschild et al., 2005).

DC-likeS has also been described in cases of interaction with prey. Specifically, this interaction was observed in 2 animals in a retrospective study involving 493 stranded cetaceans. Both animals were Risso's dolphins (*Grampus griseus*) which, at different times, were diagnosed with acute lethal DC-likeS following evidence of a recent

struggle to ingest a large squid. Both pathological findings and analysis of gas bubble composition led to the diagnosis (Fernández et al., 2017).

### **Supportive evidence of gas embolism: fishing net entrapment**

The presence of gas embolism has also been described in marine mammals caught in fishing nets, being mainly observed in seals, porpoises, and dolphins (Moore et al., 2009). Since these animals die at depth due to entrapment, the chemical composition of the gas bubbles presented is a clear reflection of the gases accumulated in tissues during diving. Nitrogen was the mayor component of the gas bubbles found in these entrapments, evidencing that marine mammals accumulate this inert gas, and that morphological and physiological adaptations limit this accumulation but do not prevent it (Bernaldo de Quirós et al., 2013).

### **2.5.2.2. RISK FACTORS OF DC-likeS IN CETACEANS**

To understand the incidence of DC-likeS in marine mammals it's necessary to differentiate between deep diving species and shallow diving species since conditions affecting diving, such as breath-holding time, temperature decrease or pressure increase, are critical at greater depths (Kooyman and Ponganis, 1998). Shallow divers are theoretically less at risk of developing DC-likeS due to their diving profiles that involve a low accumulation of dissolved gases (Houser et al., 2001). On the other hand, beaked whales are one of the cetacean families most at risk for DC-likeS due to their characteristic deep and long dives, where gas accumulation is greater. In fact, the depth record in mammals is held by a beaked whale at 2992 meters, performing a dive lasting 137.5 minutes (Schorr et al., 2014). The dive time record in mammals is also set by other beaked whale at 222 minutes (Quick et al., 2020).

### **2.5.2.3. DIAGNOSTIC OF DC-likeS IN CETACEANS**

The diagnosis of DC-likeS in cetaceans, unlike in human medicine and sea turtles, cannot be performed *in vivo*, being pathology the key to the diagnosis in these species. This is done by means of a standard necropsy of the animals, observing gas bubbles and the lesions associated with them, which will be developed in the pathology section of this thesis.

Ultrasound has been used in live cetaceans to detect gas bubbles. With this method, gas bubbles have been observed in kidney and hepatic portal veins of different species of dolphins (Dennison et al., 2011) as well as in the brain of a California sea lion (Van Bonn et al., 2013), but with unknown aetiology. On the other hand, gas bubbles were not observed in dolphins trained to perform repeated dives (Dennison et al., 2011), so it is necessary to further investigate this possibility of *in vivo* diagnosis.

## **2.6. PATHOLOGY OF DECOMPRESSION SICKNESS**

### **2.6.1. DECOMPRESSION PATHOLOGY IN HUMANS**

When a decompression accident leads to death, the forensic study begins with collecting the medical history and diving data. Thanks to the new technologies applied in diving nowadays, dive computers accurately indicate depth, duration, ascent rates, water temperature, gas used from the cylinder, pressure, etc. These computers have valuable data that can indicate inadequate practices or changes in the dive profile (Edmonds et al., 2015).

In case of a suspected case of DCS, post-mortem imaging techniques are always used before autopsy, a procedure that could introduce gas artifact. These techniques include radiography, computed axial tomography or magnetic resonance imaging, which are increasingly common. With these techniques it is possible to quantify the amount of gas and its location, mainly in the blood vessels in DCS (When and Williams, 2009). Even so, these techniques should be evaluated carefully as the presence of gas may also be due to other processes, such as decomposition of the body, post-mortem decompression artifacts or resuscitation-induced gas (Edmonds et al., 2015). For this purpose, gas composition can be analyzed revealing a high concentration of nitrogen and carbon dioxide in cases of gas bubbles produced due to decompression. In contrast, in decomposition, hydrogen as a marker of putrefaction, is found in large quantities (Bajanowski et al., 1998; Bernaldo de Quirós et al., 2012b; Varlet et al., 2015).

External examination of the cadaver may reveal skin lesions that are also reported as clinical manifestations. Frequently associated with

severe lesions is cutis marmorata (**Fig. 14**), a skin lesion characterized by a marbled appearance, with erythematous areas and cyanotic changes, interrupted by pale areas (Edmonds et al., 2015).

### Gross findings

DCS internal lesions during autopsy are related to gas bubbles mainly in blood vessels of vital organs (**Fig. 14**), such as the lung or heart, and tissues with high lipid content, such as subcutaneous tissue or the myelin sheaths of neurons (Saukko and Knight, 2004). In the case of extravascular or autochthonous gas bubbles, hemorrhages (**Fig. 14**), emphysema, and necrosis are sometimes observed associated with these gas bubbles, but their development is usually within hours and may go unnoticed (Edmonds et al., 2015). Severe congestion of blood vessels of organs such as the liver, spleen, lung, or kidneys are other macroscopic findings found in DCS autopsies (Kitano and Hayashi, 1981). The most affected organ is usually the lung, where pulmonary interstitial emphysema may be denoted in gross examination. In this tissue, also edema and hemorrhages can be observed (Saukko and Knight, 2004). Pathological gross findings are confirmed microscopically (Saukko and Knight, 2004).



**Figure 14.** From left to right. Cutis marmorata (Source: *Germonpre et al., 2015*). Hemorrhages in epicardial adipose tissue of the heart (Source: *Ninomiya et al., 2013*). Gas bubbles circulating within vessels of the circle of Willis, in the base of brain (Source: *Wheen and Williams, 2009*).

### **Microscopic findings**

Microscopically, the presence of unstained intravascular oval spaces between blood components in blood vessels consisting of gas bubbles is the most common finding (Wheen and Williams, 2009). Microscopic gas bubbles in pulmonary, cerebral, subcutaneous, coronary, and mesenteric vessels, as well as dilatation of the right atrium, has been described as the most frequent locations of gas embolism (Wheen and Williams, 2009). Microscopic lesions are associated with severe circulatory disturbances caused by these gas bubbles, such as congestion, edema and hemorrhages in the liver, spleen, lungs, kidneys, and other visceral organs (Kitano and Hayashi, 1981).

The histological changes seen in the central nervous system are mainly in the spinal cord (Caruso, 2003) due to the high proportion of lipids, which confers the myelin that surrounds the axons of the white matter of this structure, and the low vascular flow, being already raised by Haldane in the 1900s and later hypothesized by other studies (Francis and Mitchell, 2003). Hemorrhages and infarcts are seen in the spinal cord (Edmonds et al., 2015), and, microscopically, ring-shaped hemorrhages are seen around the affected capillaries (Saukko and Knight, 2004).

## **2.6.2. DECOMPRESSION PATHOLOGY IN MARINE ANIMALS**

### **Decompression pathology in sea turtles**

In sea turtles the approximation to the dive history in humans can be inferred from gillnet and trawl data. These data can be obtained opportunistically from those provided by fishing boats in terms of average time and depth deployment of gear nets (Fahlman et al., 2017).

In necropsies performed on sea turtles diagnosed with DCS, gas bubbles were observed in the right atrium and large blood vessels (**Fig. 15**). Spleen and lung emphysema, as well as congestion of most organs were relevant macroscopic findings (García-Párraga et al., 2014), similarly to humans. Histologically, multisystemic congestion and hemorrhages, perivascular edema, as well as intravascular gas bubbles in vital organs were also observed. Moreover, other microscopic lesions described in sea turtles were myocardial necrosis with myocyte degeneration, alveolar edema and hepatic degeneration (García-Párraga et al., 2014).

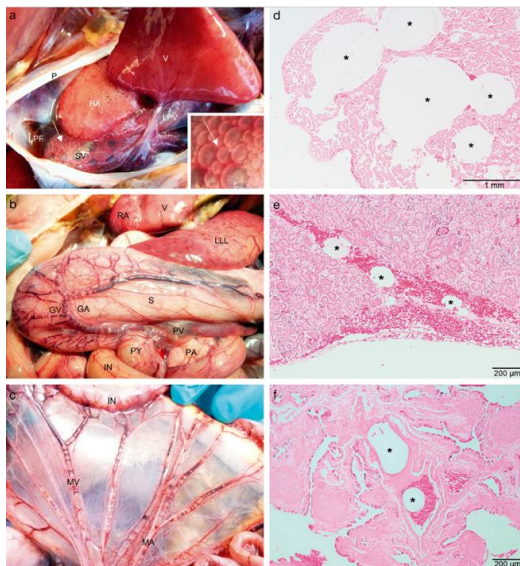


**Figure 15.** a) Macroscopic gas bubbles in the heart, specifically in the venous sinus and right atrium. b) Congestion and macroscopic gas bubbles in the gastric vasculature. c) Mesenteric blood vessels with large gas bubbles among the circulating blood. d) Confirmed microscopic gas bubbles in the right atrium of the heart, e) blood vessel from kidney, f) and lung (Source: García-Párraga et al., 2014).

### Decompression pathology in cetaceans

In contrast to humans and sea turtles, pathological findings in cetaceans are the key to diagnosis due to the clinical limitations and the impossibility of introducing large animals into a hyperbaric chamber. Necropsies must be performed promptly in cetaceans as the time elapsed since death is usually unknown and putrefaction can mask the gas bubbles previously formed by decompression (Bernaldo de Quirós et al., 2012a). Besides, cetaceans possess the blubber, an insulating layer of

adipose tissue that increases the internal temperature of the organism and accelerates the putrefaction process (IUSA field observation).

If in sea turtles the recent dive history may be inferred from gillnet and trawl data, in cetaceans it could be inferred from the stomach content. Undigested food remains in their stomachs would be indicative of recent feeding, and the distribution of the prey in the water columns, would indicate the range of depths at which the animals have been feeding (Bernaldo de Quirós et al., 2019). Generally, these animals are in good body condition with stomachs full of fresh food (Bernaldo de Quirós et al., 2019).

In cetaceans, due to logistical limitations, imaging techniques are rarely an option. Therefore, Bernaldo de Quirós et al. (2012a) developed an index method known as gas score and conducted the first study on the prevalence, distribution, composition, and amount of gas in stranded cetaceans with different decomposition status. Gas score consists of giving scores from I to VI for intravascular gas and I to III for extravascular gas, based on the amount of macroscopic gas observed in determined locations (Bernaldo de Quirós, 2011a) (**Fig. 16**). Consequently, each animal is given a total gas score, obtained from the sum of all the scores obtained, which allows for comparison.

Gas score index for intravenous bubbles.	
Gas score	Definition
0	<b>Absence of gas bubbles</b> within venous vessels (Fig. 1a, d, g).
I	<b>Occasional small bubble</b> found by carefully screening of venous vessels (Fig. 1b).
II	<b>Few bubbles:</b> Gas bubbles are more easily found but a careful screening of different venous vessels and sections of the veins is also required. The quantity of gas bubbles is easy to count. In addition, small "discontinuities of blood" can be present. These discontinuities of blood are small sections of veins showing absence of red cells and associated haemoglobin but with clear liquid instead, presumably plasma from which the red cells have retracted. There is no evidence of gas in these sections, and the veins show different grades of collapse.
III	<b>Few bubbles but larger discontinuities of blood.</b>
IV	<b>Moderate presence of gas bubbles</b> within a specific vein (Fig. 1h). The presence of gas bubbles is obvious at this score, and a careful screening for localized gas bubbles is no longer necessary. Counting gas bubbles would be a tedious but possible task.
V	<b>Abundant presence of gas bubbles</b> (Fig. 1i): many gas bubbles of different volumes would be present within the same vein making quantification of bubbles very difficult, if not impossible.
VI	<b>Complete sections of vessels filled with gas</b> (Fig. 1c, e, f). This occurs by the coalescence of gas bubbles. Quantification of bubbles is no longer possible.

Gas score index for extravascular gas underneath the organs' capsules and in adipose tissues.	
Gas score	Definition
0	<b>Absence of gas.</b>
I	<b>Scarce presence of gas:</b> only in one organ or anatomic region.
II	<b>Moderate presence of gas:</b> affecting two or three organs or anatomic regions.
III	<b>Abundant presence of gas:</b> affecting many different organs. Systemic.

**Figure 16.** The gas score index is a semiquantitative method for grading the abundance of intravascular (left) and extravascular (right) gas bubbles (Source: *Bernaldo de Quirós et al., 2016a*)

With this classification, it was observed that the amount of gas in deep diving cetaceans was greater than in shallow diving, as in the case of beaked whales (Bernaldo de Quirós et al., 2012a). In the retrospective study describing Risso's dolphins diagnosed with DC-likeS after an interaction with prey, the gas score obtained was clearly higher in these two specimens compared to animals of the same species and same decomposition status (Fernández et al., 2017), demonstrating that the gas score method is a useful tool for the diagnosis of DC-likeS. Gas score is a complementary and important tool for the diagnosis of gas-decompression pathology (Bernaldo de Quirós et al., 2016a).

A methodology of in situ sampling, storage and transport was conceived to collect samples from cetaceans stranded in areas that were difficult to access requiring further storage and transportation to the laboratory for further analysis (Bernaldo de Quirós et al., 2011b). The results of gas bubble composition in cetaceans are consistent with those described in experimental animals and humans (Bernaldo de Quirós et al., 2013). Both gas score and gas bubble composition are two tools that should be used in fresh animals or performed as soon as possible to maintain their diagnostic utility in cases of DC-likeS (Bernaldo de Quirós et al., 2013).

If in sea turtles the recent dive history may be inferred from gillnet and trawl data, in cetaceans it could be inferred from the stomach content. Undigested food remains in their stomachs would be indicative of recent feeding, and the distribution of the prey in the water columns, would indicate the range of depths at which the animals have been feeding (Bernaldo de Quirós et al., 2019).

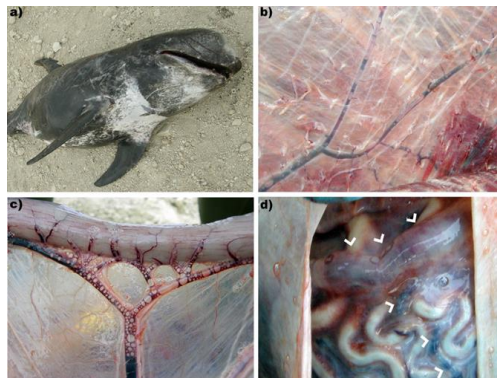
Bernaldo de Quirós et al. (2019) analyzed 6 mass strandings of beaked whales' events in different territories (Canary Islands 2002 and 2004; Almería 2006 and 2011; and Greece 2011 and 2014), describing and summarising the commonalities of DC-likeS in these events. The

main findings were abundant gas bubbles distributed in veins throughout the organism, as well as multi-organ congestion and hemorrhages, mainly in tissues rich in lipids such as the spinal cord, central nervous system, coronary or renal fat was (Bernaldo de Quirós et al., 2019). These results are similar to those described in the pathology of DCS in humans (Edmonds et al., 2015).

As in humans and sea turtles, decompressive pathology in cetaceans is mainly characterized by macroscopic and microscopic, intravascular and extravascular gas bubbles, and associated gas-bubble lesions (Fernandez et al., 2005; Fernandez et al., 2017). Hemorrhages are present in different tissues, highlighting pulmonary pleura, renal parenchyma, spinal cord, and subarachnoid space of the CNS in these animals (Fernandez et al., 2005), similarly to DCS findings in humans.

Other findings in cetaceans with DC-likeS include pulmonary and lymph node emphysema (Fernández et al., 2012), subblubber and intestinal serosal edema (Jepson et al., 2005), multifocal petechiae in acoustic fat and melon, and cavitary lesions in liver and kidney (Jepson et al., 2005).

**Figure 17.** **a)** Dead stranded Risso's dolphin after interaction with prey. **b)** Presence of intravascular gas bubbles in subcutaneous veins. **c)** Mesenteric veins with gas bubbles, some of them coalescing. **d)** Presence of coronary veins with gas bubbles that completely distend the blood vessels (arrowheads), with few amounts of blood inside. (Source: *Fernández et al., 2017*).



Microscopically associated with intravascular gas bubbles (**Fig. 18**), congestion, edema, and hemorrhages can also be seen perivascularly (Fernandez et al., 2017). Multiorgan congestion, atelectatic areas near to the pulmonary emphysematous foci and diffuse pulmonary and spinal cord edema were also observed microscopically (Fernández et al., 2017). In association with cavitary lesions, renal and hepatocellular necrosis is observed, together with the formation of fibrin thrombi (Jepson et al., 2005).

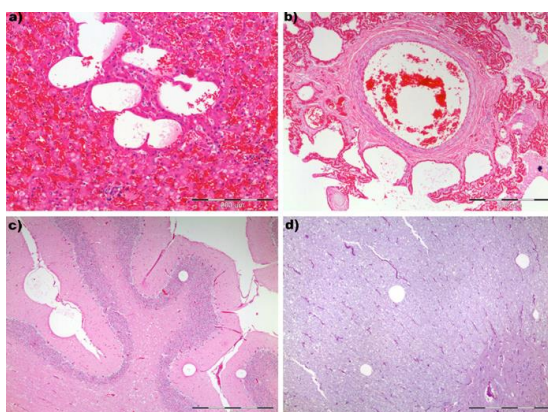


**Figure 18.** Presence of unstained circular spaces found between erythrocytes compatible with microscopic gas bubbles in **a)** liver, **b)** lung, **c)** cerebellum, and **d)** in the white matter of the spinal cord (Source: *Fernández et al., 2017*)

### 2.6.3. ENDOTHELIAL DAMAGE AND ASSOCIATED BIOMARKERS

The pathogenesis of DCS is associated mainly with the presence of circulating gas bubbles in blood (Levin et al., 1981; Huang et al., 2003; Pontier et al., 2008; Brubakk and Møllerløyken, 2009; Zhang et al., 2016; Zhang et al., 2017a). Endothelial cells are the first cell layer to enter in contact with intravascular gas bubbles, as they line the inner aspect of blood vessels. These gas bubbles may induce endothelial proinflammatory and prothrombotic phenotypes (Su et al., 2004). Endothelial function is reduced in divers after a single dive, while dysfunction appears with repetitive dives (Brubakk et al., 2005; Obad et al., 2010). The impairment of endothelial function is positively

correlated with the presence of gas bubbles (Levin et al., 1981; Zhang et al., 2016), and may continue several days after decompression (Obad et al., 2007). Some studies suggest that endothelial damage is primarily due to direct contact with gas bubbles, causing endothelial cells to express different biomarkers and reactions in response to this stress or injury (Su et al., 2004; Zhang et al., 2016). In contrast, others propose an alternative to direct damage mediated by secondary molecules such as reactive oxygen species (Madden and Laden, 2009; Wang et al., 2015a).

Endothelial cells are a source of vasoactive substances such as nitric oxide (NO), a relaxing factor responsible of vasodilation (Nossum et al., 2002), a function that is compromised when endothelial damage occurs (Wang et al., 2015a). NO maintains silenced cellular processes such as inflammation, cell proliferation, and thrombosis (Deanfield et al., 2007). When NO synthesis or activation is inhibited, gas bubble formation is increased (Wisløff et al., 2003), and when NO-releasing substances are administered, bubble formation is decreased (Wisløff et al., 2004). Thus, delving into endothelial alterations provides an important target for the understanding and prevention of DCS (Fismen et al., 2012).

### **2.6.3.1. Biomarkers of cellular damage**

Endothelial alterations and cellular damage can be studied by the quantification of biomarkers of are expressed in response to stress or damage (Su et al., 2014). For our study, aiming at obtaining translational results, these biomarkers should meet the following (1) being produced by endothelial cells, (2) being easily accessible in blood samples, tissues or cell cultures, (3) being indicators of endothelial activity, (4) being well conserved phylogenetically, and (5) having been correlated with decompressive stress. Among the biomarkers that follow these criteria

are heat shock proteins 70 and 90 (HSP70, HSP90), intercellular adhesion molecule-1 (ICAM-1) and endothelin-1 (ET-1).

### **Heat shock proteins 70 and 90 (HSP70, HSP90)**

Heat shock proteins (HSPs) are a superfamily of proteins present in all cellular organisms and highly conserved between species (Schlesinger, 1990). Their main role in physiological conditions is cellular proteostasis (Zininga et al., 2018) focusing on the folding of newly formed proteins, protein trafficking, and protein assembly, among others (Radons, 2016). They were first described in 1962 by Ritossa, based on their increased synthesis in a house fly (*Drosophila* spp.) subjected to heat stress (Ritossa, 1962), from which their name derives. Later, it was observed that they responded to other cellular stresses such as hyperoxia, hypoxia, nutrient deprivation, or exercise (Lindquist and Craig, 1988; Kregel, 2002). They receive different denominations according to their molecular weight, being HSP70 and HSP90 among the most abundant (Mayer and Bukau, 2005) and accounting for 2-5% of total proteins in some cells (Finka et al., 2015).

HSP90 participates in cell cycle control and regulates hormones and client proteins, while HSP70 participates in cellular transduction signaling, apoptosis (Macario and Conway de Macario, 2007), assembly of multiprotein complexes or binding to nascent polypeptides before their release from the ribosome (Radons, 2016). HSP90 is the most abundant HSP in cytosol of unstressed cells (Miller and Fort, 2018) and HSP70 is the most studied in eukaryotic cells (Tavaria et al., 1996). In a wide range of pathologies, HSPs expression is increased, producing a cytoprotective and immunomodulatory effect (Radons, 2016), attenuating tissue injuries (Morimoto, 1993). Hence, they are used as biomarkers of cellular damage (Zininga et al., 2018).

Several studies have proven that HSP70 is a reliable marker for the study of different cellular stresses (Matsuo et al., 2000; Szyller et al., 2022). The occurrence of DCS has also been associated with elevated expression of HSP70 in rats at levels very similar to the expression under heat stress (Huang et al., 2003), mainly observed in lung, liver, and heart of rabbits subjected to compression/decompression (Su et al., 2004). Few studies on the alteration of HSP90 related to decompressive stress have been carried out, with results differing from each other (Szyller et al., 2022).

### **Intercellular adhesion molecule 1 (ICAM-1)**

Cell adhesion molecules (CAM) are a family of transmembrane proteins involved in intercellular junctions or cells with the extracellular matrix (Bigley et al., 2008). This superfamily contains several family members, as intercellular adhesion molecules (ICAMs) or vascular cell adhesion molecules (VCAMs) (Henninger et al., 1997). Interaction between cells is mediated by the family of ICAMs. The CAM most most widely known is ICAM-1 (Anbarasan et al., 2015).

ICAM-1 is expressed in the membrane of several cell types, including endothelial cells, at low concentrations under physiological conditions (Hubbard and Rothlein, 2000). This transmembrane protein serves as a receptor for leukocytes, causing them to bind to endothelial cells and transmigrate to different tissues (Van de Stolpe & Van der Saag, 1996). Besides inflammatory cell trafficking, ICAM-1 also plays an important role in antigen presentation and signal transduction within the cell (Mukhopadhyay et al., 2016).

In response to damage or inflammation, the prothrombotic phenotype of endothelium induces the expression of ICAM-1, to facilitate this migration of immune system cells (Anbarasan et al., 2015). This type of CAM has been considered as a sensitive biomarker

reflecting direct endothelial damage (Zhang et al., 2016) and, as an endothelial disruptor. DCS causes an increase in the levels of inflammatory mediators such as cytokines or CAM (Zhang et al., 2017a). Increased expression of ICAM-1 was observed by immunohistochemistry techniques in the lungs and brains of rats after decompression (Bigley et al., 2008), remaining dysregulated for several days. It has been observed that ICAM-1 have its highest peak expression in blood serum at 24 hours post-decompression, remaining at similar values beyond 72 hours (Zhang et al., 2016).

### **Endothelin-1 (ET-1)**

Endothelins are a family of potent vasoconstrictor peptides, with three known isoforms ET-1, ET-2, and ET-3 (Inoue et al., 1989). ET-1 is the main contraction factor generated by the endothelium (Viridis et al., 2010) and the most potent vasoconstrictor factor known (Yanagisawa et al., 1988). ET-1 acts as an antagonist of the vasodilator function of NO (Boulanger and Lüscher, 1990) and are also involved in the stimulation of cardiac and smooth muscles contraction, regulation of vasoactive substances or stimulation of secretion by tissues such as kidneys or adrenals, among others (Watson and Arkininstall, 1994). Besides endothelial cells as major producers of ET-1, this substance is also produced by cardiomyocytes, neurons, Kupffer cells or renal medulla cells (Piechota et al., 2010).

ET-1 has been considered to act as a stress response, and its expression is particularly associated with different cardiac, vascular, and renal conditions (Schiffrin, 1999). When endothelial dysfunction occurs, NO bioavailability decreases causing a relative increase in ET-1 expression, release, and activity (Alabadí et al., 1997). This imbalance of vasodilator and vasoconstrictor factors contributes to hemodynamic disorders (Marasciulo et al., 2006).

Due to endothelial dysfunction generated by gas embolism, Zhang et al. (2017a) postulated that the measurement of ET-1 in blood serum could be of value as a biomarker of decompressive stress. In this study, the time course of the half elevation of ET-1 expression post-decompression ranged from 2 to 60 hours in blood serum (Zhang et al., 2017a). ET-1 has been postulated as the most sensitive biomarker for DCS, showing a positive correlation with the amount of gas bubbles (Zhang et al., 2016).

## **2.7. EXPERIMENTAL MODELS OF DECOMPRESSION SICKNESS**

Experimental animal models have been used since the early days of the discovery of DCS, from the use of a snake by Boyle to the trials with different animal species that led to Bert's findings or the creation of a hyperbaric chamber for experimental animal studies by Haldane. Although these studies were carried out more than a century ago, together with observational findings, they have laid the foundations for DCS and provided most of the information known about this disease (Ninokawa and Nordham, 2022). In addition, the advances in hyperbaric medicine of the last century have allowed the creation of increasingly accurate dive tables for the prevention of DCS and, through the experimental animal models, other essential aspects such as the therapeutic approach or pathophysiology have been investigated to deepen the knowledge of this syndrome.

Animal models are performed in different species, small rodents being the group of animals most used for the study of DCS, especially rats and rabbits, due to their availability and manageability. Other species used to a lesser extent to study this syndrome have been swine (Broome and Dick, 1998; Buttolph et al., 1998; Reuter et al., 2000; Møllerløkken et al., 2006; Laurent et al., 2013), sheep (Atkins et al., 1988; Ball et al., 1999; Cole et al., 2006), dogs (Clay, 1963; Levin et al., 1981; Francis et al., 1988), guinea pigs (Gersh et al., 1944; Eggleton et al., 1945; Brown et al., 1978), mice (Lever et al., 1966; Blatteau et al., 2012) and monkeys (Eggleton et al., 1945).

Experimental animal studies on DCS are developed by introducing anesthetized animals into hyperbaric chambers where different immersion profiles are simulated through compression and decompression protocols. These protocols vary according to the study

being performed but, in broad terms, typically involve compressions of between 6 to 9 atmospheres absolute, holding times of between 45 to 90 minutes and rapid decompressions of between 3 to 9 minutes. These simulated dive profiles result in DCS and are mainly carried out in fields such as diagnosis, risk factors, pathophysiology, gene expression and treatment/prevention.

### **2.7.1. EXPERIMENTAL MODELS OF DCS: TREATMENT**

The treatment used to eliminate or reduce the number of bubbles developed in DCS is mainly the addition of hyperbaric oxygen during recompression in the hyperbaric chamber, as postulated by Bert and implemented in humans since the 1960s. In recent decades, experimental studies have continued to investigate hyperbaric oxygen treatment (Broome and Dick, 1998; Geng et al., 2015) as well as normobaric oxygen administration (Arieli et al., 2010) or prevention by hyperbaric oxygen as a pretreatment (Arieli et al., 2009).

Other treatments have been proved to reduce severity or eliminate the clinical signs of DCS associated with the damage presumably caused by gas bubbles, such as the administration of endothelial protective drugs as simvastatin (Zhang et al., 2015), escin (Zhang et al., 2017b) or antioxidants (Obad et al., 2007). Treatment with antiplatelet drugs as clopidogrel (Bao et al., 2015) or abciximab (Lambrechts et al., 2015), hydrogen-rich saline (Ni et al., 2011), calcium channel blockers such as BTP2 (Tang et al., 2020), antidepressants such as fluoxetine (Blatteau et al., 2012), pulmonary surfactant aerolization (Yu et al., 2020) or administration of nitric oxide donors (Wisløff et al., 2004; Møllerløkken et al., 2006) appear to reduce DCS severity.

### **2.7.2. EXPERIMENTAL MODELS OF DCS: DIAGNOSTIC AND RISK FACTORS**

Other studies have increased the knowledge of DCS using diagnostic tools such as computed tomography (Reuter et al., 2000; Cole et al., 2006; Laurent et al., 2013), creating models that differentiate DCS from putrefaction by the onset time of bubbles. Following this line, Bernaldo de Quirós et al. (2012b) demonstrated by analyzing gas composition that, within 27 hours postmortem, gas bubbles found in animals with DCS are mainly composed of nitrogen rather than hydrogen, a marker of putrefaction. These studies are significant because of the controversy that the decomposition process causes gas bubbles that can mask those already formed by DCS. In addition, a simple method applicable in necropsies has also been established, known as gas score, which allows differentiating the gas produced by both processes (Bernaldo de Quirós et al., 2016a).

Other studies focused on diagnosis have shown that the presence of high amounts of gas bubbles in postmortem studies correlates with the amount previously observed with ultrasound (Bernaldo de Quirós et al., 2016b) and computed tomography (Cole et al., 2006). Other animal models have tested the application of new methods complementary to DCS diagnoses, such as gravimetric methods (Hjelde et al., 2002) or behavioral tests (Buzzacott et al., 2014).

Despite many risk factors associated with DCS, some studies show contradictory data, and it is necessary to investigate them in greater depth. The amount of fat associated with overweight is one of the most accepted and proven risk factors (Ball et al., 1999), along with advanced age (Buzzacott et al., 2016). Other risk factors that have been studied are previous treatments such as sildenafil, a potent vasodilator used mainly for male impotence, which causes greater severity of DCS (Blatteau et al., 2013); or the performance of aerobic exercise, which

protects against DCS (Wisløff and Brubakk, 2001; Wisløff et al., 2004). It has also been shown by an animal model in rats that circadian rhythm influences the onset of DCS, being a factor to be considered in underwater work (Butler et al., 2010).

### **2.7.3. EXPERIMENTAL MODELS OF DCS: PATHOLOGY**

Most of these studies focused on the study of a single system or organ. L'Abbate et al. (2010) focused their study on the liver of rats with DCS, demonstrating that gas embolism could be observed in this organ through the portal system and extensively after several hours post-decompression. Furthermore, it raised the need to clinically attend to this organ, which is usually conceived with minor importance in the pathophysiology of DCS (L'Abbate et al., 2010). Other studies have focused their animal models on describing the alterations observed in the respiratory system of sheep with DCS such as pulmonary edema and pleural effusion (Atkins et al., 1988) or in the skin describing cutaneous vascular congestion in pigs after decompression (Buttolph et al., 1988), findings that contrast with the pathology described in humans.

Thus, animal models have been established by studying the macroscopic presence of gas bubbles in the organism (**Fig. 19**) such as Lever et al. (1966) who studied the onset time of bubbles in mice, or Gersh et al. (1944) who described in guinea pigs the presence of extravascular gas bubbles in fat-rich tissues while intravascular bubbles, despite being observed in all organs, appear more numerous in blood vessels of fat-rich tissues. Eggleton et al. (1945) established different animal models to study DCS, describing that guineapigs are more susceptible to decompression than rats or rabbits or that most animals' dead by decompression have systemic formation of gas bubbles in blood. Shim et al. (1967) performed a compression-decompression

protocol in rabbits where they observed macroscopic gas embolism and extravascular gas in the animals dead by the protocol.

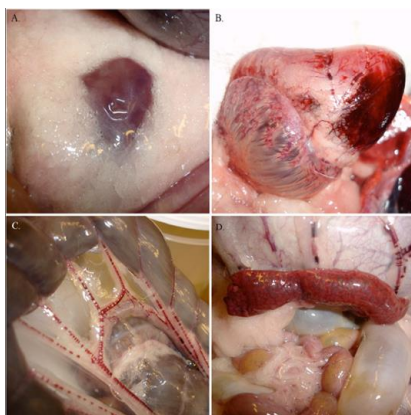


**Figure 19.** Macroscopic appearance of experimental rabbits subjected to rapid decompression. **A)** Presence of emphysema of the abdominal adipose tissue. **B)** Coronary veins with presence of gas bubbles, right atrium gas-distended and presence of apical hemorrhage in the heart. **C)** Mesenteric veins with abundant amount of gas bubbles among the circulating blood. **D)** Emphysematous spleen and gastric veins with gas bubbles. (Source: *Bernaldo de Quirós et al., 2016a*)

Experimental models with histopathological studies are few. Clay (1963) carried out a complete histopathological study of DCS in dogs. He reported pathological findings similar to those previously described, such as systemic intravascular bubbles, pulmonary congestion and edema, extravascular gas bubbles in sections of the spleen and spinal cord, among others. In addition, he analyzed by histology the bone marrow of femurs, observing gas bubbles that disrupted the structure (Clay, 1963). Francis et al. (1988) studied how extravascular gas bubbles affected the spinal cord in dogs. He described intramyelinal structures, compressing the rest of the tissue and without affecting the blood vessels. There is an absence of full pathological studies in animal models that provides a global perspective of DCS.

## **2.8. GAS BUBBLE DISEASE AS A MODEL OF DECOMPRESSION SICKNESS**

### **2.8.1. DEFINITION OF GBD**

Gas bubble disease (GBD) is a condition described in aquatic species, triggered by an excess of total dissolved gases (TDG) in the water, a process known as water supersaturation. Exposure to this water leads to the formation of systemic gas bubbles, both intravascular and extravascular (D'Aoust and Smith, 1974). This disease is widely described in freshwater and saltwater fish (Bouck et al., 1976; Weitkamp and Katz, 1980), but also been observed in other aquatic vertebrates (Tsai et al., 2017) and invertebrates (Goldberg, 1978; Ross et al., 2017).

Given the similarities in terms of the pathophysiology triggered by these gas bubbles and DCS, particularly gas embolism, several authors have postulated the usefulness of a fish model of GBD for the study of DCS (D'Aoust and Smith, 1974; Marking, 1987; Speare, 2010; Machova et al., 2017). Since the 1970s, there has been an increased interest in the study of this disease as a model of DCS, and, secondarily, to increase the knowledge about GBD, which has raised in frequency due to human activities (Speare, 2010).

#### **Total dissolved gases in water**

The most relevant atmospheric gases in percentage are nitrogen (78.08%), oxygen (20.95%), and argon (0.93%). The other relevant atmospheric gases present (the remaining 0.04%) are carbon dioxide, neon, and helium (Harvey, 1975). The solubility of atmospheric gases in water depends on their partial pressure in the atmosphere and will be affected mainly by two factors related to water, such as hydrostatic pressure and temperature. An increase in hydrostatic pressure increases solubility of atmospheric gases and, inversely, increased water

temperature decreases their solubility (Speare, 2010). The pressure of the gases dissolved in the water tends to equilibrate with the atmospheric pressure. Considering at sea level there is 1 atmosphere of pressure (760 mmHg), the TDG value for saturated water will be approximately this value. In practice, it is assumed that 760 mmHg of TDG is 100% TDG saturation in water (Marking, 1987) and TDG supersaturation occurs above these levels. Initially it was postulated that nitrogen was the cause of GBD, but Weitkamp and Katz (1980) concluded that TDG was a better indicator to determine the potential of this disease.

### **Water supersaturation in natural conditions**

Supersaturation of water occurs under natural conditions as in groundwater. Aquifers are subjected to different pressures and temperatures (Marking, 1987). The pressure exerted on these groundwaters causes gases to be more soluble in them. When this water rises to the surface and the pressure decreases or temperatures increases, supersaturated water is generated (Weitkamp and Katz, 1980).

In waterfalls, atmospheric gases are trapped by the hydrostatic pressure exerted when the water mass falls. If the hydrostatic pressure is greater than the atmospheric pressure, it causes the atmospheric gases to dissolve, causing an increase of TDG in this water. Supersaturated water in cascades of up to 134% has been described (Harvey, 1975). Other examples of water supersaturation in natural conditions include extensive algal bloom (Woodbury, 1941), increased photosynthetic activity (Renfro, 1963) and water round ice formation (Colt, 1986).

### **Water supersaturation by anthropogenic causes**

The generation of supersaturated water is associated with anthropogenic activities, and it has been observed mainly in large-scale hydroelectric projects, representing high mortalities of fish populations

(Speare, 2010). It has also been described due to air injection failures in aquaculture facilities (Harvey and Smith, 1961).

Hydroelectric facilities are characterized by large waterfalls between dams of a river, where a hydraulic turbine sends the energy received from the flow of water to an electric generator, converting hydraulic energy into electrical energy. These plants transport large volumes of water which, as explained above in a natural waterfall (**Fig. 20**), trap atmospheric gases as they fall over dams and force them to dissolve due to the pressure exerted (Marking, 1987). This supersaturated water has been shown to maintain similar percentages of TDG along the length of the water flow to the next spillway (Marking, 1987) and has long been associated with GBD (Weitkamp and Katz, 1980). High levels of supersaturated water have been detected up to 180 km away from a dam fall (Feng et al., 2014).



**Figure 20.** From left to right. McNary dam on the Columbia River (Source: *US army corps of engineers*). The victory falls of the Zambezi River, located on the border between Zambia and Zimbabwe, UNESCO World Heritage Site since 1989 (Source: *National Geographic*).

Due to the cooling procedures of these large-scale hydroelectric structures and other industrial plants, where river water is used to capture heat from the machinery and is returned to the river, local temperature increases have been observed in these rivers, increasing TDG as explained in natural aquifers and thus favouring the occurrence of GBD in fish inhabiting those waters (Marking, 1987; Yuan et al., 2022).

On the other hand, the rise of aquaculture implies the stocking of high fish densities, requiring the flow of large bodies of water and the use of aerators for greater oxygenation to supply large aquaculture facilities (Marking, 1987). It has been demonstrated that failures in aeration systems can lead to an increase in TDG and so, to the presence of GBD (Edsall and Smith, 1991). Additionally, accidental entrainment and dissolution of gases through water intake pipe can occur in fish culture facilities, observed mainly in incompletely immersed intake pipes, resulting also in GBD (Harvey and Smith, 1961). GBD has also been described due to the intentional increase of temperatures in aquaculture facilities to favour fish growth (Ebel, 1971).

Another possible trigger of GBD is the transport of fish at altitude, causing a pressure change (Hauck, 1986). This practice is frequently carried out by helicopters transporting smolts from hatcheries to river areas for restocking or in the case of transporting tropical species to aquariums (Roberts, 2012). The risk of supersaturation of a fish depends on the TDG pressure in the organism minus the ambient hydrostatic pressure. This term is known as decompensated pressure differential (Colt, 1983). At depth, the risk of supersaturation decreases because the hydrostatic pressure increases, reducing the unbalanced differential. If a fish surfaces, the hydrostatic pressure decreases and the unbalanced differential increases, causing the gas in tissues to come out of solution and form gas bubbles. Thus, a reduction in ambient pressure will decrease the hydrostatic pressure and increase the unbalanced pressure differential, which occurs during air transport (Hauck, 1986).

### **2.8.2. HISTORY OF GBD**

In 1857, the German physiologist Felix Hoppe-Seyler (1825-1895) noticed external signs of gas bubbles in fish subjected to an experimental vacuum (Hoppe-Seyler, 1857) and, a few years later, Paul

Bert, in his experiments on barophysiology, noted similar findings when subjecting these aquatic animals to high pressures (Bert, 1873). It was not until years later that an American bacteriologist named Frederic Gorham (1871-1933) (**Fig. 21**) provided a complete description of the disease. This first description of GBD occurred in 1898 in a public aquarium of Massachusetts, where Gorham also discovered that the water in the aquarium was getting supersaturated because of the high hydrostatic pressure exerted by the fall of the water supply pump into the aquarium, trapping the atmospheric gas (Gorham, 1901).



Frederic Doble Gorham  
1871-1933

**Figure 21.** Portrait of the American bacteriologist Frederic Gorham, who provides the first complete description of GBD (Source: *Round, 1933*).

Gorham described gas bubbles in fins and eyes causing a condition known as "pop-eye" referring to severe exophthalmia, and less frequently in gills or skin (Gorham, 1901). He also noted that these gas-filled vesicles increased in size with exposure time to supersaturated water, resulting in the loss of equilibrium of the fish. A few years later, in 1905, internal lesions associated with GBD were described for the first time (Marsh and Gorham, 1905). These consisted of gas embolism that could be observed as a few single bubbles up to complete vessel occlusions. In the heart, gas movement was seen with each beat, sometimes even without the presence of blood in the cardiac chambers. The most affected blood vessels were the main vessels of the gill filaments. Thus, it was concluded in this first documented pathological

study of GBD that death was associated with gas embolism (Marsh and Gorham, 1905).

In this first complete GBD report, Marsh and Gorham also documented the disease in naturally supersaturated freshwater; rainbow trout (*Salmo gairdneri*) showing clinical signs very similar to those described by Gorham in the Massachusetts saltwater aquarium. They suggested the hypothesis that susceptibility to increased TDG in water may vary according to fish species. For example, goldfish (*Carassius auratus*) were more resistant to the same level of TDG than trout and other cyprinids (Marsh and Gorham, 1905).

This work was the basis for the knowledge of GBD, with very few records until the mid-1960s (Weitkamp and Katz, 1980). In those years, few studies on GBD due to supersaturated water stand out, associated with extensive algal bloom (Woodbury, 1941), increased photosynthetic activity (Renfro, 1963), and in hatcheries due to air entry through water supply (Embody, 1934; Dannevig and Dannevig, 1950).

The first reference on GBD in hydroelectric projects arose in the Columbia River system (United States) in 1964, where the presence of this disease was observed in adult salmonids (Westgard, 1964). From this first report, GBD began to be observed more frequently, resulting in the implementation of TDG supersaturation measurement as a water quality parameter in this system. Thus, in the first measurements in 1966 and 1967, values of 120-130% of TDG supersaturation were obtained, causing that fish captured presented GBD, due to long stays in these waters (Ebel, 1969).

In 1970, following Ebel's study (Ebel, 1969), the U.S. Environmental Protection Agency addressed the problem of supersaturated water by setting maximum TDG supersaturation limits to 120%, to reduce the prevalence of the disease (USEPA, 1971). These

regulatory measures, which are still in application, are implemented during the smolt migration season, reducing the mass of water that falls through the different spillways of the dams and, therefore, reducing the TDG of the water. Even so, the regulation makes exceptions in the case of events with high water load, such as heavy rains, which leads to increases in TDG and mortalities per GBD. In 1975, Harvey analyzed TDG levels in different locations of the Columbia River system, obtaining up to 26 locations where the measurement revealed levels greater than 140% TDG supersaturation (Harvey, 1975). Due to exceptions to the established regulation, over the last 40 years fish mortalities have been reported by numerous authors in the Columbia River (Pauley and Nakatani, 1967; Beiningen and Ebel, 1970; Bouck et al., 1970; Backmann and Evans, 2002; McGrath et al. 2006; Brosnan et al., 2016)

Another large-scale hydropower system was installed in the early 21st century on the world's third largest river, the Yangtze River (China), a project called the Three Gorges Dam, in response to increasing energy demand (Cao et al., 2020). The Yangtze River is known for its extensive ecosystem inhabited by a wide variety of fish species. In 2014 the hydropower project attracted the attention of the Chinese authorities for the death of 40 tons of fish, presenting GBD due to large floods that led to increased water mass in the dam and elevated TDG levels (Ni et al., 2014). Since its opening in 2006 and after the 2014 mortality episode, other GBD records have been associated with these supersaturated waters (Tan et al., 2006; Cao et al., 2019). Numerous authors have directed their experimental studies towards the survival of endemic species in this river (Huang et al., 2010; Liu et al., 2011; Chen et al., 2012; Liang et al., 2013; Cao et al., 2015; Wang et al., 2015b; Cao et al., 2019; Ji et al., 2019; Xue et al., 2019; Cao et al., 2019; Cao et al., 2020, Deng et al., 2020; Fan et al., 2020; Ji et al., 2021), that

are facing extinction due to the alterations of the waters they inhabit (Li et al., 2019).

Other cases of massive mortalities by GBD have also been described in Canada or Norway (Heggberget, 1984), where survival studies of saltwater species have also been conducted (Gunnarsli et al., 2008; Gunnarsli et al., 2009).

### **2.8.3. PATHOGENESIS OF GBD**

The pathogenesis of GBD is founded on the fact that supersaturated water contacts the gills of fish for gaseous exchange. The osmotic pressures of the gill membrane on the side in contact with the water and on the side in contact with the blood vessels tend to equilibrate and, since the saturation point is similar in both fluids, any excess of gas in the water will transfer to the bloodstream (Marking, 1987). Gas bubbles can then form when gas escapes from the solution because the sum of dissolved gas pressures exceeds the sum of hydrostatic pressure and the rest of compensatory pressures (Bouck, 1980) similarly to DCS.

The cause of death of GBD is associated with asphyxia as gas emboli are usually found in the gill vessels, causing blood stasis and anoxia. This occlusion of the gill vessels causes a decrease in gas exchange, reduced respiration, and leads to the death (Marking, 1987). Primary findings are gas embolism and emphysema in tissues, triggering the response to endothelial damage and associated secondary lesions (Bouck, 1980). These aspects will be addressed later in the section of comparative pathophysiology.

## **2.8.4. CLINICAL FEATURES, RISK FACTORS AND TREATMENT OF GBD**

### **Clinical features**

Although GBD has now been clinically detected in a wide variety of species and life stages (Bouck et al., 1976), the tolerance and survival vary between species and stages of life, presenting variable clinical signs with similar TDG level and exposure time (Weitkamp and Katz, 1980). Even in populations with similar individuals, individuality plays a fundamental role in this disease, determining the survival of some and death of others (Speare, 2010), similarly to DCS (Shim et al., 1967; L'abbate et al., 2010). The most typical clinical signs of GBD will be addressed next.

The behavior of fish with GBD is often described as lethargy, loss of equilibrium, erratic swimming with periods of inactivity and spasms (Lund and Heggberget, 1985; Machado et al., 1987). It is common to observe a decrease in feeding because gas bubbles in eyes can cause blindness (Speare, 2010). Machado et al. (1987) also describe violent turns during swimming, and, after an episode of convulsions lasting minutes, death occurs, frequently with the operculum and mouth open. In fish populations, Bouck (1980) described three stages of GBD: 1) incremental gas bubble formation, 2) acute deaths, and 3) eventual death of those animals that survived GBD, from GBD sequelae (Bouck, 1980).

In early life stages, gas bubbles can be observed externally in subcutaneous tissue of head and tail (Liang et al., 2013), while in adults gas bubbles are frequently formed in the gills, fins, and eyes (Roberts, 2012). Gas bubbles in the eyes produce exophthalmia, which can be unilateral or bilateral, although its observation is variable and does not always appear (Pauley and Nakatani, 1967), being more associated with

subacute or chronic cases of the disease (Machova et al., 2017). In subacute cases of GBD, the dorsal and caudal fins are mainly affected, with gas bubbles of different sizes. In severe cases of GBD large gas bubbles are seen in all fins of the fish (Machova et al., 2017).

### **Risk factors**

Regarding fish risk factors, age and size of the fish elicits a different response to TDG supersaturation levels (Weitkamp and Katz, 1980). For example, at the same level of TDG, eggs seem to be more tolerant than juveniles of the same species (Weitkamp and Katz, 1980). This could be due to the hydrostatic pressure they maintain under their capsule (Alderdice and Jensen, 1985). It is postulated that sensitivity to TDG supersaturation is lower in early stages, increases in juveniles and decreases again in adults (Weitkamp and Katz, 1980). There is controversy on this aspect of GBD as other authors postulate that sensitivity to TDG supersaturation is inversely proportional to the size of the fish (Cornacchia and Colt, 1984). However, there is a scientific agreement that adulthood is considered the most resistant life to elevated TDG levels (Gunnarsli et al., 2008).

In experimental studies where fish could move freely, some species and individuals have demonstrated the ability to detect and avoid supersaturation (Bouck, 1980; Stevens et al., 1980). This was more relevant in TDG supersaturation levels above 135% (Huang et al., 2010). Fish may experience supersaturation depending on the depth, i.e., pressure, they are at, since supersaturation depends on ambient pressure. With the same level of TDG in the water and as the ambient pressure increases (i.e., depth increases), the less supersaturation the fish will experience (Weitkamp et al., 2003). Therefore, fish in deeper water will be less supersaturated than those at the surface of the same waters, due to the increase of environmental pressure. It is estimated that the supersaturation experienced by fish descends 10% for each meter of

depth reached (Weitkamp et al., 2003). For example, with a surface TDG supersaturation measurement of 130%, a fish descending to a depth of 1 meter will experience a supersaturation of 120%, at 2 meters 110% and successively (Weitkamp et al., 2003) (**Fig. 22**). This % saturation-to-depth relationship will make GBD more severe in shallow water (Johnson et al., 2007). It has been shown that fish in surface waters suffer more severe GBD and that, those same individuals placed in cages at greater depths can alleviate disease symptoms and reduce mortality (Cao et al., 2019), similarly to a recompression treatment of DCS.

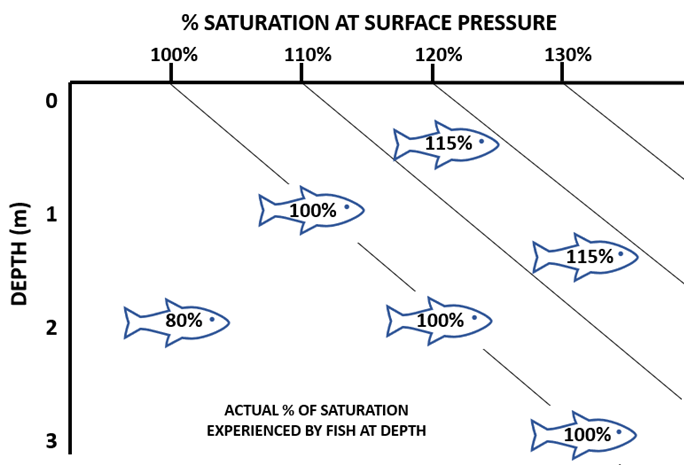


**Figure 22.** Diagram showing varying saturation at different depths (Adapted from Weitkamp et al., 2003).

Regarding water risk factors, taking into account that temperature and pressure modify TDG levels, the factors that determine the severity of GBD are the degree of water supersaturation and the time of exposure (Weitkamp and Katz, 1980). The close relationship between these two factors has been studied in hydroelectric projects, observing that chronic exposures to a percentage of 102% TDG supersaturation can produce disease in some fish in the population, while as TDG increases, morbidity increases (Weitkamp and Katz, 1980). Chronic GBD is suggested to occur at levels below 110% of TDG supersaturation and

with long exposure times (weeks to months), where GBD-related symptomatology is barely observed (Gunnarsli et al., 2008), although cases of individuals dying at these supersaturation levels have been described (Dawley and Ebel, 1975). Chronic GBD can act as a stressor for feeding and growth, increasing vulnerability to predators and reproduction of the subjected species, as well as favoring the presence of secondary infections (Bouck, 1980; Marking, 1987; Mesa and Warren, 1997).

The value of 120% TDG supersaturation appears to be the cut-off value for the onset of acute GBD leading to death (Huang et al., 2010) and it seems to be the tolerated limit for maintaining a high probability of survival in most species (Cao et al., 2015; Wang et al., 2015b; Cao et al., 2020; Deng et al., 2020; Fan et al., 2020). A study in the Columbia River system determined that the presence of signs of GBD at 120-125% TDG supersaturation was 5% and increased to 45% when exposed to TDG supersaturation over 135%, suggesting that the prevalence of disease below 120% is low (Weitkamp et al., 2003). TDG supersaturation levels of 125% are considered fatal since fish that do not die acutely of GBD, do not survive long, suggesting that they cannot overcome the effects of this disease (Cao et al., 2015). TDG supersaturation values of 140% cause acute GBD (in just a few hours most) in fish (Weitkamp et al., 2003).

Most experimental studies have focused on TDG supersaturation levels below 150%, similar to those that can occur in the waters of large dams. This allowed the analysis of the disease from the point of view of different variables such as age, species, feeding, reproduction, concomitant diseases, etc.

## Treatment

“Recompression”: placing the affected fish in deeper water that is not supersaturated or to water that is not supersaturated is an efficient treatment for fish exposed to TDG supersaturation below 125% (Cao et al., 2020). Even animals with near-death behavior due to GBD, recovered when moved to water with 100% TDG supersaturation (Knittel et al., 1980). The prognosis of survival will depend first on the species and larval stage, followed by the time and degree of supersaturation to which the fish was subjected (Pauley and Nakatani, 1967).

### 2.8.5. PATHOLOGY OF GBD

The most observed external lesions include subcutaneous emphysema causing skin crepitus and emphysema in all fins (Machado et al., 1987) (**Fig. 23**). Internally, main macroscopic findings are gas bubbles within the blood vessels of different organs (Pauley and Nakatani, 1967), especially in the gill and ventral aorta (**Fig. 23**), where the amount of gas bubbles is very large, distending the vessels and displacing the blood. Gas bubble associated lesions are petechial hemorrhages in gills and opercular areas (Machado et al., 1987), oedema, congestion, and swollen gill filaments (Edsall and Smith, 1991), and hepatic degenerative changes (Pauley and Nakatani, 1967). In cases of chronic exposure, ascites and muscle changes may be observed (Weitkamp and Katz, 1980).

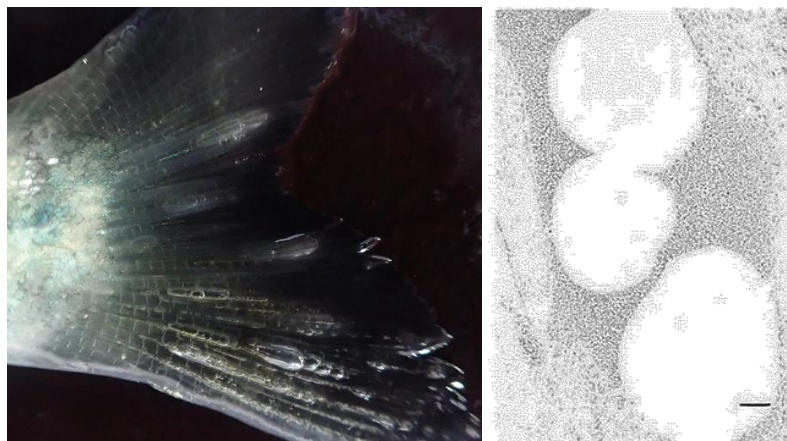


**Figure 23.** From left to right. Presence of emphysema in the caudal fin (Source: *Stenberg et al., 2022*). Microscopic gas bubbles between the red blood cells of the bulbus arteriosus and ventral aorta (Source: *Smith, 1988*).

In histopathology, edema of the secondary lamellae of the gills with degeneration of the respiratory epithelium is observed (Speare, 2010). Epithelial hyperplasia and fusion of secondary lamellae are observed in some gill areas, in agreement with gross findings (Machado et al., 1987). In addition, intravascular gas bubbles can be seen occluding gill vessels, which can be a cause of acute mortality. Other microscopic findings are edema and disruption of the intestinal mucosa, degeneration of the renal tubular epithelium, hepatic, and muscular changes (Roberts, 2012).

In the eye, histological lesions such as gas bubbles in choroidal vessels or emphysema can occasionally be observed. In addition, degeneration of the optic nerve, muscle, and adjacent connective tissue due to emphysema may also be seen (Machado et al., 1987). Inflammatory changes associated with the presence of gas bubbles were observed as edema, compression, and degeneration of the connective tissue adjacent to the bubbles. Occasionally neutrophils near the locations of these structures (Speare, 2010).

### **2.8.6. COMPARATIVE PATHOPHYSIOLOGY BETWEEN GBD AND DCS**

From the point of view of bubble formation, bubble growth and persistence, the nature of these aspects is very similar between GBD and DCS. In DCS there is a supersaturation of blood and tissues after decompression, causing the appearance of gas bubbles in the circulatory system and other tissues. Lesions associated with vascular damage are observed in primary tissues such as the CNS. In the case of GBD, exposure to supersaturated water causes the development of gas bubbles in the vasculature and well-perfused tissues, showing lesions associated with the same pathophysiological pattern of DCS (Machado et al., 1987).

The pathophysiological mechanisms causing gas bubbles in both diseases are mainly vascular. The mechanical damage produced by the presence of these structures in circulation is observed with the occlusion of blood vessels, i.e., gill vessels in fish and pulmonary vessels in mammals (Edsall and Smith, 1991) (Tanoue et al., 1987).

In both diseases biochemical damage triggers an inflammatory response and the coagulation cascade (Philp, 1974; Casillas et al., 1975). Thrombogenesis is well studied in DCS (Levin et al., 1981; Tanoue et al., 1987), while in GBD it is suspected that gas bubbles may cause thrombi (Smith, 1988).

Activation of coagulation mechanisms causes disseminated intravascular coagulation (DIC), also observed in DCS (Levin et al., 1981). Gas bubbles from DCS have been shown to cause direct action on the endothelium and platelets, causing the release of endothelial damage factors leading to DIC (Warren et al., 1973). Endothelial damage has also been shown to be directly related to GBD (Speare, 1991) and is recognized as a generator of DIC due to exposure of

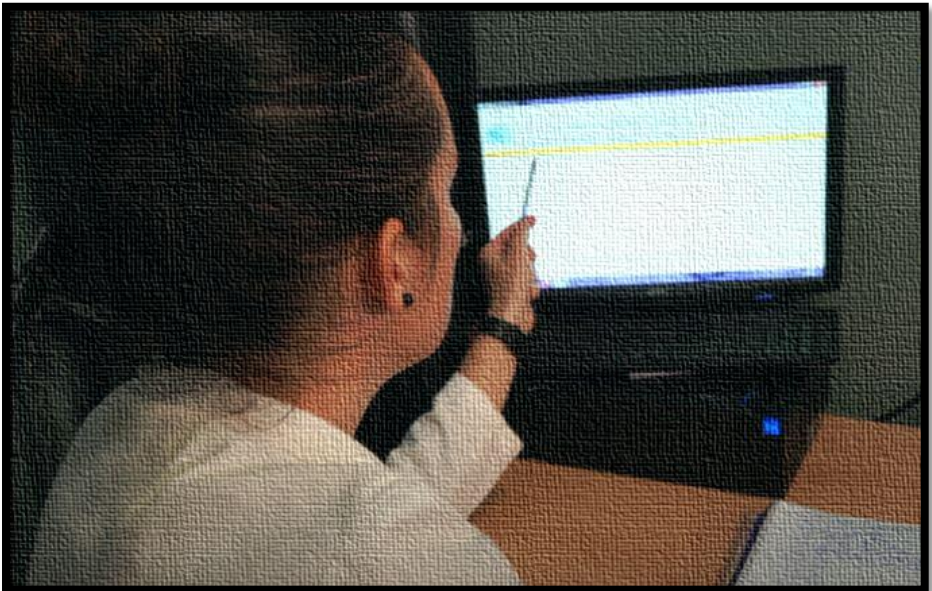
subendothelial collagen and by triggering the coagulation cascade (Speare, 2010).

Another consequence of endothelial damage caused by gas bubbles is the activation of leukocytes in DCS (Levin et al., 1981), this perivascular leukocyte response has also been observed in fish with GBD (Speare, 1991). The similarities in the interaction of gas bubbles and endothelium between GBD and DCS make it possible to propose a GBD model for the study of the endothelial effects of gas bubbles in DCS (Speare, 2010).

The study of tissue damage biomarkers in fish is relatively recent, not being studied to date the association of this type of biomarkers with gas embolism. Several studies have previously described the presence of biomarkers in fish (Poder et al., 1991; Hyndman and Evans, 2007; Roberts et al., 2010), sometimes associating their expression with cellular stress (Basu et al., 2002; Padmini and Usha Rani, 2008; Padmini, 2010; Wang et al., 2015a; Zhai et al., 2021). Therefore, in this thesis we will explore if these biomarkers are expressed with gas embolism in fish and thus validate the fish model for this purpose.



### 3. METHODOLOGY





To achieve the objectives of this thesis project, two experimental animal models were carried out, in rabbits and fish. While the experimental model in rabbits subjected to compression/decompression in a hyperbaric chamber to provoke DCS is part of a larger study developed prior to this thesis, the experimental model in fish was designed and developed entirely in this project. This model consisted of the reproduction of experimental GBD through the production of supersaturated water by means of a low-pressure vessel associated with a pressurized aquarium. Both experimental models were developed to obtain a comparative pathological view with DC-likeS in cetaceans, DCS in humans and sea turtles, using experimental DCS and GBD as a comparative pathological model for the study of this disease.

Both experimental models were submitted to their corresponding ethical committees. The model in rabbits was approved by the Norwegian committee for animal experiments (Reference: 2154) and the ethical committee for animal experiments of the University of Las Palmas de Gran Canaria (Reference: CEEBA-HUGCDN 002/2010), while the experimental model in fish was approved by the latter ethics committee (Reference: CEEA-ULPGC 4-2018R1) and by the competent authority of the government of the Canary Islands.

### **3.1. RABBIT EXPERIMENTAL MODEL**

The experimental model in rabbits was designed and used by Dr. Yara Bernaldo de Quirós Miranda in her doctoral thesis (Bernaldo de Quirós, 2011a). For the present thesis we will use only the pathological data of rabbits subjected to compression/decompression to perform the complete pathological study. In addition, to complement this study, the databank of cetaceans diagnosed with DC-likeS was used to perform the comparison of pathological lesions between the experimental model and DC-likeS in cetaceans.

The experimental model in rabbits was designed by creating three groups: compression/decompression (I), air injection (II) and putrefaction (III). Bernaldo de Quirós created this model to study and compare the composition of gas bubbles generated by decompression, by air injection, and by the processes derived from decomposition. To characterize the presence, abundance, and distribution of gas in vascular and extravascular locations, the researcher developed a score index named as Gas Score (explained in the section “Decompression pathology consistent with DCS in cetaceans”). The animals in the compression/decompression group presented statistically higher gas scores than any of the animals in the other groups, and the gas was more widely distributed.

In addition, another part of Bernaldo de Quirós’ doctoral thesis consisted of using imaging techniques to evaluate the abundance of gas bubbles after decompression *in vivo* and correlate it with the Gas Score *post-mortem*. In the present thesis, a complementary study was performed by doing a pathological exam of the tissue-samples previously collected by Bernaldo de Quirós and comparing these results with the findings in cetaceans diagnosed with DC-likeS by our group.

### **Animals**

Tissue samples from 18 New Zealand White Rabbits (NZWR) were studied. These rabbits were all males and weighed  $3.15 \pm 0.65$  kg. Of these, 14 animals were subjected to a compression/decompression protocol (C/D group), while 4 of them were control rabbits (Control group). Only fresh necropsied animals, within 12h *post-mortem*, were included in this study.

### **Pretreatment**

Animals from both groups were anesthetized during all the procedure. Anesthesia consisted of the subcutaneous administration of

Medetomidine (0.5 mg/Kg) and Ketamine (25 mg/Kg), achieving surgical anesthesia in a few minutes. The anesthesia protocol was administered again at removal from the hyperbaric chamber, to ensure anesthesia throughout the entire experiment.

### **Compression/decompression model (C/D model)**

Rabbits were compressed in pairs to 8 absolute atmospheres (ATA) in a dry hyperbaric chamber (Animal Chamber System, NTNU, Haugesund, Norway). When 8 ATA was reached, the animals were maintained for 45 minutes at that pressure after which, in search of a dive profile inducing explosive decompression, rapid decompression was performed at a rate of 0.33 meters per second. Rabbits were kept anesthetized for a 1-hour observation period after decompression, after which animals were euthanized if still alive. Euthanasia was performed with a peritoneal injection of 200 mg/kg of dilute pentobarbital. At the end of the experiment, two subgroups of the C/D group were obtained, the group of animals that died within 1-hour observation period post-decompression (C/D dead group) and the group of animals that survived decompression and were anesthetized 1 hour later (C/D euthanized group).

### **Control group**

To reproduce the experimental conditions, 4 control animals were anesthetized and subsequently euthanized following the same anesthesia and euthanasia protocol as the C/D euthanized group.

### **Dissection, external exploration, and Gas score**

Necropsies were carried out individually by placing the rabbits in the dorsal decubitus position and performing the dissections carefully to preserve the large blood vessels intact, following the protocol established by Bernaldo de Quirós (2011a). This consisted of an external

exploration of the carcass and removal of the skin with special care in examining the subcutaneous vessels in search of gas bubbles. Next, the abdominal cavity was opened, observing the mesenteric and renal blood vessels. The thoracic cavity was then opened to access the heart and large vessels such as the aorta and caudal vena cava. Taking advantage of the opening of the abdominal cavity, the presence of possible subcapsular gas or gas in fat tissues was also evaluated.

To study the mode of abundance of gas bubbles in the various locations, we used the information provided by the Gas score, a gradient system created by Bernaldo de Quirós (2011a), based on 6 grades to classify the intravascular locations (I-VI) and 3 grades for the extravascular locations (I-III) (**State of the art section, Fig. 16**). Each animal thus obtained a total gas score consisting of the sum of all the locations studied. Thus, in this thesis we studied the mode of gas scores for the different locations of each group, C/D euthanized, C/D dead and control.

Once the gas score was performed, the routine necropsy protocol was continued and representative samples of the lung, trachea, superficial cervical lymph node, spleen, central nervous system, heart, liver, stomach, intestines, mesenteric lymph node, kidney, urinary bladder, and skeletal muscle were collected, fixed in 10% buffered formalin, processed routinely, embedded in paraffin wax and sections of 5  $\mu\text{m}$  were cut and stained with standard hematoxylin and eosin for histopathological analysis (Suvarna et al., 2018). To evidence changes in heart and skeletal muscle, sections of both tissues were also stained with phosphotungstic acid hematoxylin and Masson's trichrome respectively (Suvarna et al., 2018).

### **Cetacean data used for comparison with the DCS model**

To perform the pathological comparison between experimental decompression in animal models and DC-likeS in cetaceans, we resorted to the IUSA sample bank to use samples from stranded cetaceans diagnosed with DC-likeS. Necropsy reports and histological slides belonged to 31 cetaceans stranded coinciding in time and space with naval military maneuvers: eight Cuvier's beaked whales (*Ziphius cavirostris*), one Blainville's beaked whale (*Mesoplodon densirostris*), and one Gervais's beaked whale (*Mesoplodon europaeus*) stranded in the islands of Fuerteventura and Lanzarote (Spain) in 2002 (Fernández et al., 2005); four Cuvier's beaked whales stranded on these same islands in 2004 (Fernández et al., 2012); four Cuvier's beaked whales stranded in 2006 and one Cuvier's beaked whale stranded in 2011, both in Almeria (Spain) (Arbelo et al., 2008; Bernaldo de Quirós et al., 2019); ten Cuvier's beaked whale mass stranding in Corfú (Greece) in 2011 (Bernaldo de Quirós et al., 2011b). In addition, we added the cases of 2 Risso's dolphins (*Grampus griseus*) diagnosed with DC-likeS due to interaction with large prey (Fernández et al., 2017).

## **3.2. FISH EXPERIMENTAL MODEL**

The experimental model in fish was designed to induce severe GBD. This required the development of machinery capable of producing supersaturated water. Once produced, this supersaturated water must be able to be transferred to an aquarium where the fish will be introduced and where it will be kept with stable values during the experimental hours. Both the machinery set-up as well as the pilot experiments, and the experimental model designed were carried out at the experimental animal facilities of the veterinary faculty of the University of Las Palmas de Gran Canaria (Canary Islands, Spain).

### **3.2.1. WATER SUPERSATURATION**

The first step of producing supersaturated water experimentally was carried out by acquiring a low-pressure vessel, using the scheme developed by Bouck et al. (1976) to design it in conjunction with an engineering company (IBERCO S.L., Spain) (**Fig. 24**). This low-pressure vessel was composed of different components, highlighting the dissolution tube and the pressurized tank. The dissolution tube is a structure filled with porous material of decreasing diameter, which causes pressure to be exerted as the water passes through this structure. In this tube atmospheric air is injected from the bottle and forced to dissolve in the water by successive passes through these materials, producing supersaturated water. The tank is the pressurized structure where the supersaturated water may be stored.

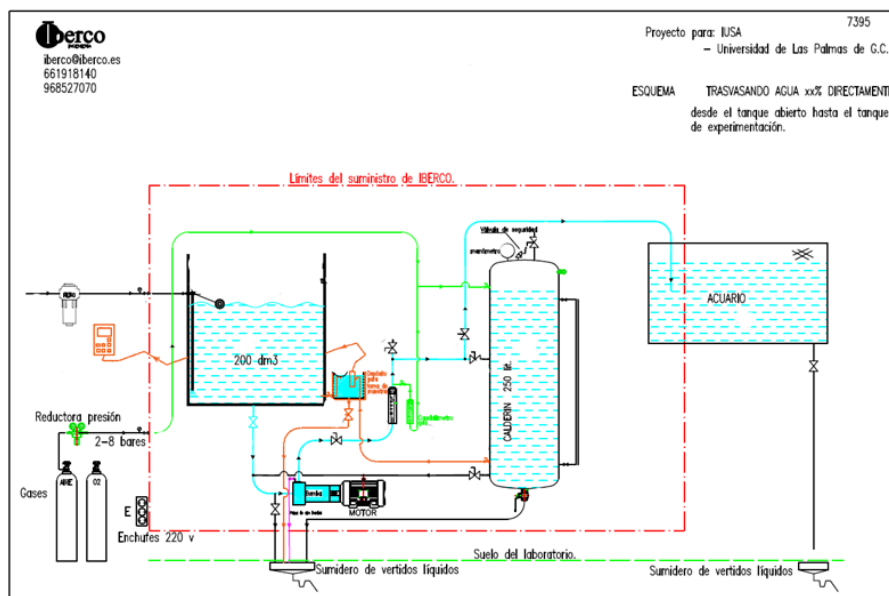


**Figure 24.** Schematic drawing of the components of the low-pressure vessel (*IBERCO S.L.*).

## Measurement and control of supersaturated water parameters

A TDG sensor (Manta+ Trimeter probe, Eureka water probes, USA) was used to monitor the percentage of TDG of the water. This sensor also monitors temperature values and is connected via USB to a computer to obtain real-time values of the parameters. These values can be plotted in excel to obtain graphs of the TDG behavior.

### Water supersaturation with open aquarium

As a first option, the production of supersaturated water was considered using the low-pressure vessel coupled to an open aquarium (**Fig. 25**) following the literature (referencias). Once the desired TDG supersaturation value monitored by the TDG sensor was reached in the low-pressure vessel, the supersaturated water was transferred to an open aquarium where the fish would be introduced and maintained during the

## Comparative study of gas-bubble lesions using experimental models

experimental hours, placing the TDG sensor in the open aquarium to control the values.

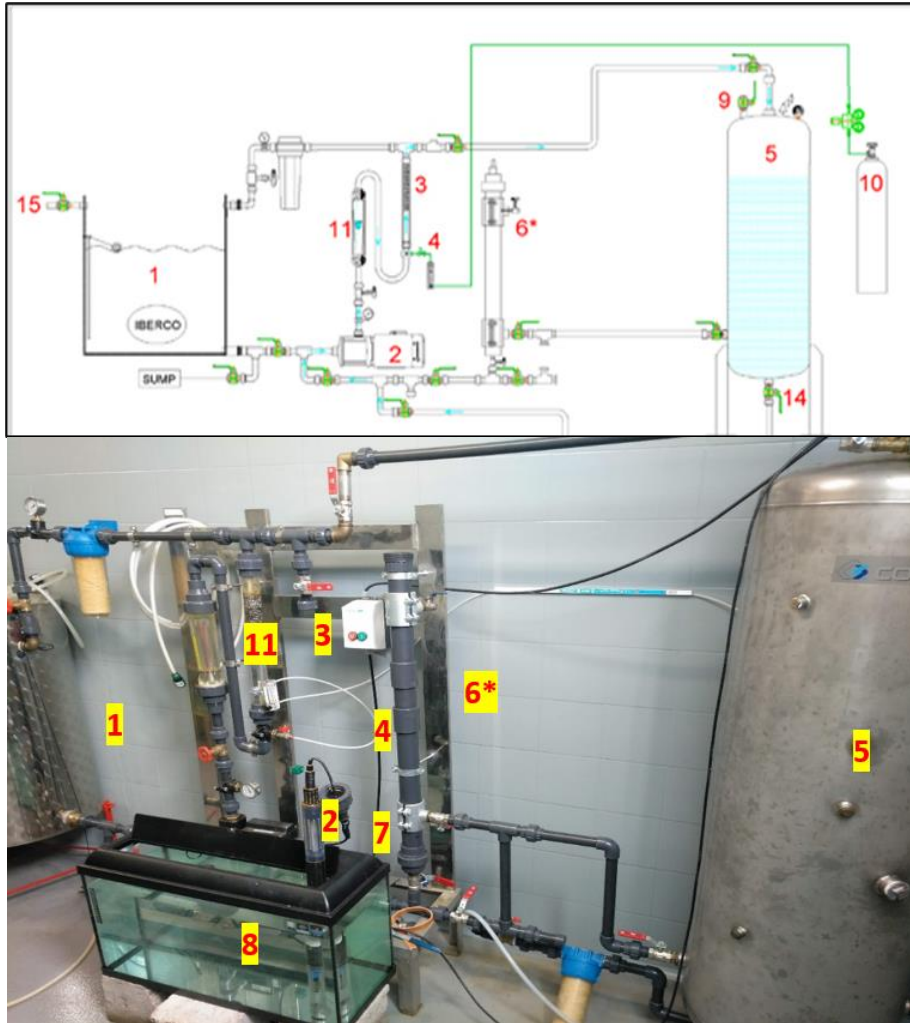


**Figure 25.** Supersaturated water production system components. (1) Open vessel. (2) Motor pump. (3) Dissolution tube. (4) Synthetic air injection valve. (5) Pressurized tank. (6\*) TDG and temperature sensor. (7) TDG and temperature sensor inside the aquarium. (8) Open aquarium. (9) Pressurized tank vent valve. (10) Synthetic air bottle. (11) Flow meter. (14) Pressurized tank outlet valve. (15) Running water inlet.

Water supersaturation was achieved as follows: first, the open vessel (max. 200L; **Fig. 25. 1**) was filled with a total of 150L by means of the tap water valve (**Fig. 25. 15**). Then, the motor pump (Grundfos, Model: CM10-1 ARAE-AVBE CAAN) (**Fig. 25. 2**) was started to distribute the water to the pressurized tank (max. 3 ATA; 250L) (**Fig. 25. 5**). The open vessel was isolated when only 20L remained in it to prevent air from entering into the system. The 130L of water from the pressurized tank was recirculated through the system, passing the water from the pressurized tank through the motor pump, the flowmeter, the dilution tube, and back to the pressurized tank. The TDG sensor was placed between the pressurized tank and the motor pump to obtain TDG values during recirculation.

After several passes, synthetic atmospheric bottle air (Premier-X50S 200.0B) was injected through the injector at the beginning of the dissolution tube. The amount of air introduced was regulated at a rate of 10-20L/min, with a bottle outlet pressure of 3 bar. The pressure gauge of the pressurized tank indicated the pressure obtained, allowing a pressure up to 3 ATA. This limit of 3 ATA was achieved after 5 minutes of air injection and the subsequent recirculation. Recirculation was kept constant at a flow rate of 3000L/h, until TDG supersaturation values of 150% or above were achieved. At this point, the motor pump was stopped, and water was transferred by pressure differential from the pressurized tank to the open aquarium through a pipe, filling up to 80L in the open aquarium (**Fig. 26**). During the filling maneuver, the TDG sensor was moved to the aquarium for constant monitoring of TDG values, obtaining graphs in which the value decreased exponentially (**Fig. 26**).

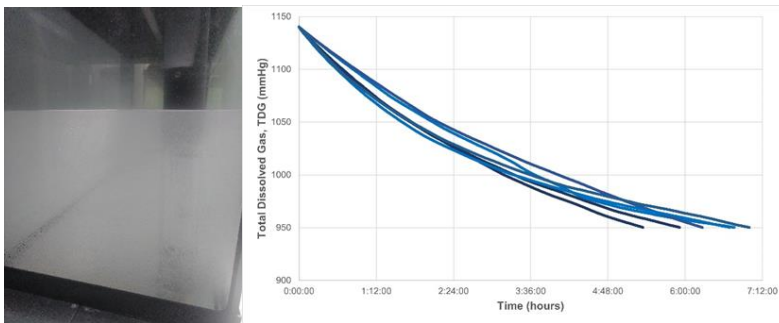


**Figure 26.** Transfer of supersaturated water into the open aquarium with TDG sensor monitoring the process. Behavior of TDG in supersaturated water kept watertight inside an open aquarium. A significant decrease is observed over a period of 7 hours.

### **Water supersaturation with pressurized aquarium and constant recirculation**

To ensure maintenance of TDG values within the water to which the fish are exposed, it was necessary to maintain pressure in the entire circuit by adding to the design a pressurized aquarium (IBERCO S.L.), directly connected to the system (**Fig. 27**). The generation of supersaturated water was modified according to **Figure 28**: the open vessel (**Fig. 28. 1**) was filled with tap water and transferred by starting the motor pump (**Fig. 28. 2**) to the pressurized tank (**Fig. 28. 5**), as explained in the previous section. In this case, during the transfer, the vent valves of the pressurized aquarium (**Fig. 28. 8**) and the pressurized tank (**Fig. 28. 9**) were kept open to facilitate the elimination of residual air in the system.

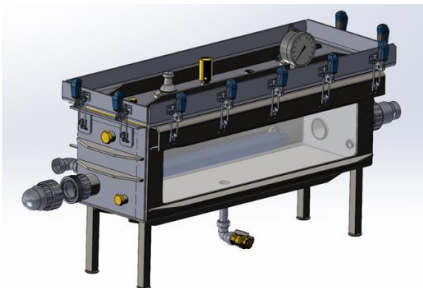


**Figure 27.** schematic design of the pressurized aquarium supplied by *IBERCO S.L.*

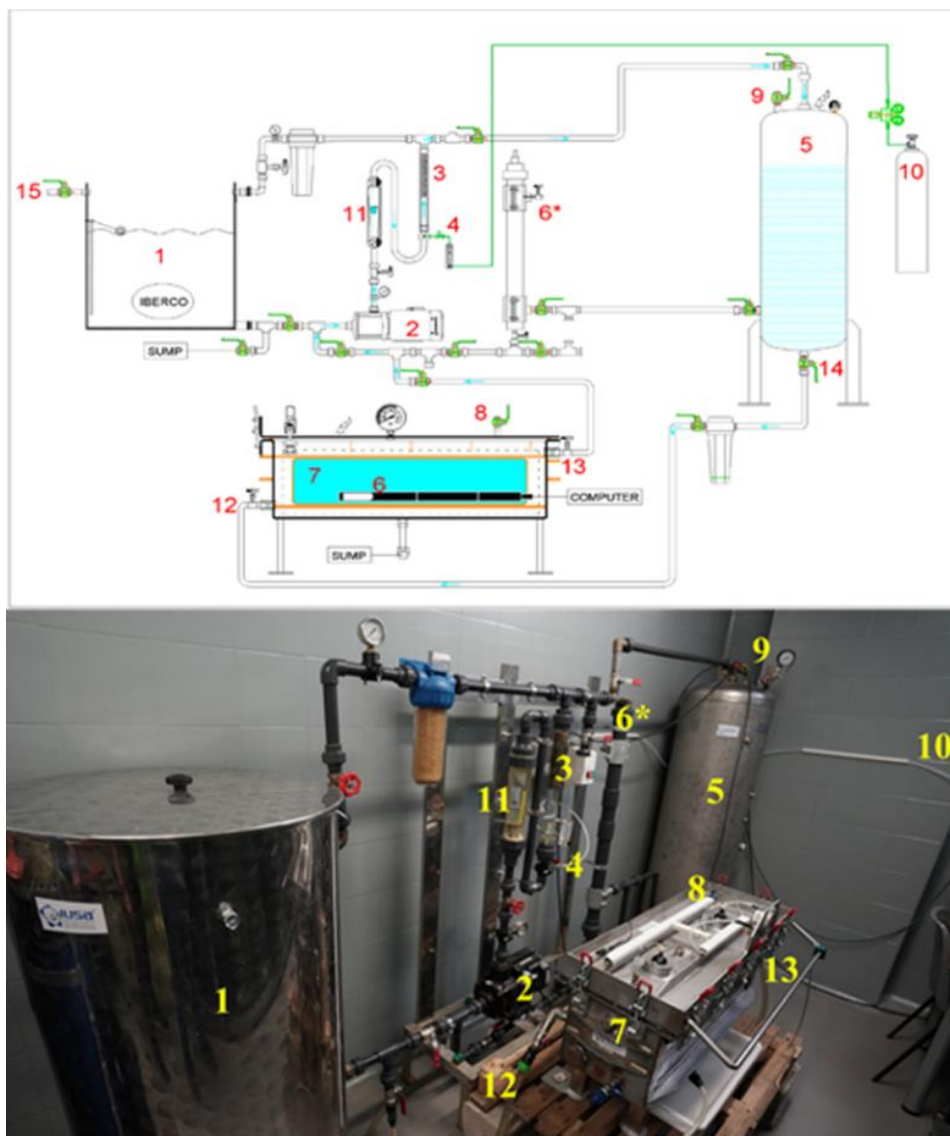


**Figure 28.** Supersaturated water production system components. (1) Open vessel (2) Motor pump (3) Dissolution tube (4) Synthetic air injection valve (5) Pressurized tank (6) TDG and temperature sensor (6\*) TDG and temperature sensor inside the open circuit (7) Pressurized aquarium (8) Pressurized aquarium vent valve (9) Pressurized tank vent valve (10) Synthetic air bottle (11) Flow meter (12) Pressurized aquarium inlet valve (13) Pressurized aquarium outlet valve (14) Pressurized tank outlet valve (15) Running water inlet.

Once all the water had been transferred to the pressurized tank, the open vessel was isolated from the system and water was recirculated between the pressurized tank and the pressurized aquarium with the vent valves of both pressurized structures open. After that, the vent valves were closed, and synthetic atmospheric bottle air (Premier-X50S 200.0B) was injected (**Fig. 28. 4**). The amount of air injected, regulated by flowmeter, in this circuit modification was dependent on the maximum pressure of the pressurized aquarium (0.5 bar). When this pressure was reached, the air injection was stopped and the water was kept in constant recirculation of 3000 L/h, passing through the 3 important elements of the circuit: pressurized aquarium, dissolution tube, and pressurized tank. This constant recirculation was maintained for several minutes to favor the dissolution of the injected gas until reaching a dynamic equilibrium between the liquid and gas phase, determined by constantly measuring TDG values in the pressurized aquarium (**Fig. 28. 6**).

Once it was assessed that the TDG remained constant with this new design, the aquarium was opened simulating the introduction of a fish into the pressurized aquarium to adjust the procedure and to assess the behavior of this parameter when the aquarium was opened. This was done by stopping first the motor pump and water recirculation, then isolating the aquarium from the system by closing the inlet tap (**Fig. 28. 12**) and the outlet tap (**Fig. 28. 13**), venting and de-pressurizing the aquarium through its valve (**Fig. 28. 8**) and opening the 9 quick closes to simulate the introduction of a fish. Then the quick closes were closed again, followed by the vent valve. Finally, the water inlet and outlet valves were reopened to restart the circulation of supersaturated water.

These experiments were performed at different times and with different TDG supersaturation values, varying between 150% and 180%, in order to adjust the parameters. Through these tests, it was calculated that the outlet pressure of the synthetic air bottle should be at 3 bar, with

a flow rate of 10-20L/min for 4-6 minutes. Thus, after this air injection time, recirculation at 3000 L/h would be maintained for approximately 1.5 hours, reaching constant TDG levels. These supersaturation levels varied between 160% and 180%, taking into account that the longer the experimental time, the more the TDG tends to stabilize.

### **3.2.2. PILOT TESTS**

#### **Fish**

Fish, 10 adult goldfish (*Carassius auratus*) of  $112.8 \pm 11.74$  g and  $16.95 \pm 0.60$  cm, were purchased from a certified fish distributor in Las Palmas de Gran Canaria (Canary Islands-Spain). Upon arrival at the experimental animal facility, the goldfish were kept for 1 month in acclimatization. During this time, they were stimulated with a natural photoperiod of 12 hours of light and 12 hours of darkness and were fed with a commercial pellet (Tetra Goldfish) twice a day. Every two days, water parameters, such as temperature (23-25 °C), dissolved oxygen ( $> 6.0$  mg/ dm<sup>3</sup>), and chemical parameters were monitored by means of a colorimetric strip kit (nitrate, 10 mg/dm<sup>3</sup>; nitrite, 0 mg/dm<sup>3</sup>; pH,6.8; total hardness, 80-300 mg/dm<sup>3</sup>; chlorine, 0 mg/dm<sup>3</sup>).

#### **Exposure to supersaturated water and generation of GBD**

To assess the exposure time to supersaturated water necessary to generate severe GBD, we performed sequential pilot experiments (n=2; one fish at a time) starting at 3 h of exposure, and incremented the time of exposure in a stepwise manner, doubling the exposure time until the expected outcome, i.e. severe gas bubble production, was achieved. During the exposure, the animal's behavior was continuously monitored, and once the experimental hours had elapsed, fish were euthanized and necropsied, checking for gas bubbles and lesions indicative of severe GBD. Hence, the exposure times tested were: 3h, 6h, 12h, and 18h. The

18h exposure group was initially set at 24h, but at 18h the humane endpoint was reached. The humane end point is when the procedure is causing unnecessary pain or suffering to the animal that should be alleviated, and it's determined by the investigator on each clinical setting. In the case of our experiment, the humane endpoint was established when the fish lost buoyancy and presented erratic swimming or lethargy.

In addition to these 4 experimental groups (n=8), a control group (n=2) was added: fish were individually introduced into the pressurized aquarium for 18h without pressure, to reproduce the possible stress generated when transferring the fish from the acclimatization aquarium to the experimental aquarium.

### **Clinical signs**

The behavior of the fish was monitored throughout the hours of exposure of each group, including the monitoring of opercular beat and swimming frequencies, establishing baseline values by examining the control group. For example, the opercular beat frequencies in the control group were approximately 2 /sec, and control fish took 10 sec to swim from one side of the aquarium to the other. It was considered an abnormal behaviour when the opercular beat frequency or the swim speed was 2 times higher than the control. The appearance of external lesions was also registered, paying special attention to the loss of scales, hemorrhages in fins or visible gas bubbles in skin, fins, and eyes.

### **Macroscopic evaluation**

Once the experimental hours were completed or the humane end point was reached, the animals were euthanized by adding 2-phenoxyethanol in a 10L cube of water, at a concentration of 0.6 ml/L. Then, fish were placed in right lateral decubitus and an external inspection was performed using a stereo microscope, with particular

focus on the integument, gills, fins, and eyes, (**Fig. 29**). Next, the coelomic cavity was dissected, incising the ventral midline from the anus to the operculum. This dissection was performed carefully trying to preserve most of the blood vessels for examination together with the internal organs, also using the stereo microscope.

**Figure 29.**  
Stereomicroscope for  
external and internal  
examination of fish  
during necropsy.



### Microscopic evaluation

For microscopic evaluation, representative samples of fins, eyes, gills, swim bladder, liver, spleen, gonads, digestive tract, heart, anterior and posterior kidney, central nervous system, spinal cord (**Fig. 30**), and axial muscles were collected and placed in 10% formalin for histological processing. Formalin-fixed tissues were transferred to the tissue processor that performs dehydration, cleaning, and paraffin imbibition of the tissues, to finally cut 4  $\mu\text{m}$  samples and routinely stain them with hematoxylin and eosin (H&E) for further observation under the microscope.



**Figure 30.** Samples  
obtained from spinal  
cord and central nervous  
system sections for  
histological processing.

### 3.2.3. FISH MODEL OF GAS-BUBBLE LESIONS

Adult goldfish (*Carassius auratus*), 10 females and 10 males of  $116.1 \pm 11.3$  g weight and  $17.2 \pm 0.5$  cm long, were obtained from Tropical Centre (ICA Canarias). Fish were divided into two groups: control group (n=10) and GBD group (n=10). Fish in the GBD group were individually subjected to supersaturated water with TDG supersaturation between 164-174% in the pressurized aquarium for 18 hours as described above. Experimental procedures and postmortem procedures were carried out as previously described for the pilot study. An addition to this study was the use of a gas score index to evaluate the presence, abundance, and distribution of gas bubbles following Bernaldo de Quirós et al. (2012a). For this purpose the following a gas score from I to VI was given to the following vascular locations: fin, opercular, cranial and caudal subcutaneous, swim bladder, and posterior cardinal veins, as well as the ventral and dorsal aorta. For extravascular locations, a gas score from I to III was given, considering visceral fat emphysema of the coelomic cavity and fin emphysema. The gas score of all the locations was summed to obtain a total gas score for each fish.

#### Molecular analyses

Another addition to this study was molecular analyses. Posterior kidney, gills, heart, and ventral aorta samples of 6 GBD group fish and 6 control group fish were collected for gene expression analysis (**Fig. 31**). Samples were rinsed in PBS buffer to remove blood and then placed in cryotubes containing 1 ml each of RNA-later (Sigma-Aldrich, Dorset, UK). These cryotubes were first left for 24 h at 4°C and subsequently frozen at -80°C for proper preservation until RNA extraction. The total number of cryotubes was 48, corresponding to 4 samples for each of the 6-control fish (Control 1 - Control 6) and the 6 GBD fish (GBD 1 - GBD 6).

**Figure 31.** Samples washed in PBS buffer and stored in cryotubes with RNA-latter.



## Gene selection and primer design

The target genes studied in goldfish (*Carassius auratus*) are shown in **Table 1**. To perform real-time quantitative polymerase chain reaction (RT-qPCR), the sequences corresponding to the open reading frame (ORF) of these target genes were selected, aligned and primers were designed for the conserved regions of each one of them using the information provided by the GenBank database (NCBI).

TARGET GENES	GENE ID
Heat Shock Proteins 70 (HSP70)	AB092839
Heat Shock Proteins 90 (HSP90)	LOC113120568
Endothelin-1 (E-1)	LOC113062581
Intercellular Adhesion Molecule 1 (ICAM-1)	LOC113042392

**Table 1.** Target genes to study in experimental fish of the GBD model and their identification.

These primers were ordered from Biotein S.L. (Las Palmas de Gran Canaria, Spain) and are detailed in **Table 2**. Following GeNorm, housekeeping genes were selected and designed to normalize the results obtained from the target genes, considering that these genes are known to maintain a constant and stable expression level in the tissues of an organism. Thus, elongation factor 1 alpha (EF1 $\alpha$ ) and beta 2 microglobin (B2M) were selected.

GENES	PRIMER	SEQUENCE
<b>HSP70</b>	FORWARD PRIMER	ACCTACTCAGACAACCAGCC
	REVERSE PRIMER	CCACTGCCGACACATTTAGG
<b>HSP90</b>	FORWARD PRIMER	GCTTCGAGGTGCTGTACATG
	REVERSE PRIMER	TTGGCCTTGTCTTCCTCCAT
<b>E-1</b>	FORWARD PRIMER	AGCGCTCAGTAACAGAACCT
	REVERSE PRIMER	CGTTGTCTGTTTGTCTGCCA
<b>ICAM-1</b>	FORWARD PRIMER	GGCAGTATCAGCTCCAGTGT
	REVERSE PRIMER	CACACCAGTACTGAGCTCCA
<b>EF1<math>\alpha</math></b>	FORWARD PRIMER	GATTGTTGCTGGTGGTGTG
	REVERSE PRIMER	GCAGGGTTGTAGCCGATTT
<b>B2M</b>	FORWARD PRIMER	GCCCTGTTCTGTGTGCTGTA
	REVERSE PRIMER	AAGGTGACGCTCTTGGTGAG

**Table 2.** Target gene primers and housekeeping gene primers with their respective sequences.

### **Disruption and homogenization with TissueLyser II**

The procedure for RNA extraction from selected tissues (RNeasy Plus Universal Mini Kit-Qiagen, Cat. 73404) was performed with 20-30 mg of each tissue, removing the samples from the tube with RNA-later where they were stored after collection, taking special care to remove excess reagent or possible crystals formed around the tissue.

Each tissue was placed in 2 ml microcentrifuge tubes containing a 5 mm diameter stainless steel beads for tissue disruption, adding 900  $\mu$ l of Qiazol Lysis Reagent per tube at room temperature. The tubes were

then placed in the TissueLyser II (Qiagen, Cat. 85300) microcentrifuge tube adapter sets, activating the equipment for 2-minute periods at 20 Hz. The procedure was repeated several times, varying the positions of the microtubes within the equipment until homogenization was observed. Due to the different characteristics of the selected tissues, the operating times of the TissueLyser II varied, being necessary 3 periods of 2 minutes each for posterior kidney samples, 4 periods for heart and gill samples, and 6 periods for ventral aorta samples.

Once all the contents of the tubes were homogenized, the lysate was pipetted into new microcentrifuge tubes and placed at room temperature for 5 minutes, favoring the dissociation of the nucleoprotein complexes.

The following protocol steps were performed for each sample tube:

1. 100  $\mu$ l of Genomic DNA Removal Solution was added, shaking vigorously for 15 seconds. This step reduces contamination with genomic DNA from the aqueous phase.
2. 180  $\mu$ l of chloroform was added and shaken again vigorously for another 15 seconds to produce a phase separation.
3. The tube was left to stand for 3 minutes at room temperature.
4. Samples were centrifuged at 12000 xg for 15 minutes at 4°C. Three separate phases were obtained as a colorless upper phase or aqueous phase containing the RNA, a white interphase, and a red lower phase known as the organic phase.
5. 600  $\mu$ l of the upper or aqueous phase containing the RNA was transferred to a new microcentrifuge tube and another 600  $\mu$ l of 70% ethanol was added and mixed by pipetting.

6. Once mixed, 700  $\mu$ l of the sample was transferred to a 2 ml collection tube with a RNeasy Mini spin column (Qiagen) placed inside. This tube was centrifuged at 8000 xg for 15 seconds at room temperature.

7. The discharge flow after centrifugation was removed and the tube with the RNeasy Mini spin column was reused, transferring the remaining contents of the tube from step 5, and performing the centrifugation of step 6 again, also removing the subsequent discharge flow.

8. To clean the RNeasy Mini spin column membrane, two ethanol-containing buffers (Buffer RWT and Buffer RPE) provided by the kit used were used. First, 700  $\mu$ l of Buffer RWT was added and the centrifugation of step 6 was repeated. The discharge flow was removed, the column was carefully extracted, and the collection tube was completely emptied, taking special care that the column did not come into contact with the discharge flow during its removal and that no residues remained in the tube.

9. The column was reintroduced into the same empty collection tube and 500  $\mu$ l of Buffer RPE was added, centrifuging again with the conditions of step 6, and removing the post centrifugation discharge flow.

10. A new Buffer RPE pass was performed, again adding 500  $\mu$ l of this buffer and centrifuging at 8000 xg, this time for a longer period of time (2 min) to ensure drying of the RNeasy spin column and to remove possible residual ethanol from the buffers that may interfere with the samples.

11. The discharge flow was then removed, and the column was placed in a new 1.5 ml collection tube, to which 30  $\mu$ l of RNase-free water was added and centrifuged at 8000 xg for 1 minute to elute the

RNA, leaving the contents in the collection tube at  $-80^{\circ}\text{C}$  until next procedure.

### **RNA quantification and quality by spectrophotometry**

The Nanovue Plus spectrophotometer (GE Healthcare), a device that measures, among other functions, the concentration and purity of RNA, DNA, and proteins, was used for RNA quantification and quality control. Prior to the measurement of each sample, nuclease-free water blanks were used. Thus, 2  $\mu\text{l}$  of purified RNA from the collection tube obtained in the previous procedure were pipetted over the sample deposition point in the spectrophotometer, taking special care to avoid introducing bubbles and closing the lid. Along with the sample concentration data (**Table 3**), absorbance values were obtained at a ratio of 260:280, obtaining sample ratios above 1.8, which indicates high purity.

### **Complementary DNA synthesis**

Retroviral reverse transcriptase retrotranscribes a strand of messenger RNA (mRNA) into a single complementary DNA (cDNA). To perform this synthesis, High-capacity cDNA reverse transcription kit of 200 reactions (Thermo Fisher Scientific, Cat. 4368814) was used. To prepare a 20  $\mu\text{l}$  reaction, a 10  $\mu\text{l}$  Reverse Transcription (RT) master mix was made on ice by mixing 2  $\mu\text{l}$  of 10X RT buffer, 0.8  $\mu\text{l}$  of 100mM 25X deoxynucleotide triphosphate (dNTP) mix, 2  $\mu\text{l}$  of 10X RT Random primers and 4.2  $\mu\text{l}$  of nuclease-free water. This mix was prepared for each reaction to be generated.

With the RT master mix prepared, 10  $\mu\text{l}$  of it was pipetted into each well of a 96-well reaction plate and 10  $\mu\text{l}$  of each sample RNA was added, pipetting repeatedly to mix both solutions and discarding the pipette tip after each mix. The plate was sealed and centrifuged briefly to remove possible bubbles formed during mixing and placed on ice.

In addition to samples, negative controls were used where RT master mix was mixed with water instead of RNA as a no-template control (C-NTC) and controls without RT (C-RT-) where RNA from a sample was mixed with an RT master mix with no added retrotranscriptase.

Reverse transcription was then performed by programming the thermal cycler with the following conditions: step 1 at 25°C for 10 minutes; step 2 incubation at 37°C for 120 minutes; step 3 of 85°C for 5 minutes and step 4 at 4°C maintained; and setting the reaction volume to 20 µl, starting the thermal cycler upon insertion of the plate. In addition, the synthesized cDNA products were visualized in 1% agarose gel, applying an electric current of 90 millivolts for 30-35 minutes and using a UV transilluminator (Bio-Rad UV Transilluminator).

### **Quantification of cDNA by fluorometry**

To quantify the cDNA synthesized in the previous step, the Qubit ssDNA Assay kit (Invitrogen, Cat. Q10212) associated to a fluorometer Qubit 3.0 (Invitrogen) was used. Qubit 3.0 is a fluorometric quantification kit for DNA, RNA or proteins that employs probes that selectively bind to each of these molecules. This specific and selective binding to its target RNA, proteins, double-stranded DNA (dsDNA) or single-stranded DNA (ssDNA) as our case, minimizes the effects of contaminants in the sample that may interfere with their quantification. This kit is composed of component A or reagent being dimethyl sulfoxide (DMSO), component B or buffer, component C or standard 1 and component D or standard 2.

First the working solution was prepared by diluting the Qubit ssDNA reagent in Qubit ssDNA buffer with a ratio 1:200, considering that the final maximum amount of all tubes should be 200 µl. Because 10 µl of each standard is used, 190 µl of working solution is added to the

standard tubes, while 1  $\mu\text{l}$  of synthesized cDNA is used in the sample tubes, resulting in the addition of 199  $\mu\text{l}$  of working solution. Each tube was vortexed for 5 seconds, paying special attention not to generate bubbles, and allowed to stand for 2 minutes at room temperature.

First, a standard line or calibration curve is created with the fluorometer reading of the two tubes of standards, which contain known and specific concentrations for each type of molecule to be quantified, ssDNA in this case. After obtaining this calibration curve, the sample tubes with cDNA are read, obtaining results as shown in **Table 3**.

SAMPLES	CODE	TISSUE	RNA CONCENTRATION (ng/ $\mu\text{l}$ ) SPECTROPHOTOMETRY	cDNA CONCENTRATION (ng/ $\mu\text{l}$ ) FLUOROMETRY
Control 1	1700	Heart	189.2	102
Control 2	1701	Heart	107.6	58.8
Control 3	1702	Heart	404	124
Control 4	1703	Heart	56	48.2
Control 5	1704	Heart	303.6	107
Control 6	1705	Heart	44.8	36.8
GBD 1	1706	Heart	76	54.8
GBD 2	1707	Heart	45.2	36.2
GBD 3	1708	Heart	135.6	86.2
GBD 4	1709	Heart	69.6	53
GBD 5	1710	Heart	86	68.2
GBD 6	1711	Heart	140.8	77
Control 1	1712	V. Aorta	65.2	42
Control 2	1713	V. Aorta	98.4	64.4
Control 3	1714	V. Aorta	77.6	52.6
Control 4	1715	V. Aorta	112	83.4
Control 5	1716	V. Aorta	19.6	25.2
Control 6	1717	V. Aorta	197.6	116
GBD 1	1718	V. Aorta	70	59.4
GBD 2	1719	V. Aorta	136	106
GBD 3	1720	V. Aorta	472.8	121

Comparative study of gas-bubble lesions using experimental models

SAMPLES	CODE	TISSUE	RNA CONCENTRATION (ng/ $\mu$ l) SPECTROPHOTOMETRY	cDNA CONCENTRATION (ng/ $\mu$ l) FLUOROMETRY
GBD 4	1721	V. Aorta	82.4	65.8
GBD 5	1722	V. Aorta	170	105
GBD 6	1723	V. Aorta	103.2	88.8
Control 1	1724	P. Kidney	1558	130
Control 2	1725	P. Kidney	1347	117
Control 3	1726	P. Kidney	1976	147
Control 4	1727	P. Kidney	1170	92.8
Control 5	1728	P. Kidney	1526	102
Control 6	1729	P. Kidney	1404	124
GBD 1	1730	P. Kidney	2238	139
GBD 2	1731	P. Kidney	1593	120
GBD 3	1732	P. Kidney	1318	108
GBD 4	1733	P. Kidney	2144	121
GBD 5	1734	P. Kidney	1556	119
GBD 6	1735	P. Kidney	1390	116
Control 1	1736	Gills	1964	88.6
Control 2	1737	Gills	1903	97
Control 3	1738	Gills	621	55.6
Control 4	1739	Gills	1006	67
Control 5	1740	Gills	1953	87
Control 6	1741	Gills	1412	69.8
GBD 1	1742	Gills	938	55.6
GBD 2	1743	Gills	716.8	49.4
GBD 3	1744	Gills	916.8	46.4
GBD 4	1745	Gills	1088	71.6
GBD 5	1746	Gills	1353	57
GBD 6	1747	Gills	1878	75

**Table 3.** RNA concentrations measured by spectrophotometry and cDNA concentration by fluorometry of each sample.

### qPCR optimization with gene-specific primers

The QuantStudio 12K Flex Real-Time PCR System (Applied Biosystem) was used to adjust the amplification conditions, setting the concentrations of the primer pairs used as well as the PCR reaction program. TB Green Premix Ex Taq II kit (TII RNaseH PLus, Takara, Cat. RR820A) was used. This kit includes Takara Ex Taq HS DNA polymerase, a DNA polymerase characterized as a hot-start PCR enzyme that prevents the amplification of non-specific fragments or anomalous formations, performing a highly sensitive detection. The PCR amplifies a target sequence from a minimal portion of DNA. The procedure consists of repetitive cycles of denaturation of the DNA strand, banding of the designed primers to the corresponding fragment and elongation causing the DNA polymerase to synthesize new DNA strands from the banded primers.

To monitor DNA amplification in real time, this kit provides an intercalating agent, in this case TB Green, a fluorescent molecule that binds to the DNA double strand and produces fluorescence, which allows monitoring the amplified DNA by melting curve analysis (**Fig. 32**).

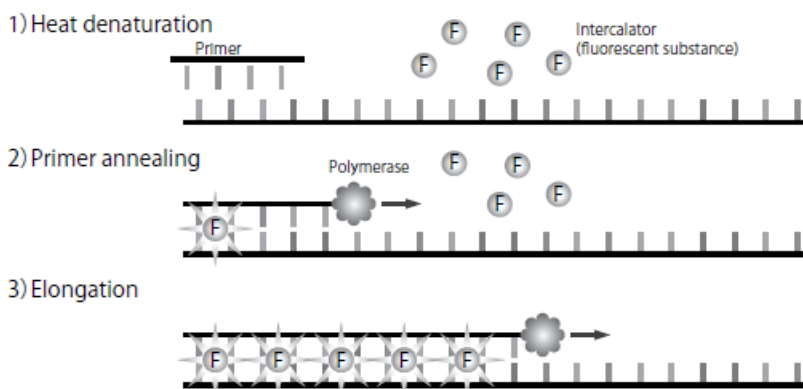


**Figure 32.** Performance of the TB Green PCR kit.

To calculate the efficiency of primers, 1:10 dilutions of the cDNA (at 20ng, 2 ng, and 0.2 ng concentration) were performed. The PCR program was set up with the following temperatures and times. The initial denaturation phase was set at 95°C for 30 seconds, followed by the PCR phase, carrying out 40 cycles consisting of a first denaturation step at 95°C for 5 seconds and continued by a banding temperature step at 62°C for 1 minute. Finally, the melting curve was performed in 3 steps, the first at 95°C for 15 seconds, the second at 62°C for 1 minute and finally step 3 or dissociation at 95°C for 15 seconds.

The amplification efficiencies of the primer pairs detected were given as valid between 90-110%, obtaining for each gene the efficiency percentages described in **Table 4**.

GENES	SLOPE	R <sup>2</sup>	EFFICIENCY (%)
<b>HSP70</b>	-3.185	0.992	106.7
<b>HSP90</b>	-3.293	0.998	101.2
<b>E-1</b>	-3.286	0.99	101.51
<b>ICAM-1</b>	-3.129	0.98	105.74
<b>EF1<math>\alpha</math></b>	-3.489	0.992	93.48
<b>B2M</b>	-3.235	0.999	103.74

**Table 4.** Efficiency and correlation (R<sup>2</sup>) of the melting curves for each gene.

### Quantification of samples by Real Time quantitative PCR (RT-qPCR)

After the specific primer pair for each gene (target and housekeeping genes) was set up, the amplification of each gene was carried out for each of the 48 samples. In addition, each cDNA sample was amplified by performing 3 technical replicates. Negative controls (C-NTC and C-RT-) were also included in each PCR, distributing the 96 well-plates for each gene (**Fig. 33**). The total volume prepared for each sample well was 10  $\mu$ l, being 1  $\mu$ l of cDNA to be analyzed, 5  $\mu$ l of TB Green Premix Ex Taq II, 0.2  $\mu$ l ROX Reference Dye II (50X, supplied in the kit), 0.2  $\mu$ l of forward and reverse specific primers for each gene and 3.4  $\mu$ l of ddH<sub>2</sub>O. The amplification programs were set as mentioned above.

	1	2	3	4	5	6	7	8	9	10	11	12
<b>A</b>	1700	1700	1700	1708	1708	1708	1716	1716	1716			NTC
<b>B</b>	1701	1701	1701	1709	1709	1709	1717	1717	1717			
<b>C</b>	1702	1702	1702	1710	1710	1710	1718	1718	1718			NTC
<b>D</b>	1703	1703	1703	1711	1711	1711	1719	1719	1719			
<b>E</b>	1704	1704	1704	1712	1712	1712	1720	1720	1720			RT-
<b>F</b>	1705	1705	1705	1713	1713	1713	1721	1721	1721			
<b>G</b>	1706	1706	1706	1714	1714	1714	1722	1722	1722			RT-
<b>H</b>	1707	1707	1707	1715	1715	1715	1723	1723	1723			

**Figure 33.** 96 well-plates with the distribution of each sample and of the positive and negative controls.

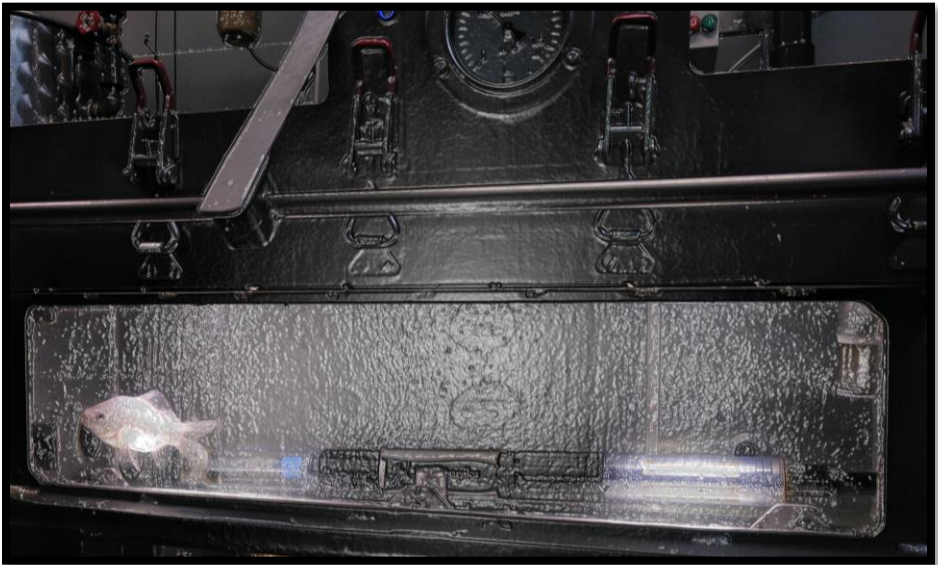
Gene quantification results obtained from RT-qPCR were analyzed using Design & Analysis Software v.2.4.3 (Thermo Fisher Scientific). Cycle threshold (Ct) values were obtained using the automatic baseline and applied to all amplicons of the same primer set. The fold change in expression of target genes (HSP70, HSP90, E-1,

ICAM-1) were normalized with values of RNA content from reference genes (EF2 $\alpha$ , B2M) and calculated using the  $2^{-\Delta C_t}$  method (Livak and Schmittgen, 2001).

### **Statistical analysis**

Statistical analyses were performed to analyze differences in biomarker gene concentration between control and GBD fish and were carried out with the SPSS software package (SPSS version 29 for Windows, IBM). Analyses were performed at a significance level of 5% ( $p$  value  $<0.05$ ) and data with significance level of 10% ( $p$  value  $<0.1$ ) were also considered. To determine whether to use parametric or nonparametric statistical tests, first, the homogeneity of variance and normal distribution of the data was studied. The requirements for parametric tests were not met so data were analyzed by a non-parametric test: Kruskal-Wallis's test. Primers at given locations that showed statistical significance ( $p <0.05$ ) or near statistical significance ( $p <0.1$ ) were further explored for correlation with the total gas score of each of the 6 GBD fish. For this correlation, Spearman's correlation coefficient was used, and the data were analyzed with R software package (version 3.3.1; R Development Core Team) for Windows.

## 4. SCIENTIFIC PUBLICATIONS





# I. Decompressive pathology in cetaceans based on an experimental pathological model

**Velázquez-Wallraf, A.,** Fernández, A., Caballero, M.J., Møllerløkken, A., Jepson, P.D., Andrada, M., & Bernaldo de Quirós, Y. (2021). Decompressive pathology in cetaceans based on an experimental pathological model. *Frontiers in Veterinary Science*, 8, 676499. <https://doi.org/10.3389/fvets.2021.676499>





# Decompressive Pathology in Cetaceans Based on an Experimental Pathological Model

Alicia Velázquez-Wallraf<sup>1</sup>, Antonio Fernández<sup>1</sup>, María José Caballero<sup>1\*</sup>, Andreas Møllerløkken<sup>2</sup>, Paul D. Jepson<sup>3</sup>, Marisa Andrada<sup>1\*</sup> and Yara Bernaldo de Quirós<sup>1</sup>

<sup>1</sup> Veterinary Histology and Pathology, Atlantic Center for Cetacean Research, University Institute of Animal Health and Food Safety (IUSA), Veterinary School, University of Las Palmas de Gran Canaria, Canary Islands, Spain, <sup>2</sup> Faculty of Engineering, Norwegian University of Science and Technology, NTNU, Trondheim, Norway, <sup>3</sup> Institute of Zoology, Zoological Society of London, London, United Kingdom

## OPEN ACCESS

### Edited by:

Stephen Raverty,  
Animal Health Center, Canada

### Reviewed by:

Weigang Xu,  
Naval Medical University, China  
Sophie Dennison,  
TeleVet Imaging Solutions, PLLC,  
United States  
Claudia Kusmic,  
Italian National Research Council, Italy

### \*Correspondence:

María José Caballero  
mariejose.caballero@ulpgc.es  
Marisa Andrada  
marisaana.andrada@ulpgc.es

### Specialty section:

This article was submitted to  
Veterinary Experimental and  
Diagnostic Pathology,  
a section of the journal  
Frontiers in Veterinary Science

**Received:** 05 March 2021

**Accepted:** 26 April 2021

**Published:** 08 June 2021

### Citation:

Velázquez-Wallraf A, Fernández A,  
Caballero MJ, Møllerløkken A,  
Jepson PD, Andrada M and Bernaldo  
de Quirós Y (2021) Decompressive  
Pathology in Cetaceans Based on an  
Experimental Pathological Model.  
Front. Vet. Sci. 8:676499.  
doi: 10.3389/fvets.2021.676499

Decompression sickness (DCS) is a widely known clinical syndrome in human medicine, mainly in divers, related to the formation of intravascular and extravascular gas bubbles. Gas embolism and decompression-like sickness have also been described in wild animals, such as cetaceans. It was hypothesized that adaptations to the marine environment protected them from DCS, but in 2003, decompression-like sickness was described for the first time in beaked whales, challenging this dogma. Since then, several episodes of mass strandings of beaked whales coincidental in time and space with naval maneuvers have been recorded and diagnosed with DCS. The diagnosis of human DCS is based on the presence of clinical symptoms and the detection of gas embolism by ultrasound, but in cetaceans, the diagnosis is limited to forensic investigations. For this reason, it is necessary to resort to experimental animal models to support the pathological diagnosis of DCS in cetaceans. The objective of this study is to validate the pathological results of cetaceans through an experimental rabbit model wherein a complete and detailed histopathological analysis was performed. Gross and histopathological results were very similar in the experimental animal model compared to stranded cetaceans with DCS, with the presence of gas embolism systemically distributed as well as emphysema and hemorrhages as primary lesions in different organs. The experimental data reinforces the pathological findings found in cetaceans with DCS as well as the hypothesis that individuality plays an essential role in DCS, as it has previously been proposed in animal models and human diving medicine.

**Keywords:** gas bubble, stranded cetaceans, pathology, rabbit model, decompression sickness

## INTRODUCTION

Decompression sickness (DCS) is a widely known clinical syndrome in human medicine, mainly in recreational and professional divers. It is considered to occur when the sum of the gases dissolved in the tissues exceeds the environmental pressure, causing the formation of intravascular and extravascular gas bubbles. The presence of gas embolism as noted by ultrasound must be observed for its confirmatory clinical diagnosis. In these cases, the patient is treated with a hyperbaric chamber. If the gas and the symptoms resolve, the diagnosis of DCS is definitive (1). In forensic

investigations, gas bubble-related lesions are the main findings (2, 3). These bubbles can result in mechanical, biochemical, and embolic damage with different severity levels depending on their number and their size (1). The respiratory system is the most affected organ by DCS when the amount of bubbles exceeds the pulmonary capillaries' capacity to eliminate them, resulting in severe lung damage (4).

Cetaceans are mammals that returned to the marine environment 60 million years ago and have developed behavioral, anatomical, and physiological adaptations for this new habitat, including those related to diving (5). It was hypothesized that these adaptations protected them from possible DCS, but in 2003, lesions compatible with DCS were described for the first time in beaked whales stranded coincidentally in time and space with naval exercises using high-intensity and mid-frequency active sonars (6, 7). This first description of a decompression-like sickness in beaked whales broke the dogma that cetaceans were immune to this disease (7). These findings have also been found in other beaked whale (BW) strandings associated with naval maneuvers (8–11) as well as in Risso's dolphins but, in this case, were caused naturally due to an interaction with their preys during feeding (12). Gas embolism and decompression-like sickness have also been described in other wild animals such as sea turtles (13).

In cetaceans, the diagnosis of DCS is limited to forensic investigations and its pathological gas bubble-associated lesions since a clinical diagnosis is not possible due to obvious logistical and ethical restrictions. For this reason, it is necessary to resort to experimental animal models to contrast the macroscopic and microscopic lesions and to support the pathological diagnosis described in marine mammals affected by DCS. To our knowledge, there are very few publications focused on the pathological study of DCS in humans or other species (14–17), and almost all the articles on animal experimentation focus on the analysis of specific tissues for the application of preventive treatments in DCS (4, 18–20). Furthermore, there is no pathological comparative study showing gross and histological findings in experimental and natural DCS. Therefore, the objective of this study is to validate the pathological results of cetaceans through an experimental model wherein a complete and detailed histopathological analysis is performed. For this purpose, an experimental rabbit model was performed in which severe DCS is reproduced, presenting the pathological results in these animals and then comparing them with the pathological findings in cetaceans.

## MATERIALS AND METHODS

For this study, 18 males of New Zealand white rabbits of  $3.15 \pm 0.65$  kg were used. These animals were divided into compression/decompression model (C/D) ( $n = 14$ ) and control group (C) ( $n = 4$ ).

All experiments were accomplished following the European Union's laboratory animals' regulation and were conducted under surgical anesthesia: subcutaneous injections of medetomidine (0.5 mg/kg) and ketamine (25 mg/kg). The

C/D model was carried out in the experimental animal facilities of St. Olav University Hospital NTNU, Norway (Trondheim, Norway), and the Norwegian Committee for Animal Experiments approved the protocol (2154). The control group was carried out in the experimental animal facilities of Dr. Negrin University Hospital (Las Palmas de Gran Canaria, Spain), and the Ethical Committee for Animal Experiments of the University of Las Palmas de Gran Canaria approved the protocol (CEEBA-HUGCDN 002/2010).

### The Compression/Decompression Model

The rabbits were anesthetized with the protocol described above and compressed in pairs in a dry, hyperbaric chamber (Animal Chamber System, NUT, Haugesund, Norway) with a diving profile selected to induce severe decompression stress with excessive amounts of intra-corporal gas formation: eight absolute atmospheres during 45 min, followed by fast decompression (0.33 m/s) to one atmosphere (21). One animal appeared dead when recovered from the chamber, and it remains unclear at what time during the treatment the animal died; thus, it was withdrawn from the study. The animals were monitored for 1 h after decompression. A group of animals ( $n = 8$ ) died within 25 min post-decompression (C/D mortality group), while the rest ( $n = 5$ ) survived the observation period of 1 h and were euthanized with an intraperitoneal injection of diluted pentobarbital (200 mg/kg) (C/D euthanized group).

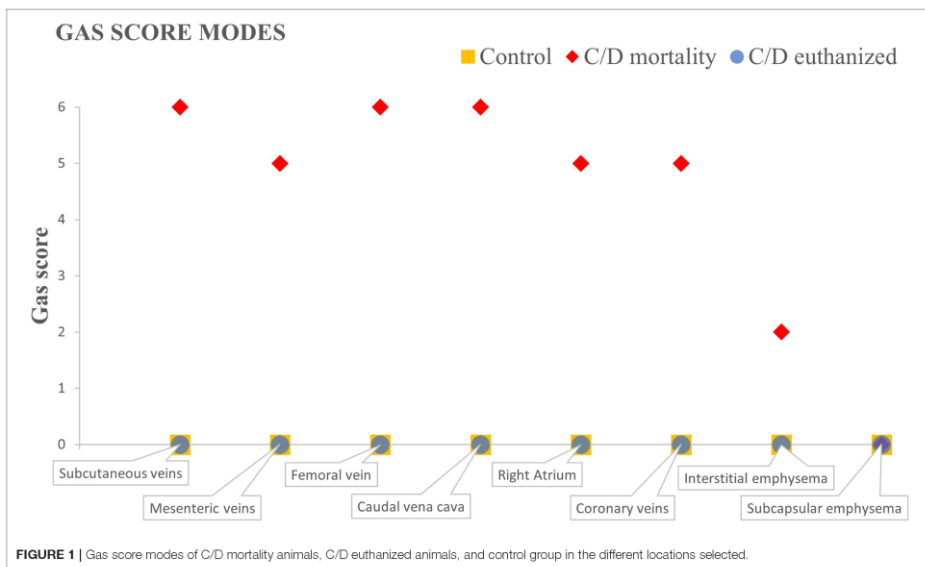
### Control Group

The rabbits were first anesthetized with the protocol described above and later euthanized with an intraperitoneal injection of diluted pentobarbital (200 mg/kg) as in the C/D euthanized group.

### Pathological Study

Necropsy was carried out for each rabbit in a dorsal decubitus position. Dissection was carefully done to avoid severing large blood vessels following the method of Bernaldo de Quirós et al. (22) to characterize the presence of intravascular and extravascular gas bubbles using a gas score index. This index-based method consists of giving a gas score from 0 to 6 for each of the defined vascular locations (i.e., subcutaneous veins, femoral veins, mesenteric veins, caudal vena cava, coronary veins, and to the right atrium) and a gas score from 0 to 3 to describe the presence and distribution of extravascular gas (i.e., subcapsular and interstitial emphysema) that may affect different organs. The sum of the gas score of each intravascular and extravascular location calculates the total gas score in each rabbit. In the current study, the mode of each group for intra- and extravascular locations has been calculated.

Representative samples of the lung, trachea, superficial cervical lymph node, spleen, central nervous system, heart, liver, stomach, small and large intestine, mesenteric lymph node, kidney, urinary bladder, and skeletal muscle (gastrocnemius) were collected and fixed in 10% buffered formalin. These tissues were processed routinely and embedded in paraffin wax, and 5- $\mu$ m-thick sections were cut and stained with hematoxylin and eosin (23)



for microscopic analysis. Histological sections from the heart and skeletal muscle were also stained with phosphotungstic acid hematoxylin and Masson's trichrome (23), respectively, to evidence changes in skeletal and cardiac musculature.

### Comparison With Cetacean Decompressive Pathology

The histopathological results from the animal model were compared with the necropsy reports and histology slides from stranded cetaceans that have been studied and diagnosed with DCS by our research group. This included 31 animals: eight Cuvier's BWs (*Ziphius cavirostris*), one Blainville's BW (*Mesoplodon densirostris*), one Gervais's BW (*Mesoplodon europaeus*) stranded in the islands of Fuerteventura and Lanzarote (Spain) in 2002 (7); four Cuvier's BWs stranded on these same islands in 2004 (8); four Cuvier's BWs stranded in 2006 and one Cuvier's BWs stranded in 2011, both in Almeria (Spain) (9, 10); 10 Cuvier's BW mass stranding in Corfú (Greece) in 2011 (11), all of them coincidental in time and space with naval exercises; and two Risso's dolphins (*Grampus griseus*) that were diagnosed with a decompressive disease after an interaction with a prey (12). Since the pathological results of these animals have already been published, the comparison with the original pathological results from this study will be addressed in the Discussion section.

## RESULTS

### Presence, Distribution, and Amount of Bubbles

Rabbits from the control group presented very few or an absence of gas bubbles. One animal presented few gas bubbles in the mesenteric veins, occasional bubbles in the subcutaneous veins, and scarce bubbles in the adipose tissue (total gas score: 4). One more animal presented only occasional gas bubbles in the mesenteric veins (total gas score: 1). These results were previously reported by Bernaldo de Quirós et al. (22). The resulting gas score mode calculated in this study for all locations was 0 (Figure 1) since the two remaining animals showed no bubbles.

In rabbits from the C/D mortality group, gas bubbles were observed in abundant numbers and/or filling complete vessel sections in the subcutaneous veins, the femoral veins, the mesenteric veins (Figure 2E), the caudal vena cava, the right atrium (Figure 2C), and the coronary veins. In addition, a sparse or moderate presence of subcapsular and interstitial emphysema was observed. The gas score mode in the subcutaneous veins, the femoral vein, and the caudal vena cava was 6, while the mesenteric and the coronary veins, along with the right atrium, had a gas score mode of 5 (Figure 1). The gas score mode for interstitial emphysema in this group was 2, while that of subcapsular emphysema was 0. The total gas score ranged from 29 to 40 (22). Additionally, large amounts of gas bubbles were found disseminated through other vascular locations.

Gas bubbles were not found in the C/D euthanized group, with a total gas score of 0 in all animals and a gas score mode for all locations of 0 (22).

## Gross Examination and Histopathology

### Control Group

Gross findings in this group showed congestion in different organs, such as lung (3/4, 75%), liver (3/4, 75%), kidney (3/4, 75%), spleen (2/4, 50%), and brain (1/4, 25%), and mild multifocal petechial hemorrhages in thymus (3/4, 75%). These findings were confirmed histologically. No other histopathological findings were observed, except hyper eosinophilia (2/4, 50%) and vacuolization (2/4, 50%) in muscular cardiac fibers and vacuolization of hepatocytes (1/4, 25%).

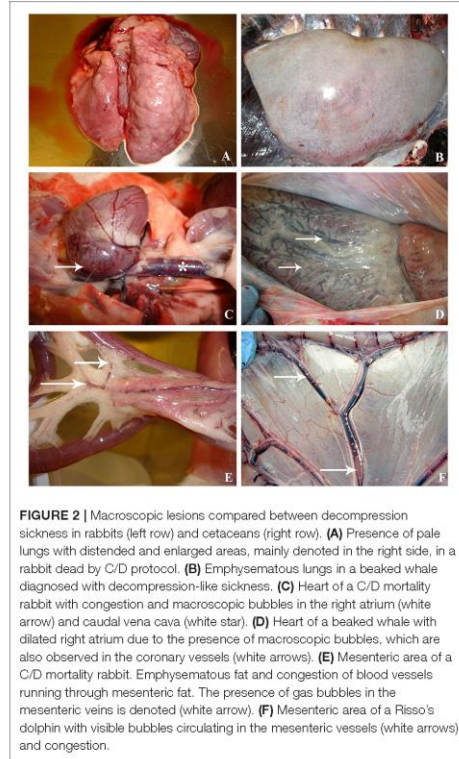
### C/D Model: Mortality Group

Emphysema was the predominant lesion observed in the lung of C/D mortality animals (6/8, 75%), with grossly voluminous, pale, and gas-distended pulmonary areas (Figure 2A). Other lung findings were congestion (3/8, 38%) and alveolar edema evidenced by exudation of fluid from the cut surface (2/8, 25%). The lung's microscopic appearance showed mild to severe emphysema in all animals (8/8, 100%). Besides these, mild pulmonary congestion (7/8, 88%) and alveolar hemorrhages ranging from mild focal hemorrhages to severe multifocal hemorrhages (4/8, 50%) as well as microscopic intravascular bubble-like round empty spaces surrounded by blood cells (3/8, 38%) were observed (Figure 3A).

Marked subcapsular splenic emphysema was observed (3/8, 38%). Histological emphysema was confirmed in six out of eight animals (75%). Gross cavities underneath the splenic capsule and within splenic parenchyma were observed microscopically along with mild splenic congestion (7/8, 88%). Cerebral congestion was seen in four cases of C/D mortality animals (4/8, 50%), and two animals showed, microscopically, mild local to extensive hemorrhages in the meningeal area and around cerebral capillaries (2/8, 25%) (Figure 3E).

The most relevant finding in the heart was the presence of hemorrhages, mainly in the right ventricle, in the group of C/D mortality animals (3/8, 38%). Mild hemorrhages were confirmed microscopically (4/8, 50%) (Figure 3C), while two showed bubble-like cavities in cardiac capillaries (2/8, 25%). Acute changes such as mild hyaline changes of muscle fibers as well as hyper eosinophilia and mild intracytoplasmic vacuolization of injured cardiomyocytes were observed in seven animals out of eight (88%). In contrast, contraction band fibers were detected in only one animal (1/8, 13%). Cardiac muscle fibers were separated by expanded interstitial spaces filled with pale pink material, indicating mild interstitial edema (3/8, 38%).

In the liver of C/D mortality animals, mild hepatomegaly and general congestion were the main gross findings (5/8, 63%). Histologically, moderate congestion was confirmed by the distention of central veins and sinusoids. Mild vacuolization of centrilobular hepatocytes with cytoplasmic ballooning of these cells was also observed (4/8, 50%). Renal congestion was also



found in this group (4/8, 50%). Microscopic vascular bubble-like cavities were also observed (2/8, 25%).

Other findings in this group were emphysema (7/8, 88%) and vascular congestion (4/8, 50%) associated with the adipose tissue. At the microscopic analysis of this group's skeletal muscle, acute changes such as mild hyper eosinophilia were found in seven animals out of eight (88%) as well as interfibrillar mild interstitial edema (4/8, 50%).

### C/D Model: Euthanized Group

The lung of C/D euthanized animals showed emphysema (2/5, 40%), while edema was present in one animal of five (20%). Histologically, 100% of animals presented mild lung emphysema, mild congestion (3/5, 60%), and multifocal alveolar hemorrhages (1/5, 20%). While splenic subcapsular emphysema was only macroscopically observed in one animal (1/5, 20%) and congestion in two animals (2/5, 40%), the microscopic analysis revealed mild splenic congestion in 100% of animals (5/5, 100%) and subcapsular and parenchymal emphysema in 80% of animals

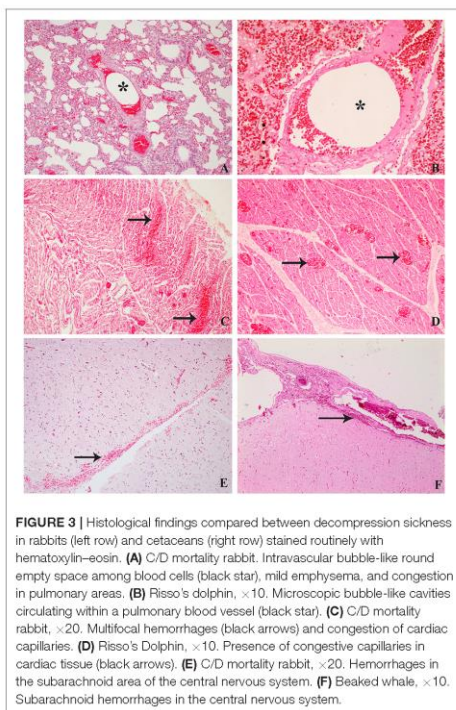


**FIGURE 3 |** Histological findings compared between decompression sickness in rabbits (left row) and cetaceans (right row) stained routinely with hematoxylin–eosin. **(A)** C/D mortality rabbit. Intravascular bubble-like round empty space among blood cells (black star), mild emphysema, and congestion in pulmonary areas. **(B)** Risso's dolphin,  $\times 10$ . Microscopic bubble-like cavities circulating within a pulmonary blood vessel (black star). **(C)** C/D mortality rabbit,  $\times 20$ . Multifocal hemorrhages (black arrows) and congestion of cardiac capillaries. **(D)** Risso's Dolphin,  $\times 10$ . Presence of congestive capillaries in cardiac tissue (black arrows). **(E)** C/D mortality rabbit,  $\times 20$ . Hemorrhages in the subarachnoid area of the central nervous system. **(F)** Beaked whale,  $\times 10$ . Subarachnoid hemorrhages in the central nervous system.

(4/5). In the brain, gross and microscopic congestion was found (2/5, 40%).

The heart showed no gross lesions in this group, whereas acute cardiomyocyte changes, intracytoplasmic vacuolization, and hyper eosinophilia were detected microscopically in 100% of animals (5/5). Mild congestion (2/5, 40%), mild hemorrhages (2/5, 40%) as well as mild interstitial edema (1/5, 20%) were also observed in this group.

Hepatic congestion was present in four animals out of five (80%) in this group and mild congestion (5/5, 100%) with mild hepatocytic vacuolization (3/5, 60%). Renal congestion was observed in 40% (2/5), while congestion was observed in 100% (5/5), with intravascular bubble-like cavities in 60% of the animals (3/5).

Other findings in this group were congestion of the adipose tissue (2/5, 40%) and muscle fiber hyper eosinophilia as well as wavy fibers in two animals (2/5, 40%).

### Comparative Results

As shown in **Figure 1**, where the different gas score modes of each group are represented, both the control and the C/D euthanized

animals do not present macroscopic bubbles in any defined location for the gas score. The C/D mortality group presents bubbles in all locations, varying between abundant number of bubbles and completely filling vessel sections, except the presence of few bubbles leading to interstitial emphysema and the absence of subcapsular emphysema.

As shown in **Tables 1, 2**, the presence of microscopic bubble-like cavities was another finding also observed with greater incidence in the group of C/D mortality, with these bubbles observed in capillaries and small-sized blood vessels of the lung (38%), the heart (25%), and the kidney (25%). In the C/D euthanized group, the presence of these microscopic bubble-like cavities was lower in kidney, although with a relevant percentage (60%).

Pulmonary and splenic emphysema was observed in both groups. Emphysema in the adipose tissue was only seen in the C/D mortality group. Hemorrhages were more prevalent in different organs of the C/D mortality group, with hemorrhages present in the lung (50%), heart (50%), and brain (25%). The C/D euthanized group presented lower hemorrhages in the lung (20%) and heart (40%). No hemorrhages were seen in the brain.

Other relevant lesions observed were interfibrillar edema in cardiac (38% in C/D mortality and 20% in C/D euthanized) and skeletal muscles (50% in C/D mortality group) as well as hyper eosinophilia in these fibers (88% in C/D mortality group and 40% in C/D euthanized group). Congestion was seen in most of the organs in all groups.

### DISCUSSION

The main pathological finding in rabbits that died by experimental compression/decompression was the presence of a large amount of gas bubbles widely distributed throughout both the central and peripheral venous circulation. Emphysema (mainly in the lung, spleen, and adipose tissue) and hemorrhages in the lung, heart, and brain were the second main gross and histological finding in those rabbits. These pathological findings have also been described in beaked whales (Family *Ziphiidae*) and Risso's dolphins (*Grampus griseus*) that died of decompression-like sickness (7–12) (**Figure 3D**). Nevertheless, these lesions were absent in the rabbits that survived for 1 h after decompression.

The abundance, distribution, and gas composition of the animals from this study have been previously described in detail by Bernaldo de Quirós et al. (21). Thus, we will only briefly summarize those results here in order to compare them with the results from cetaceans. Macroscopic gas was observed massively and systematically distributed in rabbits that died due to a compression/decompression protocol. These results are in agreement with other studies such as those of Eggleton et al. (14), Lever et al. (16), or Shim et al. (17), carried out with guinea pigs, mice, and rabbits, respectively. In stranded cetaceans, the abundance and distribution of macroscopic gas were also analyzed in the two stranded Risso's dolphins diagnosed with a decompression-like sickness as the cause of death, being also systemically distributed (12) (**Figures 2D,F**).

# Comparative study of gas-bubble lesions using experimental models

**TABLE 1 |** Macroscopic findings in each group of rabbits and organs.

	Lung				Heart	Thymus	Liver	Kidney	Spleen		Brain		Fat
	Congestion	Edema	Emphysema	Pneumonia	Hemorrhages	Petechiae	Congestion	Congestion	Congestion	Emphysema	Congestion	Congestion	Emphysema
C/D Mortality	3/8 (38%)	2/8 (25%)	6/8 (75%)	1/8 (13%)	3/8 (38%)	0/8 (0%)	5/8 (63%)	4/8 (50%)	1/8 (13%)	3/8 (38%)	4/8 (50%)	4/8 (50%)	7/8 (88%)
C/D Euthanized	0/5 (0%)	1/5 (20%)	2/5 (40%)	0/5 (0%)	0/5 (0%)	0/5 (0%)	4/5 (80%)	2/5 (40%)	2/5 (40%)	1/5 (20%)	2/5 (40%)	2/5 (40%)	0/5 (0%)
Control	3/4 (75%)	0/4 (0%)	0/4 (0%)	1/4 (25%)	0/4 (0%)	3/4 (75%)	3/4 (75%)	3/4 (75%)	2/4 (50%)	0/4 (0%)	1/4 (25%)	0/4 (0%)	0/4 (0%)

**TABLE 2 |** Microscopic findings in each group of rabbits and organs.

	Lung							Heart						
	Bubble-like cavities	Congestion	Edema	Emphysema	Hemorrhages	Pneumonia	Thrombi	Bubble-like cavities	Congestion	Contraction band necrosis	Edema	Hemorrhages	Hyper-eosinophilia	Vacuolization
C/D mortality	3/8 (38%)	7/8 (88%)	0/8 (0%)	8/8 (100%)	4/8 (50%)	1/8 (13%)	0/8 (0%)	2/8 (25%)	7/8 (88%)	1/8 (13%)	3/8 (38%)	4/8 (50%)	7/8 (88%)	7/8 (88%)
C/D euthanized	0/5 (0%)	3/5 (60%)	0/5 (0%)	5/5 (100%)	1/5 (20%)	0/5 (0%)	0/5 (0%)	0/5 (0%)	2/5 (40%)	0/5 (0%)	1/5 (20%)	2/5 (40%)	5/5 (100%)	5/5 (100%)
Control	0/4 (0%)	3/4 (75%)	0/4 (0%)	0/4 (0%)	0/4 (0%)	1/4 (25%)	0/4 (0%)	0/4 (0%)	1/4 (25%)	0/4 (0%)	0/4 (0%)	0/4 (0%)	2/4 (50%)	2/4 (50%)

	Liver		Kidney		Spleen		Brain		Skeletal muscle		
	Congestion	Vacuolization	Bubble-like cavities	Congestion	Congestion	Emphysema	Congestion	Hemorrhages	Edema	Hyper-eosinophilia	Wavy fibers
C/D mortality	5/8 (63%)	4/8 (50%)	2/8 (25%)	8/8 (100%)	7/8 (88%)	6/8 (75%)	4/8 (50%)	2/8 (25%)	4/8 (50%)	7/8 (88%)	1/8 (13%)
C/D euthanized	5/5 (100%)	3/5 (60%)	3/5 (60%)	5/5 (100%)	5/5 (100%)	4/5 (80%)	2/5 (40%)	0/5 (0%)	0/5 (0%)	2/5 (40%)	2/5 (40%)
Control	1/4 (25%)	1/4 (25%)	0/4 (0%)	3/4 (75%)	3/4 (75%)	0/4 (0%)	0/4 (0%)	0/4 (0%)	0/4 (0%)	0/4 (0%)	0/4 (0%)

Microscopic bubble-like cavities (i.e., small round to oval non-staining spaces that sometimes displaced erythrocytes) were observed within blood capillaries and small vessels from the lung, heart, and kidneys of the rabbits that died after decompression as well as in the kidney of animals that survived decompression and were euthanized. Microscopic gas embolism in the lung small pulmonary arteries, capillaries, and veins has been previously described, such as that of Geng et al. (4) in decompressed rabbits. L'Abbate et al. (24) also described microscopic bubbles in hepatic sinusoids from rats. In cetaceans diagnosed with a decompression-like sickness as the cause of death, abundant microscopic gas embolism was observed in renal capillaries, subcapsular veins, hepatic sinusoids, and pulmonary (Figure 3B), coronary, intestinal, and meningeal vessels (7, 10, 12).

These microscopic lesions were also observed in cetaceans, disrupting the white matter structure of the brain and spinal cord (7, 8). Similarly, micro-bubbles in the nervous system have been described in human medicine, being primarily seen in the spinal cord (25). It has been hypothesized that the low vascular supply and the high lipid content of the spinal white matter, conferred by the myelin that covers the axons, increase the affinity of inert gases for this structure (26). Thus, most CNS lesions are described in the spinal cord's white matter, such as punctured hemorrhages, spongiosis, axon swelling, and myelin degeneration (27). Microscopic bubble-like cavities were not observed in the brain or cranial spinal cord of the rabbits, but only the cranial part of the spinal cord was sampled. Future studies should aim at investigating the entire spinal cord.

Gas composition analysis of the gas embolism was performed in the rabbits of this study (21) and in some of the cetaceans diagnosed with a decompression-like sickness. These included a beaked whale stranded in association with naval exercises (11) and Risso's dolphins after a deadly prey interaction (12). In all cases, nitrogen was the main compound, followed by CO<sub>2</sub>. Hydrogen, a putrefaction marker, was absent or present in low quantities.

The most affected organ in all the rabbits from the C/D model was the lung. Mild to severe pulmonary emphysema was observed in all of them, while no control rabbits showed pulmonary emphysema. Similar results have been observed in other animal models of decompressive sickness with rats and rabbits (4, 19, 20, 28) as well as in mass stranded beaked whales associated with military exercises and in single stranded Risso's dolphins analyzed in this comparative study (7, 12) (Figure 2B).

Emphysema in other locations, such as the spleen and the adipose tissue of the abdominal cavity and mesenteric areas, was also observed in rabbits. Although splenic emphysema was observed to be affecting both groups in the C/D model, the severity was more critical in the rabbits that died after decompression, with severe emphysematous spleens vs. the mild emphysema of the spleens of rabbits that survived decompression and were euthanized. Clay (15) also described that half of the dogs analyzed presented macroscopic and microscopic gas in the spleen, which sometimes displaced the splenic follicles.

The adipose tissue (i.e., mesenteric, abdominal, and coronary fat depots) presented mild multifocal emphysema in most rabbits

that died after decompression. Since nitrogen is more soluble in fatty tissues than in non-fat tissues (17), the relevant presence of bubbles within the adipose tissue in animals that have died by DCS was probably a macroscopic finding to be considered in the assessment of this disease. In the case of the cetaceans diagnosed with DCS, emphysema in the adipose tissue was evident in most cases, being more evident in the coronary fatty deposits and beneath the renal capsule (7, 12).

Another relevant injury found in the rabbits that died after decompression was hemorrhages in different organs. Bubbles can cause vasoconstriction, leading to the presence of ischemia, edema, and hemorrhages in target organs such as the lung (3). Severe pulmonary hemorrhages were present in the rabbits that died from compression–decompression than those that survived decompression after 1 h. Pulmonary hemorrhages have also been described in rats (19, 29), rabbits (4), and stranded cetaceans with pathological signs of DCS (7, 12).

The beaked whales in the mass strandings were all diagnosed with decompressive-like sickness (7, 8) that showed macroscopically acute disseminated hemorrhages in different organs, being especially severe in the CNS. These multifocal hemorrhages were mainly in subarachnoid areas, spinal cord, and meninges (Figure 3F). These findings are similar to those presented in rabbits from this study. In addition to hemorrhages in the CNS, vascular congestion, myelin degeneration, axon swelling, and pericapillary edema are common findings in pigs, humans, or rats (19, 26, 27, 30). However, in this experimental model, only congestion and brain-associated hemorrhages in the subarachnoid space were observed.

Interstitial and alveolar pulmonary edema was observed in all groups. This edema has also been macroscopically described in other experimental models that reproduced DCS in rats, sheep, and rabbits (4, 20, 28, 31). In these models, pulmonary edema was one of the most observed lesions, along with emphysema. According to Atkins et al. (31), pulmonary edema is related to the development of pulmonary hypertension and increased permeability of blood capillaries due to the contact of microbubbles with the endothelium, inducing the release of intracellular calcium, causing damage to endothelial cells, increasing their permeability, and allowing the release of protein-rich fluid into the intracellular space (20). In this experimental model, the low number of affected rabbits and all groups' presence do not seem relevant to this finding. Cetaceans diagnosed with DCS also had diffuse pulmonary edema (8) and non-specific lesions linked to different causes of death.

Acute muscle changes were associated with ischemic damage caused by stressful situations. In this study, these changes were found in muscular tissues such as skeletal muscle and myocardium. These acute changes usually occur within minutes after ischemia, including contraction band necrosis and wavy fibers' presence. These changes are well studied in other recent studies that analyzed the stress to which cetaceans were exposed while stranding alive (32) (Figure 3C). In this study, these two lesions were reported in fewer animals than expected (1/8 animals in the mortality group presented both lesions and 2/5 animals in the euthanized group presented wavy fibers). Other acute changes such as hyper eosinophilia and intracytoplasmic

vacuolization were observed in the cardiac and skeletal muscle of animals that died after decompression and, to a lesser extent, in those that survived and were euthanized. Since in the rabbits all the procedures were carried out under surgical anesthesia, this might prevent the appearance of some stress-related lesions.

Vacuolization of hepatocytes was observed in the C/D model, with the rabbits that died by the protocol being more affected. L'Abbate et al. (24) conducted a study on the changes observed in rats' liver after undergoing a rapid decompression protocol. Thus, hepatocellular vacuolization was not observed in spontaneous death or in the group euthanized after 3 h, but it was observed in the animals euthanized at 24 h, with different severity levels. These findings are dissimilar to those obtained in our study, where the animals that died shortly after decompression had more marked hepatocellular vacuolization than those that were euthanized at 1 h post-decompression.

While in this study no fibrin microthrombi were observed in the compression/decompression model, pulmonary arterial microthrombi have been described in other studies of DCS with similar protocols, such as in the study of Tanoue et al. (33), where rabbits were exposed to a compression protocol of 6 ATA for 40 min and rapid decompression of 5 min, and the animals euthanized immediately after decompression showed these microthrombi in large arteries of the lung, or in the study of Geng et al. (4), where thrombosis was seen in small pulmonary arteries, capillaries, and veins (798 ATA for 1 h, rapid decompression for 5 min in rabbits). Arieli et al. (18), with a rat model subjected to 12'49 ATA for 33 min and a rapid decompression in 6 min, also described the blood alterations generated by the microbubbles and the platelets' consequent activation which increased the presence of microthrombi and disseminated intravascular coagulation. In cetaceans, the presence of these microthrombi associated with decompression-like sickness was not observed.

In summary, it is necessary to highlight the difference between the severe presence of systemic gas embolism and associated gas lesions in rabbits dead by decompression vs. the absence or lower incidence in euthanized animals. Other studies have observed that, despite exposing individuals with a similar profile (species, sex, age, and weight) to the same protocol, bubble formation and lethality are highly variable (17, 24). Based on this, cetaceans exposed to the same diving profile and subjected to the same stress can present different results, with some animals developing a lethal DCS, while others may survive.

In conclusion, the rabbits that died after decompression presented large quantities of macroscopic and microscopic gas bubbles systemically distributed, emphysema, and hemorrhages in multiple vital organs. Most of the lesions described were probably due to the bubbles' mechanical and embolic damage.

These same lesions have been described in cetaceans, consistent with a decompression-like sickness, reinforcing the pathological findings found. Besides this, almost half of the rabbits that survived for 1 h after decompression did not show the same lesions or severity. It reveals that individuality plays an essential role in this disease as it has previously been hypothesized in animal models and human diving medicine.

## DATA AVAILABILITY STATEMENT

The original contributions presented in the study are included in the article/supplementary material, further inquiries can be directed to the corresponding authors.

## ETHICS STATEMENT

The animal study was reviewed and approved by Norwegian Committee for Animal Experiments (2154) and the Ethical Committee for Animal Experiments of the University of las Palmas de Gran Canaria (CEEBA-HUGCDN 002/2010).

## AUTHOR CONTRIBUTIONS

AF, AM, and YB took charge of conceptualization. AF and AM took charge of funding. AV-W contributed to writing. YB, MC, AM, MA, and AV-W contributed to the experimental procedures and laboratory analyses. AV-W, YB, MC, and MA took charge of the pathological studies. All the authors contributed to review and editing. AF, YB, and MC supervised the study.

## FUNDING

This study was supported by the National Project PGC2018-101226-B-I00 and the Canary Islands Government, which has funded and provided support to the stranding network. AV-W was funded by the University Professor Formation fellowship from the Spanish Ministry of Education (FPU17/00763). This work was also supported by the Liaison Committee between the Central Norway Regional Health Authority and the Norwegian University of Science and Technology, grant number 46028600.

## ACKNOWLEDGMENTS

The authors would like to thank all colleagues from the University of las Palmas de Gran Canaria (Spain) and volunteers of the Cetacean Stranding Network who contributed to this work and the hyperbaric medicine division of the Norwegian University of Science and Technology (Norway) for its scientific contribution.

## REFERENCES

1. Vann RD, Butler FK, Mitchell SJ, Moon RE. Decompression illness. *Lancet*. (2011) 377:153–64. doi: 10.1016/S0140-6736(10)61085-9

2. Edmonds C, Bennett M, Lippmann J, Mitchell SJ. *Diving Subaquatic Medicine*. 5th ed. Boca Raton, FL: CRC Press (2015). doi: 10.1201/b18700
3. Pekka S, Knight B. *Knight's Forensic Pathology*. 3rd ed. London: Edward Arnold Ltd (2004). p. 488–90.

4. Geng M, Zhou L, Liu X, Li P. Hyperbaric oxygen treatment reduced the lung injury of type II decompression sickness. *Int J Clin Exp Pathol.* (2015) 8:1791–803.
5. Ponganis PJ, Koymann GL, Ridway SH. Comparative diving physiology. In: Brubakk AO, Neuman TS, editors. *Bennett and Elliott's Physiology and Medicine of Diving*. 5th ed. New York, NY: Saunders Elsevier Science Ltd (2003). p. 221–6.
6. Jepson PD, Arbelo M, Deaville R, Patterson I, Castro P, Baker, et al. Gas-bubble lesions in stranded cetaceans. *Nature.* (2003) 425:575–6. doi: 10.1038/425575a
7. Fernández A, Edwards J, Rodríguez E, de los Monteros A, Herráez P, Castro, et al. "Gas and fat embolic syndrome" involving a mass stranding of beaked whales (Family Ziphiidae) exposed to anthropogenic sonar signals. *Vet Pathol.* (2005) 42:446–57. doi: 10.1354/vp.42-4-446
8. Fernández A, Sierra E, Martín V, Méndez M, Sacchini S, Bernaldo de Quiros Y, et al. Last "Atypical" beaked whales mass stranding in the canary islands (July, 2004). *J Marine Sci Res Dev.* (2012) 2.2. doi: 10.4172/2155-9910.1000107
9. Bernaldo de Quiros Y, Fernández A, Baird RW, Brownell RL, Jr, Aguilar del Soto N, Allen D, et al. Advances in research on the impacts of anti-submarine sonar on beaked whales. *Proc R Soc B.* (2019) 286:20182533. doi: 10.1098/rspb.2018.2533
10. Arbelo M, Bernaldo de Quiros Y, Sierra E, Méndez M, Godinho A, Ramirez G, et al. Atypical beaked whale mass stranding in Almería's coast: pathological study. *Int J Anim Sound Rec.* (2008) 17:293–323. doi: 10.1080/09524622.2008.9753853
11. Bernaldo de Quiros Y, González-Díaz Ó, Saavedra P, Arbelo M, Sierra E, Sacchini, et al. Methodology for in situ gas sampling, transport and laboratory analysis of gases from stranded cetaceans. *Sci Report.* (2011) 1:193. doi: 10.1038/srep00193
12. Fernández A, Sierra E, Díaz-Delgado J, Sacchini S, Sanchez-Paz Y, Suarez-Santana C, et al. Deadly acute decompression sickness in risso's dolphins. *Sci Rep.* (2017) 7:13621. doi: 10.1038/s41598-017-14038-z
13. García-Párraga D, Crespo-Picazo JL, Bernaldo de Quiros Y, Cervera V, Martí-Bonmati L, Díaz-Delgado I, et al. Decompression sickness ('the bends') in sea turtles. *Dis Aquat Org.* (2014) 111:191–205. doi: 10.3354/dao02790
14. Eggleton P, Elsdon S, Fegler J, Hebb C. A study of the effects of rapid 'decompression' in certain animals. *J Physiol.* (1945) 104:129–50. doi: 10.1113/jphysiol.1945.sp004111
15. Clay JR. Histopathology of experimental decompression sickness. *Aerosp Med.* (1963) 34:1107–10.
16. Lever MI, Miller KW, Paton WDM, Smith EB. Experiments on the genesis of bubbles as a result of rapid decompression. *J Physiol.* (1966) 184:964–9. doi: 10.1113/jphysiol.1966.sp007960
17. Shim SS, Patterson FR, Kendall MJ. Hyperbaric chamber and decompression sickness: an experimental study. *Can Med Assoc J.* (1967) 97:1263–72.
18. Arieli R, Baron E, Abramovich A. Combined effect of denudation and denitrogenation on the risk of decompression sickness in rats. *J Appl Physiol.* (2009) 106:1453–8. doi: 10.1152/jappphysiol.91146.2008
19. Ni X, Cai Z, Fan D, Liu Y, Zhang R, Liu, et al. Protective effect of hydrogen-rich saline on decompression sickness in rats. *Aviat Space Environ Med.* (2011) 82:604–9. doi: 10.3357/ASEM.2964.2011
20. Tang S, Liao W, Wu S, Pao H, Huang K, Chu S. The blockade of store-operated calcium channels improves decompression sickness in rats. *Front Physiol.* (2020) 10:1616. doi: 10.3389/fphys.2019.01616
21. Bernaldo de Quiros Y, González-Díaz O, Møllerløkken A, Brubakk A, Hjelde A, Saavedra, et al. Differentiation at autopsy between in vivo gas embolism and putrefaction using gas composition analysis. *Int J Legal Med.* (2013) 127:437–45. doi: 10.1007/s00414-012-0783-6
22. Bernaldo de Quiros Y, Saavedra P, Møllerløkken A, Brubakk A, Jørgensen A, González-Díaz, et al. Differentiation at necropsy between in vivo gas embolism and putrefaction using a gas score. *Vet Sci Res J.* (2016) 106:48–55. doi: 10.1016/j.rvsc.2016.03.007
23. Suvarna S, Layton C, Bancroft J. *Bancroft's Theory and Practice of Histological Techniques*. 7th ed. Philadelphia: Churchill Livingstone of Elsevier (2018).
24. L'Abbate A, Kusmic C, Matteucci M, Pelosi G, Narari A, Pagliazzo, et al. Gas embolization of the liver in a rat model of rapid decompression. *Am J Physiol Regul Integr Comp Physiol.* (2010) 299:R673–82. doi: 10.1152/ajpregu.00699.2009
25. Caruso JL. Pathology of diving accidents. In: Brubakk AO, Neuman TS, editors. *Bennett Elliott's: Physiology Medicine of Diving*. 5th ed. Eastbourne: Saunders Elsevier (2003). p. 729–43.
26. Francis T, Mitchell S. Pathophysiology of decompression sickness. In: Bove A, editor. *Bove Davis' Diving Medicine*. 4th ed. Philadelphia: Saunders (2004). p. 165–83. doi: 10.1016/B978-0-7216-9424-5.50014-9
27. Broome JR, Dick EJ, Jr. Neurological decompression illness in swine. *Aviat Space Environ Med.* (1996) 67:207–13.
28. Zhang K, Wang D, Jiang Z, Ning X, Buzzacott P, Xu W. Endothelial dysfunction correlates with decompression bubbles in rats. *Sci Rep.* (2016) 6:33390. doi: 10.1038/srep33390
29. Bao X, Chen H, Fang Y, Yuan H, You P, Ma J, et al. Clopidogrel reduces the inflammatory response of lung in a rat model of decompression sickness. *Respir Physiol Neurobiol.* (2015) 211:9–16. doi: 10.1016/j.resp.2015.02.003
30. Dick EJ, Jr, Broome JR, Hayward II. Acute neurologic decompression illness in pigs: lesions of the spinal cord and brain. *Lab Anim Sci.* (1997) 47:50–7.
31. Atkins C, Lehner C, Beck K, Dubielzig R, Nordheim E, Lamphier E. Experimental respiratory decompression sickness in sheep. *J Appl Physiol.* (1988) 65:1163–71. doi: 10.1152/jappl.1988.65.3.1163
32. Cámara N, Sierra E, Fernández-Maldonado C, Espinosa de los Monteros A, Arbelo M, Fernández A, et al. Stress cardiomyopathy in stranded cetaceans: a histological, histochemical and immunohistochemical study. *Vet Rec.* (2019) 185:694. doi: 10.1113/vr.105562
33. Tanoue K, Mano Y, Kuroiwa K, Suzuki H, Shibayama M, Yamazaki H. Consumption of platelets in decompression sickness of rabbits. *J Appl Physiol.* (1987) 62:1772–9. doi: 10.1152/jappl.1987.62.5.1772

**Conflict of Interest:** The authors declare that the research was conducted in the absence of any commercial or financial relationships that could be construed as a potential conflict of interest.

Copyright © 2021 Velázquez-Wallraf, Fernández, Caballero, Møllerløkken, Jepson, Andrade and Bernaldo de Quiros. This is an open-access article distributed under the terms of the Creative Commons Attribution License (CC BY). The use, distribution or reproduction in other forums is permitted, provided the original author(s) and the copyright owner(s) are credited and that the original publication in this journal is cited, in accordance with accepted academic practice. No use, distribution or reproduction is permitted which does not comply with these terms.



## II. Establishment of a fish model to study gas-bubble lesions

**Velázquez-Wallraf, A.**, Fernández, A., Caballero, M.J., Arregui, M., González-Díaz, O., Betancor, M.B., & Bernaldo de Quirós, Y. (2022). Establishment of a fish model to study gas-bubble lesions. *Scientific Reports*, 12, 6592. <https://doi.org/10.1038/s41598-022-10539-8>.





OPEN

## Establishment of a fish model to study gas-bubble lesions

Alicia Velázquez-Wallraf<sup>1</sup>, Antonio Fernández<sup>1</sup>, María José Caballero<sup>1</sup>✉, Marina Arregui<sup>1</sup>, Óscar González Díaz<sup>2</sup>, Mónica B. Betancor<sup>3</sup> & Yara Bernaldo de Quirós<sup>1,4</sup>

Decompression sickness (DCS) is a clinical syndrome caused by the formation of systemic intravascular and extravascular gas bubbles. The presence of these bubbles in blood vessels is known as gas embolism. DCS has been described in humans and animals such as sea turtles and cetaceans. To delve deeper into DCS, experimental models in terrestrial mammals subjected to compression/decompression in a hyperbaric chamber have been used. Fish can suffer from gas bubble disease (GBD), characterized by the formation of intravascular and extravascular systemic gas bubbles, similarly to that observed in DCS. Given these similarities and the fact that fish develop this disease naturally in supersaturated water, they could be used as an alternative experimental model for the study of the pathophysiological aspect of gas bubbles. The objective of this study was to obtain a reproducible model for GBD in fish by an engineering system and a complete pathological study, validating this model for the study of the physiopathology of gas related lesions in DCS. A massive and severe GBD was achieved by exposing the fish for 18 h to TDG values of 162–163%, characterized by the presence of severe hemorrhages and the visualization of massive quantities of macroscopic and microscopic gas bubbles, systemically distributed, circulating through different large vessels of experimental fish. These pathological findings were the same as those described in small mammals for the study of explosive DCS by hyperbaric chamber, validating the translational usefulness of this first fish model to study the gas-bubbles lesions associated to DCS from a pathological standpoint.

Decompression sickness (DCS) is a clinical syndrome described mainly in professional and recreational scuba divers, presenting symptoms such as muscle and joint pain, difficult breathing, weakness, dizziness, numbness, skin rashes, and neurological symptoms among others<sup>1</sup>. DCS was first described in 1878 by Bert<sup>2</sup>, reporting these symptoms in caisson workers returning to the surface after finishing their shifts underwater. This disease is caused by the formation of systemic intravascular and extravascular gas bubbles when the sum of the partial pressures of dissolved gases in the tissues exceeds the atmospheric pressure<sup>3</sup>. The presence of gas bubbles in blood vessels is known as gas embolism and can lead to mechanical and biochemical alterations.

DCS has also been described in wild animals such as sea turtles<sup>4</sup> and cetaceans<sup>5–12</sup>, presumably caused by the alteration of their diving profile and diving response with regards to a stressor<sup>4,7</sup>. In most cases, these alterations were associated with anthropogenic activities such as the use of high-intensity mid-frequency sonar in military naval maneuvers coincident in time and space with mass strandings<sup>8–9</sup> or bycatch<sup>4</sup>, but it has also been described in stressing large prey interactions<sup>12</sup>. A severe form of DCS has been described in these species, namely explosive decompression sickness characterized by a lethal gas embolism, which in humans rarely occurs except in cases of severe diving accidents<sup>13</sup>.

To delve deeper into DCS, experimental models in terrestrial mammals subjected to compression/decompression in a hyperbaric chamber have been used. In some of these models, mainly developed in rats and rabbits, compressions were performed for a variable period (6–8 absolute atmospheres, 40–90 min) followed by rapid decompression (3–5 min), aiming to induce severe DCS<sup>14–19</sup>. These models have allowed comparison with marine mammals affected by DCS, showing very similar pathology findings<sup>20</sup>.

Fish can suffer from gas bubble disease (GBD), characterized by the formation of intravascular and extravascular systemic gas bubbles, similarly to gas bubbles observed in DCS. GBD has been extensively studied, mainly

<sup>1</sup>Veterinary Histology and Pathology, Atlantic Center for Cetacean Research, University Institute of Animal Health and Food Safety (IUSA), Veterinary School, University of Las Palmas de Gran Canaria (ULPGC), Canary Islands, Spain. <sup>2</sup>Physical and Chemical Instrumental Center for the Development of Applied Research Technology and Scientific Estate, Institute for Environmental Studies and Natural Resources (I-UNAT), University of Las Palmas de Gran Canaria (ULPGC), Las Palmas, Spain. <sup>3</sup>Institute of Aquaculture, Faculty of Natural Sciences, University of Stirling, Stirling, UK. <sup>4</sup>Department of Integrative Physiology, University of Colorado Boulder, Boulder, CO, USA. ✉email: mariajose.caballero@ulpgc.es

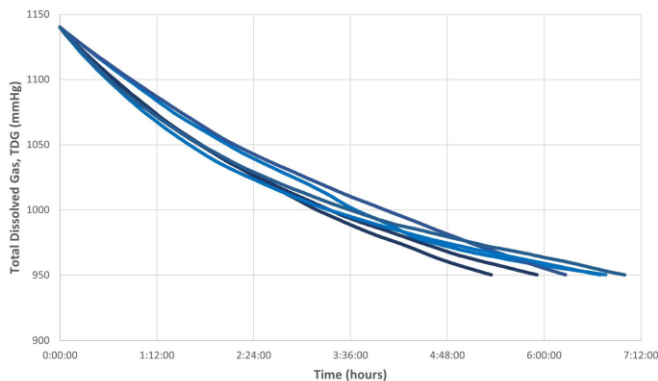


**Figure 1.** Graphical representation of the evolution of supersaturated water in an open aquarium without recirculation based on experiments performed from 1140 mmHg (150% of TDG). Each line corresponds to six different experiments with a similar pattern of TDG decrease in all of them.

in large dam areas where the discharge of significant amounts of water from one dam level to another entrains and dissolves atmospheric air causing an increase in total dissolved gases (TDG) in the water<sup>21</sup>. Clinical signs have been observed in live fish inhabiting these supersaturated waters, such as loss of buoyancy and erratic swimming, along with pathological signs such as gas bubbles in eyes and fins<sup>22</sup>. Fish experimental studies on GBD have mainly focused on the survival of the different fish species and life stages at different TDG values<sup>21–24</sup>.

Several authors have described the usefulness of an *in vivo* model of GBD to study gas embolism related to DCS, from the perspective of the formation of intravascular gas bubbles, their growth and subsequent endothelial pathophysiology, that are common to both diseases<sup>25–27</sup>. Given the similarities between GBD and DCS and the fact that fish develop this disease naturally, they could be used as an alternative experimental model following the replacement principle in accordance with European laboratory animal regulations (Directive 2010/63/EU of the European Parliament). Hence, the main objective of the present study was to obtain a reproducible model for massive GBD in fish. In order to achieve this aim, an engineering system was implemented to produce and maintain over time high concentrations of TDG, and the clinical diagnosis of GBD was confirmed with a complete pathological study validating, for the first time, this fish model to study the gas bubbles associated lesions similar to DCS from a pathological standpoint.

## Results

**Generation of supersaturated water with an open aquarium.** An engineering system was designed (see “Methods”) to produce supersaturated water with high percentages of TDG following the existing literature<sup>38,39</sup>. Once the desired TDG was achieved, the supersaturated water was transferred to an open aquarium, where it remained stagnant. The results showed a decrease of TDG with time when using the open aquarium and without recirculating the water. This decrease was observed from a value of 150–125% in approximately 6 h (Fig. 1).

**Generation of supersaturated water with a pressurized aquarium.** The significant decrease in TDG forced to modify the initial circuit by designing and introducing, for the first time, a pressurized aquarium (Fig. 2), creating a closed circuit with constant recirculation (Fig. 3). This new design was able to produce TDG water of around 160% and 180% successfully and to maintain it stable over time.

The time at which it was simulated to introduce a fish into the pressurized aquarium (see “Methods”) had no effect on TDG values, since this simulation caused a slight decrease due to depressurization followed by fast recovery of TDG. Figure 4 shows the simulation maneuver of fish introduction through the descending peak and rapid recovery to stable values, behaving similarly in the different trials performed with different TDG values and times.

Therefore, a model graph of the TDG behavior is established (Fig. 5) that shows the global overview of the tests performed without fish. The TDG values over time graphs can be divided into different stages: stage I (green) in which the supersaturation of the flowing water occurs, stage II (orange) in which the maximum TDG value for a given experiment is reached and is maintained stable (plateau), stage III (gray) where TDG values dropped briefly and abruptly (reverse peak) with a quick recovery to a TDG value closed to stage II, reflecting the isolation and opening of the pressurized aquarium to simulate the introduction of the fish and the subsequent recirculation of supersaturated water once the aquarium was closed again, and stage IV (yellow), where TDG values are stable again (Fig. 5).

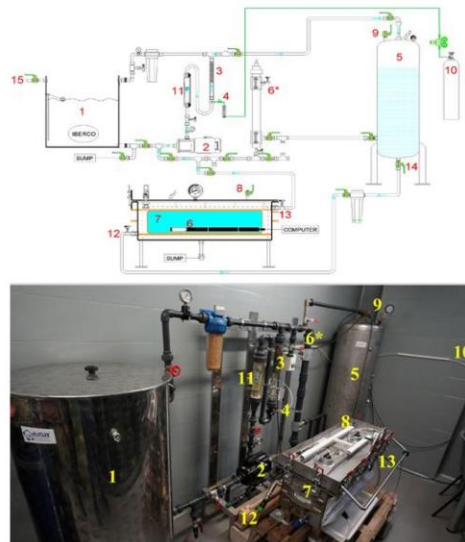


**Figure 2.** Supersaturated water production system components. (1) Open vessel. (2) Motor pump. (3) Dissolution tube. (4) Synthetic air injection valve. (5) Pressurized tank. (6) TDG and temperature sensor. (6\*) TDG and temperature sensor inside the open circuit. (7) Pressurized aquarium. (8) Pressurized aquarium vent valve. (9) Pressurized tank vent valve. (10) Synthetic air bottle. (11) Flow meter. (12) Pressurized aquarium inlet valve. (13) Pressurized aquarium outlet valve. (14) Pressurized tank outlet valve. (15) Running water inlet.

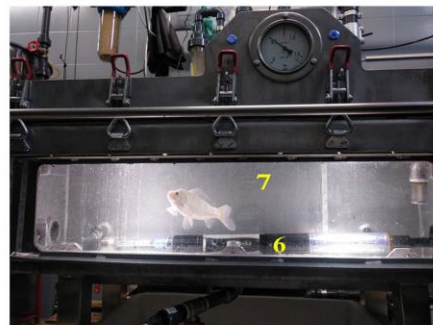


**Figure 3.** Detail of pressurized aquarium during a fish experiment. TDG and temperature sensor (6). Pressurized aquarium (7).

The pilot test results showed that the maximum TDG was reached (stage II) after 90 min, although 30–60 more minutes were necessary to confirm that the TDG was stable, at which time the fish may be introduced.

**Pilot tests: fish exposure.** Fish were exposed to TDG values between 160 and 180%. TDG was maintained stable in all tests (Fig. 6). The 3 h, 6 h, and 12 h groups presented GBD, although it was not massive, regardless of exposure to very high TDG values, so the 18 h group was sequentially resorted to. The 18 h group

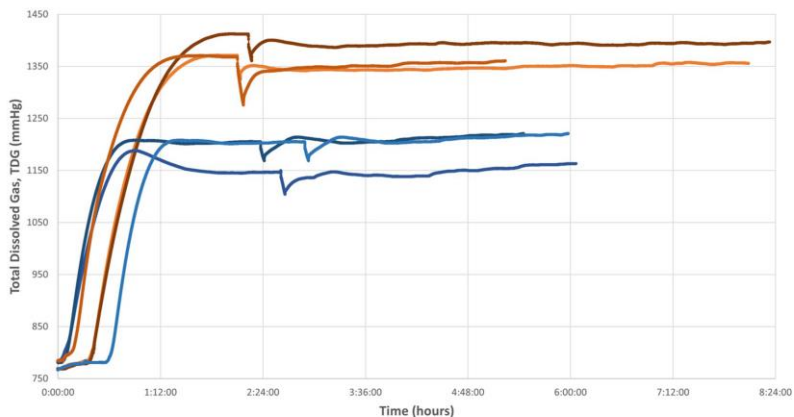


**Figure 4.** TDG plots represent the pilot tests without fish. The orange lines represent the group in which a high TDG value (180%) was reached, while the blue lines represent the experiments with a TDG of approximately 150%. The peaks observed in the different tests represent the simulation of fish introduction.

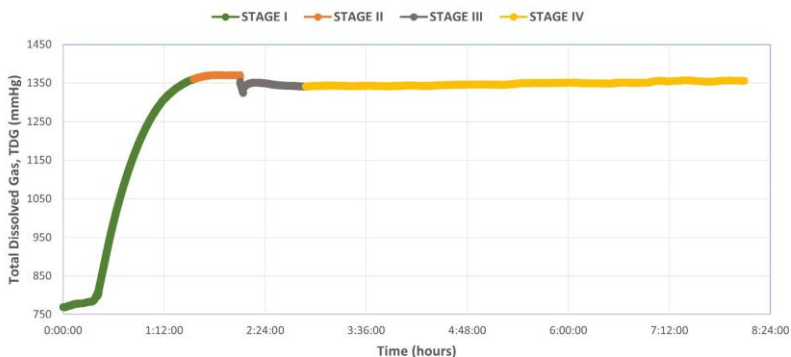


**Figure 5.** Diagram of the 4 phases into which the water supersaturation procedure can be divided. Phase I (green) represents the increase of TDG in the water due to the addition of compressed air from a cylinder. Phase II (orange): stabilization or plateau phase of the TDG value. Phase III (gray): simulation of the introduction of a fish into the pressurized aquarium representing the loss of TDG when depressurizing the aquarium and the rapid recovery of the value. Phase IV (yellow): stabilization of TDG post-simulation, which remains constant over time.

was initially planned for a time exposure of 24 h, following the same reasoning of doubling the hours from the previous group treatment, but both fish reached the humane endpoint at 18 h, showing signs of loss of buoyancy and lethargy. TDG average values for the 18 h group was of 162% and 163%.

**Clinical signs.** The clinical signs of the 18 h-fish group are described below (details of all groups are provided in the Supplementary Material). Thus, both fish from the 18 h group presented the same clinical signs when introduced into the pressurized aquarium. They immediately presented intense agitation, denoted by swimming back and forth, being three times faster than control fish. In addition, they showed intense opercular beat frequency, two times faster than control fish. Between 5 and 10 min after the experiment started, fish were paralyzed at the bottom of the pressurized aquarium. From then on, they were less steady and tried to swim, slowly recovering their regular swimming pattern and speed and their standard opercular beat frequency. Small gas bubbles were visible in the lateral and anal fins after 30 min of exposure, becoming visually larger in between

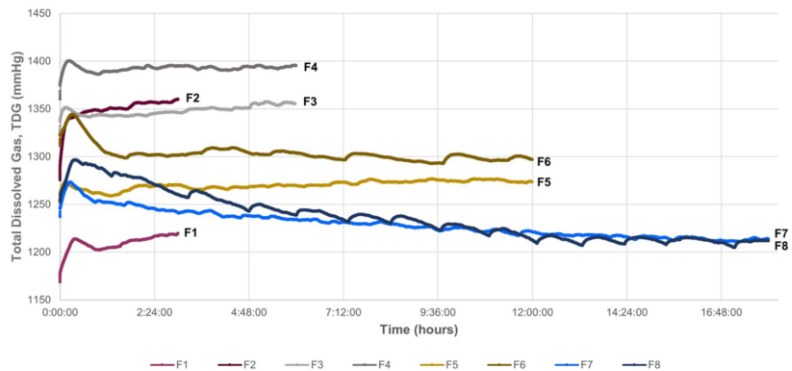


**Figure 6.** Representation of the evolution of TDG values from the introduction of the fish to the end of the exposure time for each experimental fish. F1–F2 correspond to the 3 h group, F3–F4 to the 6 h group, F5–F6 to the 12 h group, and F7–F8 to the 18 h model group.

1 and 2 h of exposure. Between 6 and 12 h of the experiment, many gas bubbles in all fins were recorded. In the last interval (12–18 h), the fish presented some loss of scales. At 17 h of exposure, the fish returned to the bottom of the pressurized aquarium, showed erratic movements, loss of buoyancy, and rigidity of the pectoral fins with very severe hemorrhages, congestion, and gas bubbles, as well as in the rest of the fins. The fish were euthanized at this point, following the pre-established humane endpoint.

**Macroscopic findings.** The macroscopic findings of the 18 h-fish group are described below (details of all groups are provided in the Supplementary Material). All fins presented severe emphysema, multifocal hemorrhagic areas, and gas bubbles within the congestive vessels, either *in vivo* (Fig. 7A) and post-euthanasia (Fig. 7B–D). Gas bubbles were also observed within the vessels of the medial side of the opercula. Additionally, the fish presented loss of scales, mainly around the base of the tail, where the skin was crepitant to the touch denoting mild subcutaneous emphysema. The gills presented severe congestion.

Internal examination of the organs revealed the presence of large amounts of gas bubbles in the heart, ventral aorta (Fig. 7E), posterior cardinal veins, gonads veins (Fig. 7F), swim bladder vasculature, and in the intercostal vessels. In addition, severe generalized organ congestion, denoted mainly in liver, kidney, and spleen, and moderate emphysema of visceral fat were also observed.

**Microscopic findings.** The microscopic findings of the 18 h-fish group are described below (details of all groups are provided in the Supplementary Material). Large non-staining dilations compatible with emphysema and severe congestion were observed in fins (Fig. 8A), along with moderate multifocal hemorrhages and some intravascular bubble-like round empty spaces among blood cells. Gills presented severe congestive areas with large gas bubbles circulating within capillaries associated with primary lamellae. Severe congestion was also observed in spleen and posterior kidney, with the latter showing some hemorrhagic areas among the renal tubules. Rete mirabile of swim bladder, liver, ocular structures, and central nervous system showed moderate congestive appearance. The same circular structures were observed among the blood displacing the erythrocytes inside vascular structures of posterior kidney (Fig. 8B), spleen (Fig. 8C), liver, digestive tract, eyes, central nervous system (Fig. 8D), gills (Fig. 8E), and between blood of heart's ventricle (Fig. 8F).

## Discussion

A massive GBD in fish with the presence of severe gas-bubble lesions similar to that seen in explosive DCS in other species. (e.g., humans, cetaceans, rabbits, rats)<sup>1–19</sup> was achieved by exposing the fish for 18 h to TDG values of 162–163%, validating a new experimental model from the point of view of the study of gas bubble pathophysiology, alternative to rabbits and rats following the 3Rs replacement principle.

The Directive 2010/63/EU of the European Parliament states that in the case that the use of live animals is necessary, an animal species with a lower capacity to feel pain, suffering, distress, or lasting harm that can be extrapolated to the target species should be used. Following these reasons, the development of this work and the use of fish as a model organism for DCS has a great value on the development of new approaches that allow the implementation of the 3Rs principles.

Unlike rabbits and rats, fish can develop GBD naturally when large quantities of water fall from one dam level to another, entraining atmospheric gas, causing an increase in TDG. D'Aoust and Smith<sup>35</sup> were the first authors to describe GBD in fish as a useful *in vivo* model to study DCS. From the point of view of the development of gas bubbles, first intravascular and well perfused tissues, their growth and the consequences triggered by their

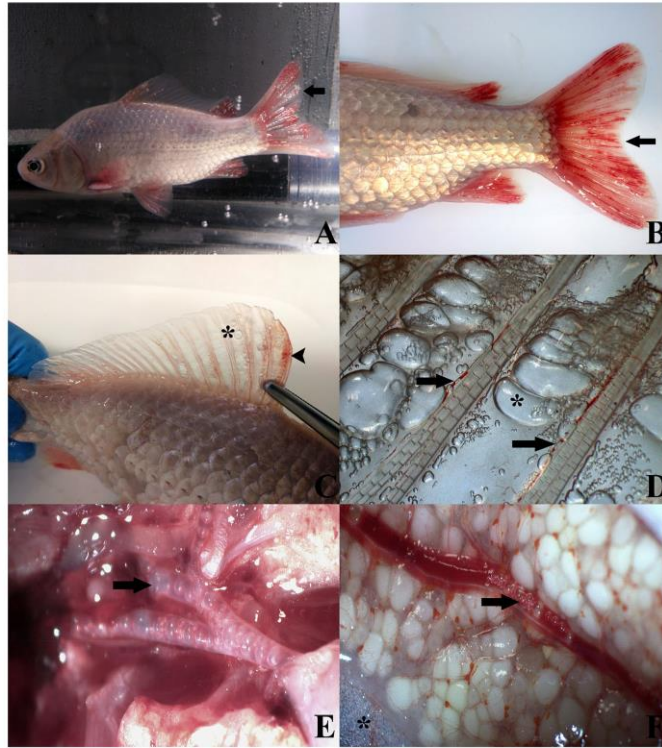


**Figure 7.** Macroscopic appearance of the 18-h fish group. (A) Fish alive inside the pressurized aquarium in the last hours of the experiment. Emphysema, congestion, and hemorrhages are observed in all fins. (B) External examination of the fish after euthanasia. Presence of the similar lesions observed in vivo. (C) Dorsal fin with the presence of emphysema (star) and multifocal hemorrhages (arrowhead). (D) Detail of dorsal fin with gas bubbles in blood vessels (arrows) and emphysema (star). (E) Ventral aorta at its exit from the bulbus arteriosus filled with gas. (F) Gas bubbles circulating in the gonadal vessel and presence of emphysema of the adjacent adipose tissue.

presence, Speare<sup>36</sup> also considered GBD as an interesting model to deepen in the pathophysiological aspects of gas embolism in DCS.

Most previous studies on the GBD in fish focused on the tolerance and survival of different species and life stages to specific TDG values<sup>21,28,39</sup>. The present study differs from these previous manuscripts in the goal and approach since the aim was to reproduce a massive GBD as a model to study systemic massive gas bubbles related to explosive DCS.

The first step in order to achieve a model of massive GBD was to be able to produce water saturated with high levels of TDG and to maintain those levels along the duration of the experiment. Most previous experimental studies described stable TDG values while recirculating water with an open tank<sup>39</sup>. However, we could not recirculate the water in these conditions due to the differences in pressure between the open aquarium and the rest of the circuit, preventing the correct operation of the motor pump and causing more water outflow than inflow, leading to overflowing of the aquarium. Hence, the supersaturated water was transferred from the tank to the open aquarium and remained steady to observe how the TDG values behaved. In this case, the loss of TDG was almost immediately causing a rapid exponential decrease, as shown in Fig. 1. For this reason, a pressurized aquarium was added to the design, enabling the same pressure throughout the circuit and allowing constant recirculation of water. As a result, TDG values remained constant in these conditions during the study period (Fig. 4).

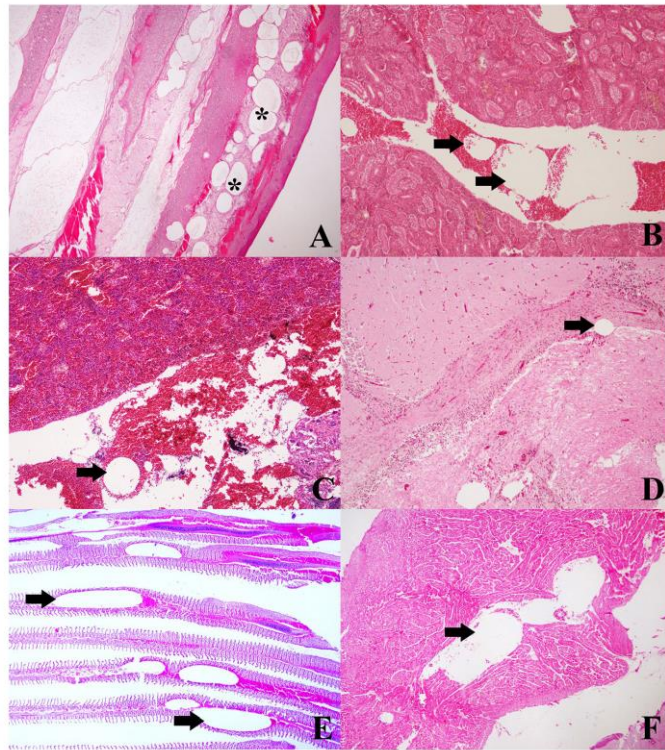


**Figure 8.** Microscopic findings of the 18-h fish group stained routinely with hematoxylin–eosin. (A) Fins displays the presence of emphysema (stars) and congestion.  $\times 4$ . (B) Posterior kidney with large, unstained, circular to oval structures between blood components (arrows).  $\times 10$ . (C) Gas bubble-like in the spleen (arrow), along with congestion.  $\times 10$ . (D) Congestion and dilatation of blood vessels in the brain (arrow).  $\times 10$ . (E) Blood vessels of primary gill lamellae with large caliber bubble-like gas, circumscribed by blood cells (arrows).  $\times 4$ . (F) Ventricle cavity of the heart with presence of displaced blood around an oval, unstained structure compatible with gas bubble (arrow).  $\times 4$ .

Once the stable parameters were achieved, the next step was to perform the experiments by introducing the fish. Although most experiments on GBD in supersaturated water have been conducted with fish of the family *Cyprinidae*, none have been conducted with *Carassius auratus*. The choice of this species was based on the fact that carp are fish that acclimatize very well to new environments, are economically accessible, and are easily marketed.

The pathology of GBD, in non-experimental studies, is described in both living and dead fish as gas bubbles and hemorrhages in fins<sup>28,32,34,40</sup>, as well as gill congestion and hemorrhages, along with exophthalmia<sup>31,41</sup>. In addition, microscopic lesions such as gas bubbles in blood vessels, hemorrhages, and congestion in different tissues, attributed to GBD, have been described<sup>42,43</sup>. In the first test performed (3 h with TDG 160–178%) fish showed signs of GBD but at a mild level, with presence of few gas bubbles in fins and vascular locations, together with mild hemorrhages and organic congestion. The aim of establishing a comparative model of gas-bubbles lesions from DCS led to the development of a massive GBD model where the presence of extravascular and intravascular gas bubbles is severe and massive, throughout most of the vascular system. By sequentially repeating the tests and doubling the exposure time we reproduced this massive GBD model, after 18 h of exposure to TDG values of 162–163%. This model was characterized by the presence of severe hemorrhages, congestion, and gas bubbles in the fins as well as the visualization of circulating macroscopic gas bubbles by different large vessels (Fig. 7), coupled with microscopic confirmation of massive quantities of gas bubbles systematically distributed, hemorrhages,

and multi-organ congestion (Fig. 8). Overall, pathological findings were the same as those described in small mammals for the study of gas-bubbles lesions in explosive DCS by hyperbaric chamber<sup>4,16,18,20</sup>, validating the translational usefulness of this model from a pathological standpoint.

As described by Marking<sup>44</sup>, gas excess in the water is rapidly transmitted to the bloodstream of the fish as the osmotic pressures between the two sides of the gill membrane tend to equalize and both blood and water have similar saturation points. This might explain why gas bubbles form in fish with low supersaturations, in comparison with other species.

The main limitation of this experimental model in fish is from the point of view of raising the questions of how and when intravascular and extravascular gas bubbles are formed. Therefore, it could not be applied to studies focused on the origin and formation of these gas bubbles in human DCS, but it could be considered for the study of the consequences of these gas bubbles.

In conclusion, a massive GBD with severe intravascular and extravascular gas bubbles similar to gas-bubbles lesions related to DCS was reproduced when goldfish were exposed during 18 h to TDG values between 162 and 163% in a pressurized aquarium. The clinical diagnose was confirmed by means of a pathological study. This represents the first establishment of a fish model as an alternative model to rodents and other mammals for the study of gas bubbles produced in DCS in humans and it could be a useful model to deepen in the pathophysiology of gas bubbles in tissues.

## Methods

**Generation of supersaturated water with an open aquarium.** Following the scheme of Bouck et al.<sup>38</sup> and taking into account that the dissolution of gas in water depends on pressure and temperature, in order to obtain supersaturated water at a constant temperature, it is necessary to exert pressure. Thus, these authors, by microdispensing water in an aeration tank, forced the gas to dissolve. Therefore, with this scheme as baseline<sup>38</sup>, a dissolution tube was designed, filled with porous materials of decreasing diameters, which broke the gas bubbles from the air injected. Supersaturated water was obtained forcing, with constant recirculation, the dissolution of gas and, therefore, increasing the TDG of the water.

The engineering circuit (IBERCO S.L., Spain) was composed of several structures shown in Fig. 2: (1) an open vessel which was filled with water from the tap, (2) a motor pump (Grundfos, Model: CM 10-1 ARAE-AVBE CAAN) to circulate water within the circuit, (3) a dissolution tube with (4) air injector, (5) a pressurized tank (max. 3 ATA; 250 L) to increase the pressure and favor the dissolution of gas into water and to store it, (6\*) a TDG sensor (Manta + Trimeter probe, Eureka water probes, USA) placed within the circuit to control for TDG values. Once the desired TDG value was reached in the pressurized tank, the water was transferred to the open aquarium, and the TDG sensor was moved into the aquarium to ensure TDG exposure along the duration of the experiments.

**Generation of supersaturated water with a pressurized aquarium.** The circuit was modified by adding a (7) pressurized aquarium (Fig. 3) (max 0.5 bar; 70 L) (IBERCO S.L., Spain). To produce supersaturated water (Fig. 2), first (1) the open vessel was filled with tap water at ambient pressure (the vent valves from (8) the pressurized aquarium and (9) tank were opened) with the help of (2) the motor pump. Then, both vent valves were closed, and (10) pressurized synthetic atmospheric air (Premier-X50S 200.0B) was injected (4). The amount of synthetic air injected was regulated using a flow meter connected to the circuit. When the maximum pressure of the circuit was reached (0.5 bar), no more air was injected, and the water was continuously recirculated (3000 L/h) from the dissolution tube to the pressurized tank and vice versa for several minutes to favor the dissolution of the gas remaining in the head space of the pressurized tank until a dynamic equilibrium between the gas and the liquid phase within the circuit was reached (determined by a constant reading of TDG values) and to ensure a homogenous TDG water mixture.

**Pilot tests: parameter settings without fish.** To adjust the parameters of the experimental model, different tests without fish were initially carried out following the supersaturated water production scheme explained above. In these pilot tests, the amount of synthetic air injected and recirculating time was varied, with the main objective of achieving a stable TDG value of more than 150% during the entire experiment. To test how high TDG values the system could produce and maintain stability over time, two different TDG ranges of around 150% and 180% TDG were tested. These values were reached by setting the outlet pressure of the synthetic air bottle at 3 bar, with a flow rate of 10–20 L/min for 4–6 min.

Since in the fish exposure experiments, it is necessary to open the pressurized aquarium in order to introduce the fish, causing an inevitable pressure loss in the circuit, the effect of this pressure drop in the TDG was analyzed by simulating the introduction of the fish during the pilot tests. Once the TDG was stabilized around the desired value, the recirculation of the water was stopped, and the aquarium was depressurized and opened, simulating the introduction of a fish. Then, the aquarium was closed, and the water was recirculated again through the circuit. We tested for different times at which introducing the fish.

**Pilot tests: fish exposure.** 10 adult goldfish (*Carassius auratus*) of  $112.8 \pm 11.74$  g and  $16.95 \pm 0.60$  cm were purchased from a certified fish distributor in Las Palmas de Gran Canaria (Spain) and acclimatized during 4 weeks in tanks at the experimental animal facility (EGC00616436) of the University of Las Palmas de Gran Canaria (Spain). The fish were kept under a natural photoperiod of 12:12 h light:dark cycle. Water chemistry parameters were assessed every 2 days using a colorimetric test kit (nitrate, 10 mg/dm<sup>3</sup>; nitrite, 0 mg/dm<sup>3</sup>; pH, 6.8; total hardness, 80–300 mg/dm<sup>3</sup>; chlorine, 0 mg/dm<sup>3</sup>). Dissolved oxygen (> 6.0 mg/dm<sup>3</sup>) and temperature (23–25 °C) were also measured. Fish were fed a commercial pellet (Tetra Goldfish) diet two times a day.

Fish experiments ( $n=8$ ) were performed sequentially by increasing time exposure and TDG values to determine the parameters triggering a massive GBD in adult goldfish, which was confirmed through pathological studies. The experiments started with 3 h of exposure. If massive production of gas bubbles were not observed, then the time was increased (3 h (h), 6 h, 12 h, and 18 h). TDG values were established based on the results of previous non-fish experiments so that these were in the range of 160–180%. These values reflect this range of amplitude since TDG tends to stabilize as exposure time increases. A humane endpoint (18 h) was established when the fish showed loss of buoyancy, erratic swimming, and lethargy. Two control animals were placed in the pressurized aquarium without recirculation of water for 18 h.

**Clinical signs.** Clinical monitoring of the fish was performed throughout the exposure time, with the observation of fish behavior as well as swimming and opercular beat frequency. In addition, the presence of possible external lesions such as the appearance of gas bubbles and hemorrhages in fins and loss of scales or subcutaneous emphysema were monitored. Thus, the intense opercular beat frequency value was established when the value was 2–4 times faster than normal based on control fish ( $\pm 2$  openings/s). In the same way, intense agitation was determined when fish swim 2–3 times faster than regular swimming based on control fish ( $\pm 10$  s swimming from one side of the aquarium to the other).

**Macroscopic evaluation.** Fish were euthanized with 2-phenoxyethanol (0.6 ml/L). Necropsy was immediately performed by a thorough external examination with an especial focus on describing lesions on fins, eyes, integument, and gills. Similarly, the coelomic cavity was dissected carefully from the anus to the ventral area of the operculum via the midline to expose the organs and visualize the blood vessels. A stereo microscope was used for the visualization of gas bubbles.

**Microscopic evaluation.** Samples of gill, fins, heart, swim bladder, digestive tract, liver, spleen, anterior and posterior kidney, gonads, muscle, eyes, and central nervous system were collected in 10% formalin for subsequent histopathological study. The formalin-fixed tissues were dehydrated, cleared, and embedded in paraffin, and sectioned at 4  $\mu$ m. The obtained samples were routinely stained with hematoxylin and eosin (H&E) and microscopically observed by two pathologists.

**Approval for animal experiments.** Experimental procedures were approved by the ethical committee of the University of Las Palmas de Gran Canaria and authorized by the competent authority of the Canary Islands Government (CEEA-ULPGC 4-2018R1). All the trials were designed and performed to result in the death of as few animals as possible and reduce the duration and intensity of suffering according to the relevant guidelines and regulations (Directive 2010/63/EU). Authors complied with the ARRIVE guidelines.

#### Data availability

All data generated during and/or analyzed during the current study are available from the corresponding author on reasonable request.

Received: 8 November 2021; Accepted: 1 April 2022

Published online: 21 April 2022

#### References

- Edmonds, C., Bennett, M., Lippmann, J. & Mitchell, S. *Diving and Subaquatic Medicine* (CRC Press, 2015). <https://doi.org/10.1201/b18700>.
- Bert, P. *La Pression Barométrique: Recherches de Physiologie Expérimentale* (Masson, 1878).
- Vann, R. D., Butler, F. K., Mitchell, S. J. & Moon, R. E. Decompression illness. *Lancet* **377**, 153–164. [https://doi.org/10.1016/S0140-6736\(10\)61085-9](https://doi.org/10.1016/S0140-6736(10)61085-9) (2011).
- García-Párraga, D. *et al.* Decompression sickness ('the bends') in sea turtles. *Dis. Aquat. Organ.* **111**, 191–205. <https://doi.org/10.3354/dao02790> (2014).
- Jepson, P. D. *et al.* Gas-bubble lesions in stranded cetaceans. *Nature* **425**, 575–576. <https://doi.org/10.1038/425575a> (2003).
- Fernández, A. *et al.* "Gas and fat embolic syndrome" involving a mass stranding of beaked whales (family Ziphiidae) exposed to anthropogenic sonar signals. *Vet. Pathol.* **42**, 446–457. <https://doi.org/10.1354/vp.42-4-446> (2005).
- Bernaldo de Quiros, Y. *et al.* Advances in research on the impacts of anti-submarine sonar on beaked whales. *Proc. Biol. Sci.* **286**, 20182533. <https://doi.org/10.1098/rspb.2018.2533> (2019).
- Fernández, A. *et al.* Whales, sonar and decompression sickness (reply): Pathology. *Nature* **428**, 2–2. <https://doi.org/10.1038/nature02528a> (2004).
- Bernaldo de Quiros, Y. *et al.* Methodology for in situ gas sampling, transport and laboratory analysis of gases from stranded cetaceans. *Sci. Rep.* **1**, 193. <https://doi.org/10.1038/srep00193> (2011).
- Arbelo, M. *et al.* Pathology and causes of death of stranded cetaceans in the Canary Islands (1999–2005). *Dis. Aquat. Organ.* **103**, 87–99. <https://doi.org/10.3354/dao02558> (2013).
- Díaz-Delgado, I. *et al.* Pathologic findings and causes of death of stranded cetaceans in the Canary Islands (2006–2012). *PLoS One* **13**, e0204444. <https://doi.org/10.1371/journal.pone.0204444> (2018).
- Fernández, A. *et al.* Deadly acute decompression sickness in Risso's dolphins. *Sci. Rep.* **7**, 13621. <https://doi.org/10.1038/s41598-017-14038-z> (2017).
- Francis, T. J. & Mitchell, S. I. Pathophysiology of decompression sickness. In *Bove and Davis' Diving Medicine* 4th edn 165–183 (Elsevier, 2004). <https://doi.org/10.1016/B978-0-7216-9424-5.50014-9>.
- Tanoue, K. *et al.* Consumption of platelets in decompression sickness of rabbits. *J. Appl. Physiol.* **62**, 1772–1779. <https://doi.org/10.1152/jappl.1987.62.5.1772> (1987).
- Bernaldo de Quiros, Y. *et al.* Differentiation at autopsy between in vivo gas embolism and putrefaction using gas composition analysis. *Int. J. Legal Med.* **127**, 437–445 (2013).

16. Geng, M., Zhou, L., Liu, X. & Li, P. Hyperbaric oxygen treatment reduced the lung injury of type II decompression sickness. *Int. J. Clin. Exp. Pathol.* **8**, 1797–1803 (2015).
17. Bernaldo de Quiros, Y. *et al.* Bubbles quantified in vivo by ultrasound relates to amount of gas detected post-mortem in rabbits decompressed from high pressure. *Front. Physiol.* **7**, 310. <https://doi.org/10.3389/fphys.2016.00310> (2016).
18. Zhang, K. *et al.* Endothelial dysfunction correlates with decompression bubbles in rats. *Sci. Rep.* **6**, 33390. <https://doi.org/10.1038/srep33390> (2016).
19. Tang, S.-E. *et al.* The blockade of store-operated calcium channels improves decompression sickness in rats. *Front. Physiol.* **10**, 1616. <https://doi.org/10.3389/fphys.2019.01616> (2019).
20. Velázquez-Wallraf, A. *et al.* Decompressive pathology in cetaceans based on an experimental pathological model. *Front. Vet. Sci.* **8**, 676499. <https://doi.org/10.3389/fvets.2021.676499> (2021).
21. Chen, S.-C. *et al.* Effects of total dissolved gas supersaturated water on lethality and catalase activity of Chinese sucker (*Mystocyprinus asiaticus* Bleeker). *J. Zhejiang Univ. Sci. B* **13**, 791–796. <https://doi.org/10.1631/jzus.B1200022> (2012).
22. Cao, C. *et al.* Effects of continuous acute and intermittent exposure on the tolerance of juvenile yellow catfish (*Pelteobagrus fulvifurcatus*) in total dissolved gas supersaturated water. *Ecotoxicol. Environ. Saf.* **201**, 110855. <https://doi.org/10.1016/j.ecoenv.2020.110855> (2020).
23. Stevens, D. G., Nebeker, A. V. & Baker, R. J. Avoidance responses of salmon and trout to air-supersaturated water. *Trans. Am. Fish. Soc.* **109**, 751–754. [https://doi.org/10.1577/1548-8659\(1980\)109%3c751:AROSAT%3e2.0.CO;2](https://doi.org/10.1577/1548-8659(1980)109%3c751:AROSAT%3e2.0.CO;2) (1980).
24. Weitkamp, D. E. & Katz, M. A review of dissolved gas supersaturation literature. *Trans. Am. Fish. Soc.* **109**, 659–702. [https://doi.org/10.1577/1548-8659\(1980\)109%3c659:ARODGS%3e2.0.CO;2](https://doi.org/10.1577/1548-8659(1980)109%3c659:ARODGS%3e2.0.CO;2) (1980).
25. Dawley, E. M. & Ebel, W. J. Effects of various concentrations of dissolved atmospheric gas on juvenile Chinook Salmon and Steelhead Trout. *Fish. Bull.* **73**, 787–796 (1975).
26. Geist, D. R., Linley, T. J., Cullinan, V. & Deng, Z. The effects of total dissolved gas on chum salmon fry survival, growth, gas bubble disease, and seawater tolerance. *N. Am. J. Fish. Manage.* **33**, 200–215. <https://doi.org/10.1080/02755947.2012.750634> (2013).
27. Liang, R.-F., Li, B., Li, K.-F. & Tuo, Y.-C. Effect of total dissolved gas supersaturated water on early life of David's schizothoracin (*Schizothorax davidi*). *J. Zhejiang Univ. Sci. B* **14**, 632–639. <https://doi.org/10.1631/jzus.B1200364> (2013).
28. Cao, L. *et al.* The tolerance threshold of Chinese sucker to total dissolved gas supersaturation. *Aquac. Res.* **47**, 2804–2813. <https://doi.org/10.1111/are.12730> (2015).
29. Wang, Y., Li, K., Li, J., Li, R. & Deng, Y. Tolerance and avoidance characteristics of prenat's Schizothoracin *Schizothorax prenanti* to total dissolved gas supersaturated water. *N. Am. J. Fish. Manage.* **35**, 827–834. <https://doi.org/10.1080/02755947.2015.1052160> (2015).
30. Ji, Q. *et al.* The tolerance characteristics of resident fish in the upper Yangtze River under varying gas supersaturation. *Int. J. Environ. Res. Public Health* **16**, 2021. <https://doi.org/10.3390/ijerph16112021> (2019).
31. Xue, S., Wang, Y., Liang, R., Li, K. & Li, R. Effects of total dissolved gas supersaturation in fish of different sizes and species. *Int. J. Environ. Res. Public Health* **16**, 2444. <https://doi.org/10.3390/ijerph16132444> (2019).
32. Deng, Y. *et al.* Effect of total dissolved gas supersaturation on the survival of bighead carp (*Hypophthalmichthys nobilis*). *Animals (Basel)* **10**, 166. <https://doi.org/10.3390/ani10010166> (2020).
33. Fan, Z. *et al.* Effect of total dissolved gas supersaturation on the tolerance of grass carp (*Ctenopharyngodon idellus*). *Environ. Sci. Res.* **32**, 25. <https://doi.org/10.1186/s12302-020-00330-9> (2020).
34. Ji, Q. *et al.* Total dissolved gases induced tolerance and avoidance behaviors in pelagic fish in the Yangtze River, China. *Ecotoxicol. Environ. Saf.* **216**, 112218. <https://doi.org/10.1016/j.ecoenv.2021.112218> (2021).
35. DAoust, B. & Smith, L. Bends in fish. *Comp. Biochem. Physiol. A Physiol.* **49**, 311–321 (1974).
36. Speare, D. J. Disorders associated with exposure to excess dissolved gases. In *Fish Disease and Disorders: Noninfectious Disorders* (eds Leatherland, J. F. & Woo, P. T. K.) 207–224 (CABI Publishing, 1998).
37. Roberts, R. *Fish Pathology* 4th edn. (Wiley-Blackwell, 2012).
38. Bouck, G. R., Nebeker, A. V., & Stevens, D. G. Mortality, saltwater adaptation and reproduction of fish exposed to gas supersaturated water. EPA-600/3-76-054, United States Environmental Protection Agency, Corvallis, Oregon, USA (1976).
39. Huang, X., Li, K.-F., Du, J. & Li, R. Effects of gas supersaturation on lethality and avoidance responses in juvenile rock carp (*Procypris rabaudi* Zhang). *J. Zhejiang Univ. Sci. B* **11**, 806–811. <https://doi.org/10.1631/jzus.B1000006> (2010).
40. Liu, X. *et al.* Lethal effect of total dissolved gas-supersaturated water with suspended sediment on river sturgeon (*Acipenser dabryanus*). *Sci. Rep.* **9**, 13373. <https://doi.org/10.1038/s41598-019-49800-y> (2019).
41. Yuan, Y., Wang, Y., Zhou, C., An, R. & Li, K. Tolerance of prenat's Schizothoracin *Schizothorax prenanti* to total dissolved gas supersaturated water at varying temperature. *N. Am. J. Aquac.* **80**, 107–115. <https://doi.org/10.1002/naaq.10007> (2018).
42. Smith, C. E. Communications. Histopathology of gas bubble disease in juvenile rainbow trout. *Prog. Fish-Cult.* **50**, 98–103. [https://doi.org/10.1577/1548-8640\(1988\)050%3c0098:CHOGBD%3e2.3.CO;2](https://doi.org/10.1577/1548-8640(1988)050%3c0098:CHOGBD%3e2.3.CO;2) (1988).
43. Pauley, G. B. & Nakatani, R. E. Histopathology of "gas-bubble" disease in salmon fingerlings. *J. Fish. Res. Board Can.* **24**, 867–871. <https://doi.org/10.1139/f67-073> (1967).
44. Marking, L. *Gas Supersaturation in Fisheries* (United States Department of the Interior, Fish and Wildlife Service, 1987).

## Acknowledgements

The authors would like to thank the engineering team of IBERCO S.L., especially Jacinto Paredes, for the design and attention to this project. This work was supported by the National Project PGC2018-101226-B-I00. In addition, AV-W was funded by the University Professor Formation fellowship from the Spanish Ministry of Education (FPU17/00763), and YBdQ was funded by the Marie Skłodowska-Curie Actions (MSCA) fellowship H2020-MSCA-IF-GF-2019 ref#89227.

## Author contributions

A.F., M.J., Y.B., O.G.: conceptualization. A.F.: funding. A.V.: writing. Y.B., M.J., M.B., M.A., and A.V.: experimental procedures and laboratory analyses. A.V., Y.B., M.J. and M.A.: pathological studies. All authors: review and editing. A.F., Y.B. and M.J.: supervision.

## Competing interests

The authors declare no competing interests.

## Additional information

**Supplementary Information** The online version contains supplementary material available at <https://doi.org/10.1038/s41598-022-10539-8>.

**Correspondence** and requests for materials should be addressed to M.J.C.

**Reprints and permissions information** is available at [www.nature.com/reprints](http://www.nature.com/reprints).

**Publisher's note** Springer Nature remains neutral with regard to jurisdictional claims in published maps and institutional affiliations.



**Open Access** This article is licensed under a Creative Commons Attribution 4.0 International License, which permits use, sharing, adaptation, distribution and reproduction in any medium or format, as long as you give appropriate credit to the original author(s) and the source, provide a link to the Creative Commons licence, and indicate if changes were made. The images or other third party material in this article are included in the article's Creative Commons licence, unless indicated otherwise in a credit line to the material. If material is not included in the article's Creative Commons licence and your intended use is not permitted by statutory regulation or exceeds the permitted use, you will need to obtain permission directly from the copyright holder. To view a copy of this licence, visit <http://creativecommons.org/licenses/by/4.0/>.

© The Author(s) 2022



### III. Biomarkers related to gas embolism: gas score, pathology, and gene expression in a gas bubble disease model

**Velázquez-Wallraf, A.**, Caballero, M.J., Fernández, A., Betancor, M.B., Saavedra, P., Hemingway, H.W., & Bernaldo de Quirós, Y. *PLOS ONE*, Accepted for publication on July 1, 2023. <https://doi.org/10.1371/journal.pone.0288659>



## FORMAL ACCEPTANCE LETTER

Notification of Formal Acceptance for PONE-D-23-04319R2 -  
[EMID:4124ff9a7ae904c7]

em.pone.0.847ae6.f537d8e4@editorialmanager.com  
<em.pone.0.847ae6.f537d8e4@editorialmanager.com>  
en nombre de  
PLOS ONE <em@editorialmanager.com>

Mié 05/07/2023 22:04

Para: Alicia Sofía Velázquez Wallraf <alicia.velazquez101@alu.ulpgc.es>

You are being carbon copied ("cc:'d") on an e-mail "To" "Maria José Caballero"  
mariajose.caballero@ulpgc.es

CC: alicia.velazquez101@alu.ulpgc.es, antonio.fernandez@ulpgc.es, m.b.betancor@stir.ac.uk,  
pedro.saavedra@ulpgc.es, holden.hemingway@colorado.edu, yara.bernaldo@ulpgc.es

PONE-D-23-04319R2

Biomarkers related to gas embolism: gas score, pathology, and gene expression in a gas bubble disease model.

Dear Dr. Caballero:

I'm pleased to inform you that your manuscript has been deemed suitable for publication in PLOS ONE. Congratulations! Your manuscript is now with our production department.

If your institution or institutions have a press office, please let them know about your upcoming paper now to help maximize its impact. If they'll be preparing press materials, please inform our press team within the next 48 hours. Your manuscript will remain under strict press embargo until 2 pm Eastern Time on the date of publication. For more information please contact [onepress@plos.org](mailto:onepress@plos.org).

If we can help with anything else, please email us at [plosone@plos.org](mailto:plosone@plos.org).

Thank you for submitting your work to PLOS ONE and supporting open access.

Kind regards,  
PLOS ONE Editorial Office Staff

on behalf of  
Dr. Jayonta Bhattacharjee  
Academic Editor  
PLOS ONE


Maria José Caballero ▾

[Home](#) [Main Menu](#) [Submit a Manuscript](#) [About ▾](#) [Help ▾](#)

← **Submissions with Production Completed**

**Contents:** This page lists all submissions where production has been completed.

Page: 1 of 1 (1 total submissions) Results per page 10 ▾

Action	Manuscript Number	DOI	Title	Initial Date Submitted	Final Decision Date
<a href="#">Action Links</a>	PONE-D-23-04319R2	10.1371/journal.pone.0288669	Biomarkers related to gas embolism: gas score, pathology, and gene expression in a gas bubble disease model.	Feb 14 2023 7:08AM	Jul 1 2023 12:39AM

Page: 1 of 1 (1 total submissions) Results per page 10 ▾

1 **Biomarkers related to gas embolism: gas score,**  
2 **pathology, and gene expression in a gas bubble disease**  
3 **model.**

4 **Alicia Velázquez-Wallraf<sup>1</sup>, María José Caballero<sup>1\*</sup>, Antonio Fernández<sup>1</sup>, Mónica**  
5 **B. Betancor<sup>2</sup>, Pedro Saavedra<sup>3</sup>, Holden W. Hemingway<sup>4</sup>, Yara Bernaldo de**  
6 **Quirós<sup>1,4</sup>.**

7 **1** Veterinary Histology and Pathology, Atlantic Center for Cetacean Research, University Institute of  
8 Animal Health and Food Safety (IUSA), Veterinary School, University of Las Palmas de Gran Canaria  
9 (ULPGC), Canary Islands, Spain. **2** Institute of Aquaculture, Faculty of Natural Sciences, University of  
10 Stirling, Stirling, UK. **3** Department of Mathematics, University of Las Palmas de Gran Canaria  
11 (ULPGC), Canary Islands, Spain. **4** Department of Integrative Physiology, University of Colorado  
12 Boulder, Boulder, CO, USA.

13 \* mariajose.caballero@ulpgc.es (MJC)

14 **Abstract**

15 Fish exposed to water supersaturated with dissolved gas experience gas embolism similar  
16 to decompression sickness (DCS), known as gas bubble disease (GBD) in fish. GBD has  
17 been postulated as an alternative to traditional mammals' models on DCS. Gas embolism  
18 can cause mechanical and biochemical damage, generating pathophysiological responses.  
19 Increased expression of biomarkers of cell damage such as the heat shock protein (HSP)  
20 family, endothelin 1 (ET-1) or intercellular adhesion molecule 1 (ICAM-1) has been  
21 observed, being a possible target for further studies of gas embolism. The GBD model  
22 consisted of exposing fish to supersaturation in water with approximately 170% total  
23 dissolved gas (TDG) for 18 hours, producing severe gas embolism. This diagnosis was  
24 confirmed by a complete histopathological exam and the gas score method. HSP70  
25 showed a statistically significant upregulation compared to the control in all the studied  
26 organs ( $p < 0.02$ ). Gills and heart showed upregulation of HSP90 with statistical  
27 significance ( $p = 0.015$  and  $p = 0.02$ , respectively). In addition, HSP70 gene expression  
28 in gills was positively correlated with gas score ( $p = 0.033$ ). These results suggest that  
29 gas embolism modify the expression of different biomarkers, with HSP70 being shown  
30 as a strong marker of this process. Furthermore, gas score is a useful tool to study the  
31 abundance of gas bubbles, although individual variability always remains present. These  
32 results support the validity of the GBD model in fish to study gas embolism in diseases  
33 such as DCS.

34 **Introduction**

35 The circulation of gas bubbles through the vascular system is known as gas embolism. It  
36 can be developed under different conditions, including the accidental introduction of gas  
37 during surgical and medical procedures [1,2], penetrating traumas [3], as well as in  
38 pathological processes such as barotraumas and decompression sickness (DCS) that can  
39 produce intra- and extravascular gas bubbles [4]. Depending on the cause of gas  
40 embolism, the abundance and distribution of gas bubbles may differ [1]. DCS is mostly

41 described in human divers [5], although it has also been reported in cetaceans [6,7] and  
42 marine turtle [8]. Fish experienced a gas embolism similar to DCS named gas bubble  
43 disease (GBD) [9,10].

44 GBD and DCS share similarities in terms of pathophysiology, the latter has previously  
45 been postulated as an experimental model for studying DCS [10-13]. Velázquez-Wallraf  
46 et al. [14] reported the study of GBD in fish as an alternative to traditional mammals'  
47 models for the study of gas embolism and DCS in accordance with the replacement  
48 principle from the European regulations for the use of laboratory animals (Directive  
49 2010/63/EU of the European Parliament).

50 GBD occurs in fish when the water where they inhabit gets supersaturated of dissolved  
51 gases [15]. This disease has been responsible for high fish mortalities mainly described  
52 in large hydroelectric projects where, due to the force exerted by the water mass falling  
53 from one dam to another, atmospheric gases are entrained and forced to dissolve [10].  
54 Exposure of fish to these supersaturated waters causes the development of intravascular  
55 and extravascular gas bubbles [11], which varying in severity depending on the total  
56 dissolved gas (TDG) values and length of exposure [15]. TDG supersaturation values  
57 higher than 120% have triggered acute GBD and lead to death of some fish [15].

58 Gas embolism can cause mechanical and biochemical damage [16], generating  
59 pathophysiological responses, notably from endothelial cells, the first cell line to  
60 encounter intravascular gas bubbles [17]. Regarding GBD, Speare et al. (1991) [18] were  
61 the first to describe GBD lesions related to endothelial damage. Although the mechanism  
62 remains unclear, two possible pathways of endothelial cell activation have been  
63 hypothesized [18]. Direct activation by contact of the gas bubbles with the endothelial  
64 wall cells themselves has been proposed [19] and, on the other, indirect activation by the  
65 formation of molecules secondary to gas embolism [20]. Regarding direct activation, gas  
66 bubbles are foreign surfaces that cause a circulating blood-bubble interface [21]. This  
67 foreign interface may generate activation of plasma proteins, platelet aggregation, leading  
68 to thrombogenesis [22] and consequent thrombocytopenia [23], involving cell adhesion  
69 molecules, such as intercellular adhesion molecule 1 (ICAM-1). ICAM-1 is expressed  
70 by endothelial cells in response to the call of proinflammatory cytokines, facilitating the  
71 migration of leukocytes across the endothelium into inflamed tissue [24]. In addition,  
72 endothelial cells respond to bubble contact by generating biomarkers of endothelial stress,  
73 such as the heat shock protein (HSP) family [17]. The consequent endothelial dysfunction  
74 causes a decrease in nitric oxide (NO), a vasodilator molecule, that generates a relative  
75 increase in vasoconstriction factors, mainly endothelin-1 (ET-1). Therefore, activation of  
76 the expressed biomarkers due to the above circumstances represents an important target  
77 for further investigation of gas embolism [25].

78 In this study, we tested the hypothesis that GBD in fish induces similar vascular and  
79 cellular responses to other gas embolisms, such as DCS in mammals, and if it can be used  
80 as an alternative experimental model. To test this hypothesis, we first induced a severe  
81 GBD in a group of goldfish (*Carassius auratus*), we evaluated tissue damage through  
82 pathology, we assessed the presence, distribution, and amount of gas bubbles in several  
83 intra- and extravascular locations and analyzed the expression of different biomarkers

84 that have previously been associated with the consequent biochemical damage of gas  
85 embolism in other laboratory animals.

## 86 **Material and methods**

### 87 **Experimental fish**

88 For this study, 20 goldfish (*Carassius auratus*), 10 males and 10 females (weight: 116.1  
89  $\pm$  11.3 g; length: 17.2  $\pm$  0.5 cm long), were purchased from Tropical Centre (ICA  
90 Canarias). Fish were kept in tap water conditioned with JBL Biotopol and JBL Denitrol,  
91 according to the manufacturer's instructions, with a natural photoperiod of 12:12h  
92 light:dark cycle and fed twice daily. Using a colorimetric test kit, water parameters such  
93 as nitrate and nitrite concentration ( $<10$  mg/dm<sup>3</sup> nitrate, 0 mg/dm<sup>3</sup> nitrite), pH ( $\pm 6.8$ ), total  
94 hardness (80-300 mg/dm<sup>3</sup>) and chlorine (0 mg/dm<sup>3</sup>) were measured every two days, along  
95 with measurement of temperature (23-25 °C) and dissolved oxygen ( $>6.0$  mg/ dm<sup>3</sup>).

### 96 **Experimental procedures**

97 Fish were evenly divided into two treatment groups: control group (n=10) and GBD group  
98 (n=10). Fish in the GBD group were individually introduced into a pressurized aquarium  
99 for 18 hours with supersaturated water produced following Velázquez-Wallraf et al. [14].  
100 This supersaturated water was produced using a pressure vessel (max. 3 ATA) coupled  
101 to a pressurized aquarium (max. 0.5 bar) through constant recirculation of the water.  
102 Briefly, the vessel was filled with tap water at ambient pressure, the water was  
103 recirculated throughout the circuit with the help of a motor pump and pressurized  
104 synthetic atmospheric air was injected until reaching the maximum pressure of the circuit.  
105 At that time, the water was kept in constant recirculation, passing through a dissolution  
106 tube composed of small-diameter porous materials that forced the gas to dissolve in the  
107 water, until a dynamic equilibrium between the liquid phase and the gas phase was  
108 obtained. This entire process was controlled by a TDG sensor with real-time values.

109 Fish were introduced in the pressurized aquarium when TDG supersaturation levels of  
110  $169 \pm 5\%$  were reached in agreement with Velázquez-Wallraf et al. [14]. Fish from the  
111 control group were placed in the same aquarium but without exerting pressure or  
112 recirculation of water, so the TDG saturation level was 100% during the 18 hours of  
113 control test. During the exposure, activity and clinical signs were monitored and  
114 registered, paying special attention to opercular movements frequency, swimming  
115 behavior, presence of gas bubbles in fins or eyes, loss of scales, hemorrhages, or  
116 subcutaneous emphysema, as described by Velázquez-Wallraf et al. [14]. After 18 hours,  
117 fish from both groups were euthanized with 2-phenoxyethanol (0.6 ml/L).

### 118 **Gas score: presence, amount, and distribution of gas bubbles**

119 Before dissection, the eyes, integument, gills, and fins were examined under a stereo  
120 microscope for the presence of gas bubbles and lesions. Later, the coelomic cavity was  
121 carefully opened to enable the visualization of internal organs and vasculature, and  
122 presence, amount, and distribution of intravascular and extravascular gas bubbles, was  
123 evaluated using a gas score index [26] adapted to fish. The locations used for the

124 assessment of intravascular gas bubbles were fin, opercular, cranial and caudal  
125 subcutaneous, swim bladder and posterior cardinal veins, as well as ventral and dorsal  
126 aorta. Intravascular locations were graded from 0 to 6, while extravascular locations were  
127 graded from 0 to 3 (Table 1). In the extravascular locations, the gas score was based on  
128 the presence of emphysema in the visceral fat and fins. Total gas score was calculated by  
129 the summation of the gas score index for each location. Gas score ranged from 0 to 54.

130 **Table 1. Definition of gas score index.** Gas score definition for post-mortem examinations, following  
131 Bernaldo de Quirós et al. [25].

GAS SCORE	DEFINITION
<b>INTRAVASCULAR LOCATIONS</b>	
GRADE 0	Absence of bubbles
GRADE 1	Occasional bubble
GRADE 2	Few bubbles
GRADE 3	Few bubbles and discontinuities of blood
GRADE 4	Moderate presence of bubbles
GRADE 5	Abundant presence of bubbles
GRADE 6	Complete sections filled with gas
<b>EXTRAVASCULAR LOCATIONS</b>	
GRADE 0	Absence of gas
GRADE 1	Scarce presence (1 organ affected)
GRADE 2	Moderate presence of gas (more than 1 organ)
GRADE 3	Abundant presence of gas (systemic)

132

### 133 Gross and histopathological evaluation

134 Simultaneously to the gas score, external and internal organs were examined  
135 macroscopically for lesions, and representative samples were collected and fixed in 10%  
136 buffered formalin. Samples were processed routinely, embedded in paraffin wax and 4-  
137  $\mu$ m-thick sections were cut and stained with hematoxylin and eosin (H&E) [27] and  
138 examined by two pathologists. Additionally, samples were also pretreated with chromic  
139 acid to fix lipids prior to paraffin-embedding [28]. Lipids were stained with Oil O Red  
140 and the tissue was counterstained with Mayer's hematoxylin to discriminate between gas  
141 and fat emboli [29].

### 142 Gene expression analysis by real-time qPCR

143 Molecular studies of biomarkers of vascular damage were carried out in 6 fish from each  
144 group. Samples of posterior kidney, gills, heart, and ventral aorta were collected in  
145 cryotubes with 1 ml of RNA-later (Sigma-Aldrich, Dorset, UK), maintained for 24 hours  
146 at 4 °C and then preserved at -80 °C until RNA extraction from the samples was  
147 performed. Sequences corresponding to the open reading frame (ORF) for selected genes,  
148 HSP70, HSP90, E-1, and ICAM-1, for *Carassius auratus* were aligned using NCBI  
149 BLAST sequence alignment analysis (NIH) and primers designed on common conserved  
150 regions (Table 2). In addition, elongation factor 1-alpha (EF1 $\alpha$ ) and beta-2 microglobulin  
151 (B2M) were chosen as reference (housekeeping) genes, according to GeNorm.

152 **Table 2. Target and reference genes.** Sequences of designed primers and the efficiency and correlation  
153 values of each gene.

GEN	PRIMER	SEQUENCE	STANDARD CURVE QUALITY
<b>HSP70</b>	FORWARD PRIMER	ACCTACTCAGACAACCAGCC	R <sup>2</sup> = 0.992
	REVERSE PRIMER	CCACTGCCGACACATTTAGG	E= 106.7%
<b>HSP90</b>	FORWARD PRIMER	GCTTCGAGGTGCTGTACATG	R <sup>2</sup> = 0.998
	REVERSE PRIMER	TTGGCCTTGCTCTCCAT	E= 101.2%
<b>ET-1</b>	FORWARD PRIMER	AGCGCTCAGTAACAGAACCT	R <sup>2</sup> = 0.99
	REVERSE PRIMER	CGTTGTCTGTTGTCTGCCA	E= 101.51%
<b>ICAM-1</b>	FORWARD PRIMER	GGCAGTATCAGCTCCAGTGT	R <sup>2</sup> = 0.98
	REVERSE PRIMER	CACACCAGTACTGAGCTCCA	E= 105.74%
<b>EF1α</b>	FORWARD PRIMER	GATTGTTGCTGGTGGTGTG	R <sup>2</sup> = 0.992
	REVERSE PRIMER	GCAGGGTTGTAGCCGATT	E= 93.48%
<b>B2M</b>	FORWARD PRIMER	GCCCTGTTCTGTGTCTGTA	R <sup>2</sup> = 0.999
	REVERSE PRIMER	AAGGTGACGCTCTTGTTGAG	E= 103.74%

154

155 Target tissues were dissected and homogenized in tubes with 900 µl of Qiazol Lysis  
 156 Reagent using a stainless-steel bead in Tissuelyser II (Qiagen, Hilden, Germany), and  
 157 following the manufacturer's instructions for total RNA extraction. Isolated RNA was  
 158 quantified via spectrophotometry (Nanovue plus spectrophotometer, Biochrom Ltd.,  
 159 Cambridge, UK). RNA quality was estimated by visualization on 1% agarose gel with an  
 160 UV transilluminator (Bio-Rad, California, USA). Complementary DNA (cDNA) was  
 161 synthesized from 10 µl of extracted RNA using the High-capacity cDNA reverse  
 162 transcription kit (Thermo Fisher scientific, Massachusetts, USA), and performing reverse  
 163 transcription by thermocycler. To quantify this cDNA synthesis, a Qubit fluorometer  
 164 (Thermo Fisher scientific, Massachusetts, USA) was used together with a Qubit ssDNA  
 165 Assay kit, performing standard curves.

166 Confirmation of correct amplification of selected reference and target genes was carried  
 167 out previously as follows: melting-curve analysis for each primer set was conducted to  
 168 further confirm the specificity of PCR amplification. To calculate the PCR amplification  
 169 efficiency of each primer set, serial dilution of cDNA from the samples and no-template  
 170 control were used as templates for Real-Time quantitative PCR (RT-qPCR). The standard  
 171 curve was generated for the calculation of amplification efficiency (E) and correlation  
 172 coefficients (R<sup>2</sup>) of each primer set. These values are listed in **Table 2** and were  
 173 calculated to ensure that the efficiency is above 90% for all primer pairs.

174 RT-qPCR was carried out using QuantStudio 12k flex RT-qPCR system (Applied  
 175 Biosystems, Warrington, UK) in 96 well-plates in triplicates (technical replicates). The  
 176 total volume per reaction was set at 10 µl, containing 1 µl of cDNA sample (1:10 diluted),  
 177 5 µl of TB Green™ Premix Ex Taq™ II-Tli RNaseH Plus (Takara Bio Inc., Kusatsu,  
 178 Japan), 0.2 µl ROX Reference Dye II (50X; Takara Bio Inc.), 0.2 µl of forward and

179 reverse specific primers for each gene and 3.4  $\mu$ l of ddH<sub>2</sub>O. In addition, no-template  
180 control (CNTC) and RT negative control (CRT) were used as negative controls for each  
181 primer set. The amplification programs were set as an initial denaturation step at 95°C for  
182 30 sec, followed by 40 PCR cycles: 5 s at 95°C, 1 min at 62°C for annealing temperature.

183 The RT-qPCR data were analyzed using Design & Analysis Software v.2.4.3 (Thermo  
184 Fisher scientific, Massachusetts, USA). Cycle threshold (Ct) values were obtained using  
185 auto baseline and applied to all amplicons of the same primer set. The fold change in  
186 expression of target genes (HSP70, HSP90, ET-1, ICAM-1) was calculated using the 2<sup>-  
187  $\Delta$ Ct</sup> method [30]. Gene expression of each sample was normalized with the geometric  
188 mean of RNA content of reference genes (EF1 $\alpha$ , B2M).

### 189 **Statistical analysis**

190 The differences in biomarker gene concentration in control fish vs fish with GBD were  
191 analysed by Mann-Whitney test. Biomarker genes that were found to be statistically  
192 significant different ( $p < 0.05$ ) or near statistically significantly different ( $p < 0.1$ ), the  
193 correlation of these gene concentrations and total gas score was evaluated by Spearman's  
194 correlation coefficient. The significance level used for all statistical tests performed was  
195  $p$  value  $< 0.05$ . SPSS software package (version 29.0; SPSS, IBM) and R software  
196 package (version 3.3.1; R Development Core Team) for Windows were used. Statistical  
197 power was calculated by post hoc test with a significance level of 0.05, using G\*power  
198 software (version 3.1.9.6; Heinrich-Heine-Universität Düsseldorf).

## 199 **Results**

### 200 **Fish behavior and clinical signs under exposure to** 201 **supersaturated water**

202 During the treatment, all fish from the GBD group showed clinical signs consistent with  
203 severe GBD such as increased opercular and swimming frequency along with the  
204 presence of gas bubbles in the fins. The presence and size of these gas bubbles increased  
205 with time spent in pressurized and supersaturated water. In the last two experimental  
206 hours, fish presented with erratic movements, loss of buoyancy along with severe  
207 hemorrhages and gas bubbles in the fins. Control fish showed no behavioral or clinical  
208 signs during observation.

### 209 **Gas score: presence, amount, and distribution of gas bubbles**

210 The results obtained at each intravascular and extravascular location, as well as the total  
211 gas score of the GBD group are shown in **Fig 1**. In the GBD group, half of the studied  
212 intravascular locations presented a mode gas score of 5: fin veins (90% of the fish) (**Fig**  
213 **2A**), posterior cardinal veins (60%) (**Fig 2B**), ventral aorta (50%) (**Fig 2C**), and dorsal  
214 aorta (30%). The subcutaneous caudal (50%) (**Fig 2D**) and opercular veins (30%)  
215 presented a mode gas score of 4; and the subcutaneous cranial (60%) (**Fig 2E**) and swim  
216 bladder (50%) vein had a mode gas score of 3 (**Fig 2F**). Within the two extravascular

# Comparative study of gas-bubble lesions using experimental models

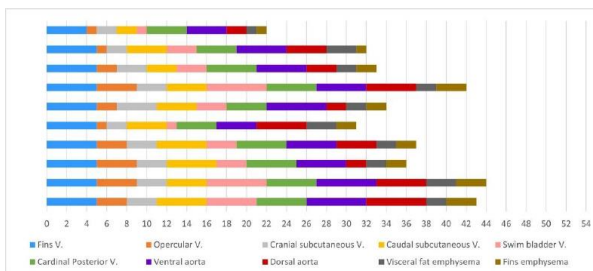
PLOS ONE

Manuscript draft: PONE-D-23-04319R2.

Accepted for publication on July 1, 2023.

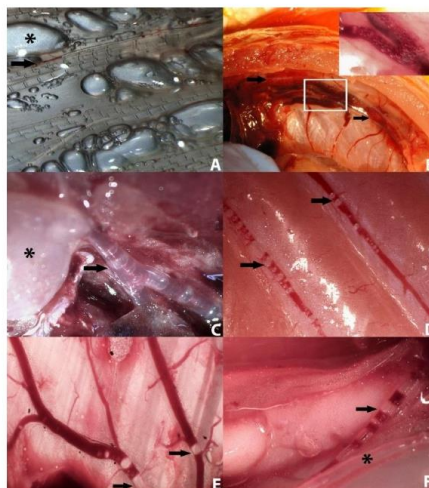
10.1371/journal.pone.0288659

217 locations studied, mode gas score was 2, both in visceral fat emphysema (60%) and fin  
218 emphysema (50%). All the control animals showed a total gas score of 0.



219

220 **Fig 1. Gas score results.** Gas scores obtained in the intravascular (0-6 scores) and extravascular (0-3  
221 scores) locations of each fish in the GBD group. The total gas score of each fish is also shown.



222

223 **Fig 2. Gas score locations under stereo microscope.** **A)** Fins. Presence of large gas discontinuities in  
224 the blood vessels (arrow) causing a gas score 5, together with emphysema (star), graded with gas score of  
225 3. **B)** Posterior cardinal veins. Presence of abundant gas bubbles along their entire course (arrows), with  
226 gas score 5. Detail of gas bubbles at the beginning of the posterior cardinal veins from the caudal vein  
227 (inset). **C)** Heart and ventral aorta. Gas score 5 with abundant presence of gas bubbles at the exit of the  
228 ventral aorta (arrow) from the bulbus arteriosus (star), which appears gas dilated. **D)** Caudal subcutaneous  
229 veins with moderate presence of bubbles (arrows). Gas score 4. **E)** Cranial subcutaneous veins with few  
230 bubbles inside, although with a discontinuity (arrows). Gas score 3. **F)** The vein of the swim bladder with  
231 abundant presence of gas bubbles (arrow), running parallel to the pneumatic duct (star). Gas score 5.

232 **Gross and histopathological evaluation**

233 Externally, the presence of subcutaneous emphysema was denoted by skin in 70% of fish  
234 (7/10), coinciding with areas where the loss of scales was observed in vivo. Fins presented  
235 emphysema and hemorrhages in all animals (100%, 10/10) (Figs 3A and 3B), being the  
236 pectoral fins (90%, 9/10) followed by the caudal fins (50%, 5/10) the most affected  
237 locations. The gills presented severe hemorrhages (70%, 7/10) (Fig 3C).

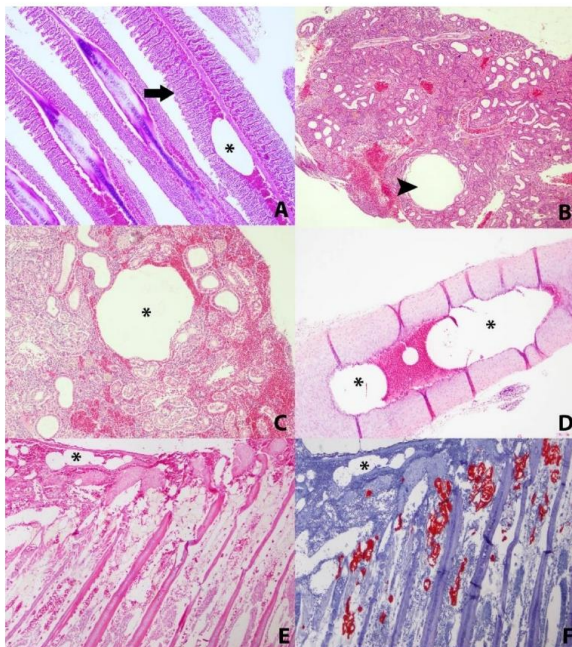


238  
239 **Fig 3. Macroscopic lesions.** A) Presence of hemorrhages and emphysema in the fins, pectoral fins with  
240 greater affection. B) Fins with greater detail of the emphysema (star) and the hemorrhages described, as  
241 well as a bubble in a blood vessel. C) Presence of hemorrhage in the gills, appreciated in the ventral area  
242 of the gills. D) Portion of liver surrounded by visceral fat, which presents an emphysematous aspect.

243 In the opening of the coelomic cavity, emphysema of the visceral adipose tissue stood out  
244 in most animals (70%, 7/10) (Fig 3D). In addition, the swim bladder was hyperinflated  
245 (90%, 9/10) and the bulbus arteriosus of the heart appeared distended due to the presence  
246 of gas (100%, 10/10). Multiorgan congestion was observed: fins (70%, 7/10), gills  
247 (100%/10/10/10), posterior kidney (90%, 9/10), liver (90%, 9/10), spleen (70%, 7/10),  
248 and central nervous system (50%, 5/10).

249 Microscopically, notable findings were emphysema of fins (100%, 10/10) observed as  
250 gas-distended areas between the fin rays, together with congestion (100%, 10/10). In  
251 some animals, hemorrhages due to the rupture of larger congested blood vessels were  
252 observed in the fins (60%, 6/10). The gills showed remarkably consistent microscopic  
253 congestion (100%, 10/10) and hemorrhages (70%, 7/10), together with fusion of the  
254 secondary lamellae in some animals (50%, 5/10) (Fig 4A). In the posterior kidney,  
255 severely dilated blood vessels were observed (90%, 9/10), without the presence of  
256 circulating blood, while in those with the presence of blood, congestion was observed  
257 (100%, 10/10) (Fig 4B). Intravascular bubble-like round empty spaces among blood cells  
258 were identified in different blood vessels. These were predominantly observed in fins  
259 (90%, 9/10), gills (90%, 9/10) and posterior kidney (80%, 8/10) in considerable amounts.

260 In other organs intravascular gas bubbles were also observed but only in some animals,  
 261 such as ventral aorta (30%, 3/10) (**Fig 4D**), in the coronary veins of the heart (30%, 3/10),  
 262 spleen (20%, 2/10), gonads (20%, 2/10), and liver (10%, 1/10). These structures were  
 263 neither stained by H&E or Oil Red, confirming that they were gas bubbles (**Figs 4E** and  
 264 **4F**). Multiorgan congestion was confirmed via microscopic visualization.



265

266 **Fig 4. Microscopic lesions.** A) Gills with the presence of a large gas bubble in the central vessel of the  
 267 primary lamella (star). There is also fusion of the secondary lamellae (arrow). HxEx10. B) Posterior  
 268 kidney with presence of vascular dilations (arrowhead) and congestion of blood vessels. HxEx4. C)  
 269 Posterior kidney with presence of large gas bubble displacing blood components to the periphery (star).  
 270 HxEx10. D) Ventral aorta at origin of the arterial bulb, showing gas bubbles inside (star). HxEx10. E)  
 271 Gas bubbles at the base of a holobranch (star). HxEx4. F) Control of gas bubbles on the same sample as  
 272 above. Chromic acid x4.

273 The macroscopic and microscopic pathological findings of each fish, as well as the  
 274 degrees of severity shown, are described in **Table 3** and **Table 4**. Examination of the  
 275 control group revealed no pathological findings.

PLOS ONE | <https://doi.org/10.1371/journal.pone.0241022> Accepted for publication on July 1, 2022

FISH	INTEGUMENT		FINS					EYES		GILLS	
	Increased mucus production	Subcutaneous emphysema	Emphysema	Congestion	Hemorrhages	Most affected fins	Exophthalmia	Congestion	Hemorrhages		
GBD 1	X	Mo	Mo	Mo	Mo	Pectoral, anal, and ventral	X	Mo	Mo		
GBD 2	X	Mo	S	S	Mo	Pectoral	-	Mo	Mo		
GBD 3	X	-	Mo	S	S	Pectoral	-	S	S		
GBD 4	-	Mo	Mo	S	S	Pectoral and caudal	X	Mi	-		
GBD 5	X	Mi	Mi	-	Mi	Pectoral, ventral, and anal	X	S	S		
GBD 6	-	-	Mo	Mo	Mo	Pectoral and caudal	X	Mo	-		
GBD 7	-	-	S	-	S	Pectoral and caudal	-	Mi	Mi		
GBD 8	X	Mi	Mo	-	Mo	Pectoral and dorsal	X	Mo	Mo		
GBD 9	X	Mo	Mo	Mo	Mo	Lateral, caudal, and ventral	X	Mo	Mo		
GBD 10	X	Mi	Mi	Mi	Mi	Pectoral and caudal	X	Mo	-		
<b>TOTAL</b>	Yes= 7/10 (70%) No= 3/10	S= 0/10 Mo= 4/10 (40%) Mi= 3/10 (30%) Yes= 7/10 (70%) No= 3/10	S= 2/10 (20%) Mo= 6/10 (60%) Mi= 2/10 (20%) Yes= 10/10 (100%) No= 0/10	S= 3/10 (30%) Mo= 3/10 (30%) Mi= 1/10 (10%) Yes= 7/10 (70%) No= 3/10	S= 3/10 (30%) Mo= 5/10 (50%) Mi= 2/10 (20%) Yes= 10/10 (100%) No= 0/10	P: 9/10 (90%) C: 5/10 (50%) V: 3/10 (30%) A: 2/10 (20%) L: 1/10 (10%) D: 1/10 (10%)	Yes= 6/10 (60%) No= 4/10	S= 2/10 (20%) Mo= 6/10 (60%) Mi= 2/10 (20%) Yes= 10/10 (100%) No= 0/10	S= 2/10 (20%) Mo= 4/10 (40%) Mi= 1/10 (10%) Yes= 7/10 (70%) No= 3/10		

FISH	ADIPOSE TISSUE	SWIM BLADDER	LIVER	SPLEEN	DIGESTIVE TRACT	POSTERIOR KIDNEY	CENTRAL NERVOUS SYSTEM	HEART
	Emphysema	Hyperinflation	Congestion	Congestion	Gas-distended	Emphysema	Congestion	Gas distended bulb
GBD 1	Mi	X	Mi	Mo	-	Mo	Mi	S
GBD 2	Mi	X	Mi	-	-	-	Mi	S
GBD 3	Mo	X	Mo	Mo	S	S	S	-
GBD 4	Mo	-	S	-	Mo	-	-	Mo
GBD 5	Mo	X	Mo	-	-	Mi	-	Mi
GBD 6	-	X	Mi	Mo	-	-	Mo	Mo
GBD 7	Mo	X	Mo	Mo	Mi	-	Mo	-
GBD 8	Mo	X	-	Mo	Mi	-	S	-
GBD 9	Mi	X	Mo	Mi	-	Mi	Mo	S
GBD 10	-	X	Mo	Mi	-	Mo	Mi	Mi
<b>TOTAL</b>	S= 0/10 Mo= 4/10 (40%) Mi= 3/10 (30%) Yes= 7/10 (70%) No= 3/10	Yes= 9/10 (90%) No= 1/10	S= 1/10 (10%) Mo= 5/10 (50%) Mi= 3/10 (30%) Yes= 9/10 (90%) No= 1/10	S= 0/10 Mo= 5/10 (50%) Mi= 2/10 (20%) Yes= 7/10 (70%) No= 3/10	S= 1/10 (10%) Mo= 1/10 (10%) Mi= 2/10 (20%) Yes= 4/10 (40%) No= 6/10 (60%)	S= 1/10 (10%) Mo= 1/10 (10%) Mi= 2/10 (20%) Yes= 4/10 (40%) No= 6/10 (60%)	S= 0/10 Mo= 1/10 (10%) Mi= 4/10 (40%) Yes= 5/10 (50%) No= 5/10	S= 5/10 (50%) Mo= 3/10 (30%) Mi= 2/10 (20%) Yes= 10/10 (100%) No= 0/10

276 Table 3. Macroscopic findings and degrees of severity. Macroscopic lesions were categorized as presence (X) or absence (-) and, in those cases where a severity could be attributed to the lesion, the degree of the lesion was specified, i.e., mild (Mi), moderate (Mo) or severe (S). In the total section, the presence (Yes) and the degrees of severity for each lesion were highlighted in bold.

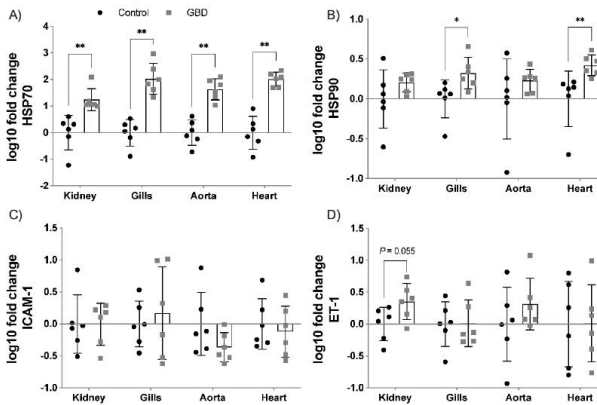
PLOS ONE | <https://doi.org/10.1371/journal.pone.0241022> Accepted for publication on July 1, 2022

FISH	EMPHYSEMA		CONGESTION		HEMORRHAGES		GAS BUBBLES		EYES		GILLS		LIVER		SPLEEN		
	Congestion	Gas bubbles	Congestion	Gas bubbles	Congestion	Gas bubbles	Congestion	Gas bubbles	Congestion	Gas bubbles	Congestion	Gas bubbles	Congestion	Gas bubbles	Congestion	Gas bubbles	
GBD 1	Mi	Mi	-	-	-	S	Mo	S	Mo	S	Mo	S	Mo	Mi	Mi	-	
GBD 2	Mo	Mi	-	Mo	-	Mo	Mo	-	Mo	Mo	Mo	Mo	Mo	Mi	Mi	-	
GBD 3	S	S	S	Mo	S	Mi	Mo	S	Mo	Mo	Mo	Mo	Mo	S	Mo	Mo	
GBD 4	S	S	S	S	S	Mi	S	Mo	Mo	Mo	Mo	Mo	Mo	S	Mo	-	
GBD 5	Mo	S	Mo	Mo	Mo	Mi	Mo	Mo	-	Mo	Mo	Mo	Mo	-	Mi	-	
GBD 6	S	Mi	Mi	Mi	-	Mi	-	-	-	Mo	Mo	Mo	Mo	-	Mi	-	
GBD 7	Mo	Mo	Mo	Mo	Mo	S	S	S	S	-	-	Mo	Mo	Mi	Mi	-	
GBD 8	Mo	Mo	Mo	Mo	Mo	S	Mo	Mo	Mo	Mi	Mi	Mo	Mo	Mi	Mo	-	
GBD 9	S	S	Mo	S	Mo	S	Mi	-	Mo	Mo	Mo	Mo	Mo	Mi	Mi	-	
GBD 10	Mi	Mi	-	Mi	Mi	Mi	Mi	-	Mi	-	Mo	Mo	Mo	Mi	Mi	-	
<b>TOTAL</b>	S= 4/10 (40%) Mo= 2/10 (20%) Mi= 4/10 (40%) Yes= 10/10 (100%) No= 0/10	S= 4/10 (40%) Mo= 2/10 (20%) Mi= 4/10 (40%) Yes= 10/10 (100%) No= 0/10	S= 1/10 (10%) Mo= 4/10 (40%) Mi= 1/10 (10%) Yes= 6/10 (60%) No= 4/10	S= 3/10 (30%) Mo= 4/10 (40%) Mi= 2/10 (20%) Yes= 9/10 (90%) No= 1/10	S= 0/10 Mo= 3/10 (30%) Mi= 4/10 (40%) Yes= 7/10 (70%) No= 3/10	S= 5/10 (50%) Mo= 2/10 (20%) Mi= 2/10 (20%) Yes= 10/10 (100%) No= 0/10	S= 3/10 (30%) Mo= 3/10 (30%) Mi= 2/10 (20%) Yes= 8/10 (80%) No= 2/10	S= 1/10 (10%) Mo= 4/10 (40%) Mi= 2/10 (20%) Yes= 7/10 (70%) No= 3/10	S= 1/10 (10%) Mo= 0/10 Mi= 3/10 (30%) Yes= 4/10 (40%) No= 6/10 (60%)	S= 1/10 (10%) Mo= 0/10 Mi= 3/10 (30%) Yes= 4/10 (40%) No= 6/10 (60%)	S= 0/10 Mo= 1/10 (10%) Mi= 4/10 (40%) Yes= 5/10 (50%) No= 5/10	S= 0/10 Mo= 1/10 (10%) Mi= 3/10 (30%) Yes= 4/10 (40%) No= 6/10 (60%)	S= 0/10 Mo= 1/10 (10%) Mi= 3/10 (30%) Yes= 4/10 (40%) No= 6/10 (60%)	S= 0/10 Mo= 1/10 (10%) Mi= 3/10 (30%) Yes= 4/10 (40%) No= 6/10 (60%)	S= 0/10 Mo= 3/10 (30%) Mi= 4/10 (40%) Yes= 7/10 (70%) No= 3/10	S= 0/10 Mo= 3/10 (30%) Mi= 4/10 (40%) Yes= 7/10 (70%) No= 3/10	S= 0/10 Mo= 1/10 (10%) Mi= 1/10 (10%) Yes= 2/10 (20%) No= 8/10

279 Table 4. Microscopic findings and degrees of severity. Microscopic lesions were categorized as presence (X) or absence (-) and, in those cases where a severity could be attributed to the lesion, the degree of the lesion was specified, i.e., mild (Mi), moderate (Mo) or severe (S). In the total section, the presence (Yes) and the degrees of severity for each lesion were highlighted in bold.

282 **Gene expression analysis**

283 Gene expression results were logarithmically transformed and were expressed as mean  $\pm$   
 284 standard error of the mean (SEM) (Fig 5). The expression of HSP70 and HSP90 genes  
 285 were significantly increased in gills ( $p = 0.002$ ;  $p = 0.015$ , respectively) and heart ( $p =$   
 286  $0.002$  in both). HSP70 gene expression was also significantly increased in the posterior  
 287 kidney and ventral aorta ( $p = 0.002$  in both), compared to the control group. ET-1 in  
 288 posterior kidney and ventral aorta, HSP90 in posterior kidney, and ICAM-1 in gills  
 289 showed a tendency towards upregulation compared to the control group although no  
 290 statistically significant differences were observed. Results of statistical power for each  
 291 biomarker expression performed are described in S1 Table. HSP70 expression statistical  
 292 analyses in the four tissues had high statistical power (>90%).

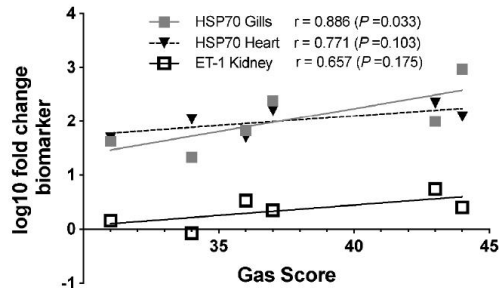


293

294 **Fig 5. Gene expression of biomarkers in selected tissues.** Log-transformed gene expression of the four  
 295 biomarkers in the tissues studied from the control group and the GBD group. Statistically significant  
 296 differences were observed in HSP70 for the four tissues and in HSP90 for gills and heart. Other results  
 297 such as HSP90 in posterior kidney, ET-1 in posterior kidney and ventral aorta, as well as ICAM-1 in gills  
 298 showed tendency to upregulation compared to the control group without reaching statistical significance.

299 **Correlation between gas score and genes expression**

300 HSP70 expression in gills correlated strongly with total gas score, with statistically  
 301 significant results ( $r = 0.886$ ,  $p = 0.033$ ). Additionally, a tendency to correlate was found  
 302 for HSP70 expression in the heart and ET-1 expression in the posterior kidney with total  
 303 gas score, although these correlations were not statistically significant ( $r = 0.771$ ,  $p =$   
 304  $0.103$ ; and  $r = 0.657$ ,  $p = 0.175$  respectively) (Fig 6). Results of statistical power of  
 305 correlation studies performed are described in S2 Table. HSP70 in gills and heart with  
 306 total gas score had a correlation with high statistical power (>90%).



307

308 **Fig 6. Correlation between total gas score and gene expression of biomarkers.** There is a significant  
 309 correlation between total gas score and HSP70 expression in gills, while ET-1 in posterior kidney and  
 310 HSP70 in heart exhibit a trend but with no statistically significant correlation with total gas score.

### 311 Discussion

312 In the present study, we reproduced gas embolism as seen in DCS in fish (i.e., GBD)  
 313 following Velázquez-Wallraf et al. [14]. The diagnosis of severe gas embolism was  
 314 confirmed through a complete histopathological study and the gas score method. HSP70,  
 315 HSP90, ET-1 and ICAM-1 genes were upregulated in different tissues of fish with GBD.  
 316 These results were statistically significant in the case of HSP70 in the four tissues studied  
 317 and in HSP90 in both gills and heart. ET-1 in posterior kidney and ventral aorta, HSP90  
 318 in the posterior kidney, and ICAM-1 in the gills had a tendency to increase their  
 319 expression compared to control group, although without statistical significance. HSP70  
 320 gene expression in gills correlated positively with total gas score.

321 The dissolution of atmospheric gas in the water of large dams occurs continuously, due  
 322 to the constant fall of water from one reservoir to another causing nearby waters to remain  
 323 supersaturated [15]. Velázquez-Wallraf et al. [14], attempted to reproduce this open  
 324 environment experimentally through an open aquarium, observing that gases were rapidly  
 325 released to the atmosphere with a consequent loss of the TDG values of the water. They  
 326 resorted to a pressurized aquarium to maintain constant recirculation of the water and  
 327 stable TDG values [14]. The effect of this closed environment on the fish was measured  
 328 through the control group fish, with no relevant behavioral change or clinical sign  
 329 observed [14]. The control group of the present study also did not show behavioral  
 330 alterations or clinical signs related to the pressurized aquarium.

331 The main macroscopic and microscopic findings were gas bubbles systemically  
 332 distributed. Other main pathological findings included: emphysema in fins, subcutaneous  
 333 tissue, and adipose tissue, hemorrhages in fins, gills, and posterior kidney, and multiorgan  
 334 congestion. These pathological findings were consistent with those described previously  
 335 by our group [14] and other studies of GBD in fish [31-35].

336 All fish in the GBD treatment group had a relatively high total gas score, although there  
337 was some inter-individual variability. This inter-individual variability was observed in  
338 the opercular veins, swim bladder vein, caudal subcutaneous veins, or the dorsal aorta.  
339 Hence, these locations were considered the most relevant to evaluate the severity of the  
340 gas embolism. Individual variability has been postulated to play a determining role in  
341 diseases that produce gas embolism [36, 37].

342 Increased amount of gas bubbles in vascular locations systemically distributed have been  
343 also reported in DCS experimental models: in guinea pigs [38], dogs [39, 40], mice [41],  
344 rabbits [26, 36, 42, 43], sheep [44], swine [45-47], rats [17, 37, 48-50], and in natural  
345 occurring DCS in humans [51, 52], cetaceans [7, 53-56] and sea turtles [8]. The gas score  
346 index was validated as a method to evaluate the presence of gas bubbles postmortem by  
347 correlating this index with the amount of gas bubbles seen by ultrasound in vivo in the  
348 right heart of rabbits [57]. The gas score has been used as a diagnostic tool for gas  
349 embolism [26, 55, 58], with the affected animals showing high total gas scores, in  
350 agreement with the present study.

351 Circulating intravascular gas bubbles trigger activation of the vascular endothelium,  
352 widely described in diseases such as DCS [59, 60] and GBD. For example, Speare et al.  
353 [18] related for the first time that GBD lesions were associated with endothelial damage.  
354 This generates a stress response of the organism, causing the emergence of different  
355 biomarkers [61].

356 HSPs are a superfamily of proteins that regulate different physiological processes mainly  
357 related to other proteins [62]. As a defense mechanism, the expression of these proteins  
358 can be increased under different stresses, especially thermal, oxidative, or hypoxic [63].  
359 The main role of HSP70, one of the most studied HSPs, is cytoprotection [64] and  
360 participation in the cell growth by mediating the production of nascent proteins [65].

361 HSP70 expression in gills, heart, posterior kidney, and ventral aorta showed a statistically  
362 significant pattern of upregulation in the GBD group. The gills were the location with the  
363 greatest magnitude difference between groups. The gills are the tissue that functionally  
364 resembles the lung in mammals [66]. Considering this, our results are in agreement with  
365 previous studies that showed an increase in HSP70 expression in lung, liver, and heart of  
366 rabbits [19], and in lungs of rats [61]. HSP70 expression in tissues has been postulated by  
367 several studies as a stress biomarker [67-69].

368 HSP90 showed a statistically significant upregulation in gills and heart. HSP90 is mainly  
369 a constitutive protein that, in certain circumstances, is induced to regulate client proteins  
370 in response to damage [70]. HSP90 expression following decompressive stress was not  
371 significantly elevated in tissues in contrast to the expression of HSP70 in the few existing  
372 studies measuring this marker, probably because baseline tissue expression levels of  
373 HSP90 in physiological situations are already high [25, 71]. In this study, the significant  
374 upregulation of HSP90 in gills and heart might be explained by the severity of the gas  
375 embolism.

376 Zhang et al., [72] suggested that elevated levels of ET-1 in blood serum after  
377 decompressive stress might be used to evidence endothelial stress in DCS. ET-1 is the

378 most potent vasoconstrictor factor known and it is secreted mainly by endothelial cells  
379 [73]. Although vascular endothelium is the most abundant source of ET-1 in the organism  
380 [74], this peptide is also secreted by the tubular cells of the renal medulla [75]. The  
381 posterior kidney is a highly vascularized organ, lodging in the perirenal area large caliber  
382 blood vessels such as posterior cardinal veins or the dorsal aorta [76], but also with small  
383 caliber arterioles and venules from malpighian corpuscle, where gas bubbles can easily  
384 get trapped and cause mechanical and biochemical damage. In our study, ET-1 tended to  
385 increase its expression in the posterior kidney and ventral aorta of GBD fish, but it was  
386 not statistically significant. These results could be used as a premise to test if ET-1 is  
387 elevated in blood serum of fish with GBD, and if this marker would be the best marker  
388 of gas embolism induced endothelial damage as suggested by Zhang et al. [72], since  
389 markers in blood serum accumulate over a course time if the half-life of the molecule is  
390 relatively high. This accumulation effect might provide a larger magnitude of difference  
391 between groups compared to expression alone in tissues. Therefore, the tendency to  
392 upregulation shown in both posterior kidney and ventral aorta for this biomarker is to be  
393 expected.

394 In the present study, no significant differences in ICAM-1 expression were found in the  
395 GBD group, in contrast to other studies [72, 77]. ICAM-1 is a transmembrane protein that  
396 is mainly located in the membrane of endothelial cells and leukocytes [78], allowing the  
397 transmigration of the latter through the endothelium to inflamed tissues [79]. Increased  
398 expression of ICAM-1 in lungs of rats with gas embolism after decompression has been  
399 observed by immunohistochemistry [77]. Some authors report that increases in  
400 expression of this molecule is slight in animals with gas embolism [80] while others  
401 consider it potentially as a valid parameter for endothelial dysfunction [72]. The  
402 differences in results from our study compared to the literature may be due to the  
403 experimental design, either because of the difference in ICAM-1 detection techniques and  
404 localization (tissue/blood serum) or that our model may not reach the time necessary to  
405 produce an inflammatory response sufficient to highly express this biomarker in tissues.

406 Total gas score presented a statistically significant correlation with HSP70 in gills. In the  
407 case of HSP70 in heart and ET-1 in posterior kidney, there was a tendency to correlate  
408 with the total gas score, but it was not statistically significant. These organs are highly  
409 perfused; therefore, the greater the amount of gas bubbles circulating through the vascular  
410 structures, the greater the expression of biomarkers associated with stress and endothelial  
411 dysfunction should be observed. ET-1 in blood serum correlated positively with the  
412 amount of gas bubbles observed in rats [17].

413 The correlations between gene upregulation and the gas score demonstrate that the  
414 damage was produced by the gas bubbles. In the case of the remaining correlations that  
415 did not exhibit a statistical significance, it is probably related to the limitations of this  
416 study: small sample size, the semiquantitative nature of the gas score index, and small  
417 variability in total gas score. Future studies should increase the sample size but also  
418 induce different degrees of severity of gas score so correlations between gas score and  
419 other markers can be better established. Furthermore, the gas score is a semiquantitative  
420 variable and the gene expression of markers a quantitative variable, consequently the  
421 correlation study performed cannot discriminate as much as if both variables were

422 quantitative. Still, with these limitations, we were able to detect a statistically significant  
423 correlation between total gas score and HSP70 expression in gills, and a tendency to  
424 correlate with no statistical significance between total gas score and HSP90 in gills and  
425 heart, and ET-1 in posterior kidney. Power analysis for correlations with total gas score  
426 showed that HSP70 in both gills and heart had high statistical power (>90%) while the  
427 trend to correlation with ET-1 in the posterior kidney showed acceptable statistical power  
428 (>70%) and may be promising correlations with a larger sample size.

429 The limitation of the sample size also applies to those biomarkers that, showing a  
430 tendency to upregulation, did not present statistically significant differences, being  
431 starting points for future studies with a larger sample size. The power analyses indicated  
432 that significance may have been reached if sample size were larger. On the other hand,  
433 the effect size of the non-significant samples was very small, requiring an excessively  
434 large sample size to achieve statistical significance, suggesting that there were no  
435 differences for GBD vs control for those markers. Overall, our study suggests that fish  
436 with GBD might be a valid model to experimentally study gas embolism and DCS and  
437 its effects similar to other traditional laboratory animals (i.e., mice, rats, and rabbits) but  
438 in a species with lower capacity to feel pain following the 3Rs replacement principle  
439 (Directive 2010/63/EU of the European Parliament).

440 In conclusion, fish with severe gas embolism showed an increase in HSPs, mainly HSP70,  
441 and a positive correlation with the gas score. Our results confirmed that HSP70 is a strong  
442 marker of gas embolism as has previously been demonstrated in other animal models,  
443 validating this model for the study of gas embolism and its effects. These results validated  
444 fish with GBD as a model for further investigation of the pathophysiological pathways of  
445 gas embolism, with the possibility of extrapolating the results to other susceptible species  
446 such as cetaceans, sea turtles or humans.

## 447 Acknowledgments

448 We would like to thank Diego Lozano Peral of the Supercomputing and Bioinnovation  
449 Center (SCBI) of the University of Malaga for the gene analysis of the samples  
450 performed; and Jacinto Paredes from IBERCO S.L., for the design and attention to this  
451 project.

## 452 References

- 453 1. Muth CM, Shank ES. Gas Embolism. *New Engl J Med*. 2000;342(7):476–482. doi:  
454 10.1056/NEJM200002173420706
- 455 2. Van Hulst RA, Klein J, Lachmann B. Gas embolism: pathophysiology and treatment. *Clin*  
456 *Physiol Funct I*. 2003;23(5):237–246. doi: 10.1046/j.1475-097X.2003.00505.x
- 457 3. Saukko P, Knight B. *Knight's Forensic Pathology*. Florida: CRC Press; 2013, p. 488–491.
- 458 4. Vann R, Butler F, Mitchell S, Moon R. Decompression illness. *Lancet*.  
459 2011;377(9760):153–164. doi: 10.1016/S0140-6736(10)61085-9
- 460 5. Edmonds C, Bennett M, Lippmann J, Mitchell SJ. *Diving Subaquatic Medicine*. 5th ed.,  
461 Florida: CRC Press; 2015, p. 123–202.
- 462 6. Jepson PD, Arbelo M, Deaville R, Patterson IA, Castro P, Baker JR, et al. Gas-bubble  
463 lesions in stranded cetaceans. *Nature*. 2003;425(6958):575–576. doi: 10.1038/425575a

- 464 7. Fernández A, Edwards JF, Rodríguez F, de los Monteros AE, Herráez P, Castro P, et al.  
465 “gas and fat embolic syndrome” involving a mass stranding of beaked whales (family  
466 ziphiidae) exposed to anthropogenic sonar signals. *Vet Pathol.* 2005;42(4):446–457. doi:  
467 10.1354/vp.42-4-446
- 468 8. García-Párraga D, Crespo-Picazo JL, de Quirós YB, Cervera V, Martí-Bonmati L, Díaz-  
469 Delgado J, et al. Decompression sickness (‘the bends’) in sea turtles. *Dis Aquat Org.*  
470 2014;111(3):191–205. doi: 10.3354/dao02790
- 471 9. Bouck GR. Etiology of gas bubble disease. *Trans Am Fish Soc.* 1980;109(6):703–707. doi:  
472 10.1577/1548-8659(1980)109<703:EOGBD>2.0.CO;2
- 473 10. Marking L. Gas supersaturation in fisheries. Fish and wildlife leaflet. Washington DC:  
474 United States Department of the Interior, Fish and Wildlife Service; 1987.
- 475 11. D’Aoust BG, Smith LS. Bends in fish. *Comp Biochem Physiol.* 1974;49(2):311–321. doi:  
476 10.1016/0300-9629(74)90122-4
- 477 12. Speare DJ. Disorders associated with exposure to excess dissolved gases. In: Leatherland  
478 JF, Woo PTK, editors. *Fish Disease and Disorders: 2. Non-infectious Disorders.*  
479 Oxfordshire: CAB International; 2010; pp. 342-356.
- 480 13. Machova J, Faina R, Randak T, Valentova O, Steinbach C, Kocour Kroupova H, et al. Fish  
481 death caused by gas bubble disease: A case report. *Vet Med (Praha).* 2017;62(4):231–237.  
482 doi: 10.17221/153/2016-VETMED
- 483 14. Velázquez-Wallraf A, Fernández A, Caballero MJ, Arregui M, González Díaz Ó, Betancor  
484 MB, et al. Establishment of a fish model to study gas-bubble lesions. *Sci Rep.*  
485 2022;12(6592). doi: 10.1038/s41598-022-10539-8
- 486 15. Weitkamp DE, Katz M. A review of dissolved gas supersaturation literature. *Trans Am*  
487 *Fish Soc.* 1980;109(6):659–702. doi:  
488 10.1577/15488659(1980)109<659:ARODGS>2.0.CO;2
- 489 16. Mahon RT, Regis DP. Decompression and decompression sickness. *Compr Physiol.*  
490 2014;4(3):1157–1175. doi: 10.1002/cphy.c130039
- 491 17. Zhang K, Wang D, Jiang Z, Ning X, Buzzacott P, Xu W. Endothelial dysfunction  
492 correlates with decompression bubbles in rats. *Sci Rep.* 2016;6:33390. doi:  
493 10.1038/srep33390
- 494 18. Speare, DJ. Endothelial lesions associated with gas bubble disease in fish. *J. Comp. Pathol.*  
495 1991;104(3):327-335. doi: 10.1016/S0021-9975(08)80044-8
- 496 19. Su C-L, Wu C-P, Chen S-Y, Kang B-H, Huang K-L, Lin Y-C. Acclimatization to  
497 neurological decompression sickness in rabbits. *Am J Physiol Regul Integr Comp Physiol.*  
498 2004;287(5):R1214-1218. doi: 10.1152/ajpregu.00260.2004
- 499 20. Madden LA, Laden G. Gas bubbles may not be the underlying cause of decompression  
500 illness – the at-depth endothelial dysfunction hypothesis. *Med Hypotheses.*  
501 2009;72(4):389–392. doi: 10.1016/j.mehy.2008.11.022
- 502 21. Kitano M, Kawashima M, Hayashi K. Experimental studies on decompression sickness. *J*  
503 *Orthop Traumatol.* 1978;27:653–658.
- 504 22. Warren BA, Philp RB, Inwood MJ. The ultrastructural morphology of air embolism:  
505 platelet adhesion to the interface and endothelial damage. *Br J Exp Pathol.* 1973;54(2):163-  
506 172.
- 507 23. Pontier JM, Blatteau JE, Vallée N. Blood platelet count and severity of decompression  
508 sickness in rats after a provocative dive. *Aviat Space Environ Med.* 2008;79(8):761–764.  
509 doi: 10.3357/ASEM.2299.2008
- 510 24. Yang L, Froio RM, Sciuto TE, Dvorak AM, Alon R, Lusinskas FW. ICAM-1 regulates  
511 neutrophil adhesion and transcellular migration of TNF- $\alpha$ -activated vascular endothelium  
512 under flow. *Blood.* 2005;106(2):584–592. doi: 10.1182/blood-2004-12-4942

- 513 25. Fismen L, Hjelde A, Svardal AM, Djurhuus R. Differential effects on nitric oxide synthase,  
514 heat shock proteins and glutathione in human endothelial cells exposed to heat stress and  
515 simulated diving. *Eur J Appl Physiol.* 2012;112(7):2717–2725. doi: 10.1007/s00421-011-  
516 2241-4
- 517 26. Bemaldo de Quirós Y, Saavedra P, Møllerløkken A, Brubakk AO, Jørgensen A, González-  
518 Díaz O, et al. Differentiation at necropsy between in vivo gas embolism and putrefaction  
519 using a gas score. *Res Vet Sci.* 2016a;106:48–55. doi: 10.1016/j.rvsc.2016.03.007
- 520 27. Bancroft J, Layton C. The hematoxylin and eosin. In: Suvama S, Layton C, Bancroft J,  
521 editors. *Bancroft's Theory and Practice of Histological Techniques.* 7th ed. Philadelphia:  
522 Churchill Livingstone of Elsevier; 2012. pp. 173-186.
- 523 28. Tracy RE, Walia P. A method to fix lipids for staining fat embolism in paraffin sections.  
524 *Histopathology.* 2002;41(1):75–79. doi: 10.1046/j.1365-2559.2002.01414.x
- 525 29. Tracy RE, Walia P. Lipid fixation for fat staining in paraffin sections applied to lesions of  
526 atherosclerosis. *Virchows Archiv.* 2004;445(1):22-26. doi: 10.1007/s00428-004-1036-y
- 527 30. Livak KJ, Schmittgen TD. Analysis of relative gene expression data using real-time  
528 quantitative PCR and the 2<sup>-ΔΔCT</sup> method. *Methods.* 2001;25(4):402–408. doi:  
529 10.1006/meth.2001.1262
- 530 31. Pauley GB, Nakatani RE. Histopathology of "gas-bubble" disease in Salmon Fingerlings. *J*  
531 *Fish Res Board Can.* 1967;24(4):867–871. doi: 10.1139/f67-073
- 532 32. Smith CE. Communications: Histopathology of Gas Bubble Disease in juvenile rainbow  
533 trout. *Prog Fish-Cult.* 1988;50(2):98–103. doi: 10.1577/1548-  
534 8640(1988)050<0098:chogbd>2.3.co;2
- 535 33. Cao L, Li K, Liang R, Chen S, Jiang W, Li R. The tolerance threshold of Chinese sucker to  
536 total dissolved gas supersaturation. *Aquac Res.* 2015;47(9):2804–2813. doi:  
537 10.1111/are.12730
- 538 34. Deng Y, Cao C, Liu X, Yuan Q, Feng C, Shi H, et al. Effect of total dissolved gas  
539 supersaturation on the survival of Bighead carp (*Hypophthalmichthys nobilis*). *Animals.*  
540 2020;10(1):166. doi: 10.3390/ani10010166
- 541 35. Ji Q, Li K, Wang Y, Liang R, Feng J, Yuan Q, et al. Total dissolved gases induced  
542 tolerance and avoidance behaviors in pelagic fish in the Yangtze River, China. *Ecotoxicol*  
543 *Environ Saf.* 2021;216:112218. doi: 10.1016/j.ecoenv.2021.112218
- 544 36. Shim SS, Patterson FP, Kendall MJ. Hyperbaric Chamber and Decompression Sickness:  
545 An Experimental Study. *Can Med Assoc J.* 1967;97(21):1263-1272.
- 546 37. L'Abbate A, Kusmic C, Matteucci M, Pelosi G, Navari A, Pagliazzo A, et al. Gas  
547 embolization of the liver in a rat model of rapid decompression. *Am J Physiol Regul Integr*  
548 *Comp Physiol.* 2010;299(2):673-682. doi: 10.1152/ajpregu.00699.2009
- 549 38. Eggleton P, Elsdon SR, Fegler J, Hebb CO. A study of the effects of rapid 'decompression'  
550 in certain animals. *Physiol J.* 1945;104(2):129–150. doi: 10.1113/jphysiol.1945.sp004111
- 551 39. Bert, P. *La Pression Barometrique: Recherches de Physiologie Experimentale* (Masson,  
552 1878).
- 553 40. Clay JR. Histopathology of experimental decompression sickness. *Aerosp Med.*  
554 1963;34:1107–1110.
- 555 41. Lever MJ, Miller KW, Paton WD, Smith EB. Experiments on the genesis of bubbles as a  
556 result of rapid decompression. *Physiol J.* 1966;184(4):964–969. doi:  
557 10.1113/jphysiol.1966.sp007960
- 558 42. Tanoue K, Mano Y, Kuroiwa K, Suzuki H, Shibayama M, Yamazaki H. Consumption of  
559 platelets in decompression sickness of rabbits. *J Appl Physiol.* 1987;62:1772–1779. doi:  
560 10.1152/jappl.1987.62.5.1772
- 561 43. Geng M, Zhou L, Liu X, Li P. Hyperbaric oxygen treatment reduced the lung injury of type  
562 II decompression sickness. *Int J Clin Exp Pathol.* 2015;8(2):1791–1803.

- 563 44. Atkins C, Lehner C, Beck K, Dubielzig R, Nordheim E, Lanphier E. Experimental  
564 respiratory decompression sickness in sheep. *J Appl Physiol.* 1988;65:1163–1171. doi:  
565 10.1152/jappl.1988.65.3.1163
- 566 45. Broome JR, Dick EJ, Jr. Neurological decompression illness in swine. *Aviat Space Environ*  
567 *Med.* 1996;67:207–213.
- 568 46. Dick EJ, Jr, Broome JR, Hayward IJ. Acute neurologic decompression illness in pigs:  
569 lesions of the spinal cord and brain. *Lab Anim Sci.* 1997; 47:50–57.
- 570 47. Buttolph TB, Dick Jr EJ, Toner CB, Broome JR, Williams R, Kang YH et al. Cutaneous  
571 lesions in swine after decompression: histopathology and ultrastructure. *Undersea Hyperb*  
572 *Med.* 1998;25(2), 115-121.
- 573 48. Anieli R, Boaron E, Abramovich A. Combined effect of denucleation and denitrogenation  
574 on the risk of decompression sickness in rats. *J Appl Physiol.* 2009;106:1453–1458. doi:  
575 10.1152/jappphysiol.91146.2008
- 576 49. Ni X, Cai Z, Fan D, Liu Y, Zhang R, Liu, et al. Protective effect of hydrogenrich saline on  
577 decompression sickness in rats. *Aviat Space EnvironMed.* 2011;82:604–609. doi:  
578 10.3357/ASEM.2964.2011
- 579 50. Tang S, Liao W, Wu S, Pao H, Huang K, Chu S. The blockade of storeoperated calcium  
580 channels improves decompression sickness in rats. *Front Physiol.* (2020) 10:1616. doi:  
581 10.3389/fphys.2019.01616
- 582 51. Caruso JL. Pathology of diving accidents. In: Brubakk AO, Neuman TS, editors. *Bennett*  
583 *Elliott's: Physiology Medicine of Diving.* 5th ed. Eastbourne: Saunders Elsevier (2003). p.  
584 729–43.
- 585 52. Francis T, Mitchell S. Pathophysiology of decompression sickness. In: Bove A, editor.  
586 *Bove Davis' Diving Medicine.* 4th ed. Philadelphia: Saunders (2004). pp.165–183. doi:  
587 10.1016/B978-0-7216-9424-5.50014-9
- 588 53. Arbelo M, Bernaldo de Quirós Y, Sierra E, Méndez M, Godinho A, Ramirez G, et al.  
589 Atypical beaked whale mass stranding in Almeria's coast: pathological study. *Int J Anim*  
590 *Sound Rec.* 2008;17:293–323. doi: 10.1080/09524622.2008.9753853
- 591 54. Fernández A, Sierra E, Martín V, Méndez M, Sacchini S, Bernaldo de Quirós Y et al. Last  
592 "Atypical" beaked whales mass stranding in the Canary Islands (July, 2004). *J Mar Sci Res*  
593 *Dev.* 2012;2(107). doi: 10.4172/2155-9910.1000107
- 594 55. Fernández A, Sierra E, Diaz-Delgado J, Sacchini S, Sánchez-Paz Y, Suárez-Santana C, et  
595 al. Deadly acute decompression sickness in Risso's Dolphins. *Sci Rep.* 2017;7(1):13621.  
596 doi: 10.1038/s41598-017-14038-z
- 597 56. Bernaldo de Quirós Y, Fernández A, Baird RW, Brownell RL, Jr Aguilar del Soto N, Allen  
598 D et al. Advances in research on the impacts of anti-submarine sonar on beaked whales.  
599 *Proc Royal Soc B.* 2019;286(1895):20182533. doi: 10.1098/rspb.2018.2533
- 600 57. Bernaldo de Quirós Y, Møllerløkken A, Havnes MB, Brubakk AO, González-Díaz O,  
601 Fernández A. Bubbles quantified in vivo by ultrasound relates to amount of gas detected  
602 post-mortem in rabbits decompressed from high pressure. *Front Physiol.* 2016b;7:310. doi:  
603 10.3389/fphys.2016.00310
- 604 58. Velázquez-Wallraf A, Fernández A, Caballero MJ, Møllerløkken A, Jepson PD, Andrada  
605 M, et al. Decompressive pathology in cetaceans based on an experimental pathological  
606 model. *Front Vet Sci.* 2021;8:676499. doi: 10.3389/fvets.2021.676499
- 607 59. Lambrechts K, Pontier J-M, Mazur A, Theron M, Buzzacott P, Wang Q, et al. Mechanism  
608 of action of antiplatelet drugs on decompression sickness in rats: A protective effect of  
609 anti-GPIIb/IIIa therapy. *J Appl Physiol.* 2015;118(10):1234–1239. doi:  
610 10.1152/jappphysiol.00125.2015

- 611 60. Wang Q, Mazur A, Guerrero F, Lambrechts K, Buzzacott P, Belhomme M, et al.  
 612 Antioxidants, endothelial dysfunction, and DCS: In vitro and in vivo study. *J Appl Physiol*.  
 613 2015;119(12):1355–1362. doi: 10.1152/jappphysiol.00167.2015
- 614 61. Huang K-L, Wu C-P, Chen Y-L, Kang B-H, Lin Y-C. Heat stress attenuates air bubble-  
 615 induced acute lung injury: A novel mechanism of diving acclimatization. *J Appl Physiol*.  
 616 2003;94(4):1485–1490. doi: 10.1152/jappphysiol.00952.2002
- 617 62. Tutar L, Tutar Y. Heat shock proteins; an overview. *Curr Pharm Biotechnol*.  
 618 2010;11(2):216–222. doi: 10.2174/138920110790909632
- 619 63. Lindquist S, Craig EA. The heat-shock proteins. *Annu Rev Genet*. 1988;22:631–677. doi:  
 620 10.1146/annurev.ge.22.120188.003215
- 621 64. Park KH, Cozier F, Ong OC, Caprioli J. Induction of heat shock protein 72 protects retinal  
 622 ganglion cells in a rat glaucoma model. *Invest Ophthalmol Vis Sci*. 2001;42(7):1522–1530.
- 623 65. Miller DJ, Fort PE. Heat shock proteins regulatory role in neurodevelopment. *Front*  
 624 *Neurosci*. 2018;12:821. doi: 10.3389/fnins.2018.00821
- 625 66. Weibel ER. Morphological basis of alveolar-capillary gas exchange. *Physiol Rev*.  
 626 1973;53(2):419–495. doi: 10.1152/physrev.1973.53.2.419
- 627 67. Matsuo H, Shinomiya N, Suzuki S. Hyperbaric stress during saturation diving induces  
 628 lymphocyte subset changes and heat shock protein expression. *Undersea Hyperb Med*.  
 629 2000;27(1):37–41.
- 630 68. Domoto H, Iwaya K, Ikomi F, Matsuo H, Tadano Y, Fujii S, et al. Up-regulation of  
 631 antioxidant proteins in the plasma proteome during saturation diving: Unique coincidence  
 632 under hypobaric hypoxia. *PLoS ONE*. 2016;11(10):e0163804. doi:  
 633 10.1371/journal.pone.0163804
- 634 69. Szyller J, Kozakiewicz M, Siemontowski P, Kaczerska D. Oxidative stress, hsp70/hsp90  
 635 and Enos/inos serum levels in professional divers during Hyperbaric Exposition.  
 636 *Antioxidants*. 2022;11(5):1008. doi: 10.3390/antiox11051008
- 637 70. Latchman D. Heat shock proteins and cardiac protection. *Cardiovasc Res*. 2001;51(4):637–  
 638 646. doi: 10.1016/s0008-6363(01)00354-6
- 639 71. Djuhuus R, Nossum V, Lundsett N, Hovin W, Svardal AM, Havnes MB, et al. Simulated  
 640 diving after heat stress potentiates the induction of heat shock protein 70 and elevates  
 641 glutathione in Human Endothelial Cells. *Cell Stress Chaperones*. 2009;15(4):405–414. doi:  
 642 10.1007/s12192-009-0156-3
- 643 72. Zhang K, Wang M, Wang H, Liu Y, Buzzacott P, Xu W. Time course of endothelial  
 644 dysfunction induced by decompression bubbles in rats. *Front Physiol*. 2017;8:181. doi:  
 645 10.3389/fphys.2017.00181
- 646 73. Yanagisawa M, Kurihara H, Kimura S, Tomobe Y, Kobayashi M, Mitsui Y, et al. A novel  
 647 potent vasoconstrictor peptide produced by Vascular Endothelial Cells. *Nature*.  
 648 1988;332(6163):411–415. doi: 10.1038/332411a0
- 649 74. Haynes WG, Webb DJ. Contribution of endogenous generation of endothelin-1 to basal  
 650 vascular tone. *Lancet*. 1994;344(8926):852–854. doi: 10.1016/s0140-6736(94)92827-4
- 651 75. De Miguel C, Speed JS, Kasztan M, Gohar EY, Pollock DM. Endothelin-1 and the kidney.  
 652 *Curr Opin Nephrol Hypertens*. 2016;25(1):35–41. doi: 10.1097/mnh.0000000000000185
- 653 76. Mok HK. The posterior cardinal veins and kidneys of fishes, with notes on their  
 654 phylogenetic significance. *Jpn J Ichthyol*. 1981;27(4):281–290.
- 655 77. Bigley NJ, Perymon H, Bowman GC, Hull BE, Stills HF, Henderson RA. Inflammatory  
 656 cytokines and cell adhesion molecules in a rat model of decompression sickness. *J*  
 657 *Interferon Cytokine Res*. 2008;28(2):55–63. doi: 10.1089/jir.2007.0084
- 658 78. Hubbard AK, Rothlein R. Intercellular adhesion molecule-1 (ICAM-1) expression and cell  
 659 signaling cascades. *Free Radic Biol Med*. 2000;28(9):1379–1386. doi: 10.1016/s0891-  
 660 5849(00)00223-9

- 661 79. Panés J, Perry M, Granger DN. Leukocyte-Endothelial Cell Adhesion: Avenues for  
 662 Therapeutic Intervention. *Br J Pharmacol.* 1999;126(3):537–550. doi:  
 663 10.1038/sj.bjp.0702328  
 664 80. Yu X, Xu J, Liu W, Zhang Z, He C, Xu W. Protective effects of pulmonary surfactant on  
 665 decompression sickness in rats. *J Appl Physiol.* 2021;130(2):400–407. doi:  
 666 10.1152/jappphysiol.00807.2020

667

668

669 **S1 Table.** Statistical power calculation of the biomarker’s expression study.

BIOMARKERS EXPRESSION STUDIES		P. KIDNEY	GILLS	V. AORTA	HEART
<b>HSP70</b>	Effect size	2.266	3.744	3.719	4.224
	Power (1-β error probability)	0.928	0.999	0.999	0.999
<b>HSP90</b>	Effect size	0.764	1.483	0.627	1.593
	Power (1-β error probability)	0.214	0.614	0.16	0.676
<b>ICAM-1</b>	Effect size	0.006	0.294	0.954	0.304
	Power (1-β error probability)	0.05	0.073	0.306	0.075
<b>ET-1</b>	Effect size	1.29	0.0374	0.625	0.018
	Power (1-β error probability)	0.5	0.05	0.159	0.05

670

671 **S2 Table.** Statistical power calculation of the correlation between total gas score and  
 672 biomarkers expression.

673

CORRELATION STUDIES	HSP70 Gills	HSP70 Heart	ET-1 Kidney
Effect size	0.941	0.878	0.8106
Power (1-β error probability)	0.998	0.911	0.719



## 5. CONCLUSIONS

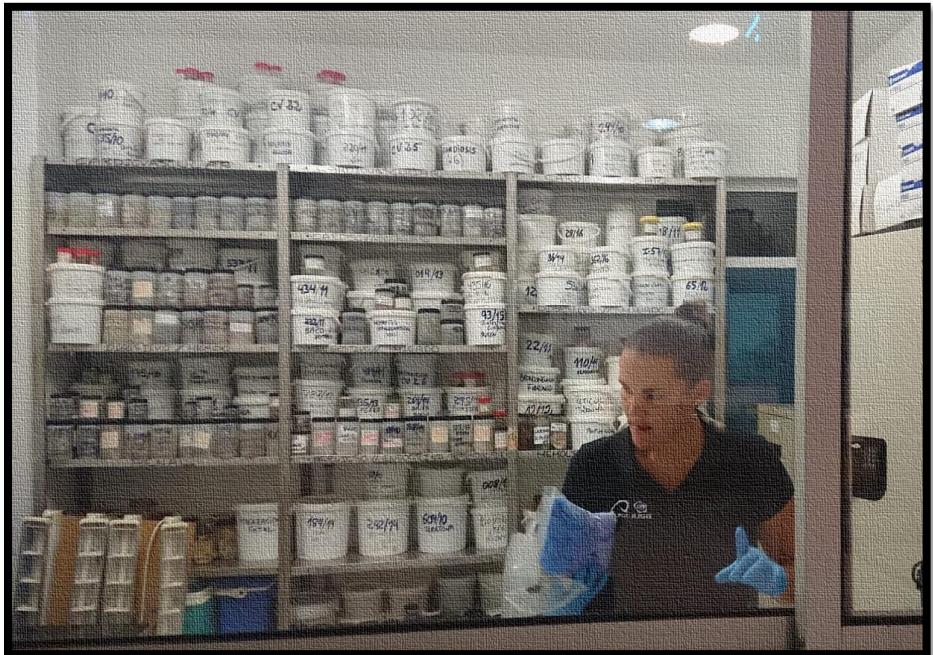




1. Predominant pathological findings in experimental rabbits exposed to a severe compression and decompression treatment were gas embolism systemically distributed, emphysema, and hemorrhages in multiple vital organs. These lesions are similar to those previously described in cetaceans with decompression-like sickness, providing further evidence of this pathology and reinforcing its diagnosis in this group of animals.
2. A massive and severe gas bubble disease model was reproduced by placing fish in water with 162-163% of total dissolved gases supersaturation for 18 hours.
3. The severe presence of intravascular and extravascular gas bubbles generated in the fish model and the associated pathological lesions such as multiorgan hemorrhages are closely related to those observed in experimental models of explosive decompression sickness.
4. The gas embolism generated in the experimental model in fish modifies the expression of different cell stress or damage markers, being HSP70 a strong marker for this process.
5. The gas score method was applied for the first time in fish, and was confirmed as a useful, easy, and low-cost tool for postmortem examinations to address the presence, distribution, and abundance of intravascular and extravascular gas bubbles also in fish.
6. The experimental results of fish with GBD validate the use of this animal model for the study of gas-bubble lesions being an alternative to the traditional use of small mammals applying the 3R's replacement principle of research
7. In both species, rabbits and fish, animals displayed different severity in gas embolism and related lesions even though they were exposed to the same experimental conditions, proving that individual variability

plays a fundamental role in decompression sickness, as previously proposed in animal models and human diving medicine.

## 6. RESUMEN EXTENDIDO





## 6.1. ANTECEDENTES Y OBJETIVOS

La enfermedad descompresiva (EDC) es un síndrome producido cuando la presión parcial de los gases disueltos en el organismo supera la presión ambiental, provocando la formación de burbujas de gas en circulación y tejidos (Vann et al., 2011). Éstas pueden provocar alteraciones mecánicas, embólicas y bioquímicas/inflamatorias (es decir, estrés o daño celular). En humanos, los principales signos clínicos graves son trastornos neurológicos, pulmonares, sistémicos y de oído interno (Lemaitre, 2009). Sujetos sometidos al mismo perfil de inmersión pueden mostrar un patrón muy diferente de formación de burbujas de gas (Nishi, 1993), siendo la variabilidad un factor a tener en cuenta en este síndrome.

La EDC se ha estudiado tradicionalmente en humanos (Francis, 2002; Vann et al., 2011), pero se ha descrito recientemente en especies marinas, como las tortugas marinas (García-Párraga et al., 2014) y los cetáceos (Jepson et al., 2003; Fernández et al., 2005). Éstos se presuponían estar protegidos frente a EDC gracias a sus adaptaciones al buceo (Piantadosi y Thalmann, 2004). Sin embargo, una patología compatible con EDC fue descrita por primera vez en un varamiento masivo de zifios coincidente en tiempo y espacio con el uso de sonar en maniobras navales (Jepson et al., 2003; Fernandez et al., 2005). Desde entonces, se ha diagnosticado enfermedad compatible con EDC en cetáceos en varios zifios varados asociados a ejercicios navales, pero también en calderones grises en interacción con sus presas (Arbelo et al., 2008; Bernaldo de Quirós et al., 2011; Fernández et al., 2012; Bernaldo de Quirós et al., 2019). Independientemente de la literatura reciente, la controversia en la comunidad científica sobre si las adaptaciones al buceo previenen la aparición de enfermedad compatible con EDC en cetáceos sigue en debate. Por ello, es necesario investigar y aportar más evidencias de esta patología en este grupo de animales marinos. A

diferencia de los humanos y las tortugas marinas, en los que el diagnóstico y estudio de la EDC es clínico, este síndrome en cetáceos sólo puede ser estudiado en animales varados mediante estudios patológicos postmortem. En medicina humana, los modelos experimentales de EDC se han utilizado tradicionalmente en pequeños mamíferos como conejos, ratas y ratones, centrándose en la prevención y potenciales tratamientos. A pesar de la extensa literatura sobre modelos experimentales de EDC, pocos han profundizado en los aspectos patológicos, siendo necesario un estudio patológico completo y actualizado para reforzar el diagnóstico patológico de enfermedad compatible con EDC.

El uso tradicional de pequeños mamíferos en EDC experimental podría ser reemplazado por un modelo alternativo de peces. Esto se postuló debido a las similitudes en la formación de burbujas de gas intravasculares y extravasculares de la enfermedad de las burbujas de gas (EBG) en peces y la EDC en mamíferos (D'Aoust y Smith, 1974; Machado et al., 1987). La EBG es una patología ampliamente descrita en peces que habitan grandes presas, donde masas de agua caen de un embalse a otro, provocando el atrapamiento y disolución de gases atmosféricos debido a la presión hidrostática (Bouck et al., 1976; Weitkamp y Katz, 1980). Por tanto, esta agua pasa a estar sobresaturada de gases disueltos y es responsable de una gran mortandad de peces en las presas. El desarrollo de un embolismo gaseoso y lesiones asociadas descritos en la EBG son muy similares a las observadas en la descompresión experimental y natural (Speare, 1998).

Teniendo en cuenta las similitudes patológicas entre EBG y EDC y aplicando el principio de reemplazo descrito en la Directiva 2010/63/UE del Parlamento Europeo que establece la necesidad de utilizar animales con menor capacidad de sentir dolor, sufrimiento o daño prolongado, podría utilizarse un modelo de embolismo gaseoso en peces como base para explorar la fisiopatología de la EDC. Este modelo

podría ser útil para el estudio de las lesiones patológicas asociadas a las burbujas de gas y para el estudio de las alteraciones bioquímicas/inflamatorias causadas por éstas en vasos sanguíneos y tejidos.

La presente investigación se ha desarrollado para ampliar el conocimiento sobre la patología y las alteraciones celulares asociadas a las lesiones por burbujas de gas. Los objetivos principales fueron:

1. Caracterizar la patología asociada a la EDC en un modelo animal bien establecido, el conejo blanco neozelandés, y comparar estos resultados con los descritos en cetáceos que presentan una patología compatible con EDC.
2. Inducir de manera rigurosa y reproducible la enfermedad de las burbujas de gas severa en peces.
3. Evaluar y validar el modelo de pez de enfermedad de las burbujas de gas severa para estudiar las lesiones por burbujas de gas y sus efectos a nivel celular en EDC.

## **6.2. RESUMEN DE LAS PUBLICACIONES CIENTÍFICAS**

### **6.2.1. PUBLICACIÓN I: Patología descompresiva en cetáceos basada en un modelo patológico experimental.**

Teniendo en cuenta los antecedentes explicados en el apartado anterior, el objetivo de esta publicación es validar los resultados patológicos observados en cetáceos mediante un modelo experimental en conejos sometidos a EDC severa.

Para este estudio se diseñaron dos grupos experimentales con un total de 18 conejos, divididos en 14 conejos sometidos a un protocolo de compresión/descompresión (grupo C/D) y 4 conejos controles (grupo control). Los animales se mantuvieron anestesiados durante ambos protocolos. El grupo C/D se comprimió en cámara hiperbárica a 8ATA durante 45 min seguido de una descompresión rápida. Se obtuvieron dos subgrupos: conejos que murieron tras descompresión (grupo C/D muertos) y aquellos supervivientes, eutanasiados tras 1h (grupo C/D eutanasiados). Los animales control fueron eutanasiados tras permanecer en la cámara hiperbárica sin presión. Las necropsias se realizaron primero evaluando el gas score, un método de puntuación del 0-6 para gas distintas localizaciones intravasculares y 0-3 para gas extravascular (Bernaldo de Quirós et al., 2016). Para los estudios estadísticos pertinentes, se utilizó la moda para cada localización elegida. Paralelamente se realizó el examen macroscópico y microscópico. Los resultados patológicos experimentales en conejos fueron comparados con 31 cetáceos diagnosticados previamente con patología descompresiva (Fernández et al., 2005; Arbelo et al., 2008; Bernaldo de Quirós et al., 2011; Fernández et al., 2012; Fernández et al., 2017; Bernaldo de Quirós et al., 2019).

Los animales control y C/D eutanasiados presentaron una moda de gas score 0 y el grupo C/D muertos modas de gas score de 5 y 6 en todas las localizaciones, con abundante número de burbujas o secciones de vasos completamente llenas de gas. El grupo C/D muertos presentó burbujas de gas macroscópicas y microscópicas distribuidas principalmente en vasos sanguíneos de pulmón, riñón y corazón. Microscópicamente estas burbujas de gas se observaban como espacios circulares a ovalados no teñidos entre las células sanguíneas (**Fig. 34**). Estos hallazgos también han sido descritos en modelos animales de EDC (Eggleton et al., 1945; Lever et al., 1966; Shim et al., 1967; L'Abbate et

al., 2010; Geng et al., 2015) y en cetáceos (**Fig. 34**) (Fernández et al., 2005; Arbelo et al., 2008; Fernández et al., 2017).



**Figura 34.** Comparativa de hallazgos patológicos entre conejos con EDC experimental (**A, C, E**) y cetáceos con diagnóstico compatible con EDC (**B, D, F**). Se observa principalmente burbujas de gas macroscópicas (flechas y asterisco blancos) y microscópicas (asteriscos negros) en estructuras vasculares de diferentes órganos como pulmón, corazón o mesenterio; así como enfisema pulmonar macroscópico y microscópico junto con hemorragias microscópicas en espacio subaracnoideo y corazón (flechas negras).

El grupo control solo presentó congestión generalizada. El órgano más afectado en el modelo C/D fue el pulmón, describiéndose hallazgos similares en modelos de EDC (Geng et al., 2015; Ni et al., 2011; Tang et al., 2020; Zhang et al., 2016) y en cetáceos (Fernández et al., 2005; Fernández et al., 2017). Además de enfisema pulmonar, se observó enfisema en bazo con mayor severidad en C/D muertos que en C/D eutanasiados, lesión descrita también por Clay (1963) en perros. Se observó enfisema multifocal leve de tejido adiposo en la mayoría de los conejos del grupo C/D muertos, concordando con cetáceos (Fernández et al., 2005; Fernández et al., 2017). Teniendo en cuenta que el nitrógeno es más soluble en tejidos grasos (Shim et al., 1967), este hallazgo debe tenerse en cuenta en el diagnóstico de la EDC.

Las burbujas de gas pueden provocar vasoconstricción, generando isquemia, edema y hemorragias en órganos diana como el pulmón (Saukko and Knight, 2004). En este estudio, se observaron hemorragias pulmonares severas en el grupo C/D muertos, en concordancia con modelos animales (Geng et al., 2015; Ni et al., 2011; Bao et al., 2015) y cetáceos (Fernández et al., 2005; Fernández et al., 2017). En zifios diagnosticados con enfermedad compatible con EDC se describió la presencia de hemorragias agudas diseminadas en el sistema nervioso central (Fernández et al., 2005), hallazgos también presentes en este estudio. Se observó edema pulmonar intersticial y alveolar en ambos grupos C/D, similar a otros modelos (Geng et al., 2015; Tang et al., 2020) y cetáceos (Fernández et al., 2012), siendo en estos estudios una de las lesiones más frecuentes junto con enfisema, a diferencia del presente estudio.

Los cambios musculares agudos se asocian a situaciones de estrés (Câmara et al., 2019). En este estudio, los cambios musculares observados fueron poco relevantes probablemente debido a la anestesia, a diferencia de lo que se observaría en cetáceos debido al estrés descompresivo. Es común que se observen microtrombos de fibrina en modelos de EDC (Tanoue et al., 1987; Geng et al., 2015), aunque en este estudio no se observaron y en cetáceos tampoco se ha relacionado su presencia. En este estudio se observó que individuos sometidos al mismo protocolo y perfiles similares pueden tener una formación de burbujas de gas variable, hecho previamente descrito (Shim et al., 1967; L'Abbate et al., 2010).

En conclusión, los conejos muertos tras descompresión presentaban mayor abundancia de burbujas de gas sistémicas, enfisema y hemorragias en órganos vitales. Las mismas lesiones han sido observadas en cetáceos con enfermedad compatible con EDC, reforzando los hallazgos patológicos. La mitad de los conejos que sobrevivieron no mostraron las mismas lesiones o severidad, revelando

que la variabilidad individual juega un papel esencial en esta enfermedad, tal y como se ha hipotetizado en otros modelos animales y medicina humana del buceo.

### **6.2.2. PUBLICACIÓN II: Establecimiento de un modelo en peces para estudiar las lesiones por burbujas de gas.**

Resumiendo lo descrito anteriormente, los peces pueden sufrir de EBG, una enfermedad caracterizada por la formación de burbujas de gas sistémicas similares a las de EDC. Los signos clínicos más frecuentes asociados a EBG son pérdida de flotabilidad, natación errática, así como burbujas de gas en ojos y aletas (Cao et al., 2020). Los estudios de EBG se han centrado principalmente en la supervivencia de especies en estas aguas (Stevens et al., 1980; Geist et al., 2013; Wang et al., 2015), siendo postulado por algunos autores un modelo in vivo de EBG para estudiar el embolismo gaseoso de la EDC, desde la perspectiva de la fisiopatología endotelial desencadenada por la presencia de estas burbujas de gas, común a ambas enfermedades (D'Aoust and Smith, 1974; Speare, 1998; Roberts, 2012). Dadas las similitudes presentadas y teniendo en cuenta el principio de reemplazo (Directiva 2010/63/UE del Parlamento Europeo), el objetivo de este estudio es obtener un modelo reproducible de EBG severa en peces para estudiar las lesiones asociadas a las burbujas de gas, similares a EDC.

Para ello, se diseñó en primer lugar un sistema para generar agua sobresaturada siguiendo el esquema de Bouck et al. (1976). Se adquirió un circuito (**Fig. 35**) conformado por una vasija de presión (5), que se rellenaba con agua corriente (15) y a la que se le inyectaba aire sintético de botella (4, 10). El agua sobresaturada se conseguía mediante recirculación constante (2) junto con el paso del gas inyectado por materiales porosos de diámetro fino (3) dispuestos dentro del circuito,

que forzaban su disolución en el agua. Esto provocaba un aumento del total de gases disueltos (TGD), que se medía de forma constante mediante un sensor de TGD (6\*). La mayoría de los estudios experimentales previos describían valores estables de TGD mientras se recirculaba el agua con un tanque abierto (Huang et al., 2010). Sin embargo, no pudimos recircular el agua en estas condiciones por las diferencias de presión entre el acuario abierto y el circuito, por lo que el agua se mantuvo estanca, observando pérdida de TGD casi inmediata. Debido a esto, se decidió modificar el circuito acoplando un acuario presurizable (7) (**Fig. 35**). Este nuevo sistema permitía la recirculación de agua sobresaturada por todo el circuito (incluido acuario presurizable) y el mantenimiento constante del TGD. Con este diseño, se realizaron pruebas piloto sin peces para ajustar parámetros, variando la cantidad de aire sintético inyectado y el tiempo de recirculación, con el objetivo de mantener un TGD superior a 1140 mmHg (saturación de 150%) durante todo el experimento.

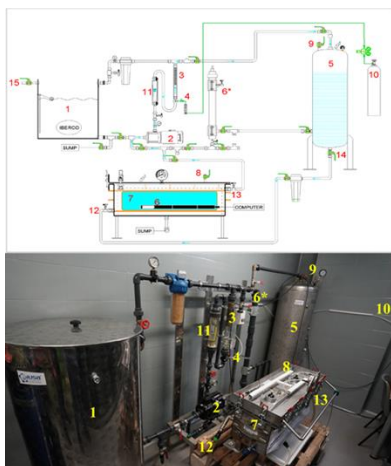


**Figura 35.** Circuito con vasija de presión y acuario presurizable. (1) Recipiente abierto (2) Motobomba (3) Tubo de disolución (4) Válvula de inyección de aire sintético (5) Vasija de presión (6) TDG y sensor de temperatura (6\*) TDG y sensor de temperatura dentro del circuito abierto (7) Acuario presurizado (10) Botella de aire sintético (15) Entrada de agua corriente.

Las pruebas piloto se realizaron con 10 carpas adultas, previa aclimatación. Los experimentos se realizaron por parejas, comenzando con 3h de exposición. Los valores de saturación de TGD se establecieron aproximadamente en 170%. Si no se observaban burbujas de gas

masivas, se duplicaba el tiempo de exposición. Se estableció un punto final humanitario cuando los peces mostraran pérdida de flotabilidad, natación errática y letargia. Se colocaron dos controles en el acuario presurizable sin recirculación de agua durante 18h. Durante toda la duración del experimento, se monitorizó a los peces observando su comportamiento, frecuencia de nado, latidos operculares y presencia de lesiones externas. Al finalizar, los peces se eutanasiaron y se realizó el examen macroscópico y microscópico.

El primer diseño con acuario abierto mostró una disminución de la saturación de TGD de 150 a 125% en 6h. Al introducir un acuario presurizado con circuito cerrado en recirculación constante, se produjo saturación de TGD mantenido de entre 160-180%. La fluctuación de TGD durante el experimento se dividió en 4 etapas. La primera, de carácter ascendente, debido a la producción de agua sobresaturada; la segunda de valor máximo de TGD y su estabilización; la tercera del leve descenso por la introducción de peces y rápida recuperación a niveles anteriores; y, por último, la cuarta de mantenimiento del TGD. Los grupos de 3h, 6h y 12h presentaron EBG, pero no masivo. El grupo de 18h se planificó inicialmente en 24h, pero ambos peces alcanzaron el punto final humanitario a las 18h, mostrando pérdida de flotabilidad y letargo. Los valores medios de saturación de TGD para el grupo de 18h fueron de 162-163% (**Fig. 36**).

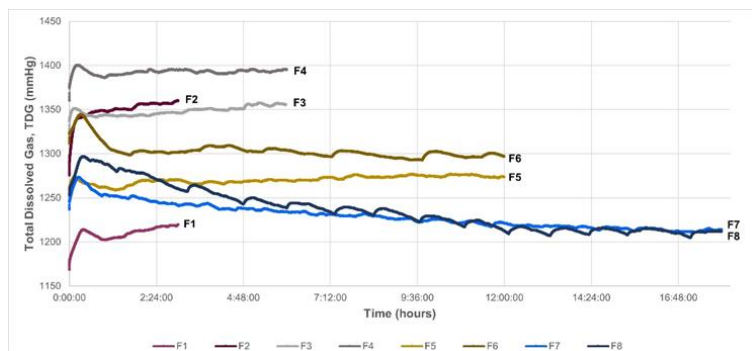


**Figura 36.** Valores de TGD desde la introducción de peces hasta el fin del tiempo experimental. F1-F2 corresponden al grupo de 3 h, F3-F4 al de 6 h, F5-F6 al de 12 h y F7-F8 al de 18 h.

Ambos peces del grupo de 18h presentaron signos clínicos similares al ser introducidos en el acuario presurizado. Agitación intensa, tres veces más frecuencia opercular que los peces control e intensa frecuencia de nado, dos veces más rápido que los controles. Entre 5-10 min tras la introducción, se paralizaron en el fondo del acuario. Después recuperaron lentamente la velocidad de nado y la frecuencia opercular habitual. Se visualizaron pequeñas burbujas de gas en las aletas laterales y anal después de 30 min de exposición, alcanzando éstas un mayor tamaño entre 1-2h de exposición. Entre las 6-12h del experimento, se registraron numerosas burbujas de gas en todas las aletas. En el último intervalo (12-18h), los peces presentaron pérdida de escamas. De 17-18h de exposición, los peces volvieron al fondo del acuario presurizado, con movimientos erráticos, pérdida de flotabilidad y rigidez de las aletas con hemorragias severas, congestión y burbujas de gas, siendo muy evidente estos signos clínicos a las 18h. Los peces fueron eutanasiados en este punto, siguiendo el punto final humanitario preestablecido.

En el examen externo, todas las aletas presentaban enfisema severo, hemorragias multifocales y burbujas de gas dentro de los vasos sanguíneos. Los peces presentaban pérdida de escamas con enfisema subcutáneo y las branquias congestión severa. Internamente, se observó la presencia de abundantes burbujas de gas en el corazón, aorta ventral, venas cardinales posteriores, venas gonadales, vena de la vejiga natatoria y venas intercostales. Además, se observó congestión generalizada severa de órganos, principalmente de hígado, riñón y bazo, y moderada de grasa visceral. Microscópicamente, se observaron grandes dilataciones no teñidas compatibles con enfisema en las aletas junto con hemorragias multifocales moderadas y algunos espacios vacíos ovalados intravasculares en forma de burbujas entre las células sanguíneas. Las

branquias presentaban áreas congestivas severas con grandes burbujas de gas en capilares sanguíneos. En el bazo y el riñón posterior se observaron burbujas de gas, mostrando este último algunas zonas hemorrágicas entre los túbulos renales. La rete mirabile de la vejiga natatoria, el hígado, las estructuras oculares y el sistema nervioso central mostraban un aspecto congestivo moderado. Las mismas estructuras circulares se observaron dentro de estructuras vasculares de hígado, tracto digestivo, ojos, sistema nervioso central, branquias y ventrículo del corazón.

La patología de EBG descrita en la literatura consiste en burbujas de gas y hemorragias en las aletas (Cao et al., 2015), congestión y hemorragias branquiales, exoftalmia (Xue et al., 2019), lesiones microscópicas como burbujas de gas en vasos sanguíneos, hemorragias y congestión en diferentes tejidos (Pauley and Nakatani, 1967), coincidiendo los hallazgos con los observados en este estudio. En general, estos hallazgos patológicos también coinciden con los de la EDC, tanto los descritos en pequeños mamíferos con EDC explosiva experimental (Geng et al., 2015; Zhang et al., 2016; Velázquez-Wallraf et al., 2021), como los de EDC natural (Fernández et al., 2005; García-Párraga et al., 2014; Edmonds, 2015), validando la traslación de este modelo desde el punto de vista patológico.

En conclusión, se reprodujo una EBG masiva con severa presencia de burbujas de gas intravasculares y extravasculares similares a las de EDC. El diagnóstico clínico se confirmó mediante un estudio patológico. Éste representa el primer establecimiento de un modelo de pez como alternativa a mamíferos para el estudio de las burbujas de gas producidas en EDC en humanos y otras especies afectadas, y podría ser un modelo útil para profundizar en la fisiopatología de las burbujas de gas en los tejidos. La principal limitación de este modelo es que no podría aplicarse a estudios del origen y formación de las burbujas en la

EDC ya que, aunque el embolismo gaseoso causado sea similar en ambas enfermedades, sus causas son diferentes.

### **6.2.3. PUBLICACIÓN III: Biomarcadores relacionados con embolismo gaseoso: gas score, patología y expresión génica en un modelo de enfermedad de las burbujas de gas.**

El embolismo gaseoso genera respuestas fisiopatológicas, particularmente en las células endoteliales (Zhang et al., 2016), la primera línea celular en entrar en contacto con las burbujas de gas intravasculares, siendo la disfunción o daño endotelial correlacionado positivamente con la presencia de éstas (Obad et al., 2007). Además, estas burbujas provocan una interfaz sangre-burbuja circulante (Kitano et al., 1978), que activa moléculas como la molécula de adhesión intercelular 1 (ICAM-1), expresada por las células endoteliales para favorecer la migración de leucocitos a través del endotelio hacia el tejido inflamado (Yang et al., 2005). Las células endoteliales también generan biomarcadores de estrés endotelial, como la familia de proteínas de estrés térmico (HSP) (Zhang et al., 2016). Las células endoteliales son una fuente de sustancias vasoactivas, como el óxido nítrico (ON), una molécula vasodilatadora que en condiciones de daño endotelial ve disminuida su producción provocando un aumento relativo de su antagonista, la endotelina 1 (ET-1). Los biomarcadores expresados representan un objetivo importante para seguir investigando el embolismo gaseoso (Fismen et al., 2012). En este estudio, probamos la hipótesis de que la EBG en peces induce respuestas vasculares y celulares similares a otras embolias gaseosas, como la EDC en mamíferos, y reforzamos su utilización como modelo experimental alternativo.

Para este estudio se utilizaron 20 carpas que, previamente aclimatadas, se dividieron en dos grupos: un grupo control de 10 animales y un grupo EBG con otros 10 animales. Los peces del grupo EBG fueron introducidos individualmente durante 18 horas en un acuario presurizado con agua sobresaturada producida siguiendo nuestra publicación anterior (Velázquez-Wallraf et al., 2022), con valores de saturación de TGD de  $169\pm 5\%$ . Los peces del grupo control se introdujeron 18 horas en el acuario presurizable, sin presión ejercida y con agua sin sobresaturar. Durante la exposición, se monitorizó el comportamiento y los signos clínicos, de acuerdo con lo descrito en nuestra publicación anterior (Velázquez-Wallraf et al., 2022).

Después de 18 horas, todos los peces fueron eutanasiados. La necropsia se realizó comenzando con el examen externo y la aplicación del método del gas score de Bernaldo de Quirós et al. (2016) adaptado a peces. Las localizaciones intravasculares elegidas fueron venas de aleta, opérculo, subcutáneas craneales y caudales, de vejiga natatoria y cardinales posteriores, así como aorta ventral y dorsal, calificadas de 0 a 6. Las localizaciones extravasculares fueron puntuadas de 0 a 3, siendo valorado el enfisema en grasa visceral y en aletas. El gas score total de cada pez se calculó con la sumatoria de todas las localizaciones. Al mismo tiempo, se realizó el estudio macroscópico y microscópico, recolectando muestras de todos los órganos. Además de realizar la tinción rutinaria con hematoxilina-eosina, las muestras se pretrataron con ácido crómico para preservar la grasa y poder confirmar que los espacios no teñidos eran burbujas de gas y no grasa.

Del total de 10 peces dentro de cada grupo, 6 fueron utilizados para el estudio de biomarcadores, almacenando en RNA-later muestras de riñón posterior, branquias, corazón y aorta ventral. Los genes seleccionados fueron HSP70, HSP90, E-1 e ICAM-1, estudiados mediante PCR cuantitativa en tiempo real (RT-qPCR) y por triplicado. Se llevaron a cabo análisis estadísticos de los resultados para evaluar la

diferencia de expresión génica entre grupo control y grupo EBG. Además, se realizó una correlación entre el gas score total y la expresión de genes con diferencias significativas o con tendencia positiva del grupo EBG. También se calculó el poder estadístico de cada resultado.

Durante el tratamiento, todos los peces del grupo EBG mostraron signos clínicos consistentes con EBG severa, como el aumento de la frecuencia opercular y natatoria junto con la presencia de burbujas de gas en las aletas. La presencia y el tamaño de estas burbujas de gas aumentó a medida que discurrían las horas experimentales. En las dos últimas horas experimentales, los peces aparecieron con movimientos erráticos, pérdida de flotabilidad junto con hemorragias graves y burbujas de gas en las aletas. En cuanto al gas score, el grupo EBG presentó cuatro localizaciones intravasculares con moda de gas score 5, dos de grado 4 y dos de grado 3. Las localizaciones extravasculares presentaron ambas modas de gas score 2, mientras que en el grupo control todas las puntuaciones fueron 0 (**Fig. 37**). Externamente, como hallazgos más relevantes, se observó enfisema subcutáneo, enfisema y hemorragia de aletas, así como hemorragias branquiales. Internamente, hiperinflación de vejiga natatoria, distensión por gas del bulbo arterioso y congestión multiorgánica fueron los hallazgos más frecuentes.

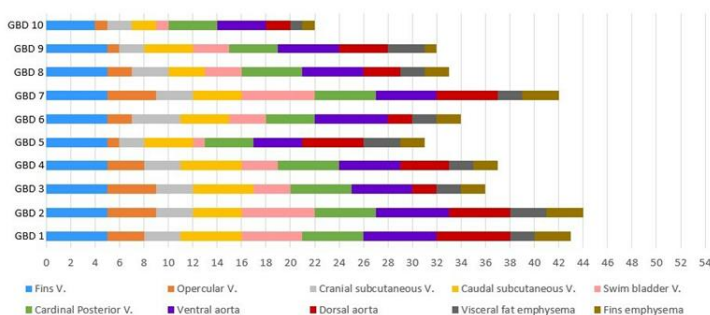


**Figura 37.** Puntuaciones de gas score obtenidas en las localizaciones intravasculares (0-6 puntos) y extravasculares (0-3) de cada pez del grupo EBG. También se muestra la puntuación total de gas score de cada pez.

Microscópicamente, se observó la congestión multiorgánica, así como enfisema y hemorragias en aletas, hemorragias y fusión de laminillas secundarias en branquias, dilatación de vasos sanguíneos y de túbulos renales del riñón posterior. Además, se visualizaron burbujas de gas abundantes en vasos sanguíneos de estos tres tejidos. En venas coronarias, de bazo, gónadas e hígado también se pudieron apreciar en menor medida estas estructuras, que no se tiñeron ni con H&E ni con Oil Red, confirmando que eran émbolos gaseosos y no grasos. En cuanto a los biomarcadores, HSP70 y HSP90 en branquias y corazón, así como HSP70 en riñón posterior y aorta ventral mostraron un aumento de expresión estadísticamente significativo en comparación con el grupo control. La ET-1 en el riñón posterior y aorta ventral, HSP90 en el riñón posterior y la ICAM-1 en las branquias presentaban una tendencia a incrementar su expresión, sin significancia estadística. Al correlacionar los marcadores con significancia estadística o tendencia a ésta con el gas score total, se observó que HSP70 en branquias tenía una correlación estadísticamente significativa. El estudio de poder estadístico determinó que los resultados de expresión de HSP70 en los cuatro tejidos, así como su correlación en branquias con el gas score total tenían un alto poder estadístico (>90%).

Los hallazgos patológicos de este estudio (**Fig. 38**) coinciden con estudios previos de este modelo (Velázquez-Wallraf et al., 2022) y otros estudios de EBG en peces (Pauley y Nakatani, 1967; Smith, 1988; Cao et al., 2015; Deng et al., 2020; Ji et al., 2021). Todos los animales EBG tenían gas score relativamente alto, aunque con cierta variabilidad. Se ha postulado que la variabilidad individual desempeña un papel determinante en las enfermedades que producen embolismo gaseoso (Shim et al., 1967; L'Abbate et al., 2010). La presencia de abundantes burbujas de gas vasculares sistémicamente distribuidas también se ha notificado en modelos experimentales de EDC (Eggleton et al., 1945; Lever et al., 1966; Tanoue et al., 1987; Arieli et al., 2009; L'abbate et al.,

2010; Zhang et al., 2016; Tang et al., 2020), y en EDC no experimental en humanos (Caruso, 2003; Francis y Mitchell, 2003), cetáceos (Fernández et al., 2005; Bernaldo de Quirós et al., 2019) y tortugas marinas (García-Párraga et al., 2014). El gas score se ha utilizado como herramienta diagnóstica de embolia gaseosa (Bernaldo de Quirós et al., 2016a; Fernández et al., 2017; Velázquez-Wallraf et al., 2021), mostrando los animales afectados puntuaciones totales de gas elevadas, en concordancia con el presente estudio.

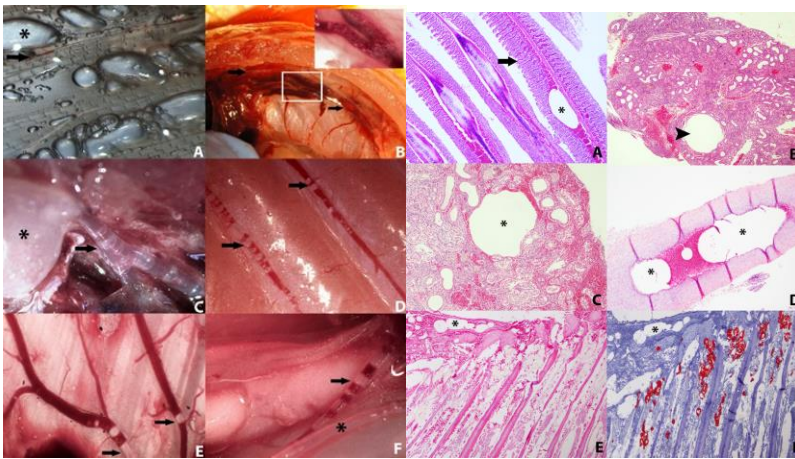


**Figura 38.** Hallazgos macroscópicos (izquierda; i) y microscópicos (derecha; d) en peces con EBG. Presencia de burbujas de gas en vasos sanguíneos como venas subcutáneas (**i.D, i.E**), aorta ventral (**i.C, d.D**), venas cardinales posteriores (**i.B**), vena de la vejiga natatoria (**i.F**), venas de la base de la holobranquia (**d.E**) o venas del riñón posterior (**d.B, d.C**). También se aprecia enfisema en aletas (**i.A**), fusión de laminillas secundarias en branquias (**d.A**).

Las burbujas de gas intravascular circulante desencadenan la activación del endotelio vascular, ampliamente descrito en enfermedades como EDC (Lambrechts et al., 2015; Wang et al., 2015). Esto genera una respuesta de estrés, provocando la puesta en escena de diferentes biomarcadores (Huang et al., 2003). Las HSPs son un mecanismo de defensa frente a estrés, especialmente térmico, oxidativo e hipóxico (Lindquist y Craig, 1988). La HSP70 mostró un patrón de aumento estadísticamente significativo de expresión en los cuatro tejidos

estudiados del grupo EBG. Estos resultados concuerdan con estudios previos de expresión de HSP70 en pulmón, hígado y corazón de conejos (Su et al., 2004), y en pulmones de ratas (Huang et al., 2003). La expresión de HSP70 en los tejidos ha sido postulada por varios estudios como un biomarcador de estrés (Matsuo et al., 2000; Domoto et al., 2016; Szyller et al., 2022). Por su parte, la HSP90 mostró un aumento estadísticamente significativo en branquias y corazón. La expresión de HSP90 tras estrés descompresivo no se ha visto significativamente aumentada, probablemente debido a que es constitutiva y sus niveles basales suelen permanecer elevados (Djurhuus et al., 2010; Fismen et al., 2012). En este estudio, este aumento podría explicarse por la severidad del embolismo gaseoso. Zhang et al. (2016) sugirieron que los elevados niveles de ET-1 en suero sanguíneo después de un estrés descompresivo podría ser una evidencia del estrés endotelial en la EDC. La ET-1 es el factor vasoconstrictor más potente conocido, siendo las células endoteliales su principal productor, aunque también otras como las células tubulares del riñón (De Miguel et al., 2016). En nuestro estudio, la ET-1 tuvo tendencia a aumentar su expresión en el riñón posterior y la aorta ventral de los peces con EBG, pero sin significancia estadística. Nuestros resultados podrían ser utilizados como premisas para probar si la ET-1 se eleva en suero sanguíneo y si este marcador fuera el mejor para inducir daño endotelial en embolismo gaseoso como sugieren Zhang et al. (2016).

La correlación de HSP70 en branquias con el gas score demuestra que el daño fue producido por las propias burbujas de gas. Las correlaciones restantes sin significancia podrían deberse a las limitaciones del estudio: pequeño tamaño muestral, naturaleza semicuantitativa del gas score y escasa variabilidad en gas score total. A pesar de ello, pudimos obtener un poder estadístico alto en los resultados de expresión de HSP70 en los 4 tejidos estudiados, así como de su correlación en branquias con el gas score total y resultados prometedores

en el caso de la correlación de gas score con expresión de HSP70 en corazón y ET-1 en riñón posterior donde probablemente, con un tamaño muestral más amplio, los resultados hubiesen sido estadísticamente significativos tal y como muestra el estudio del poder estadístico. La limitación del tamaño muestral también es aplicable a la expresión de biomarcadores que, presentando tendencia al aumento de su expresión, no fueron estadísticamente significativos. El poder estadístico de estos biomarcadores indicó que la significancia estadística podría haberse alcanzado si se hubiese utilizado un tamaño muestral mayor. Además, para las muestras que no mostraron tendencia el efecto del tamaño muestral obtenido en el análisis de poder estadístico fue muy bajo, debiendo utilizar un número excesivo de animales para haber logrado tener significancia estadística, lo que sugiere que en estos marcadores no hay diferencia entre el grupo control y el grupo EBG. Este modelo de EBG podría ser un buen modelo para estudiar experimentalmente la embolia gaseosa y sus efectos de forma similar a otros animales tradicionales de laboratorio, siguiendo el principio de reemplazo de las 3Rs.

En conclusión, los peces con embolia gaseosa grave mostraron un aumento de HSPs, principalmente HSP70, y una correlación positiva con gas score de ésta en branquias. Nuestros resultados confirmaron que la HSP70 es un marcador fuerte de embolia gaseosa como se ha demostrado previamente, validando este modelo para el estudio de la embolia gaseosa y sus efectos. Estos resultados validaron el modelo EBG para profundizar en el estudio de las vías fisiopatológicas de la embolia gaseosa, con la posibilidad de extrapolar los resultados a otras especies susceptibles.

### **6.3. CONCLUSIONES**

1. Los hallazgos patológicos predominantes en conejos experimentales expuestos a un tratamiento severo de compresión y descompresión fueron embolismo gaseoso distribuido sistémicamente, enfisema y hemorragias en múltiples órganos vitales. Estas lesiones son similares a las descritas previamente en cetáceos con patología descompresiva, proporcionando más evidencias de esta patología y reforzando su diagnóstico en este grupo de animales.

2. Se reprodujo un modelo de enfermedad masiva y severa por burbujas de gas colocando a los peces en agua con 162-163% de saturación de gases totales disueltos durante 18 horas.

3. La presencia severa de burbujas de gas intravasculares y extravasculares generadas en el modelo de peces y las lesiones patológicas asociadas como hemorragias multiorgánicas están estrechamente relacionadas con las observadas en modelos experimentales de enfermedad descompresiva explosiva.

4. El embolismo gaseoso generado en el modelo experimental en peces modifica la expresión de diferentes marcadores de estrés o daño celular, siendo la HSP70 un potente marcador de este proceso.

5. El método del “gas score” se aplicó por primera vez en peces, y se confirmó como una herramienta útil, fácil y de bajo coste para exámenes postmortem de la presencia, distribución y abundancia de burbujas de gas intravasculares y extravasculares también en peces.

6. Los resultados experimentales de peces con EBG validan el uso de este modelo animal para el estudio de lesiones por burbujas de gas siendo una alternativa al uso tradicional de pequeños mamíferos aplicando el principio de reemplazo de las 3R's de la investigación.

7. En ambas especies, conejos y peces, los animales mostraron diferente severidad de embolismo gaseoso y lesiones relacionadas a pesar de haber sido expuestos a las mismas condiciones experimentales, demostrando que la variabilidad individual juega un papel fundamental en la enfermedad descompresiva, como se ha propuesto previamente en modelos animales y en la medicina del buceo humano.

## 7. REFERENCE LIST





- Alabadí, J.A., Torregrosa, G., Miranda, F.J., Salom, J.B., Centeno, J.M., & Alborch, E. (1997). Impairment of the modulatory role of nitric oxide on the endothelin-1-elicited contraction of cerebral arteries: a pathogenetic factor in cerebral vasospasm after subarachnoid hemorrhage?. *Neurosurgery*, 41(1), 245-252. <https://doi.org/10.1097/00006123-199707000-00039>
- Alderdice, D.F., & Jensen, J.O.T. (1985). An explanation for the high resistance of incubating salmonid eggs to atmospheric gas supersaturation of water. *Aquaculture*, 49(1), 85-88. [https://doi.org/10.1016/0044-8486\(85\)90192-9](https://doi.org/10.1016/0044-8486(85)90192-9)
- Anbarasan, C., Bavaniatha, M., Latchumanadhas, K., & Mulasari, S.A. (2015). ICAM-1 molecular mechanism and genoma wide SNP's association studies. *Indian Heart Journal*, 67(3), 282-287. <https://doi.org/10.1016/j.ihj.2015.03.005>
- Arbelo, M., Bernaldo de Quirós, Y., Sierra, E., Méndez, M., Godinho, A., Ramírez, G., Caballero, M.J., & Fernández, A. (2008). Atypical beaked whale mass stranding in Almeria's coasts: pathological study. *Bioacustics*, 17(1-3), 294-297. <https://doi.org/10.1080/09524622.2008.9753853>
- Arieli, R., Boaron, E., & Abramovich, A. (2009). Combined effect of denucleation and denitrogenation on the risk of decompression sickness in rats. *Journal of Applied Physiology*, 106(4), 1453-1458. <https://doi.org/10.1152/jappphysiol.91146.2008>
- Arieli, R., Boaron, E., Arieli, Y., Abramovich, A., & Katsenelson, K. (2010). Oxygen pretreatment as protection against decompression sickness in rats: pressure and time necessary for hypothesized denucleation and renucleation. *European Journal of Applied*

*Physiology*, 111(6), 997-1005. <https://doi.org/10.1007/s00421-010-1725-y>

Arieli, R. (2017). Nanobubbles Form at Active Hydrophobic Spots on the Luminal Aspect of Blood Vessels: Consequences for Decompression Illness in Diving and Possible Implications for Autoimmune Disease—An Overview. *Frontiers in Physiology*, 8(591). <https://doi.org/10.3389/fphys.2017.00591>

Atkins, C., Lehner, C., Beck, K., Dubielzig, R., Nordheim, E., & Lanphier, E. (1988). Experimental respiratory decompression sickness in sheep. *Journal of Applied Physiology*, 65(3), 1163-1171. <https://doi.org/10.1152/jappl.1988.65.3.1163>

**B**ackmann, T.W.H., & Evans, A.F. (2002). Gas bubble trauma in adult salmonids in the Columbia River basin. *North American Journal of Fisheries Management*, 22(2), 579-584. [https://doi.org/10.1577/1548-8675\(2002\)022<0579:GBTIIA>2.0.CO;2](https://doi.org/10.1577/1548-8675(2002)022<0579:GBTIIA>2.0.CO;2)

Bajanowski, T., West, A., & Brinkmann, B. (1998). Proof of fatal air embolism. *International Journal of Legal Medicine*, 111, 208-211. <https://doi.org/10.1007/s004140050153>

Balcomb, K.C. III, & Claridge, D.E. (2001). A mass stranding of cetaceans caused by naval sonar in the Bahamas. *Bahamas Journal of Science*, 2, 2-12.

Ball, R., Lehner, C., & Parker, E. (1999). Predicting risk of decompression sickness in humans from outcomes in sheep. *Journal of Applied Physiology*, 86(6), 1920-1929. <https://doi.org/10.1152/jappl.1999.86.6.1920>

- Bao, X-C., Chen, H., Fang, Y-Q., Yuan, H-R., You, P., Ma, J., & Wang, F-F. (2015). Clopidogrel reduces the inflammatory response of lung in a rat model of decompression sickness. *Respiratory Physiology and Neurobiology*, 211, 9-16. <https://doi.org/10.1016/j.resp.2015.02.003>
- Basu, N., Todgham, A.E., Ackerman, P.A., Bibeau, M.R., Nakano, K., Schulte, P.M., & Iwama, G.K. (2002). Heat shock protein genes and their functional significance in fish. *Gene*, 295(2), 173-183. [https://doi.org/10.1016/S0378-1119\(02\)00687-X](https://doi.org/10.1016/S0378-1119(02)00687-X)
- Beiningen, K.T., & Ebel, W.J. (1970). Effect of John Day dam on dissolved nitrogen concentrations and salmon in the Columbia River, 1968. *Transactions of the American Fisheries Society*, 99(4), 664-671. [https://doi.org/10.1577/1548-8659\(1970\)99<664:EOJDDO>2.0.CO;2](https://doi.org/10.1577/1548-8659(1970)99<664:EOJDDO>2.0.CO;2)
- Bernaldo de Quirós, Y. (2011a). Methodology and Analysis of Gas Embolism: Experimental Models and Stranded Cetaceans. *PhD. Doctoral thesis*, University of Las Palmas de Gran Canaria, Las Palmas de Gran Canaria.
- Bernaldo de Quirós, Y., González-Díaz, Ó., Saavedra, P., Arbelo, M., Sierra, E., Sacchini, S., Jepson, P., Mazzariol, S., Di Guardo, G., & Fernández, A. (2011b). Methodology for in situ gas sampling, transport and laboratory analysis of gases from stranded cetaceans. *Scientific Reports*, 1(193). <https://doi.org/10.1038/srep00193>
- Bernaldo de Quirós, Y., González-Díaz, O., Arbelo, M., Sierra, E., Sacchini, S., & Fernández, A. (2012a). Decompression vs. Decomposition: Distribution, Amount, and Gas Composition of Bubbles in Stranded Marine Mammals. *Frontiers in Physiology*, 3(177). <https://doi.org/10.3389/fphys.2012.00177>

- Bernaldo de Quirós, Y., González-Díaz, O., Møllerløkken, A., Brubakk, A., Hjelde, A., Saavedra, P., & Fernández, A. (2012b). Differentiation at autopsy between in vivo gas embolism and putrefaction using gas composition analysis. *International Journal of Legal Medicine*, 127(2), 437-445. <https://doi.org/10.1007/s00414-012-0783-6>
- Bernaldo de Quirós, Y., Seewald, J., Sylva, S., Greer, B., Niemeyer, M., Bogomolni, A., & Moore, M. (2013). Compositional Discrimination of Decompression and Decomposition Gas Bubbles in Bycaught Seals and Dolphins. *PLoS ONE*, 8(12), e83994. <https://doi.org/10.1371/journal.pone.0083994>
- Bernaldo de Quirós, Y., Saavedra, P., Møllerløkken, A., Brubakk, A., Jørgensen, A., González-Díaz, O., Martín-Barrasa, J., & Fernández, A. (2016a). Differentiation at necropsy between in vivo gas embolism and putrefaction using a gas score. *Research in Veterinary Science*, 106, 48-55. <https://doi.org/10.1016/j.rvsc.2016.03.007>
- Bernaldo de Quirós, Y., Møllerløkken, A., Havnes, M., Brubakk, A., González-Díaz, O., & Fernández, A. (2016b). Bubbles Quantified In vivo by Ultrasound Relates to Amount of Gas Detected Post-mortem in Rabbits Decompressed from High Pressure. *Frontiers in Physiology*, 7(310). <https://doi.org/10.3389/fphys.2016.00310>
- Bernaldo de Quirós, Y., Fernández, A., Baird, R.W., Brownell, R.L., Jr, Aguilar del Soto, N., Allen, D., Arbelo, M., Arregui, M., Costidis, A., Fahlman, A., Frantzis, A., Gulland, F.M.D., Iñiguez, M., Johnson, M., Komnenou, A., Koopman, H., Pabst, D.A., Roe, W.D., Sierra, E., Tejedor, M., & Schorr, G. (2019). Advances in research on the impacts of anti-submarine sonar on beaked whales.

- Proceedings of the Royal Society B: Biological Sciences*. 286(1895), 20182533. <https://doi.org/10.1098/rspb.2018.2533>
- Bert, P. (1873). Influence des hautes pressions sur les poissons. *Comptes rendus des séances de la Société de Biologie de Paris*, 5, 160-161.
- Bert, P. (1878). *La Pression Barométrique : Recherches de Physiologie Expérimentale*. Paris:Masson.
- Bigley, N.J., Perymon, H., Bowman, G.C., Hull, B.E., Stills, H.F., & Henderson, R.A. (2008). Inflammatory cytokines and cell adhesion molecules in a rat model of decompression sickness. *Journal of Interferon and Cytokine Research*, 28(2), 55-63. <https://doi.org/10.1089/jir.2007.0084>
- Blatteau, J., Barre, S., Pascual, A., Castagna, O., Abraini, J., Risso, J., & Vallee, N. (2012). Protective Effects of Fluoxetine on Decompression Sickness in Mice. *PLoS ONE*, 7(11), e49069. <https://doi.org/10.1371/journal.pone.0049069>
- Blatteau, J., Brubakk, A., Gempp, E., Castagna, O., Risso, J., & Vallée, N. (2013). Sildenafil Pre-Treatment Promotes Decompression Sickness in Rats. *PLoS ONE*, 8(4), e60639. <https://doi.org/10.1371/journal.pone.0060639>
- Bouck, G.R., Chapman, G.A., Schneider, P.W., & Stevens, D.G. (1970). Observations on gas bubble disease in adult Columbia River sockeye salmon (*Oncorhynchus nerka*). Pacific Northwest laboratory, *Federal Water Quality Administration*, Corvallis, Oregon, USA.
- Bouck, G.R., Nebeker, A.V., & Stevens, D.G. (1976). Mortality, saltwater adaptation and reproduction of fish exposed to gas

supersaturated water. EPA-600/3-76-054, *United States Environmental Protection Agency*, Corvallis, Oregon, USA.

Bouck, G.R. (1980). Etiology of gas bubble disease. *Transactions of the American Fisheries Society*, 109(6), 703-707.  
[https://doi.org/10.1577/1548-8659\(1980\)109<703:EOGBD>2.0.CO;2](https://doi.org/10.1577/1548-8659(1980)109<703:EOGBD>2.0.CO;2)

Boulanger, C., & Lüscher, T.F. (1990). Release of endothelin from the porcine aorta. Inhibition by endothelium-derived nitric oxide. *The Journal of Clinical Investigation*, 85(2), 587-590.  
<https://doi.org/10.1172/JCI114477>

Bove, A. (1998). Risk of decompression sickness with patent foramen ovale. *Undersea and Hyperbaric Medicine*, 25(3), 175-178.

Boyle, R. (1670). New pneumatical experiments about respiration. *Philosophical transactions*, 5, 2011-2058.

Broome, J.R., Dutka, A.J., & McNamee, G.A. (1995). Exercise conditioning reduces the risk of neurologic decompression illness in swine. *Undersea and Hyperbaric Medicine*, 22(1), 73-85.

Broome, J.R., & Dick Jr, E.J. (1998). Neurological decompression illness in swine. *Aviation, Space and Environmental Medicine*, 67(3), 207-213.

Brosnan, I.G., Welch, D.W., & Scott, M.J. (2016). Survival rates of out-migrating yearling chinook salmon in the lower Columbia River and plume after exposure to gas-supersaturated water. *Journal of Aquatic Animal Health*, 28(4), 240-251.  
<https://doi.org/10.1080/08997659.2016.1227398>

- Brown, C., Kime, W., & Sherrer, E. (1978). Postmortem Intravascular Bubbling: A Decompression Artifact?. *Journal of Forensic Sciences*, 23(3), 511-518.
- Brubakk, A.O., Peterson, R., Grip, A., Holand, B., Onarheim, J., Segadal, K., Kunkle, T.D., & Tonjum, S. (1986). Gas bubbles in the circulation of divers after ascending excursions from 300 to 250 msw. *Journal of Applied Physiology*, 60(1), 45-51. <https://doi.org/10.1152/jappl.1986.60.1.45>
- Brubakk, A.O., & Neuman, T.S. (2003). In A.O. Brubakk & T.S. Neuman (eds), *Bennett and Elliott's physiology and medicine of diving* (5th ed., p. 800). Eastbourne: Saunders Elsevier.
- Brubakk, A.O., Duplancic, D., Valic, Z., Palada, I., Obad, A., Bakovic, D., Wisløff, U., & Dujic, Z. (2005). A single air dive reduces arterial endothelial function in man. *The Journal of Physiology*, 566(3), 901-906. <https://doi.org/10.1113/jphysiol.2005.089862>
- Brubakk, A.O., & Møllerløgken, A. (2009). The role of intra-vascular bubbles and the vascular endothelium in decompression sickness. *Diving and Hyperbaric Medicine*, 39(3), 162-169.
- Butler, B., Little, T., Sothorn, R., & Smolensky, M. (2010). Circadian study of decompression sickness symptoms and response-associated variables in rats. *Chronobiology International*, 27(1), 138-160. <https://doi.org/10.3109/07420520903398609>
- Buttolph, T.B., Dick Jr, E.J., Toner, C.B., Broome, J.R., Williams, R., Kang, Y.H., & Wilt, N.L. (1998). Cutaneous lesions in swine after decompression: histopathology and ultrastructure. *Undersea and Hyperbaric Medicine*, 25(2), 115-121.

- Buzzacott, P., Mazur, A., Wang, Q., Lambrechts, K., Theron, M., Mansourati, J., & Guerrero, F. (2014). A New Measure of Decompression Sickness in the Rat. *BioMed Research International*, 2014, 1-6. <https://doi.org/10.1155/2014/123581>
- Buzzacott, P., Theron, M., Mazur, A., Wang, Q., Lambrechts, K., Eftedal, I., Ardestani, S., & Guerrero, F. (2016). Age, weight and decompression sickness in rats. *Archives of Physiology and Biochemistry*, 122(2), 67-69. <https://doi.org/10.3109/13813455.2016.1140787>
- Cao, L. Li, K., Liang, R., Chen, S., Jiang, W., & Li, R. (2015). The tolerance threshold of Chinese sucker to total dissolved gas supersaturation. *Aquaculture Research*, 47(9), 2804-2813. <https://doi.org/10.1111/are.12730>
- Cao, L., Li, Y., An, R., Wang, Y., & Buchmann, K. (2019). Effects of water depth on GBD associated with total dissolved gas supersaturation in Chinese sucker (*Myxocyprinus asiaticus*) in upper Yangtze River. *Scientific Reports*, 9, 6828. <https://doi.org/10.1038/s41598-019-42971-8>
- Cao, C., Deng, Y., Yin, Q., Li, N., Liu, X., Shi, H., Yang, Y., & Xu, L. (2020). Effects of continuous acute and intermittent exposure on the tolerance of juvenile yellow catfish (*Pelteobagrus fulvidraco*) in total dissolved gas supersaturated water. *Ecotoxicology and Environmental Safety*, 201, 110855. <https://doi.org/10.1016/j.ecoenv.2020.110855>
- Carturan, D., Boussuges, A., Burnet, H., Fondarai, J., Vanuxem, P., & Gardette, B. (1999). Circulating venous bubbles in recreational diving: relationships with age, weight, maximal oxygen uptake and

- body fat percentage. *International Journal of Sports Medicine*, 20(6), 410–414. <https://doi.org/10.1055/s-2007-971154>
- Carturan, D., Boussuges, A., Vanuxem, P., Bar-Hen, A., Burnet, H., & Gardette, B. (2002). Ascent rate, age, maximal oxygen uptake, adiposity, and circulating venous bubbles after diving. *Journal of Applied Physiology*, 93(4), 1349–1356. <https://doi.org/10.1152/jappphysiol.00723.1999>
- Caruso, J.L. (2003). Pathology of diving accidents. In A.O. Brubakk & T.S. Neuman (eds), *Bennett and Elliott's physiology and medicine of diving* (5th ed., pp. 729-743). Eastbourne: Saunders Elsevier.
- Casillas, E., Miller, S.E., Smith, L.S., & D'Aoust, B.G. (1975). Changes in hemostatic parameters in fish following rapid decompression. *Undersea Biomedical Research*, 2(4), 267-276.
- Chen, S-C., Liu, X-Q., Jiang, W., Li, K-F., Du, J., Shen, D-Z., & Gong, Q. (2012). Effects of total dissolved gas supersaturated water on lethality and catalase activity of Chinese sucker (*Myxocyprinus asiaticus* Bleeker). *Journal of Zhejiang University Science B*, 13(10), 791-796. <https://doi.org/10.1631/jzus.B1200022>
- Clay, J.R. (1963). Histopathology of experimental decompression sickness. *Aerospace Medicine*, 34, 1107–1110.
- Cole, A., Griffiths, D., Lavender, S., Summers, P., & Rich, K. (2006). Relevance of postmortem radiology to the diagnosis of fatal cerebral gas embolism from compressed air diving. *Journal of Clinical Pathology*, 59(5), 489-491. <http://dx.doi.org/10.1136/jcp.2005.031708>

- Colt, J. (1983). The computation and reporting of dissolved gas levels. *Water research*, 17(8), 841-849. [https://doi.org/10.1016/0043-1354\(83\)90157-4](https://doi.org/10.1016/0043-1354(83)90157-4)
- Colt, J. (1986). Gas supersaturation – impact on the design and operation of aquatic systems. *Aquacultural Engineering*, 5(1), 49-85. [https://doi.org/10.1016/0144-8609\(86\)90005-1](https://doi.org/10.1016/0144-8609(86)90005-1)
- Cornacchia, J.W., & Colt, J.E. (1984). The effects of dissolved gas supersaturation on larval striped bass, *Morone saxatilis* (Walbaum). *Journal of Fish Diseases*, 7(1), 15-27. <https://doi.org/10.1111/j.1365-2761.1984.tb00903.x>
- Cross, E. R. (1962). Taravana. *Skin Diver Magazine*, 11, 42–45.
- Cross, E. R. (1965). Taravana – Diving syndrome in the Tuamotu diver. In H. Rahn & T. Yokoyama (eds), *Physiology of breathhold diving and the ama of Japan* (pp. 207–219). Washington, DC: National Academy of Science, National Research Council Publication.
- D**'Amico, A., Gisiner, R. C., Ketten, D. R., Hammock, J. A., Johnson, C., Tyack, P. L., & Mead, J. (2009). Beaked Whale Strandings and Naval Exercises. *Aquatic Mammals*, 35(4), 452–472. <https://doi.org/10.1578/AM.35.4.2009.452>
- D'Aoust, B., & Smith, L. (1974). Bends in fish. *Comparative Biochemistry and Physiology*, 49, 311-321. [https://doi.org/10.1016/0300-9629\(74\)90122-4](https://doi.org/10.1016/0300-9629(74)90122-4)
- Daily sessions of the Congress of Deputies (2004). Cdl Deputies, Editor 2004. File Number 180/000, 345.

- Dannevig, A., & Dannevig, G. (1950). Factors affecting the survival of fish larvae. *ICES Journal of Marine Science*, 16(2), 211-215. <https://doi.org/10.1093/icesjms/16.2.211>
- Dawley, E.M., & Ebel, W.J. (1975). Effects of various concentrations of dissolved atmospheric gas on juvenile chinook salmon and steelhead trout. *United States National Marine Fisheries Service, Fishery Bulletin*, 73, 787-796.
- Deanfield, J., Halcox, J., & Rabelink, T. (2007). Endothelial Function and Dysfunction. *Circulation*, 115(10), 1285-1295. <https://doi.org/10.1161/CIRCULATIONAHA.106.652859>
- Deng, Y., Cao, Y., Liu, X., Yuan, Q., Feng, C., Shi, H., Yang, Y., & Wu, Y. (2020). Effect of total dissolved gas supersaturation on the survival of bighead carp (*Hypophthalmichthys nobilis*). *Animals*, 10(1), 166. <https://doi.org/10.3390/ani10010166>
- Dennison, S., Moore, M., Fahlman, A., Moore, K., Sharp, S., Harry, C., Hoppe, J., Niemeyer, M., Lentell, B., & Wells, R. (2011). Bubbles in live-stranded dolphins. *Proceedings of the Royal Society B: Biological Sciences*, 279(1732), 1396-1404. <https://doi.org/10.1098/rspb.2011.1754>
- E**bel, W.J. (1969). Supersaturation of nitrogen in the Columbia River and its effect on salmon and steelhead trout. *United States National Marine Fisheries Service, Fishery Bulletin*, 68, 1-11.
- Ebel, W.J. (1971). Dissolved nitrogen concentrations in the Columbia and Snake Rivers in 1970 and their effect on chinook salmon and steelhead trout. *National Oceanographic and Atmospheric Administration (NOAA), Technical Report NMFS SSRF*, 646.

- Eckenhoff, R. G., Olstad, C. S., & Carrod, G. (1990). Human dose-response relationship for decompression and endogenous bubble formation. *Journal of Applied Physiology*, 69(3), 914–918. <https://doi.org/10.1152/jappl.1990.69.3.914>
- Edmonds, C., Bennett, M., Lippmann, J., & Mitchell, S.J. (2015). *Diving Subaquatic Medicine* (5th ed). Florida: CRC Press.
- Edsall, D.A., & Smith, C.E. (1991). Oxygen-induced gas bubble disease in rainbow trout, *Oncorhynchus mykiss* (Walbaum). *Aquaculture Research*, 22(2), 135-140. <https://doi.org/10.1111/j.1365-2109.1991.tb00503.x>
- Eggleton, P., Elsdon, S., Fegler, J., & Hebb, C. (1945). A study of the effects of rapid ‘decompression’ in certain animals. *The Journal of Physiology*, 104(2), 129-150. <https://doi.org/10.1113/jphysiol.1945.sp004111>
- Elliott, D.H. (1999). Early decompression experience: compressed air work. *South Pacific Underwater Medicine Society*, 29(1), 28–34.
- Emboly, G.C. (1934). Relation of temperature to the incubation period of eggs of four species of trout. *Transactions of the American Fisheries Society*, 64(1), 281-292. [https://doi.org/10.1577/1548-8659\(1934\)64\[281:ROTTTI\]2.0.CO;2](https://doi.org/10.1577/1548-8659(1934)64[281:ROTTTI]2.0.CO;2)
- European Parliament (2004). *European Parliament resolution on the environment effects of high-intensity naval sonars*. Brussels, Belgium: European Parliament.
- F**ahlman, A., Loring, S. H., Levine, G., Rocho-Levine, J., Austin, T., & Brodsky, M. (2015). Lung mechanics and pulmonary function testing in cetaceans. *Journal of Experimental Biology*, 218(13), 2030–2038. <https://doi.org/10.1242/jeb.119149>

- Fahlman, A., Crespo-Picazo, J.L., Sterba-Boatwright, B., Stacy, B.A., & García-Párraga, D. (2017). Defining risk variables causing gas embolism in loggerhead sea turtles (*Caretta caretta*) caught in trawls and gillnets. *Scientific Reports*, 7(1), 2739. <https://doi.org/10.1038/s41598-017-02819-5>
- Fahlman, A., Moore, M. J., & Wells, R. S. (2021). How Do Marine Mammals Manage and Usually Avoid Gas Emboli Formation and Gas Embolic Pathology? Critical Clues From Studies of Wild Dolphins. *Frontiers in Marine Science*, 8, 598633. <https://doi.org/10.3389/fmars.2021.598633>
- Fan, Z., Deng, Y., Yuan, Q., Liu, X., Shi, H., Feng, C., Yang, Y., & Xu, L. (2020). Effect of total dissolved gas supersaturation on the tolerance of grass carp (*Ctenopharyngodon idellus*). *Environmental Sciences Europe*, 32, 55. <https://doi.org/10.1186/s12302-020-00330-9>
- Feng, J., Li, R., Liang, R., & Shen, X. (2014). Eco-environmentally friendly operational regulation: an effective strategy to diminish the TDG supersaturation of reservoirs. *Hydrology and Earth System Sciences*, 18(3), 1213-1223. <https://doi.org/10.5194/hess-18-1213-2014>
- Fernández, A., Edwards, J. F., Rodríguez, F., de Los Monteros, A. E., Herráez, P., Castro, P., Jaber, J. R., Martín, V., & Arbelo, M. (2005). “Gas and Fat Embolic Syndrome” Involving a Mass Stranding of Beaked Whales (Family *Ziphiidae*) Exposed to Anthropogenic Sonar Signals. *Veterinary Pathology*, 42(4), 446–457. <https://doi.org/10.1354/vp.42-4-446>
- Fernández, A., Sierra, E., Martín, V., Méndez, M., Sacchini, S., Bernaldo de Quirós, Y., Andrada, M., Rivero, M., Quesada, O., & Tejedor, M. (2012). Last “Atypical” beaked whales mass stranding

in the Canary Islands (July, 2004). *Journal of Marine Science: Research and Development*, 2(107). <https://doi.org/10.4172/2155-9910.1000107>

Fernández, A., Arbelo, M., & Martín, V. (2013). Whales: no mass strandings since sonar ban. *Nature*, 497(7449), 317. <https://doi.org/10.1038/497317d>

Fernández, A., Sierra, E., Díaz-Delgado, J., Sacchini, S., Sánchez-Paz, Y., Suárez-Santana, C., Arregui, M., Arbelo, M., & Bernaldo de Quirós, Y. (2017). Deadly acute Decompression Sickness in Risso's dolphins. *Scientific Reports*, 7(1), 13621. <https://doi.org/10.1038/s41598-017-14038-z>

Ferrigno, M., & Lundgren, C.E. (2003). Breath-Hold Diving. In A.O. Brubakk & T.S. Neuman (eds), *Bennett and Elliott's physiology and medicine of diving* (5th ed, pp. 153–180). Eastbourne: Saunders Elsevier.

Finka, A., Sood, V., Quadroni, M., De los Ríos, P., & Goloubinoff, P. (2015). Quantitative proteomics of heat-treated human cells show an across-the-board mild depletion of housekeeping proteins to massively accumulate few HSPs. *Cell Stress and Chaperones*, 20, 605–620. <https://doi.org/10.1007/s12192-015-0583-2>

Fitz-Clarke, J.R. (2009). Risk of decompression sickness in extreme human breath-hold diving. *Undersea and Hyperbaric Medicine*, 36(2), 83-91.

Francis, T., Pezeshkpour, G., Dutka, A., Hallenbeck, J., & Flynn, E. (1988). Is There a Role for the Autochthonous Bubble in the Pathogenesis of Spinal Cord Decompression Sickness? *Journal of Neuropathology and Experimental Neurology*, 47(4), 475-487. <https://doi.org/10.1097/00005072-198807000-00008>

- Francis, J. (2002). Decompression sickness. *Emergency Medicine Australasia*, 14(4), 358-363. <https://doi.org/10.1046/j.1442-2026.2002.00376.x>
- Francis, T.J.R., & Mitchell, S.J. (2003). Pathophysiology of decompression sickness. In A.O. Brubakk & T.S. Neuman (eds), *Bennett and Elliott's physiology and medicine of diving* (5th ed, pp. 530–556). Eastbourne: Saunders Elsevier.
- Frantzis, A. (1998). Does acoustic testing strand whales? *Nature*, 392 (29). <https://doi.org/10.1038/32068>
- G**arcía-Párraga, D., Crespo-Picazo, J., de Quirós, Y., Cervera, V., Martí-Bonmati, L., Díaz-Delgado, J., Arbelo, M., Moore, M., Jepson, P., & Fernández, A. (2014). Decompression sickness ('the bends') in sea turtles. *Diseases of Aquatic Organisms*, 111(3), 191-205. <https://doi.org/10.3354/dao02790>
- García-Párraga, D., Lorenzo, T., Ortiz, J.L, Ortega, J., Crespo-Picazo, J.L., Cortijo, J., & Fahlman, A. (2018). Deciphering function of the pulmonary arterial sphincters in loggerhead sea turtles (*Caretta caretta*). *The Journal of Experimental Biology*, 221(23), 179820. <https://doi.org/10.1242/jeb.179820>
- Gardette, B. (1979). Correlation between decompression-sickness and circulating bubbles in 232 divers. *Undersea Biomedical Research*, 6(1): 99-107.
- Geng, M., Zhou, L., Liu, X., & Li, P. (2015). Hyperbaric oxygen treatment reduced the lung injury of type II decompression sickness. *International Journal of Clinical and Experimental Pathology*, 8(2), 1791–803.

- Germonpre, P., Balestra, C., Obeid, G., & Caers, D. (2015). Cutis Marmorata skin decompression sickness is a manifestation of brainstem bubble embolization, not of local skin bubbles. *Medical Hypotheses*, 85(6), 863-869. <https://doi.org/10.1016/j.mehy.2015.09.022>
- Gersh, I., Hawkinson, G., & Rathbun, E. (1944). Tissue and vascular bubbles after decompression from high pressure atmospheres - correlation of specific gravity with morphological changes. *Journal of Cellular and Comparative Physiology*, 24(1), 35-70. <https://doi.org/10.1002/jcp.1030240104>
- Gerth, W., & Hemmingsen, E. (1976). Gas Supersaturation Thresholds for Spontaneous Cavitation in Water with Gas Equilibration Pressures up to 570 atm. *Zeitschrift Für Naturforschung A*, 31(12), 1711-1716. <https://doi.org/10.1515/zna-1976-1240>
- Gerth, W.A., Ruterbusch, V.L., & Long, E.T. (2007). *The influence of thermal exposure on diver susceptibility to decompression sickness*. Florida: Navy Experimental Diving Unit, Tech Report #06-07.
- Goldberg, R. (1978). Some effects of gas-supersaturated sea water on *Spisula solidissima* and *Argopecten irradians*. *Aquaculture*, 14(4), 281-287. [https://doi.org/10.1016/0044-8486\(78\)90012-1](https://doi.org/10.1016/0044-8486(78)90012-1)
- Gorham, F.P. (1901). The gas bubble disease of fish and its cause. *Bulletin of the United States Fish Commission*, 19(1899), 33-37.
- Guinness World Record (2012). Deepest no-limit freedive (male). London: Guinness World Record. <https://www.guinnessworldrecords.com/world-records/673884-deepest-no-limit-freedive-male> [Accessed 6 July 2023]

- Gunnarsli, K.S., Toften, H., & Mortensen, A. (2008). Effects of nitrogen gas supersaturation on growth and survival in juvenile Atlantic cod (*Gadus morhua* L.). *Aquaculture*, 283(1-4), 175-179. <https://doi.org/10.1016/j.aquaculture.2008.06.029>
- Gunnarsli, K.S., Toften, H., & Mortensen, A. (2009). Effects of nitrogen gas supersaturation on growth and survival in larval cod (*Gadus morhua* L.). *Aquaculture*, 288(3-4), 344-348. <https://doi.org/10.1016/j.aquaculture.2008.11.039>
- H**agberg, M., & Ornhagen, H. (2003). Incidence and risk factors for symptoms of decompression sickness among male and female dive masters and instructors—a retrospective cohort study. *Undersea and Hyperbaric Medicine*, 30(2), 93-102.
- Hagen, P.T., Swcholz, D.G., & Edwards, W.D. (1984). Incidence and size of patent foramen ovale during the first decades of life: an autopsy study of 965 normal hearts. *Mayo Clinic Proceedings*, 59(1), 17–20. [https://doi.org/10.1016/S0025-6196\(12\)60336-X](https://doi.org/10.1016/S0025-6196(12)60336-X)
- Haldane, J.S. (1908). The hygiene of work in compressed air. *Journal of the Royal Society of Arts*, 56, 214–226.
- Harvey, H.H., & Smith, S.B. (1961). Supersaturation of the water supply and occurrence of gas bubble disease at Cultus Lake Trout Hatchery. *Canadian Fish Culturist*, 30, 39-46.
- Harvey, H.H. (1975). Gas diseases in fishes - a review. In W.A. Adams (ed.). *Chemistry and physics of aqueous gas solutions* (pp. 450-485). Electrochemical Society, Princeton, New Jersey, USA.
- Hauck, A.K. (1986). Gas bubble disease due to helicopter transport of young pink salmon. *Transactions of the American Fisheries Society*,

- 115(4), 630-635. [https://doi.org/10.1577/1548-8659\(1986\)115<630:GBDDTH>2.0.CO;2](https://doi.org/10.1577/1548-8659(1986)115<630:GBDDTH>2.0.CO;2)
- Heggberget, T.G. (1984). Effect of supersaturated water on fish in the river Nidelva, southern Norway. *Journal of Fish Biology*, 24(1), 65-74. <https://doi.org/10.1111/j.1095-8649.1984.tb04777.x>
- Hemmingsen, E. (1977). Spontaneous formation of bubbles in gas-supersaturated water. *Nature*, 267(5607), 141-142. <https://doi.org/10.1038/267141a0>
- Henninger, D.D., Panés, J., Eppihimer, M., Russell, J., Gerritsen, M., Anderson, D.C., & Granger, D.N. (1997). Cytokine-induced VCAM-1 and ICAM-1 expression in different organs of the mouse. *The Journal of Immunology*, 158(4), 1825-1832.
- Hicks, J.W., & Wang, T. (1996). Functional rôle of cardiac shunts in reptiles. *Journal of Experimental Zoology*, 275(2-3), 204-216. [https://doi.org/10.1002/\(SICI\)1097-010X\(19960601/15\)275:2/3<204::AID-JEZ12>3.0.CO;2-J](https://doi.org/10.1002/(SICI)1097-010X(19960601/15)275:2/3<204::AID-JEZ12>3.0.CO;2-J)
- Hjelde, A., Nossun, V., Steinsvik, M., Bagstevold, J., & Brubakk, A. (2002). Evaluation of cerebral gas retention and oedema formation in decompressed rats by using a simple gravimetric method. *Scandinavian Journal of Clinical and Laboratory Investigation*, 62(4), 263-270. <https://doi.org/10.1080/003655102760145816>
- Hochscheid, S., Bentivegna, F., Bradai, M.N., & Hays, G.C. (2007). Overwintering behaviour in sea turtles: dormancy is optional. *Marine Ecology Progress Series*, 340, 287-298.
- Hoppe-Seyler, F. (1857). Archiv für anatomie, physiologie und wissenschaftliche medizin, 24, 63-73. Cited in L. Hill and M. Greenwood, 1910. On the formation of bubbles in the vessels of

- animals submitted to partial vacuum. *Journal of Physiology* (London), 39(23).
- Houser, D.S., Howard, R., & Ridgway, S. (2001). Can diving-induced tissue nitrogen supersaturation increase the chance of acoustically driven bubble growth in marine mammals? *Journal of Theoretical Biology*, 213(2), 183-195. <https://doi.org/10.1006/jtbi.2001.2415>
- Huang, K-L., Wu, C-P., Chen, Y-L., Kang, B-H., & Lin, Y-C. (2003). Heat stress attenuates air bubble-induced acute lung injury: a novel mechanism of diving acclimatization. *Journal of Applied Physiology*, 94(4), 1485-1490. <https://doi.org/10.1152/jappphysiol.00952.2002>
- Huang, X., Li, K-F., Du, J., & Li, R. (2010). Effects of gas supersaturation on lethality and avoidance responses in juvenile rock carp (*Procypris rabaudi* Tchang). *Journal of Zhejiang University Science B*, 11, 806-811. <https://doi.org/10.1631/jzus.B1000006>
- Hubbard, A.K., & Rothlein, R. (2000). Intercellular adhesion molecule-1 (ICAM-1) expression and cell signaling cascades. *Free Radical Biology and Medicine*, 28(9), 1379-1386. [https://doi.org/10.1016/s0891-5849\(00\)00223-9](https://doi.org/10.1016/s0891-5849(00)00223-9)
- Hulman, G. (1995). The pathogenesis of fat embolism. *The Journal of Pathology*, 176(1), 3-9. <https://doi.org/10.1002/path.1711760103>
- Hyndman, K.A., & Evans, D.H. (2007). Endothelin and endothelin converting enzyme-1 in the fish gill: evolutionary and physiological perspectives. *Journal of Experimental Biology*, 210(24), 4286-4297. <https://doi.org/10.1242/jeb.009969>

**J**aminet, A. (1871). *Physical Effects of Compressed Air, and of the Causes of Pathological Symptoms Produced on Man, by Increased Atmospheric Pressure*. St. Louis, M.O. : R. & T. A. Ennis.

Janssen, I., Heymsfield, S.B., Wang, Z.M., & Ross, R. (2000). Skeletal muscle mass and distribution in 468 men and women aged 18-88 yr. *Journal of Applied Physiology*, 89(1), 81-88. <https://doi.org/10.1152/jappl.2000.89.1.81>

Jepson, P., Arbelo, M., Deaville, R., Patterson, I., Castro, P., Baker, J., Degollada, E., Ross, H., Herráez, P., Pocknell, A., Rodríguez, F., Howie, F., Espinosa, A., Reid, R., Jaber, J., Martin, V., Cunningham, A., & Fernández, A. (2003). Gas-bubble lesions in stranded cetaceans. *Nature*, 425(6958), 575-576. <https://doi.org/10.1038/425575a>

Jepson, P., Deaville, R., Patterson, I., Pocknell, A., Ross, H., Baker, J., Howie, F., Reid, R., Colloff, A., & Cunningham, A. (2005). Acute and Chronic Gas Bubble Lesions in Cetaceans Stranded in the United Kingdom. *Veterinary Pathology*, 42(3), 291-305. <https://doi.org/10.1354/vp.42-3-291>

Ji, Q., Xue, S., Yuan, Q., Yuan, Y., Wang, Y., Liang, R., Feng, J., Li, K., & Li, R. (2019). The tolerance characteristics of resident fish in the upper Yangtze River under varying gas supersaturation. *International Journal of Environmental Research and Public Health*, 16(11), 2021. <https://doi.org/10.3390/ijerph16112021>

Ji, Q., Li, K., Wang, Y., Liang, R., Feng, J., Yuan, Q., Zhang, P., & Zhu, D.Z. (2021). Total dissolved gases induced tolerance and avoidance behaviors in pelagic fish in the Yangtze River, China. *Ecotoxicology and Environmental Safety*, 216, 112218. <https://doi.org/10.1016/j.ecoenv.2021.112218>

- Jirangkul, P., Baisopon, S., Pandaeng, D., & Srisawat, P. (2021). Hyperbaric oxygen adjuvant therapy in severe mangled extremities. *Injury*, 52(11), 3511-3515. <https://doi.org/10.1016/j.injury.2021.06.033>
- Johnson, E.L., Clabough, T.S., Peery, C.A., Bennett, D.H., Bjornn, T.C., Caudill, C.C., & Richmond, M.C. (2007). Estimating adult Chinook salmon exposure to dissolved gas supersaturation downstream of hydroelectric dams using telemetry and hydrodynamic models. *River Research and Applications*, 23(9), 936-978. <https://doi.org/10.1002/rra.1019>
- Jones, J.P., & Neuman, T.S. (2003). Dysbaric osteonecrosis. In A.O. Brubakk & T.S. Neuman (eds), *Bennett and Elliott's physiology and medicine of diving* (5th ed, pp. 659-679). Eastbourne: Saunders Elsevier.
- K**amtchum Tatuene, J., Pignel, R., Pollak, P., Lovblad, K.O., Kleinschmidt, A., Vargas, M.I. (2014). Neuroimaging of diving-related decompression illness: current knowledge and perspectives. *American Journal of Neuroradiology*, 35(11), 2039-2044. <https://doi.org/10.3174/ajnr.A4005>
- Kitano, M., Kawashima, M., & Hayashi, K. (1978). Experimental Studies on Decompression Sickness. *Orthopedics and Traumatology*, 27(4), 653-658. <https://doi.org/10.5035/nishiseisai.27.653>
- Kitano, M., & Hayashi, K. (1981). Acute decompression sickness – report of an autopsy case with widespread fat embolism. *Acta Pathologica Japonica*, 31(2), 269–276.

- Knittel, M.D., Chapman, G.A., & Garton, R.R. (1980). Effects of hydrostatic pressure on steelhead survival in air-supersaturated water. *Transactions of the American Fisheries Society*, 109(6), 755-759. [https://doi.org/10.1577/1548-8659\(1980\)109<755:EOHPOS>2.0.CO;2](https://doi.org/10.1577/1548-8659(1980)109<755:EOHPOS>2.0.CO;2)
- Kohshi, K., Kinoshita, Y., Abe, H., & Okudera, T. (1998). Multiple cerebral infarction in Japanese breath-hold divers: Two case reports. *The Mount Sinai Journal of Medicine*, 65(4), 280-283.
- Kohshi, K., Denoble, P.J., Tamaki, H., Morimatsu, Y., Ishitake, T., & Lemaître, F. (2021). Decompression Illness in Repetitive Breath-Hold Diving: Why Ischemic Lesions Involve the Brain?. *Frontiers in Physiology*, 12, 711850. <https://doi.org/10.3389/fphys.2021.711850>
- Kooyman, G. (1973). Respiratory Adaptations in Marine Mammals. *American Zoologist*, 13(2), 457-468. <https://doi.org/10.1093/icb/13.2.457>
- Kooyman, G. L., & Ponganis, P. J. (1998). The Physiological Basis Of Diving To Depth: Birds and Mammals. *Annual Review of Physiology*, 60(1), 19–32. <https://doi.org/10.1146/annurev.physiol.60.1.19>
- Kregel, K.C. (2002). Heat shock proteins: modifying factors in physiological stress responses and acquired thermotolerance. *Journal of Applied Physiology*, 92(5), 2177-2186. <https://doi.org/10.1152/jappphysiol.01267.2001>
- L**ambrechts, K., Pontier, J., Mazur, A., Theron, M., Buzzacott, P., Wang, Q., Belhomme, M., & Guerrero, F. (2015). Mechanism of action of antiplatelet drugs on decompression sickness in rats: a

- protective effect of anti-GPIIb/IIIa therapy. *Journal of Applied Physiology*, 118(10), 1234-1239.  
<https://doi.org/10.1152/jappphysiol.00125.2015>
- Laurent, P., Coulange, M., Bartoli, C., Boussuges, A., Rostain, J., Luciano, M., Cohen, F., Rolland, P., Mancini, J., Piercecchi, M., Vidal, V., & Gorincour, G. (2013). Appearance of gas collections after scuba diving death: a computed tomography study in a porcine model. *International Journal of Legal Medicine*, 127(1), 177-184.  
<https://doi.org/10.1007/s00414-011-0662-6>
- Lemaitre, F., Fahlman, A., Gardette, B., & Kohshi, K. (2009). Decompression sickness in breath-hold divers: A review. *Journal Of Sports Sciences*, 27(14), 1519-1534.  
<https://doi.org/10.1080/02640410903121351>
- Lemaitre, F., Kohshi, K., Tamaki, H., Nakayasu, K., Harada, M., Okayama, M., Satou, Y., Hoshiko, M., Ishitake, T., Costalat, G., & Gardette, B. (2014). Doppler detection in Ama divers of Japan. *Wilderness and Environmental Medicine*, 25(3), 258-262.  
<https://doi.org/10.1016/j.wem.2014.02.002>
- Lever, M., Miller, K., Paton, W., & Smith, E. (1966). Experiments on the genesis of bubbles as a result of rapid decompression. *The Journal of Physiology*, 184(4), 964-969.  
<https://doi.org/10.1113/jphysiol.1966.sp007960>
- Levin, L., Stewart, G., Lynch, P., & Bove, A. (1981). Blood and blood vessel wall changes induced by decompression sickness in dogs. *Journal of Applied Physiology*, 50(5), 944-949.  
<https://doi.org/10.1152/jappl.1981.50.5.944>
- Li, N., Fu, C., Zhang, J., Liu, X., Shi, X., Yang, Y., & Shi, H. (2019). Hatching rate of Chinese sucker (*Myxocyprinus asiaticus* Bleeker)

- eggs exposed to total dissolved gas (TDG) supersaturation and the tolerance of juveniles to the interaction of TDG supersaturation and suspended sediment. *Aquaculture Research*, 50(7), 1876-1884. <https://doi.org/10.1111/are.14071>
- Liang, R-F., Li, B., Li, K-F., & Tuo, Y-C. (2013). Effect of total dissolved gas supersaturated water on early life of David's schizothoracin (*Schizothorax davidi*). *Journal of Zhejiang University Science B*, 14(7), 632-639. <https://doi.org/10.1631/jzus.B1200364>
- Lindquist, S., & Craig, EA. (1988). The heat-shock proteins. *Annual Review of Genetics*, 22, 631-677. <https://doi.org/10.1146/annurev.ge.22.120188.003215>.
- Liu, X-Q., Li, K-F., Du, J., Li, J., & Li, R. (2011). Growth rate, catalase and superoxide dismutase activities in rock carp (*Procypris rabaudi* Tchang) exposed to supersaturated total dissolved gas. *Journal of Zhejiang University Science B*, 12, 909. <https://doi.org/10.1631/jzus.B1100071>
- Livak, K.J., & Schmittgen, T.D. (2001). Analysis of relative gene expression data using real-time quantitative PCR and the  $2^{-\Delta\Delta CT}$  method. *Methods*, 25(4), 402-408. <https://doi.org/10.1006/meth.2001.1262>
- Lund, M., & Heggberget, T.G. (1985). Avoidance response of two-year-old rainbow trout, *Salmo gairdneri* Richardson, to air-supersaturated water: hydrostatic compensation. *Journal of Fish Biology*, 26(2), 193-200. <https://doi.org/10.1111/j.1095-8649.1985.tb04256.x>
- Lutcavage, M.E., Lutz, P.L., & Baier, H. (1989). Respiratory mechanics of the loggerhead sea turtle, *Caretta caretta*. *Respiration*

- Physiology*, 76(1), 13-24. [https://doi.org/10.1016/0034-5687\(89\)90014-5](https://doi.org/10.1016/0034-5687(89)90014-5)
- Lutcavage, M.E., & Lutz, P.L. (1997). Diving physiology. In: P.L. Lutz & J.A. Musick (eds), *The biology of sea turtles* (pp. 277-296). New York: CRC Press.
- M**acario, A.J.L., & Conway de Macario, E. (2007). Molecular chaperones: multiple functions, pathologies, and potential applications. *Frontiers in Bioscience*, 12, 2588-2600. <https://doi.org/10.2741/2257>
- Machado, J.P., Garling Jr., D.L., Kevern, N.R., Trapp, A.L., & Bell, T.G. (1987). Histopathology and the pathogenesis of embolism (gas bubble disease) in rainbow trout (*Salmo gairdneri*). *Canadian Journal of Fisheries and Aquatic Sciences*, 44(11), 1985-1994. <https://doi.org/10.1139/f87-243>
- Machova, J., Faina, R., Randak, T., Valentova, O., Steinbach, C., Kocour Kroupova, H., Svobodova, Z. (2017). Fish death caused by gas bubble disease: a case report. *Veterinarni Medicina*, 62, 231-237. <https://doi.org/10.17221/153/2016-VETMED>
- Madden, L.A., & Laden, G. (2009). Gas bubbles may not be the underlying cause of decompression illness—The at-depth endothelial dysfunction hypothesis. *Medical hypotheses*, 72(4), 389–392. <https://doi.org/10.1016/j.mehy.2008.11.022>
- Mahon, R. T., & Regis, D. P. (2014). Decompression and Decompression Sickness. *Comprehensive Physiology*, 4(3), 1157–1175. <https://doi.org/10.1002/cphy.c130039>
- Marasciulo, F.L., Montagnani, M., & Potenza, M.A. (2006). Endothelin-1: the yin and yang on vascular function. *Current Medicinal*

- Chemistry*, 13(14), 1655-1665.  
<https://doi.org/10.2174/092986706777441968>
- Marking, L. (1987). Gas supersaturation in fisheries. Washington, D.C.: United States Department of the Interior, Fish and Wildlife Service.
- Marsh, M.C., & Gorham, F.P. (1905). The gas disease in fishes. *Report of the United States Bureau of Fisheries*, 1904, 343-376.
- Matsuo, H., Shinomiya, N., & Suzuki, S. (2000). Hyperbaric stress during saturation diving induces lymphocyte subset changes and heat shock protein expression. *Undersea and Hyperbaric Medicine*, 27(1), 37-41.
- Mayer, M.P., & Bukau, B. (2005). Hsp70 chaperones: cellular functions and molecular mechanism. *Cellular and Molecular Life Sciences*, 62(6), 670-684. <https://doi.org/10.1007/s00018-004-4464-6>
- McGrath, K.E., Dawley, E.M., & Geist, D.R. (2006). Total dissolved gas effects on fishes of the lower Columbia River. *Pacific Northwest National Laboratory*, U.S. Army Corps of Engineers, Oregon, USA.
- Mesa, M.G., & Warren, J.J. (1997). Predator avoidance ability of juvenile chinook salmon (*Oncorhynchus tshawytscha*) subjected to sublethal exposures of gas-supersaturated water. *Canadian Journal of Fisheries and Aquatic Sciences*, 54(4), 757-764. <https://doi.org/10.1139/cjfas-54-4-757>
- Miller, D.J., & Fort, P.E. (2018). Heat Shock Proteins Regulatory Role in Neurodevelopment. *Frontiers in Neuroscience*, 12, 821. doi: 10.3389/fnins.2018.00821.
- Mitchell, S. J. (2019). DCS or DCI? The difference and why it matters. *Diving and Hyperbaric Medicine Journal*, 49(3), 152–153. <https://doi.org/10.28920/dhm49.3.152-153>

- Møllerløkken, A., Berge, V., Jørgensen, A., Wisløff, U., & Brubakk, A. (2006). Effect of a short-acting NO donor on bubble formation from a saturation dive in pigs. *Journal of Applied Physiology*, 101(6), 1541-1545. <https://doi.org/10.1152/jappphysiol.01191.2005>
- Moore, M.J., & Early, G.A. (2004). Cumulative sperm whale bone damage and the bends. *Science*, 306(5705), 2215-2215. <https://doi.org/10.1126/science.1105452>
- Moore, M.J., Bogomolni, A.L., Dennison, S.E., Early, G., Garner, M.M., Hayward, B.A., Lentell, B.J., & Rotstein, D.S. (2009). Gas bubbles in seals, dolphins, and porpoises entangled and drowned at depth in gillnets. *Veterinary Pathology*, 46(3), 536-547. <https://doi.org/10.1354/vp.08-VP-0065-M-FL>
- Morimoto, R.I. (1993). Cells in stress: transcriptional activation of heat shock genes. *Science*, 259(5100), 1409-1410. <https://doi.org/10.1126/science.8451637>
- Mukhopadhyay, S., Khaket, T.P., & Mukherjee, T.K. (2016). Intercellular Adhesion Molecule 1. In: S. Choi (ed) *Encyclopedia of Signaling Molecules*. Springer, New York, NY.
- Muth, C. M., & Shank, E. S. (2000). Gas Embolism. *New England Journal of Medicine*, 342(7), 476-482. <https://doi.org/10.1056/NEJM200002173420706>
- Ni, X-X., Cai, Z-Y., Fan, D-F., Liu, Y., Zhang, R-J., Liu, S-L., Kang, Z-M., Liu, K., Li, R-P., Sun, X-J., & Xu, W-G. (2011). Protective Effect of Hydrogen-Rich Saline on Decompression Sickness in Rats. *Aviation, Space, and Environmental Medicine*, 82(6), 604-609. <https://doi.org/10.3357/ASEM.2964.2011>

Ni, C-H., Li, Y., & Sheng, Z. (2014). The report of dead fishes in downstream of Xiluodu Dam. *Center of Fisheries Ecological Inspection of Yangtze River*, Ministry of Agriculture, China.

Ninokawa, S., & Nordham, K. (2022). Discovery of caisson disease: a dive into the history of decompression sickness. *Baylor University Medical Center Proceedings*, 35(1), 129-132. <https://doi.org/10.1080/08998280.2021.1967021>

Ninomiya, K., Ihama, Y., Yamagata, K., Fukasawa, M., Nagai, T., Fuke, C., & Miyazaki, T. (2013). An autopsy case of decompression sickness: Hemorrhages in the fat tissue and fat embolism. *Romanian Journal of Legal Medicine*, 21(1), 23-26. <https://doi.org/10.4323/rjlm.2013.23>

Nishi, R. (1993). Doppler and ultrasonic bubble detection. In A.O. Brubakk & T.S. Neuman (eds), *Bennett and Elliott's physiology and medicine of diving* (5th ed, pp. 433–453). Eastbourne: Saunders Elsevier.

Nossum, V., Hjelde, A., & Brubakk, A. (2002). Small amounts of venous gas embolism cause delayed impairment of endothelial function and increase polymorphonuclear neutrophil infiltration. *European Journal of Applied Physiology*, 86(3), 209-214. <https://doi.org/10.1007/s00421-001-0531-y>

Nukada, M. (1965). Historical development of the Ama's diving activities. In H. Rahn & T. Yokoyama (eds), *Physiology of breath-hold diving and the Ama of Japan* (pp. 25-40). Washington, DC: National Academy of Sciences, National Research Council.

**O**bad, A., Valic, Z., Palada, I., Brubakk, A.O., Modun, D., & Dujic, Z. (2007). Antioxidant pretreatment and reduced arterial endothelial

- dysfunction after diving. *Aviation, Space and Environmental Medicine*, 78(12), 1114-1120.  
<https://doi.org/10.3357/ASEM.2039.2007>
- Obad, A., Marinovic, J., Ljubkovic, M., Breskovic, T., Modun, D., Boban, M., & Dujic, Z. (2010). Successive deep dives impair endothelial function and enhance oxidative stress in man. *Clinical Physiology and Functional Imaging*, 30(6), 432-438.  
<https://doi.org/10.1111/j.1475-097X.2010.00962.x>
- P**admini, E., & Usha Rani, M. (2008). Impact of seasonal variation on HSP70 expression quantitated in stressed fish hepatocytes. *Comparative Biochemistry and Physiology Part B: Biochemistry and Molecular Biology*, 151(3), 278-285.  
<https://doi.org/10.1016/j.cbpb.2008.07.011>
- Padmini, E. (2010). Physiological adaptations of stressed fish to polluted environments: role of heat shock proteins. *Reviews of Environmental Contamination and Toxicology*, 206, 1-27.  
[https://doi.org/10.1007/978-1-4419-6260-7\\_1](https://doi.org/10.1007/978-1-4419-6260-7_1)
- Parga, M., Crespo-Picazo, J., Monteiro, D., García-Párraga, D., Hernandez, J., Swimmer, Y., Paz, S., & Stacy, N. (2020). On-board study of gas embolism in marine turtles caught in bottom trawl fisheries in the Atlantic Ocean. *Scientific Reports*, 10(1), 5561. <https://doi.org/10.1038/s41598-020-62355-7>
- Pauley, G.B., & Nakatani, R.E. (1967). Histopathology of “gas-bubble” disease in salmon fingerlings. *Journal of the Fisheries Board of Canada*, 24, 867-871. <https://doi.org/10.1139/f67-073>

- Philp, R.B. (1974). A review of blood changes associated with compression-decompression: relationship to decompression sickness. *Undersea Biomedical Research*, 1(2), 117-150.
- Piantadosi, C. A., & Thalmann, E. D. (2004). Whales, sonar and decompression sickness. *Nature*, 428(6984), 1–2. <https://doi.org/10.1038/nature02527a>
- Piechota, A., Polańczyk, A., & Gorąca, A. (2010). Role of endothelin-1 receptor blockers on hemodynamic parameters and oxidative stress. *Pharmacological Reports*, 62(1), 28–34. [https://doi.org/10.1016/s1734-1140\(10\)70240-1](https://doi.org/10.1016/s1734-1140(10)70240-1)
- Poder, T.C., Silberberg, S.D., & Rampe, D. (1991). Contraction of reptile, amphibian, and fish blood vessels by endothelin-1. *Canadian Journal of Physiology and Pharmacology*, 69(2), 215-217. <https://doi.org/10.1139/y91-032>
- Ponganis, P.J., Kooyman, G.L., & Ridgway, S. (2003). Comparative diving physiology. In A.O. Brubakk and T.S. Neuman (eds). *Bennett and Elliott's physiology and medicine of diving* (5th ed, pp. 221-226). Eastbourne: Saunders Elsevier.
- Pontier, J., Blatteau, J., & Vallée, N. (2008). Blood Platelet Count and Severity of Decompression Sickness in Rats After a Provocative Dive. *Aviation, Space, and Environmental Medicine*, 79(8), 761-764. <https://doi.org/10.3357/ASEM.2299.2008>
- Q**uick, N.J., Cioffi, W.R., Shearer, J.M., Fahlman, A., & Read, A.J. (2020). Extreme diving in mammals: first estimates of behavioural aerobic dive limits in Cuvier's beaked whales. *Journal of Experimental Biology*, 223 (18), jeb222109. <https://doi.org/10.1242/jeb.222109>

- R**adons, J. (2016). The human HSP70 family of chaperones: where do we stand? *Cell Stress Chaperones*, 21(3), 379-404. <https://doi.org/10.1007/s12192-016-0676-6>
- Renfro, W.C. (1963). Gas-bubble mortality of fishes in Galveston Bay, Texas. *Transactions of the American Fisheries Society*, 93(3), 320-322. [https://doi.org/10.1577/1548-8659\(1963\)92\[320:GMOFIG\]2.0.CO;2](https://doi.org/10.1577/1548-8659(1963)92[320:GMOFIG]2.0.CO;2)
- Reuter, M., Tetzlaff, K., Brasch, F., Gerriets, T., Weiher, M., Struck, N., Hirt, S., Hansen, J., Müller, K., & Heller, M. (2000). Computed chest tomography in an animal model for decompression sickness: radiologic, physiologic, and pathologic findings. *European Radiology*, 10(3), 534-541. <https://doi.org/10.1007/s003300050092>
- Ritossa, F. (1962). A new puffing pattern induced by temperature shock and DNP in drosophila. *Experientia*, 18, 571-573. <https://doi.org/10.1007/BF02172188>
- Roberts, R.J., Agius, C., Saliba, C., Bossier, P., & Sung, Y.Y. (2010). Heat shock proteins (chaperones) in fish and shellfish and their potential role in relation to fish health: a review. *Journal of Fish Diseases*, 33(10), 789-801. <https://doi.org/10.1111/j.1365-2761.2010.01183.x>
- Roberts, R. (2012). *Fish pathology* (4th ed). New Jersey: Wiley-Blackwell.
- Ross, P.M., Pande, A., Jones, J.B., Cope, J., & Flowers, G. (2017). First detection of gas bubble disease and Rickettsia-like organisms in *Paphies ventricosa*, a New Zealand surf clam. *Journal of Fish Diseases*, 41(1), 187-190. <https://doi.org/10.1111/jfd.12684>

Rothschild, B.M., Mitchell, E.D., Moore, M.J., & Early, G. (2005). What causes lesions in sperm whale bones?. *Science*, 308, 631–632. <https://doi.org/10.1126/science.308.5722.631c>

Round, L.A. (1933). Frederic Poole Gorham, 1871-1933. *Journal of Bacteriology*, 26(5). <https://doi.org/10.1128/jb.26.5.i2-433.1933>.

Saukko, P., & Knight, B. (2004). *Knight's Forensic Pathology* (3rd ed, pp. 488-490). London: Edward Arnold Ltd.

Schiffrin, E.L. (1999). State-of-the-art lecture. Role of endothelin-1 in hypertension. *Hypertension*, 34(4), 876-881. <https://doi.org/10.1161/01.HYP.34.4.876>

Schipke, J., Gams, E., & Kallweit, O. (2006). Decompression Sickness Following Breath-hold Diving. *Research in Sports Medicine*, 14(3), 163-178. <https://doi.org/10.1080/15438620600854710>

Schlesinger, M.J. (1990). Heat shock proteins. *The Journal of Biological Chemistry*, 265(21), 12111-12114.

Scholander, P. F. (1940). Experimental investigations on the respiratory function in diving mammals and birds. *Hvalrådets Skrifter*, 22, 5–131.

Schorr, G. S., Falcone, E. A., Moretti, D. J., & Andrews, R. D. (2014). First Long-Term Behavioral Records from Cuvier's Beaked Whales (*Ziphius cavirostris*) Reveal Record-Breaking Dives. *PLoS ONE*, 9(3), e92633. <https://doi.org/10.1371/journal.pone.0092633>

Shim, S.S, Patterson, F.P., & Kendall, M.J. (1967). Hyperbaric Chamber and Decompression Sickness: An Experimental Study. *Canadian Medical Association Journal*, 97(21), 1263-72.

- Simmonds, M., & Lopez-Jurado, L. (1991). Whales and the military. *Nature*, 351, 448. <https://doi.org/10.1038/351448a0>
- Smith, A.H. (1873). *The Effects of High Atmospheric Pressure Including the Caisson Disease* (pp. 1-53). Brooklyn, NY: Eagle Print.
- Smith, C.E. (1988). Communications: histopathology of gas bubble disease in juvenile rainbow trout. *The Progressive Fish-Culturist*, 50(2), 98-103. [https://doi.org/10.1577/1548-8640\(1988\)050<0098:CHOGBD>2.3.CO;2](https://doi.org/10.1577/1548-8640(1988)050<0098:CHOGBD>2.3.CO;2)
- Speare, D.J. (1991). Endothelial lesions associated with gas bubble disease in fish. *Journal of Comparative Pathology*, 104(3), 327-335. [https://doi.org/10.1016/S0021-9975\(08\)80044-8](https://doi.org/10.1016/S0021-9975(08)80044-8)
- Speare, D.J. (2010). Disorders associated with exposure to excess dissolved gases. In J.F. Leatherland and P.T.K. Woo (eds). *Fish Disease and Disorders: 2.Noninfectious Disorders*. Oxfordshire: CAB International.
- Spira, A. (1999). Diving and marine medicine review part II: diving diseases. *Journal of Travel Medicine*, 6(3), 180-198. <https://doi.org/10.1111/j.1708-8305.1999.tb00857.x>
- Stenberg, S.K., Velle, G., Pulg, U., & Skoglund, H. (2022). Acute effects of gas supersaturation on Atlantic salmon smolt in two Norwegian rivers. *Hydrobiologia*, 849, 527-538. <https://doi.org/10.1007/s10750-020-04439-z>
- Stevens, D.G., Nebeker, A.V., & Baker, R.J. (1980). Avoidance responses of salmon and trout to air-supersaturated water. *Transactions of the American Fisheries Society*, 109(6), 751-754. [https://doi.org/10.1577/1548-8659\(1980\)109<751:AROSAT>2.0.CO;2](https://doi.org/10.1577/1548-8659(1980)109<751:AROSAT>2.0.CO;2)

Su, C-L., Wu, C-P., Chen, S-Y., Kang, B-H., Huang, K-L., & Lin, Y-C. (2004). Acclimatization to neurological decompression sickness in rabbits. *American Journal of Physiology*, 287(5), 1214-1218. <https://doi.org/10.1152/ajpregu.00260.2004>

Szyller, J., Kozakiewicz, M., Siermontowski, P., & Kaczerska, D. (2022). Oxidative stress, hsp70/hsp90 and Enos/inos serum levels in professional divers during Hyperbaric Exposition. *Antioxidants*, 11(5), 1008. <https://doi.org/10.3390/antiox11051008>

**T**ang, S-E., Liao, W-I., Wu, S-Y., Pao, H-P., Huang, K-L., & Chu, S-J. (2020). The Blockade of Store-Operated Calcium Channels Improves Decompression Sickness in Rats. *Frontiers in Physiology*, 10, 1616. <https://doi.org/10.3389/fphys.2019.01616>

Tanoue, K., Mano, Y., Kuroiwa, K., Suzuki, H., Shibayama, M., & Yamazaki, H. (1987). Consumption of platelets in decompression sickness of rabbits. *Journal of Applied Physiology*, 62(5), 1772-1779. <https://doi.org/10.1152/jappl.1987.62.5.1772>

Tavaria, M., Gabriele, T., Kola, I., & Anderson, R.L. (1996). A hitchhiker's guide to the human Hsp70 family. *Cell Stress Chaperones*, 1(1), 23–28. [https://doi.org/10.1379/1466-1268\(1996\)001<0023:ahsgtt>2.3.co;2](https://doi.org/10.1379/1466-1268(1996)001<0023:ahsgtt>2.3.co;2)

Tikusis, P., & Gerth, W.A. (2003). Decompression Theory. In A.O. Brubakk and T.S. Neuman (eds). *Bennett and Elliott's physiology and medicine of diving* (5th ed, pp. 419-454). Eastbourne: Saunders Elsevier.

Triger C. (1845). Lettre a M. Aragao. *Comptes Rendus de L'Académie Des Sciences*, 20, 445–449.

Tsai, J.Y., Felt, S.A., Bouley, D.M., & Green, S.L. (2017). Acute and Chronic Outcomes of Gas-Bubble Disease in a Colony of African Clawed Frogs (*Xenopus laevis*). *Comparative Medicine*, 67(1), 4-10.

**U**SEPA: *United States Environmental Protection Agency* (1971). Nitrogen supersaturation in the Columbia and Snake rivers, summary report. Region 10, Seattle, Washington, USA.

**V**an Bonn, W., Dennison, S., Cook, P., & Fahlman, A. (2013). Gas bubble disease in the brain of a living California sea lion (*Zalophus californianus*). *Frontiers in Physiology*. 4, 5. <https://doi.org/10.3389/fphys.2013.00005>

Van de Stolpe, A., & Van der Saag, P.T. (1996). Intercellular adhesión molecule-1. *Journal of Molecular Medicine*, 74(1), 13-33. <https://doi.org/10.1007/BF00202069>

Vann, R., Butler, F., Mitchell, S., & Moon, R. (2011). Decompression illness. *The Lancet*, 377(9760), 153-164. [https://doi.org/10.1016/S0140-6736\(10\)61085-9](https://doi.org/10.1016/S0140-6736(10)61085-9)

Varlet, V., Smith, F., Giuliani, N., Egger, C., Rinaldi, A., Dominguez, A., Chevallier, C., Bruguier, C., Augsburger, M., Mangin, P., & Grabherr, S. (2015). When gas analysis assists with postmortem imaging to diagnose causes of death. *Forensic Science International*, 251, 1-10. <https://doi.org/10.1016/j.forsciint.2015.03.010>

Virdis, A., Ghiadoni, L., & Taddei, S. (2010). Human endotelial dysfunction: EDCFs. *Pflugers Archiv*, 459(6), 1015-1023. <https://doi.org/10.1007/s00424-009-0783-7>

- Wang, Q., Mazur, A., Guerrero, F., Lambrechts, K., Buzzacott, P., Belhomme, M. & Theron, M. (2015a). Antioxidants, endothelial dysfunction, and DCS: in vitro and in vivo study. *Journal of Applied Physiology*, 119(12), 1355-1362. <https://doi.org/10.1152/jappphysiol.00167.2015>
- Wang, Y., Li, K., Li, J., Li, R., & Deng, Y. (2015b). Tolerance and avoidance characteristics of Prenant's schizothoracin *Schizothorax prenanti* to total dissolved gas supersaturated water. *North American Journal of Fisheries Management*, 35(4), 827-834. <https://doi.org/10.1080/02755947.2015.1052160>
- Warren, B.A., Philp, R.B., & Inwood, M.J. (1973). The ultrastructural morphology of air embolism: platelet adhesion to the interface and endothelial damage. *British Journal of Experimental Pathology*, 54(2), 163-72.
- Watson, S., & Arkininstall, S. (1994). Endothelins. In: *the G protein-linked receptor facts book*. London: Academic Press, pp.111-116.
- Webb, J.T., Pilmanis, A.A., & Fischer, M.D. (2002). Moderate exercise after altitude exposure fails to induce decompression sickness. *Aviation, Space and Environmental Medicine*, 73(9), 872-875.
- Weitkamp, D.E., & Katz, M. (1980). A review of dissolved gas supersaturation literature. *Transactions of the American Fisheries Society*, 109(6), 659-702. [https://doi.org/10.1577/1548-8659\(1980\)109<659:ARODGS>2.0.CO;2](https://doi.org/10.1577/1548-8659(1980)109<659:ARODGS>2.0.CO;2)
- Weitkamp, D.E., Sullivan, R.D., Swant, T., & DosSantos, J. (2003). Behavior of resident fish relative to total dissolved gas supersaturation in the lower Clark Fork River. *Transactions of the*

- American Fisheries Society*, 132(5), 856-864.  
<https://doi.org/10.1577/T02-025>
- Westgard, R.L. (1964). Physical and biological aspects of gas-bubble disease in impounded adult chinook salmon at McNary spawning channel. *Transactions of the American Fisheries Society*, 93(3), 306-309. [https://doi.org/10.1577/1548-8659\(1964\)93\[306:PABAOG\]2.0.CO;2](https://doi.org/10.1577/1548-8659(1964)93[306:PABAOG]2.0.CO;2)
- When, L., & Williams, M. (2009). Post-mortems in recreational scuba diver deaths: The utility of radiology. *Journal of Forensic and Legal Medicine*, 16(5), 273-276. <https://doi.org/10.1016/j.jflm.2008.12.011>
- White, F.N. (1976). Circulation. In C. Gans and E.R. Dawson (eds), *Biology of the Reptilia* (pp. 275-334). New York: Academic Press.
- Wisløff, U., & Brubakk, A. (2001). Aerobic endurance training reduces bubble formation and increases survival in rats exposed to hyperbaric pressure. *The Journal of Physiology*, 537(2), 607-611. <https://doi.org/10.1111/j.1469-7793.2001.00607.x>
- Wisløff, U., Richardson, R., & Brubakk, A. (2003). NOS inhibition increases bubble formation and reduces survival in sedentary but not exercised rats. *The Journal of Physiology*, 546(2), 577-582. <https://doi.org/10.1113/jphysiol.2002.030338>
- Wisløff, U., Richardson, R., & Brubakk, A. (2004). Exercise and nitric oxide prevent bubble formation: a novel approach to the prevention of decompression sickness? *The Journal of Physiology*, 555(3), 825-829. <https://doi.org/10.1113/jphysiol.2003.055467>
- Woodbury, L.A. (1941). A sudden mortality of fishes accompanying a supersaturation of oxygen in Lake Waubesa, Wisconsin.

*Transactions of the American Fisheries Society*, 71(1), 112-117.  
[https://doi.org/10.1577/1548-8659\(1941\)71\[112:ASMOFA\]2.0.CO;2](https://doi.org/10.1577/1548-8659(1941)71[112:ASMOFA]2.0.CO;2)

**X**ue, S., Wang, Y., Liang, R., Li, K., & Li, R. (2019). Effects of total dissolved gas supersaturation in fish of different sizes and species. *International Journal of Environmental Research and Public Health*, 16(13), 2444. <https://doi.org/10.3390/ijerph16132444>

**Y**anagisawa, M., Kurihara, H., Kimura, S., Tomobe, Y., Kobayashi, M., Mitsui, Y., Yazaki, Y., Goto, K., & Masaki, T. (1988). A novel potent vasoconstrictor peptide produced by Vascular Endothelial Cells. *Nature*, 332(6163), 411–415. <https://doi.org/10.1038/332411a0>

Yu, X., Xu, J., Liu, W., Zhang, Z., He, C., & Xu, W. (2020). Protective effects of pulmonary surfactant on decompression sickness in rats. *Journal of Applied Physiology*, 130(2), 400-407. <https://doi.org/10.1152/jappphysiol.00807.2020>

Yuan, Q., Li, K., Wang, Y., Ji, Q., & Liang, R. (2022). Tolerance and growth of adult *Schizothorax prenanti* exposed and re-exposed to supersaturated gas downstream of a dam. *Water*, 14(16), 2501. <https://doi.org/10.3390/w14162501>

**Z**hai, X., Kong, W-G., Cheng, G-F., Cao, J-F., Dong, F., Han, G-K., Song, Y-L., Qin, C-J., & Xu, Z. (2021). Molecular Characterization and Expression Analysis of Intercellular Adhesion Molecule-1 (ICAM-1) Genes in Rainbow Trout (*Oncorhynchus mykiss*) in Response to Viral, Bacterial and Parasitic Challenge. *Frontiers in Immunology*, 12, 704224. <https://doi.org/10.3389/fimmu.2021.704224>

- Zhang, K., Wang, D., Xu, J., Li, R., Cai, Z., Liu, K., Zheng, J., Denoble, P.J., Fang, Y., & Xu, W. (2015). Simvastatin decreases incidence of decompression sickness in rats. *Undersea & Hyperbaric Medicine*, 42(2), 115-123.
- Zhang, K., Wang, D., Jiang, Z., Ning, X., Buzzacott, P., & Xu, W. (2016). Endothelial dysfunction correlates with decompression bubbles in rats. *Scientific Reports*, 6(1), 33390. <https://doi.org/10.1038/srep33390>
- Zhang, K., Wang, M., Wang, H., Liu, Y., Buzzacott, P., & Xu, W. (2017a). Time course of endothelial dysfunction induced by decompression bubbles in rats. *Frontiers in Physiology*, 8, 181. <https://doi.org/10.3389/fphys.2017.00181>
- Zhang, K., Jiang, Z., Ning, X., Yu, X., Xu, J., Buzzacott, P., & Xu, W. (2017b). Endothelia-Targeting Protection by Escin in Decompression Sickness Rats. *Scientific Reports*, 7, 41288. <https://doi.org/10.1038/srep41288>
- Zininga, T., Ramatsui, L., & Shonhai, A. (2018). Heat shock proteins as immunomodulants. *Molecules*, 23(11), 2846. <https://doi.org/10.3390/molecules23112846>



## 8. ABBREVIATIONS





AGE	Arterial Gas Embolism
ATA	Atmosphere Absolute
B2M	Beta 2 Microglobulin
B	Bar
BTP2	3,5-Bis Trifluoromethyl Pyrazole
C/D	Compression/Decompression
CAM	Cell Adhesion Molecules
cDNA	Complementary Deoxyribonucleic Acid
cm	Centimeters
CNS	Central Nervous System
C-NTC	No-template Control
C-RT-	Control without RT
DCI	Decompression Illness
DCS	Decompression Sickness
DC-likeS	Decompression-like Sickness
ddH <sub>2</sub> O	Double distilled water
DIC	Disseminated Intravascular Coagulation
dm <sup>3</sup>	Cubic decimeters
DMSO	Dimethyl Sulfoxide

DNA	Deoxyribonucleic Acid
dNTP	Deoxynucleotide Triphosphate
DON	Dysbaric OsteoNecrosis
dsDNA	Double-stranded DNA
e.g.	Exempli gratia (for example)
EBG	Enfermedad de las Burbujas de Gas
EDC	Enfermedad Descompresiva
EF1 $\alpha$	Elongation Factor 1 alpha
ET-1	Endothelin 1
EU	European Union
Fig	Figure
g	Grams
GBD	Gas Bubble Disease
h	Hour
HSP70	Heat Shock Protein 70
HSP90	Heat Shock Protein 90
HSPs	Heat Shock Proteins
H&E/HxE	Hematoxylin and Eosine
Hz	Hertz

i.e.	In example
ICAM-1	Intercellular Adhesion Molecule 1
IUSA	Instituto Universitario de Sanidad Animal y seguridad alimentaria
Kg	Kilograms
L	Liters
max	Maximum
MFAS	Medium Frequency Active Sonar
mg	Milligrams
min	Minutes
mm	Milimeters
mmHg	Millimeters of mercury
mRNA	Messenger Ribonucleic Acid
n	Number of individuals
NATO	North Atlantic Treaty Organization
NCBI	National Center for Biotechnology Information
ng	Nanograms
NO	Nitric Oxide
NTC	No-Template Control

NTNU	Norwegian University of Sciences and Technology
NZWR	New Zealand White Rabbit
ORF	Open Reading Frame
PBS	Phosphate Buffered Saline
PCR	Polymerase Chain Reaction
PFO	Patent Foramen Oval
RNA	Ribonucleic Acid
RT	Reverse Transcription
RT-qPCR	Real Time Quantitative Polymerase Chain Reaction
ssDNA	Single-stranded DNA
TDG	Total Dissolved Gas
TGD	Total Gases Disueltos
UE	Unión Europea
UK	United Kingdom
USA/U. S	United States of America
USB	Universal Serial Bus
UV	Ultraviolet
VCAM-1	Vascular Cell Adhesion Molecule 1

VGE	Venous Gas Embolism
x	Magnification
xg	Fuerza centrífuga
°C	Celsius degrees
μm	Micrometer
μl	Microliter



# 9. ACKNOWLEDGMENTS / AGRADECIMIENTOS / *REMERCIEMENTS*





## Comparative study of gas-bubble lesions using experimental models

Cuando empecé este camino, lo hice con muchas dudas y miedos, sin saber si era lo correcto. Me entusiasmaba la investigación y seguir ampliando conocimientos en el ámbito veterinario, pero no sabía si realmente iba a encontrar en ella mi gran pasión. Por el camino, he ido aprendiendo mucho sobre el trabajo de laboratorio, los experimentos, las necropsias, los varamientos, los entresijos de los artículos científicos y la docencia. Precisamente en este último punto es donde desbloqueé una nueva pasión. Al principio confieso que no me entusiasmaba tener que parar mi investigación para dar clases, pero, desde las primeras prácticas en anatomía, algo despertó en mí. Creo que hoy, finalizando este gran ciclo de vida, he encontrado mi verdadera pasión.

A **Antonio Fernández**, director y tutor de tesis. Gracias Toño por acogerme y confiar en mí desde el primer minuto, a pesar de los “peros”. Porque cuando entraba a tu despacho con mucha carga mental, me escuchabas, me aconsejabas y, antes de irme, siempre me hablabas de mis planes de futuro, motivándome a perseguirlos y lucharlos. Ojalá algún día podamos volver a cruzarnos con mi objetivo logrado.

A **Maria José Caballero**, directora de tesis. Gracias MJ por siempre estar ahí apoyándome, enseñándome, guiándome. Creo que hemos hecho un muy buen equipo y que hemos sufrido mucho codo a codo para que esta tesis saliera adelante desde casi cero. No me olvido de tus mil y un esquemas/dibujos para explicarme, de tu dedicación y de tu preocupación porque todo tuviera una razón, de tus abrazos tras conseguir logros importantes y de tu perseverancia cuando las cosas parecían no salir.

A **Yara Bernaldo de Quirós**, directora de tesis. Gracias Yara por mostrarme lo que realmente siente alguien apasionado por lo que hace. Aunque yo no haya logrado llegar a ese nivel de pasión por la investigación, has sido todo un ejemplo para mí de que si quieres algo en la vida solo lo consigues con trabajo, dedicación y,

sobre todo, mucha pasión. Quiero agradecerte las llamadas en la distancia y el apoyo cuando más perdida me sentía con mi futuro.

También quiero agradecer al resto de profesores que estuvieron presentes y me ayudaron en algunas fases de esta aventura, en especial a **Ayoze Castro, Miguel Rivero, Antonio Espinosa, Manuel Arbelo, Mónica Betancor y Marisa Andrada.**

**Técnicos del IUSA**, imprescindibles para que todo funcione y mi experiencia tuviera lugar, en especial a **Javier Ramos, Ani Afonso, Yehiko Camacho, Mercedes Santana y Manola Martel.** Gracias Javi por abrirme las puertas de tu sala de necropsias, de tus medias mañanas y de tu casa y familia, por siempre escucharme y apoyarme. Gracias Yehiko por tu apoyo en las labores de docencia. Fundamentales eran tus cafés y nuestros debates en el taller. Gracias Ani y Mercedes por vuestras charlas amenas y vuestra ayuda siempre en el laboratorio y con las mil y una gestiones. Gracias Manola por siempre encontrar soluciones y tenerlo todo listo y preparado con una sonrisa.

**Compañeros del IUSA.** Gracias por los buenos momentos que hemos pasado a lo largo de estos años, en varamientos, necropsias, laboratorio, almuerzos de navidad, etc. En especial a **Marina Arregui**, por ser el faro en el que me he guiado académica y emocionalmente en los primeros años de tesis. Y a **Simone Segura**, por nuestra retroalimentación en cuarentena, crucial para tomar decisiones y dar pasos hacia el futuro.

Quiero agradecer también a las instituciones que han hecho posible este proyecto, principalmente al **Instituto Universitario de Sanidad Animal y Seguridad Alimentaria**, al **Ministerio de Educación, Cultura y Deporte** del Gobierno de España a través del contrato FPU y al Proyecto PGC2018-101226-B-100 del **Ministerio de Ciencia e Innovación** del Gobierno de España, por la financiación durante estos años de tesis. A la **Universidad de las**

**Palmas de Gran Canaria**, por las instalaciones y la financiación de congresos y cursos. A la **Universidad de Lieja**, por acogerme durante mis 3 meses de estancia en Bélgica y en especial al profesor **Daniel Desmecht** y a **Axel Dubois**, mi guía durante esa experiencia. Agradecer también a la **Fundación Loro Parque** y su **Programa de Salud y Bienestar de los Animales Marinos**, así como a **Poema del mar** por su colaboración y apoyo en la investigación de Sanidad de Animales Marinos.

Por último, agradecer también a **Jacinto Paredes** de la empresa **IBERCO**, por su dedicación y esfuerzo durante toda la fase de creación y puesta en marcha de nuestra maquinaria.

En el plano personal y como base emocional de este largo camino, quiero agradecer a toda mi familia y mis amigos más cercanos el apoyo y el cariño que han depositado en mí durante esta experiencia en la que, a veces, no he podido disfrutar tanto con ellos por falta de tiempo o por la distancia que nos separa, pero siempre los he sentido muy cerca de mí. En especial:

*A Maman, Papa et Esteban, mes piliers. Maman, tu es mon oasis de paix, le portrait vivant de l'amour et de la tendresse. Merci pour ton amour inconditionnel et tes mots d'encouragement en toute circonstance. Papa, tu es mon moteur, la seule personne qui sait comment me motiver à réaliser mes rêves. Merci pour tous tes discours d'encouragement. Vous êtes tous les deux mon mélange parfait pour construire un meilleur avenir. Esteban même si, de loin, nous ne sommes pas le frère et la soeur les plus proches du monde, merci de faire en sorte que nous nous revoyions comme si nous n'avions jamais été séparés. Je vous love famille.*

A **Rosa Siebold**, mi luz y mi prometida. Si tuviera que elegir una sola cosa por la que han valido la pena estos 5 años de doctorado, con permiso de la docencia y la experiencia, es haberte conocido. Si no hubiese elegido este camino, jamás habiésemos tenido la

oportunidad de conocernos mejor en nuestra magnífica FEAGA. Gracias por aparecer en mi vida con tu amor, tus abrazos, tu apoyo incondicional, tu modo tranquilizador, tu risa contagiosa y tu locura infinita, entre miles y miles de otras cosas más. Eres mi otro pilar fundamental y siempre le estaré agradecida a esta tesis doctoral por la oportunidad de conocer a una persona tan maravillosa y única como tú.

*Papy et Mamy, mes grands-parents. Grâce à ce doctorat, j'ai également eu l'incroyable opportunité de vivre 4 mois au jour le jour avec vous. Cela a été une expérience unique et je vous en serai toujours reconnaissante. Je suis heureuse de me rappeler à quel point vous étiez fiers et attentifs lorsque je vous racontais ce que je faisais à l'Université de Liège. Une petite partie de cette thèse est la vôtre.*

*A toute ma famille Wallraf et Velázquez, notamment les Wallrakie, merci pour votre amour. Tout particulièrement à Marraine Sophie, Tati Gene et Tata Désirée, trois femmes courageuses qui ont été dans mon quotidien un exemple de lutte et de résilience. Merci pour vos conseils dans la vie.*

**Ingrid, Mathias y Lila Siebold**, mi segunda familia. Gracias por vuestro cariño desde el primer momento que nos conocimos, vuestra alegría y vuestro apoyo en estos últimos años. Sois una familia increíble y espero siempre teneros en mi vida.

*Je ne peux pas oublier mes anges gardiens, **Granny, Tonton Steph, Welita et Martin**, qui protègent chacun de mes pas depuis tout en haut et pour qui un petit bout de ce travail est également dédié.*

Se cierra una gran etapa de mi vida, pero estoy segura de que muchas más vendrán.

**GRACIAS A TODOS. MERCI À VOUS TOUS.**

















## FE DE ERRATAS DE TESIS DOCTORAL

“Comparative Study of Gas-Bubble Lesions Using Experimental Models”, por Alicia Sofía Velázquez Wallraf

### Objetivo de la fe de errata:

Corregir los valores calculados de porcentaje de saturación de gases totales disueltos para los peces que se metieron en el acuario presurizado.

### Consideraciones:

1. Los valores absolutos en milímetros de mercurio (mm Hg) de gases totales disueltos, fueron obtenidos directamente del sensor, por lo que son correctos a lo largo del texto y figuras de la presente tesis.
2. El porcentaje de saturación de gases totales disueltos es una medida relativa. Expresa el porcentaje de saturación, es decir en cuánto supera, la suma de las presiones parciales de los gases a la presión ambiental. El 100% de saturación se obtiene cuando la suma de las presiones parciales iguala la presión ambiental. Si la presión ambiental aumenta, el número de milímetros de mercurio de gases totales disueltos requeridos para obtener el 100% de saturación, aumenta también de manera proporcional.
3. Para el acuario abierto, todos los valores de porcentaje de saturación de gases totales disueltos (a 1 atm) son correctos a lo largo de la presente tesis, al tener una presión ambiental de 1 atm. Sin embargo, al tener el acuario presurizado una presión ambiental de 1.5 atm se produjo el error de cálculo a la hora de convertir los valores absolutos de gases totales disueltos de mm de Hg a porcentaje de saturación.
4. Este error de cálculo, no afecta a ningún de los resultados experimentales de la tesis: patología, índice de gas, marcadores de daño tisular, etc...
5. A continuación, se rectifican dichos valores:

Página	Párrafo	Línea	Donde dice	Debe de decir
86	3	2	varying between 150% and 180%	varying between 101% and 120%
87	1	4	varied between 160% and 180%	varied between 107% and 120%
90	1	6	supersaturation between 164-174%	supersaturation between 110-116%
155	2	2	in water with 162-163%	in water with 108-109%
166	1	15	(saturación de 150%)	(saturación de 101%)
166	2	4	aproximadamente en 170%	aproximadamente en 113%
167	2	4	de entre 160-180%	de entre 107-120%
167	2	14	fueron de 162-163%	fueron de 108-109%
171	1	7	TGD de 169±5%	TGD de 112±5%
177	2	2	agua con 162-163%	agua con 108-109%

Esta rectificación de valores también se traslada a las publicaciones II y III de la presente tesis.

**Publicación II. “Establishment of a fish model to study gas-bubble lesions”**

Página	Sección	Párrafo	Línea	Donde dice	Debe de decir
1	Abstract	-	12	TDG values of 162–163%	TDG values of 108-109%
2	Resultados	2	4	TDG water of around 160% and 180%	TDG water of around 107% and 120%
3	Resultados	3	1	TDG values between 160 and 180%.	TDG values between 107 and 120%
4	Figura 4	-	2	(180%)	(120%)
4	Figura 4	-	3	TDG of approximately 150%	TDG of approximately 101%
4	Resultados	3	6	was of 162% and 163%	was of 108% and 109%
5	Discusión	1	3	TDG values of 162-163%	TDG values of 108-109%
7	Discusión	7	4	(3 h with TDG 160–178%)	(3 h with TDG 107-119%)
7	Discusión	7	10	162-163%	108-109%
8	Discusión	10	3-4	162 and 163%	108 and 109%
8	Métodos	3	4	Than 150%	101%
8	Métodos	3	6	150% and 180% TDG	101% and 120% TDG
9	Métodos	5	5	The range of 160-180%	The range of 107-120%

**Publicación III. “Biomarkers related to gas embolism: Gas score, pathology, and gene expression in a gas bubble disease model”**

Página	Sección	Párrafo	Línea	Donde dice	Debe de decir
1	Abstract	-	8	water with approximately 170%	water with approximately 113%
3	Métodos	3	2	169 ± 5% were reached	112 ± 5% were reached